Title
Purine and pyrimidine metabolism in Tritrichomonas foetus

Author
Verham, Ronnie P.

Publication Date
1984

Peer reviewed|Thesis/dissertation

Purine and Pyrimidine Metabolism

in Tritrichomonas foetus

by

Ronnie P. Verham

DISSERTATION

Submitted in partial satisfaction of the requirements for the degree of

DOCTOR OF PHILOSOPHY

in

Pharmaceutical Chemistry

in the

GRADUATE DIVISION

of the

UNIVERSITY OF CALIFORNIA

San Francisco

Date DEC 31 1984 **University Librarian**

Degree Conferred: . . . . . .

To my wife Karen and my family, Petrus, Bie, Hendrikes and Joyce who made this all worthwhile and possible.

ACKNOWLEDGEMENTS

I wish to express my sincere appreciation to Professor C.C. Wang for his dedication to teaching, critical eye for detail and generous assistance during the entire course of this work and in the preparation of this thesis. Professor Wang's relentless drive and enthusiasm have been and remain profoundly inspirational.

I would like to thank Susan Aldritt and Hui-wen Cheng for their nucleotide conversion into nucleic acid data, Audie Rice and SinFu Tseng for assaying the purine and pyrimidine salvage enzyme activities and HUT medium work and lastly Drs. Thomas Meek and Jeffrey Coderre for their assistance in assaying thymidylate synthetase and dihydrofolate reductase activities.

I would also like to thank Rashid Aman, Meg Phillips and Alice Wang for their helpful suggestions and continual support.

Finally, I wish to express my indebtedness to my wife, Karen, whose continuing enthusiasm and encouragement contributed immeasurably to making this period of study an intensely rewarding experiance.

ABSTRACT

Tritrichomonas foetus, an anaerobic protozoan parasite, is incapable of de novo purine and pyrimidine biosynthesis. Incorporation of uracil into UMP, UDP and UTP is observed due to a high level of uracil phosphoribosyltransferase in the cellular cytoplasm of T. foetus. Uridine and cytidine are also incorporated into the nucleotide pool; but mainly through prior conversion to uracil by uridine phosphorylase and cytidine deaminase. The parasite contains no dectectable dihydrofolate reductase or thymidlyate synthetase and cannot incorporate uracil, uridine or deoxyuridine into DNA. The only means of obtaining TMP for the parasite is by thymidine phosphotransferase found in the pelletable cellular fraction of T. foetus.

Adenine, hypoxanthine, and inosine are incorporated readily into the parasites nucleotide pool via IMP. High hypoxanthine phosphoribosyltransferase, adenine deaminase and inosine phosphorylase, but no adenine phosphoribosyltransferase, inosine kinase or inosine phosphotransferase support the conclusion that adenine and inosine are converted to hypoxanthine before incorporation. Guanine and xanthine are converted to GMP and XMP by phosphoribosyltransferase activities while adenosine is incorporated by adenosine kinase.

Two enzymes involved with purine salvage in T. foetus, Hypoxanthine-Guanine-Xanthine phosphoribosyltransferase (HGXPRTase) and inosine 5'-monophosphate dehydrogenase (IMPDH), have both been purified over 500 fold and characterized. HGXPRTase has a molecular weight of 25,000 daltons, sedimentation coefficient of 3.7 S and recognizes hypoxanthine > guanine >> xanthine as substrates. Several

purine analogs including 6-mercaptopurine, 2-amino-6-thiopurine and 8-thioguanine were found to be good inhibitors of T. foetus HGXPRTase activity. In vitro growth growth studies indicate that 8-thioguanine is also a good inhibitor of T. foetus growth.

IMPDH has a molecular weight of 380,000, a subunit molecular weight of 58,000, pH optimum of 8.1, has no salt requirement and displays K_m values of 18 μM and 445 μM for IMP and NAD^+, respectively. Mycophenolic acid is an uncompetitive inhibitor of IMPDH for IMP and NAD^+ with K_i values of 9 μM and 6 μM, respectively. Mycophenolic acid is also an in vitro inhibitor of T. foetus growth with an IC_{50} of 30 μM.

TABLE OF CONTENTS

TABLE OF FIGURES

TABLE OF TABLES

INTRODUCTION

The prevention and treatment of diseases caused by microorganisms can be traced as far back as 2735 BC. The ancient Chinese physicians discovered ch'ang shang which was later identified as the antimalarial plant Dichron febrifugal (1). Present day methods for the control of disease include: a) improvements in housing, sanitation and hygiene, b) control of vectors, c) development of vaccines and d) development of chemotherapeutic agents. While all four methods will be ultimatly involved in the control of disease, I will only pursue the development of drugs. Many drugs have been develped for most diseases but there are also many problems associated with them. There is a need for a new generation of drugs that are effective against advanced stages of disease, are less toxic and are effective against "resistant" forms of the disease. Most of the present day drugs were developed empirically, with a "hit or miss" type of approach. Many compounds were selected or synthesized at random for possible screening to determine if they were of any medicinal value. A more rational approach to drug design would involve a complete and comprehensive biochemical comparison of the microorganism and host. Then, once a differance between the two are found, chemotherapeutic agents could be designed to exploit this differance.

The goal of this research project is to uncover the differances in purine and pyrimidine metabolism between a parasite and its host. A parasite, in any parasitic association, is the smaller of the

associating pair of animals while the larger is the host. Parasitism is defined as the association between two animals such that one lives and feeds, temporarily or permanently, either in or on the body of the other. The organism under study is also a protozoan, which is part of the kingdom Protista. The phylum Protozoa comprises all unicellular or acellular organisms, some forming colonies, but lacking differentiation of tissues. The basic cellular organization is of the eukaryotic type with the cell contents delineated into a large number of membrane bound organelles. Protozoa, or "one celled heterotrophs" are further divided into groups based upon their mode of locomotion and include flagellates, amoeba like organisms, ciliates and sporozoans.

The subject of this investigation is the anaerobic protozoan parasite, Tritrichomonas foetus. This urogenital trichomonad of cattle has also been refered to in the past as Trichomonas utero-vaginalis-vitulae (Mazanti), Trichomonas bovis (Riedmuller), Trichomonas genitalis (Witte), Trichomonas bovinus (Hies) and Trichomonas mazzanti (Zetti)(2). Until recently, there has been a great deal of confusion in the classification of this organism. Some classified the parasite in the genus Trichomonas (Donne') while others assigned it to the genus Tritrichomonas (Kufoid) (3-5). It wasn't until 1963 when Honigberg (6), in his revision of the order Trichomonadida, assigned the organism to Tritrichomonas. Since that time the urogenital trichomonad of cattle has been referred to as Tritrichomonas foetus.

The complete taxonomic classification of T. foetus is as follows;

kingdom-Protista

phylum-Protozoa

subphylum-Sarcomastigophora

superclass-Mastigophora

class-Zoomastigophorea

order-Trichomonadida

family-Trichomonadidae

subfamily-Tritrichomonadinae

Tritrichomonas foetus and bovine urogenital trichomoniasis is worldwide in distribution (2). The primary natural host of this trichomonad are cattle, but the pig, horse and roe deer can also harbor this parasite (7). It has been estimated that up to 30% of the cattle in some areas of south Germany and Switzerland were found to harbor T. foetus. Bovine urogenital trichomoniasis has been ranked, after brucellosis and leptospirosis, as the disease most responsible for abortions in cattle in the United States. The Agricultural Research Service of the United States Department of Agriculture estimated that between 1951 and 1960 the beef industry suffered losses exceeding $8 million due to bovine trichomoniasis (7,62).

Tritrichomonas foetus is transmitted from bulls to cows during coitus and may be cosidered strictly a venereal infection. The parasites are lodged in the prepucial cavity of the bull, but have also been found in the urethra and deeper parts of the urogenital tract

(63). Once infected, the bull is typically infected for life. Acute infection is accompanied by inflammation and swelling of the prepuce with mucopurulent discharge. These symptoms are cleared in about two weeks and then the bull is typically asymptomatic.

T. foetus trichomoniasis varies in the cow, ranging from a mild form of infection to extensive pathologic changes. The trichomonads are most numerous in the vagina 14-18 days post infection (11). There after, the parasites migrate upward through the cervix and invade the uterus. Although the primary site of infection is the uterus, the parasites may remain in the vagina causing low-grade inflammation accompanied by vaginal catarrh. In the uterus the parasites cause low grade endometritus, with uterine and cervical catarrh. If conception occurs in the infected cow, aborton usually follows. There are two types of abortion, complete and incomplete. Complete abortion is when the fetus is expelled together with the placental membranes. Cows recover, and are able to concieve later on in the case of a complete abortion. In an incomplete abortion, the membranes are retained in the uterus. If the membranes are not removed, chronic catarrhal and purulent endometritus develops. Permanent sterility results in the cow as a consequence of the destruction of uterine mucosa. Spontaneous recovery or permanent sterility are dependent upon the extent of infection and the severity of endometritus.

The pathogenicity of T. foetus infection has been thoroughly studied (12,64-66). Two hypothesis have been proposed to explain the effects of the parasitic infection. Hogue (65) proposes that the

abnormal changes observed in in vitro cultures were caused by thermostable toxins produced by the parasites. Florent (64), however, thought that the pathologic alterations were ascribable to exhaustion of nutrients by the trichomonads. Both investigators used coverglass cultures of primary chick tissue explants as their model system. Examination of various isolates of T. foetus revealed the existence of strains with different inherent pathogenicities. The differances between the strains range from a highly virulent KV_1 strain to less virulent DK_1 and UT_1 strains.

Extensive morphologic studies have been done of T. foetus by Wenrich and Emmerson (3) and also by Kirby (5). The flagellate possesses an elongated body approximately 9-25 x 3-15 microns in fixed stained preparations or 15-22.5 x 4.5-10 microns in living specimens. The discripancy between stained and living cells is not surprising since fixations cause significant shrinkage of the trichomonad cell (8). The parasite has three nearly equal anterior flagella ranging in length from 11 to 17 microns. A recurrent undulating membrane typically shorter than the body, has 3-5 waves. The external margin of the undulating membrane consists of the "accessory filament" and the attached part of the recurrent flagellum, which continues beyond the posterior end of the membrane as a free posterior flagellum. The posterior flagellum extends beyond the parasite about 16 microns. See Figure I.1.

A more detailed examination of T. foetus reveals small granules in suitable stained preparations in the axostylar capitulum. A peri-

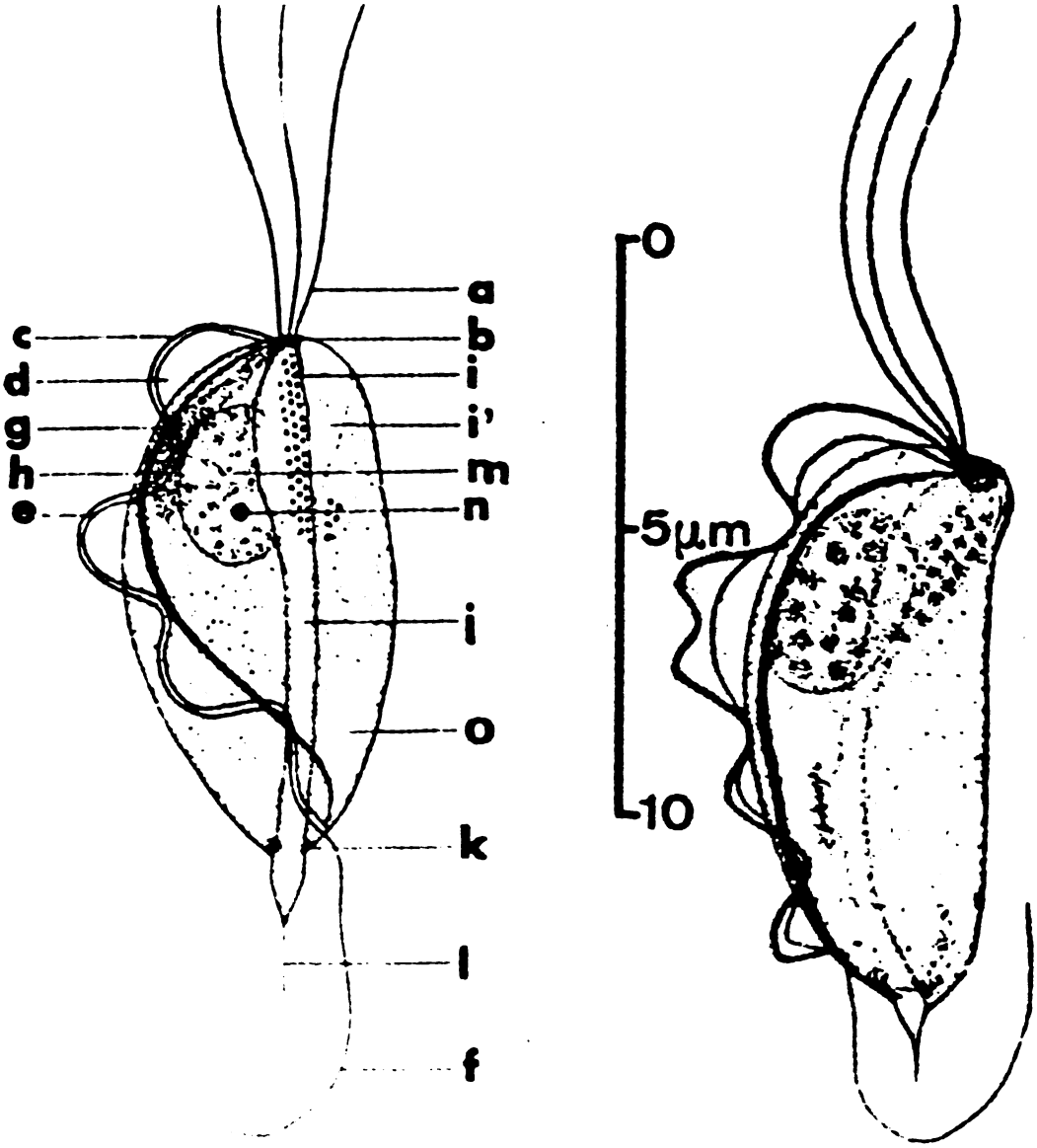

FIGURE I.1. Tritrichomonas foetus (3,5). Key to symbols: a, anterior flagella; b, kinetosomal complex; c, recurrent flagellum at the margin of the undulating membrane; d, undulating membrane; e, "accessory filament;" f, free posterior flagellum; g, costa; h, parabasal body; i, capitulum of the axostyle; i', ventral extension of the axostylar capitulum; j, trunk of the axostyle; k, pariaxostylar ring; l, terminal filamentous extension of the axostyle; m, nucleus; n, nucleolus; o, undifferentiated cytoplasm.

axostylar "chromatic" ring is also seen in the area of "emergence" of the trunk. The "chromatic" periaxostrylar ring appears to be composed of one or two rows of electron dense microbody-like inclusions similar to the paraxostylar and paracostal granules (9). The parasite poses-ses an ellipsoidal or ovoid nucleus located slightly posterior at the anterior end of the cell. In T. foetus the undulating membrane consists of two parts. The proximal part is a foldlike differentia-tion of the flagellates body surface and contains the proximal marginal lamella. The distal part has no obvious physical connection to the proximal fold but encloses the distal marginal lamella in its ventral and the microtubules of the recurrent flagellum in its dorsal area. Glycogen granules are distributed throughout the cytoplasm, being especially abundant within the axostyle.

Vaginal infections failed to stimulate humoral antibody produc-tion, but agglutinins were produced in the course of uterine trichomo-niasis in naturally and experimentally infected cattle. Evidently antigens are absorbed from the uterus and passed into the systemic circulation (14,22-24). A possible role of white blood cells in initiating an antibody response has been suggested. Phagocytosis of T. foetus by leukocytes and by macrophages in chick liver cell cultures has been reported (3,11,12). Ito et al (13) proposed that the lymphocytes and polymorphonuclear leukocytes played a role in the immunoprotection of the host organism against trichomonal infections. Experimental evidence demonstrated that cells derived from lymph glands of mice immunized with living trichomonads, when incubated with

these parasites in a suspension, caused destruction of the flagellates on contact.

Comparison of T. foetus with T. vaginalis, with the aid of agglutination, passive hemagglutination, precipitation, complement fixation and fluorescent antibody methods, show that these species have common and unique antigens (10). The discovery of 17 strains of the bovine urogenital trichomonad was found in Scotland and England alone by the agglutination method (15). There have also been reports that T. foetus strains do not change their antigenic attributes during prolonged in vitro cultivation (10,17). It is thus not certain how T. foetus evades the imunological response. Only a few of the various fractions and extracts of T. foetus were found to be immunologically active in precipitin reactions and by skin tests. The fractions reactive in the skin tests were the trichloacetic acid precipatate extracted with acetone/ether and the ethylene glycol extracted (18-20). Feinberg and Morgan (21) suggested activity of these extracts depended on the presence of some nucleoprotein substances. Analysis of the ethylene glycol fraction revealed " a complex carbohydrate to which are firmly bound amino-acids, most probably in the form of complex amino-acid-containing residue" (21). Much still remains to be learned about the immune mechanism operating in bovine urogenital trichomoniasis. There have been no reports of lasting immunity acquired by the host.

High levels of endogenous metabolism in T. foetus depends upon glycogen which is synthesized from suitable exogeneous substrates such

as glucose, galactose, mannose, maltose or sucrose (25,30). Glycogen stores are similar to mammalian glycogen; a branched α-1-4 glucosan, with a unit chain length of 15 residues (3 x 10^6 daltons) (31). Under anaerobic conditons, fructose, lactose, raffinose as well as pyruvate and lactate may be also utilized by T. foetus (30,32-34,46). In the presence or absence of exogeneous carbohydrates, Tritrichomonas foetus produces organic acids (succinate, acetate, lactate and pyruvate), CO_2 and H_2 (28-30,32,33). All carbohydrate substrates are metabolized by the bovine trichomonad via the typical glycolytic pathway (30,34). The pathway is not affected by inhibitors such as iodoacetate and fluoride (32-34). Activities for the following enzymes have been demonstrated or inferred; glycogen phosphorylase, phosphoglucomutase, hexokinase, glucose phosphate isomerase, 6-phosphofructokinase, fructose diphosphate aldolase, triose phosphate isomerase, glyceraldehyde phosphate dehydrogenase, phosphoglyceromutase, enolase, pyruvate kinase and lactate dehydrogenase (30,34).

Glycolysis is evidently the basic mechanism of glycogen utilization by T. foetus leading to the formation of phosphoenolpyruvate (PEP) (41,47). Demonstrated PEP carboxykinase, malate dehydrogenase, fumarase and fumarate reductase activities provide a facile pathway for the conversion of PEP to succinate (48). The reaction catalyzed by fumarate reductase is apparently irreversible and explains the observed excretion of succinate. There is no succinate dehydrogenase activity and all the previous enzymes are localized in the cytosol. See figure I.2.

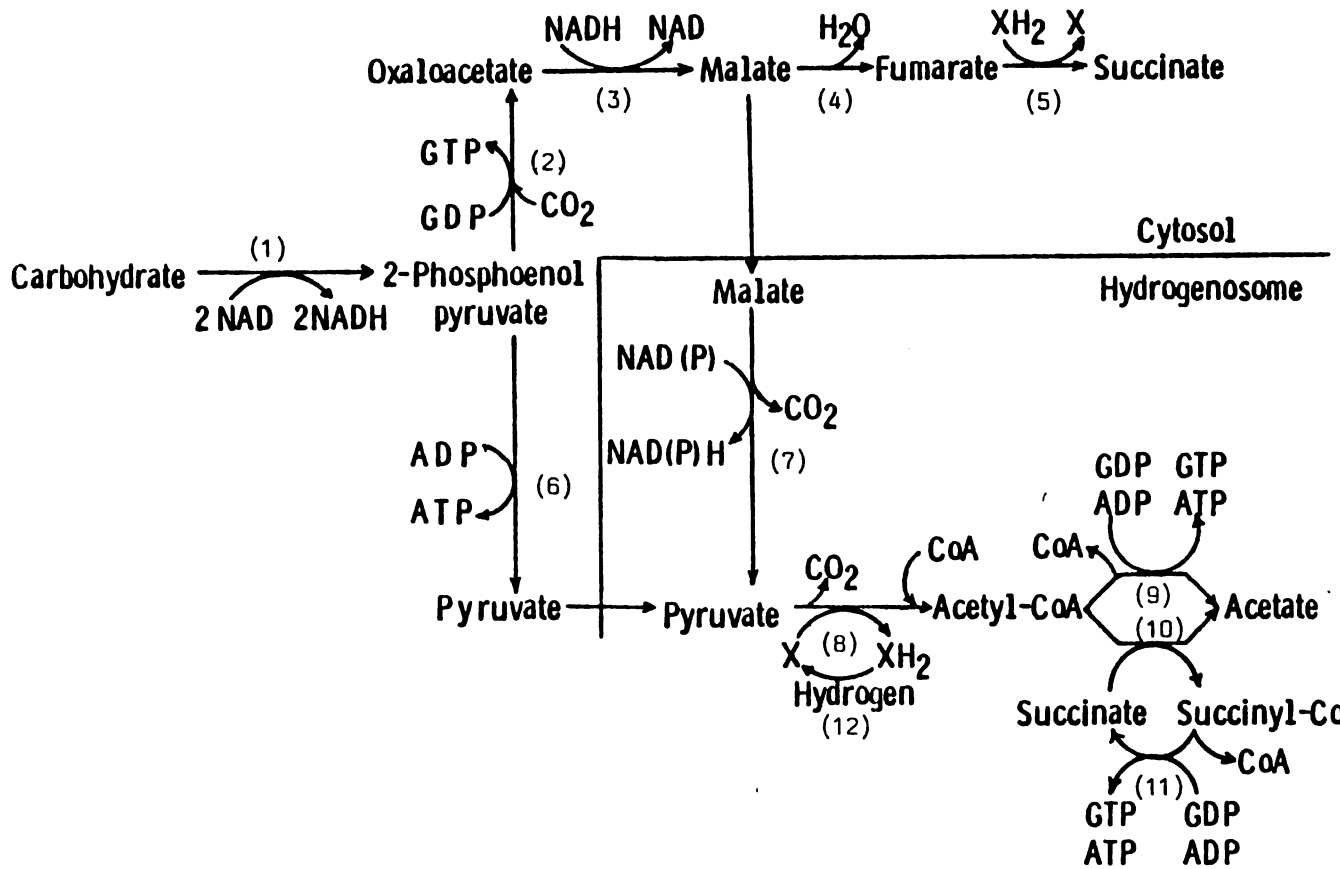

FIGURE I.2. Scheme, partly hypothetical, of carbohydrate metabolism in Tritrichomonas foetus (41). Glycolytic enzymes (1); phosphoenolpyruvate carboxykinase (GDP) (2); malate dehydrogenase (NAD) (oxaloacetate reductase) (3); fumarate hydratase (4); fumarate reductase (5); pyruvate kinase (6); malate dehydrogenase (decarboxylating, NAD(P)) (7); pyruvate dehydrogenase (ferredoxin) (8); acetate thiokinase (ADP or GDP) (9); acetate-succinate CoA transferase (10); succinate thiokinase (ADP or GDP) (11); hydrogenase (ferredoxin) (12).

The conversion of pyruvate to acetate, H_2 and CO_2 was observed using intact T. foetus at pH 4 or cell-free homogenates of this trichomonad at pH 6 (46). Pyruvate is converted from PEP via a cytoplasmic pyruvate kinase or by a malate deydrogenase (42,45).

Decarboxylating pyruvate dehydrogenase (ferredoxin-pyruvate synthase) assists the oxidation of pyruvate to acetyl CoA, CO_2 and $2H^+$. Compared to the pyruvate dehydrogenase complex from heart or kidney mitochondria, the enzyme from T. foetus was not dependent upon the participation of thiamine, pyrophosphate or lipoic acid (or the appropriate dihydrolipoyl enzymes). It did require thiol compounds for full activity. Methyl viologen, FAD, FMN or riboflavin but not NAD or NADP could serve as electron acceptors. The decarboxylating pyruvate dehydrogenase, also referred to as pyruvate:ferredoxin oxidoreductase, displayed latency suggesting its location in a membrane-bound particle.

Hydrogenase activity, in cell free extracts of T. foetus, was analyzed and compared to hydrogenase from C. pasteurianium. The enzyme from the parasite exhibited no latency, required thiol compounds and was found to utilize the same electron acceptors as pyruvate:ferredoxin oxidoreductase. There were no activities found for formate dehydrogenase, formate lyase or phosphotransacetylase in T. foetus homogenates (42).

The formation of acetyl-CoA from acetate can occur by two pathways (49). The first pathway is mediated by acetate thiokinase while the second by acetyl-CoA:succinate transferase and then

succinate thiokinase. As of yet the in vivo electron acceptor for pyruvate synthase and hydrogenase has not been identified.

Several enzymes including pyruvate synthase and hydrogenase are sensitive to oxygen. Since T. foetus is an aerotolerant anaerobe it is not surprising that it contains both catalase and superoxide dismutase (9,30,32,34,44). Most of these enzyme activities are in the cytosol while some superoxide dismutase activity is associated with the "microbody" like particles.

Isopycnic centrifugation in a sucrose gradient of the large particle fraction obtained by differential centrifugation, indicate pyruvate:ferredoxin oxidoreductase, hydrogenosome, acetate thiokinase, acetyl-CoA transferase and superoxide dismutase correspond to the paracostal and paraaxostylar granules described by light microscopists (9,43,50). These bodies lack catalase activity and were therefore not considered to be peroxisomes (9). Structural and biochemical evidence show that these bodies are also not mitochondria (25-27,50-52). In addition, these bodies contain circular DNA and cardiolipin (54,55). The term "hydrogenosomes" was proposed because these bodies are able "to use protons as terminal electron acceptors and produce molecular hydrogen". Some properties of the hydrogenosome membrane are: a) impermeable to NADH, b) the entry of pyruvate or the exit of some metabolites may be under the influence of succinate, malate or isocitrate, c) calcium ion enters the hydrogenase by active transport and d) ADP, but not GDP, is able to traverse the membrane and is dependent upon a specific translocase not inhibited by atractyloside like that

of mitochondria (40).

Information about energy production in the course of anaerobic and aerobic carbohydrate metabolism of T. foetus is incomplete. The parasite is devoid of an active tricarboxylic acid cyle, cytochromes and mitochondria (29). In the presence of added sugars, oxygen uptake of T. foetus is stimulated two fold over that observed during the glycogen-dependent endogenous metabolism (28-30,32-34,37). Aerobic metabolism is not inhibited by cyanide or azide suggesting that flavins may perhaps mediate electron transport (29-35,37,43,53). ATP to ADP levels in endogenous metabolism, in the presence of exogenous glucose and under anaerobic and aerobic conditions, allow the calculation that for each glucose molecule five and seven ATP molecules are produced anaerobically and aerobically respectively (37). Oxidative phosphorylation inhibitors such as oligomycin, amytal and atractyloside (known mitochondria respiration inhibitors) were effective only at very high concentrations. It is difficult to understand how hydrogenosomes could function in oxidative phosphorylation by Mitchell's chemiosmotic theory.

There have been several reports of NADH and NADPH oxidase found in T. foetus (9,38-40). T. foetus has two or perhaps three NADH oxidase systems. One of these oxidase systems is in the cytosol, another in the "microsomal" fraction and the third in the large granule fraction. The cytosol enzyme accounts for more than 50% of the total activity, is stimulated by Mg^{+2}, is not stimulated by ADP and displays latency. The microsomal enzyme is stimulated by ADP and

has been suggested to play a role between NADH oxidase and phosphorylation (39). The large granule fraction (hydrogenosomes) contains NADH oxidase activity with significant latency (38). It is also uncertain whether the cytosol enzyme is a separate complex or indeed just released from the microsomes.

Some other biochemical attributes of T. foetus are that it contains several hydrolases (glycosidases) such as α- and β-glucosidases, α- and β-galactosidases, α- and β-N-acetyl glucoaminidases, α- and β-fucosidases and α-rhamnosidases (56-59). The biologic significance of these hydrolases as well as of neuraminidase and hyaluronidase is still unclear. Several of the hydrolases, the protease and part of the acid phosphatase activities were found to be associated with the large granule fraction and exhibit a pH optimum of 6.0-6.5 (9,60,61).

Tritrichomonas foetus has been used for the testing of various anti-trichomonal drugs. The bovine parasite has ben used in the search for drugs against Trichomonas vaginalis because they do not pose a pathogenic hazard to the technicians and produce animal infections more readily (67,95). Michaels and Strube (65) commented that despite the existance of qualitative differances in the carbohydrate metabolism of T. foetus and T. vaginalis, many investigators have employed the bovine trichomonad in the search for drugs against T. vaginalis. A vast number of drugs have been tested in vitro and in vivo against Tritrichomonas foetus. Table I.1 illustrates the vast range of agents used against human trichomoniasis (68). The majority of compounds in Table I.1 were also tested on T. foetus but I have

made no attempt to separate the two. As Table I.1 points out, there has been an enormous amount of accumulated information on the therapy of human urogenital trichomoniasis. Steck states: "Although without any mortality, the infection gives rise to such morbidity that almost any approach to management is acceptable" (68). The conditions that existed before the introduction of metronidazole in the early 1960's is described by Keighley (69) as: " 'Flagyl' is now taken as a matter of course and a whole generation has no knowledge of the sufferings of women with trichomoniasis before its introduction- the indignities and discomfort of the perpetual local treatment, douches, paintings, insufflations and insertion of pessaries, etc. All these things women suffered for months and sometimes years on end only to relapse when the treatment was discontinued".

To date, there are no fully effective therapeutic measures for Tritrichomonas foetus trichomoniasis in cattle. Even dimetridazole, considered to be the most effective compound against this parasite when administered orally, was found to eliminate the parasites from only nine out of eleven experimentally infected cows (70-72).

As far as bulls are concerned, intravenous administration of dimetridazole along with topical administration of Baroflavine-Saalbe, acriflavine or berenil salves, appears to be fully effective (71,73,74).

The 4(5)-nitroimidazoles represent an important class of antitrichomonal agents with metronidazole and dimetridazole the drugs of choice in the treatment of human and bovine trichomonal infections

TABLE I.1: Summary of agents used against trichomonal infections (68).

INORGANIC COMPOUNDS

Group I elements: Sodium chloride, sodium bicarbonate, copper (II) sulfate, silver nitrate, argyrol, protargol, ammoniacal silver nitrate, silver lactate and silver picrate.

Group II elements: Magnesium trisilicate, magnesium sulfate, zinc chloride, zinc sulfate, zinc oxide, mercury (II) chromate, mercury (II) iodide-iodine complex, mercury oxycyanide, phenyl mercuric acetate, phenyl mercuric nitrate, mercurochrome, nitromersal and thiomerosal.

Group III elements: Borax, sodium borate, boric acid, aluminum acetate aluminum potassium sulfate (alum), aluminum zinc sulfate (zinc alum), and aluminum 2-hydroxy-naphthalene-3,6-disulfate.

Group IV elements: Lead acetate

Group V elements: Acetarsone, carbarsone, phenarsone sulfoxylate, arsphenamine, sodium arsenate, neoarsphenamine, subgallate and subsalicylate.

Other elements: Chromic acid, radium, pottassium permangante.

ACYCLIC ORGANIC COMPOUNDS

Acetic acid, lactic acid, citric acid, tartaric acid, quarternary ammonium salts, alkyl sulfonates, bromoacetic acid, thiosemicarbazones of aldehydes and ketones, dithiocarbamates, bis(thiocarbamoyl)disulfides and alicin.

ISOCYCLIC ORGANIC COMPOUNDS

Terpenoid Types: alpha-pinene, 1-terpinene-4-ol and p-cymene.

Aromatic Types

General Non-Arsenicals: DDT, phenol, cresol, hexylresorcinol, picric acid, chloramphenicol, triazenes, gentian violet, malachite green, suramin, sulfanilamide and other sulfonamide drugs.

Aromatic Arsenicals: Arsanamide, neoarsphenamine, carbarsone, acetarsone, glycobiarsol, aldarsone and phenarsone sulfoxylate.

Tetracycline Types: Tetracycline, chlortetracycline and oxytetracycline.

Steroidal Types: Testosterone, progesterone, estradiol, deoxycorticosterone and fusidic acid.

TABLE I.1 (CONT).

Other Isocyclic Types: Colchicine.

HETEROCYCLIC TYPES

Oxygen-Heterocyclic Types

Furan Derivatives: 5-nitro-2-furaldehyde, furazolidone, nifuroxime, nitrofurantoin and nifuratel.

Other small-ring oxygen Heterocyclic Types: Chelidonic acid, chelidonine, chelerythrine, aristolchic and usnic acid.

Macrolide antibiotics: Pimaracin, trichomycin, azalomycins, erythromycin, carbomycine, carbomycin, endomycin and hamycin.

Nitrogen-Heterocyclic Types

Single Nitrogen Heterocyclic Compounds

Pyrroles: Nitropyrroles, anisomycin.

Pyridines: 5-nitro-2-substituted pyridines.

Quinoline derivatives: 8-quinolinols sulfate, chlorquinalsol, 7-iodo-8-quinolinols, amonoquinolines, chloroquine, amodiaquine.

Acridine derivatives: 9-aminoacridine, acriflavine, ethacridine, quinacrine and aminoakrikhin.

Two nitrogen Heterocyclic compounds

Pyrazole derivatives: 4-nitropyrazole.

Imidazole derivatives: Azomycin, metronidazole, ornidazole, ronidazole, tinidazole.

Benzimidazoles: 2-nitrobenzimidazole.

Other two nitrogen heterocyclic compounds: 3-amino-6-methyl-4-nitro pyridazine-1-oxides, 2-amino-5- nitropyrimidines pyrimethamine, hexatidine, anthrapyrimidine, piperazine adipate and phenquone.

Other nitrogen heterocyclic types: imoctetrazoline, viomycin and fervenulin.

TABLE I.1 (CONT).

Heterocylcic types having diverse heteroatoms

Thiazoles: Forminitrazole, aminitrozole, niridazole, derivatives of 5-nitro-2-thiazolyl hydrazine and thiamorpholines.

Others: Furazolidone, nifuratel, 1,3,4-thiadiazoles and arsthinol.

CARBOHYDRATE TYPES Paromycin and streptomycin.

respectively. The structures of metronidazole and dimetridazole are shown in Figure I.3. The 5-nitroimidazoles share the following general properties; 1) they are cytotoxic leading to cell damage and death, 2) they have radiosensitizing action under anaerobic condition, 3) they are inhibitors of photosynthesis, 4) they cause mutagenic action in bacteria and fungi and 5) they exhibit high toxicity towards anaerobic prokaryotes and eukaryotes but very low toxicity to facultative and aerobic organisms. Metronidazole has been used in the treatment of protozoal diseases (trichomoniasis, giardiasis, amoebiasis, balantidiasis, bacterial diseases (caused by anaerobes like Vincents disease and post operative infections) and as a radiosensitizer of hypoxic tumours. The excellent chemotherapeutic ratio and widespread clinical application of metronidazole warrants a review of the mode of action this drug.

Studies on the antibiotic azomycin, a 2-nitroimidazole, and its anti-trichomonal properties led to the synthesis of 4(5)-nitroimidazoles. Of course, 4(5)-nitroimidazoles like metronidazole proved to be extremely potent anti-trichomonal agents. Initial observation by Ings et al (75) indicated that metronidazole inhibited both RNA and DNA synthesis. Other workers (76) using [^{14}C] metronidazole, found the label associated with the protein and DNA fractions, but not RNA. Cells were found to accumulate metronidazole and that the toxic effects and accumulation were inhibited by oxygen (77-81). The fate of metronidazole in mammals on the other hand, was much simpler. In the urine of mice, and also of human subjects, the nitro-containing

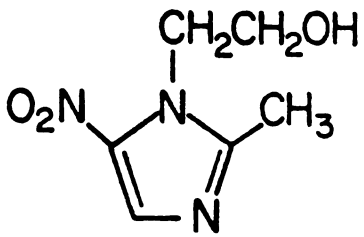

Metronidazole

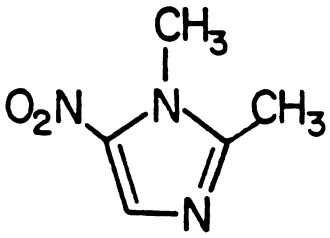

Dimetridazole

FIGURE I.3. Structures of two potent antitrichomonals.

compounds were found in the following proportions: a) the unchanged drug, 25-30%; b) 1-(2-hydroxyethyl)-2-hydroxymethyl-5-nitroimidazole, 35-40%; c) glucuronide conjugates of the compounds listed in (a) and (b), 10-14%; d) 1-acetic acid-2-methyl-5-nitroimidazole, 15-20% and e) 1-(2-hydroxyethyl)-2-carboxylic acid-5-nitroimidazole (82-84).

At this point investigators assumed that 3 steps needed to occur for metronidazole to exhibit microbicidal action in anaerobic organisms; 1) cellular uptake, 2) reductive activation and 3) toxic effects of reduced product(s). The first step involves the entry of drug into the cell. Metronidazole exhibits a linear relationship of intracellular accumulation to the external concentration in T. foetus. There is no indicaton of saturation kinetics and lacks any competitive inhibition by biologically active or inactive nitroimidazole derivatives. The most likely explainaiton for entry of metronidazole is by diffusion (77). Entry is also facilitated by a "concentration gradient". The rapid conversion of metronidazole keeps the intracellular concentration of metronidazole low and thus forms a concentration gradient from the outside to the inside of the cell. The second step, reductive activation, is thought to occur in susceptable organisms which have certain low-redox proteins (ie. ferredoxin or flavodoxin). It is apparently the ability of these organisms to reduce the nitro group of these compounds which causes the toxicity (77,86). The formation of a nitro anion radical of metronidazole has been demonstrated using intact T. foetus cells, anaerobic homogenates of T. foetus or anaerobic T. foetus hydrogenosomes (87-89). The reduction

of the nitro group of metronidazole is thought to occur by several steps as illustrated in Figure I.4.

The protein responsible for the reduction or the identity of the reduced "reactive intermediate" are still unknown. The number of electrons transferred to metronidazole in the course of in vitro reduction was determined to be four, on the basis of the results of experiments with ferredoxin, dithionite or cell homogenates (79,86). This suggests that the reduction product corresponds to a hydroxylamine derivative, yet no one has detected this intermediate. Fragmentation patterns determined by Chrystal et al (90) indicate that the reduced intermediate is extremely reactive and unstable, fragmenting in several places. Muller et al (77) have also determined that the following protein activities were unaffected by metronidazole: pyruvate:ferrdoxin succinoxidase, hydrogenase, adenylate kinase, NADH oxidase, acid phosphatase and β-N-acetylglucosaminidase. It is somewhat unfortunate that despite their significant activity, so little is known about the active inhibitory and cidal products of nitroimidazoles.

The need for new antitrichomonal drugs is evidenced by the emergence of resistant strains to metronidazole (91), the implication of carcinogenicity and mutagenicity of nitroimidazoles (92-94) and the incomplete effectiveness of dimetridazole to treat bovine tritrichomoniasis.

The scope of this research project focuses on the purine and pyrimidine metabolism of T. foetus. Parasitic protozoa have been

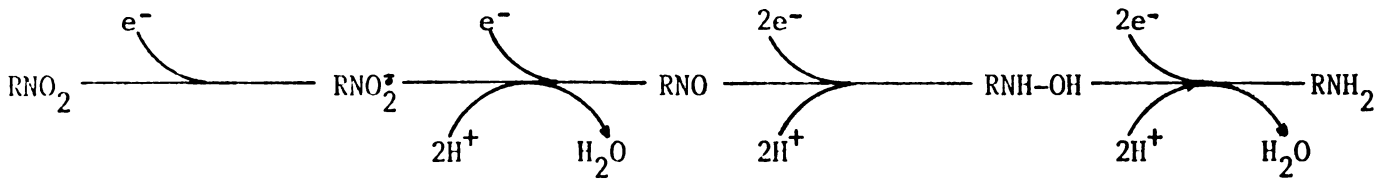

FIGURE I.4. Possible reduced intermediates of 5-nitroimidazoles.

found to be generally incapable of de novo purine biosynthesis. Trypanosoma cruzi (89), Leishmania donovani (96), Plasmodium lophurae (97), Eimeria tenella (98) and Trichomonas vaginalis are a few examples of those unable to form their purines de novo. This defiency in purine biosynthesis and the parasites reliance upon purine salvage has provided opportunites for the control of these parasites. Allopurinol, a purine analogue recognized as hypoxanthine by the parasitic salvage enzymes, exhibits antitrypanosomal and antileishmanial activities (101,102). Likewise, the purine nucleoside analogues; allopurinol riboside (103), formycin B (104) and 4-thiopyrazolopyrimidine riboside (105) have antileishmanial activity because of their recognition as substrates by the nucleoside phosphotransferase in leishmania.

On the other hand, most of the parasitic protozoa examined, Trypanosoma (89), Crithidia (100), Leishmania (102), Entamoeba (110), Eimeria (108), Toxoplasma (109) and Plasmodium (97), appear to be able to synthesize the pyrimidine ring de novo. The exceptions however, may be the anaerobic flagellates, Trichomonas vaginalis (106) and Giardia lamblia (107). Another anaerobic flagellate, Tritrichomonas foetus remains to be examined. From the previous discussion we anticipate T. foetus to be incapable of both de novo purine and pyrimidine biosynthesis. The absence of both pathways and their probable reliance on exogenous sources for purine and pyrimidine requirments, should provide us with ample opportunities for chemotherapeutic attack. It is the aim of this project to identify potential targets

in the purine and pyrimidine metabolism of Tritrichomonas foetus for our rational approach to antiparasitic drug design.

Chapter 1

PYRIMIDINE METABOLISM IN TRITRICHOMONAS FOETUS

INTRODUCTION

The synthesis and salvage of pyrimidines represent an important and essential pathway for all organisms. These basic components are needed in the synthesis of both RNA and DNA. Mammalian sources rely on both the synthesis and salvage of pyrimidines. De novo synthesis begins with simple precursors, CO_2, glutamine and aspartate to form UMP (See Figure 1.1). UMP is then modified to form the pyrimidine nucleoside triphosphates required by the cell (UTP, CTP, dTTP, dCTP). These later reactions are catalyzed by the following enzymes: 1) kinases establish an equilibrium between UMP, UDP and UTP (in general the monophosphate, diphosphate and triphosphate), 2) CTP synthetase produces CTP from UTP, 3) Ribonucleotide reductase converts UDP and CDP to dUDP and dCDP, and 4) Thymidylate synthetase forms TMP from dUMP. The "dTMP synthesis cycle" has been a focal point in cancer chemotherapy. See Figure 1.2. Analogs of dihydrofolate , such as aminopterin and amethopterin (methotrexate), are potent inhibitors of dihydrofolate reductase and are used in the treatment of acute leukemia and choriocarcinoma. There are two enzymes primarily responsible for the salvage of pyrimidine bases. Both uridine and thymidine phosphorylase covert their respective bases into nucleosides. The salvage of nucleosides, uridine and thymidine, are facilitated by uridine and thymidine kinases, respectively. A summary of the nomen-

clature involved in mammalian pyrimidine interconversion and salvage is shown in Figure 1.3.

All parasitic protozoa examined to date, Trypanosoma (89), Crithidia (100), Leishmania (102), Entamoeba (110), Eimeria (108), Toxoplasma (109), and Plasmodium (97) appear to be able to synthesize their pyrimidines de novo. The evidence for this conclusion is derived mainly from studies of the composition of minimal defined media required to support the growth of these organisms. Additional evidence from the incorporation of exogeneorus radioactive bicarbonate and orotate into the pyrimidine rings and the presence of some of the enzymes involved in pyrimidine biosynthesis suggest the ability to form pyrimidines de novo. The exceptions however, may be the anaerobic flagellates. Hill et al (106) have shown that Trichomonas vaginalis lacks aspartate transcarbamoylase, dihyroorotase, dihydroorotate dehydrogenase and orotate phosphoribosyltransferase in its crude extract. Wang and Cheng (138) provided further evidence of the parasites lack of de novo pyrimidine synthesis and revealed a simple salvage pathway. Similarly, Giardia lamblia was found by Lindmark and Jarroll (107), to be incapable of incorporating aspartate or orotate into the cold trichloracetic acid-insoluble (nucleic acid) fraction and were unable to demonstrate the enzymes of the de novo pyrimidine synthesis pathway. This evidence indicates that both T. vaginalis and G. lamblia are unable to synthesize pyrimidines de novo. It also suggests that another closely related anaerobic flagellate, Tritrichomonas foetus, is likely incapable of de novo pyrimidine synthesis.

This chapter examines the pyrimidine synthetic capablity of T. foetus and also the trichomonads pyrimidine salvage pathways in the organism. Potential sites for antitrichomonal chemotherapeutic intervention will also be identified.

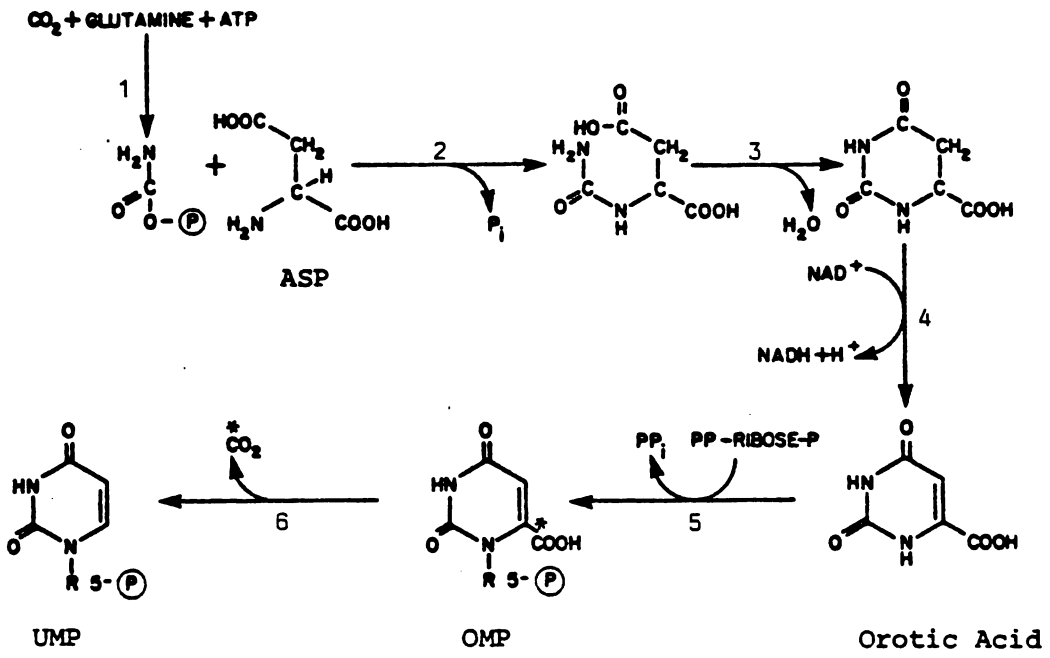

FIGURE 1.1. Pyrimidine de novo biosynthesis in mammals. Enzymes: 1, Carbamoyl phosphate synthetase; 2, Aspartate transcarbamoylase; 3, Dihydroorotase; 4, Dihydroorotate dehydrogenase; 5, Orotate phosphoribosyltransferase; 6, Orotidylic acid decarboxylase. PRPP, phosphoribosylpyrophosphate.

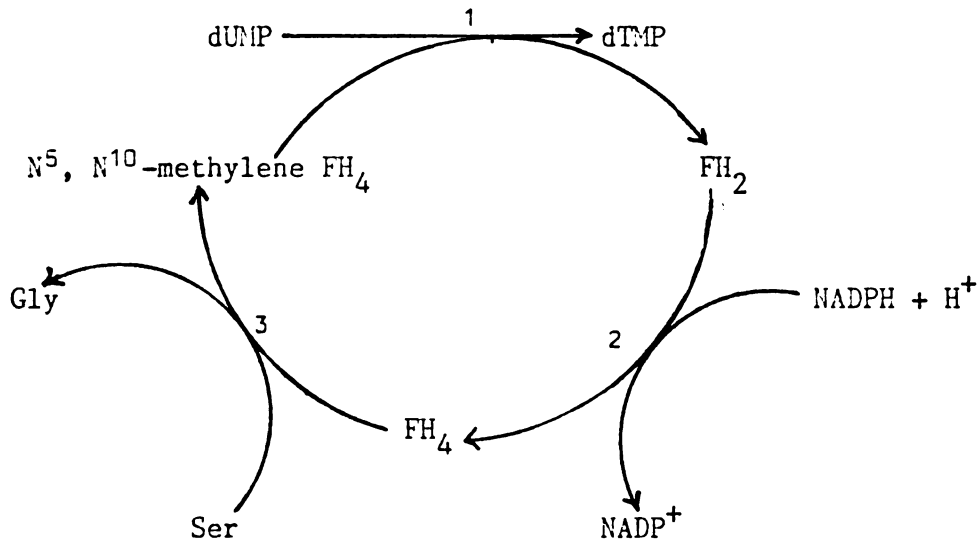

FIGURE 1.2. Thymidylate Synthase Cycle. Enzymes: 1, Thymidylate synthase; 2, Dihydrofolate reductase; 3, Serine transhydroxymethylase. FH_2, dihydrofolate; FH_4, tetrahydrofolate;.

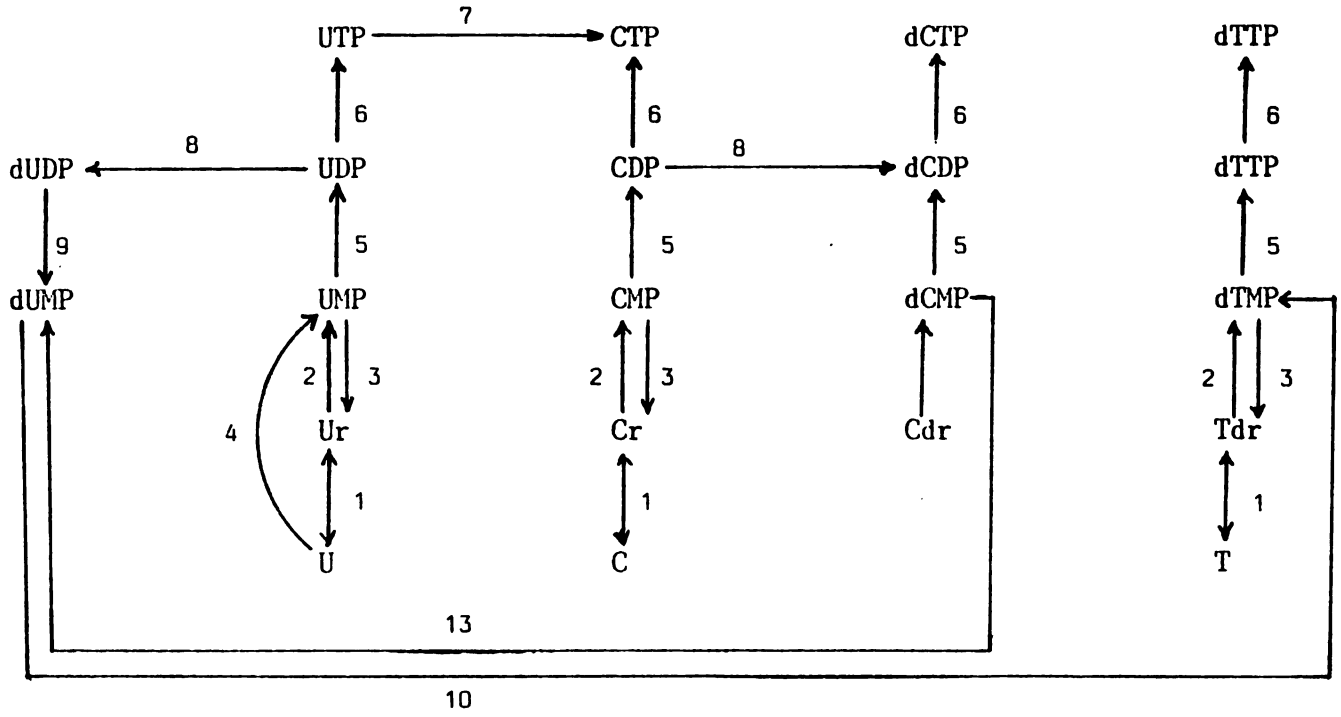

FIGURE 1.3. Enzymes involved in the salvage and interconversion of pyrimidines. Enzymes: 1, Nucleoside phosphorylase; 2, Nucleoside kinase; 3, NMP phosphatase; 4, Phosphoribosyltransferase; 5, NMP kinase; 7, CTP synthetase; 8, Ribonucleotide reductase; 9, NDP phosphatase; 10, Thymidylate synthase; 11, Cytidine deaminase; 12, Deoxycytidine kinase; 13, Deoxycytidylate aminohydrolase. U, uracil; Ur, uridine; C, cytosine; Cr, cytidine; Cdr, deoxycytidine; T, thymine; Tdr, thymidine.

Materials and Methods

CULTURES

T. foetus, strain KV_1, was cultivated in Diamonds TYM medium pH 7.2 supplemented with 10% heat inactivated horse serum, 1% antibiotic/antimycotic mixture at 37°C (114). Cells in midlogarithmic phase of growth were used for all the studies. See appendix for more details.

CHEMICALS

Radiolabels; [2-^{14}C]uracil (55.2 mCi/mmole), [6-^{14}C]orotic acid (61.0 mCi/mmole), [methyl-^{14}C]thymine (54.0 mCi/mmole), [2-^{14}C]cytosine (61.0 mCi/mmole), $NaH^{14}CO3$ (30.2 mCi/mmole), [U-^{14}C]L-aspartate (219 mCi/mmole), [methyl-^{3}H]thymidine (20.0 Ci/mmole), [6-^{3}H]uracil, [5,6-^{3}H]uridine (49.4 mCi/mmole) and [5-^{3}H]cytidine (50.1 mCi/mole) were purchased from New England Nuclear, Amersham or ICN. Aquasol 2 was obtained from New England Nuclear also. Enzyme samples were purchased from Sigma. All other chemicals used were of the highest purities commercially available.

PRECURSOR INCORPORATION INTO THE NUCLEOTIDE POOL

Midlogarithmic phase of growth cells were collected by centrifugation. The cells were washed and resuspended in 30 mM NaH_2PO_4, 22 mM NaCl and 20 mM glucose (PSG) at a final cell concentration of 10^8 cells/ml. Radiolabeled substrate, 3 microcurie, was added to the cell

suspension and incubated at 37°C. Nucleotides were extracted by the procedure of Wang and Simashkevich (98). Aliquots were removed at various times and acidified with perchloric acid to stop the reaction. After 30 minutes in an ice bath, the precipatate was removed by centrifugation and the supernatant neutralized with KOH. The sample was then filtered through PEI-cellulose (32 mg) loaded upon a GF/B filter equilibrated with 5.0 mM NH_4OAc pH 5.0. The filter was washed two times with 10 ml of 5.0 mM NH_4OAC pH 5.0 buffer and the PEI-adsorbed radioactivity was determined with a Beckman LS-3133T liquid scintillation counter. In pulse-chase experiments, the cell suspension was washed free of radioactivity and resuspended in PSG with unlabeled substrate. The incubation was then continued with aliquots being removed and treated like before.

HPLC

Nucleotides were identified by ion-exchange HPLC using Model 110A pumps and Model 420 controller. Samples were loaded onto an Ultrasil AX (10 micron) 4.6 x 250 mm column, equilibrated with 7 mM KH_2PO_4 buffer pH 3.8. The nucleotides were eluted by a programed gradient from 7 mM KH_2PO_4 pH 3.8 to 250 mM KH_2PO_4, 500 mM KCl pH 4.5. Nucleosides and bases were identified by reverse phase chromatography with an ODS-Ultrasphere (5 micron) 4.6 x 250 mm column. The column was equilibrated with 7 mM KH_2PO_4 pH 6.0 and samples were eluted by a gradient from 7 mM KH_2PO_4 pH 6.0 to 100% acetonitrile. The effluent was monitored at 254 nm in a Beckman 160 UV absorbance detector and radioactivity determined in a Flo-one radioactive flow detector

(Radiomatic, Tampa, Fl.). The outputs of both detectors were recorded in a Kipp and Zonen BD 41 dual chart recorder and analyzed with a Hewlett-Packard 3390A integrator.

PRECURSOR INCORPORATION INTO NUCLEIC ACID

The procedure used was a modification of that used by Morse et al (137). T. foetus cells, after 2 hours incubation with radiolabeled substrate, were washed with PSG and dissolved in 0.25 M NaOH containing calf thymus DNA at 0.5 mg/ml and unlabeled precursor at 0.5 mg/ml. The solution was incubated overnight at 37°C. The DNA and protein were precipitated with cold 5% trichloroacetic acid, washed and collected on a 0.45 micron Millipore cellulose nitrate filter. Radioactivity associated with the hot 5% trichloroacetic acid pellets were considered to be due to protein. Radioactivites were then measured by LSC.

Precursor incorporation into RNA was determined by dissolving cells in a solution containing sodium dodecyl sulfate (SDS) at 10 mg/ml, E. coli ribosomal RNA at 0.5 mg/ml and unlabeled precursor at 0.25 mg/ml. Cold 5% trichloroacetic acid was immediatly added to the solution and then allowed to sit overnight. The resulting pellet was washed and treated with 0.3 M KOH for 16 hours at 37°C. The solution was neutralized with 0.3 M perchloric acid and radioactivity in the supernatant fraction determined by LSC.

ENZYME ASSAYS

Phosphoribosyltransferase- Activities were measured by a modified procedure of Schmidt et al (136). Phosphoribosyltransferase activities were determined in 100 mM Tris-HCl pH 7.8, 7 mM $MgCl_2$, 1.0 mM 5-phosphoribosyl-1-pyrophosphate (PRPP), 0.05 mg/ml bovine serum albumin (BSA) and 0.02 mM radioactive substrate. The reaction mixture was incubated with enzyme at 37°C for 10 minutes and terminated by the addition of ice cold 2 mM unlabeled substrate. The resulting solution was filtered through PEI-cellulose GF/B filter and radioactivity measured by LSC.

Nucleoside kinase- Nucleoside kinase activities were assayed by the method of Nelson et al (103) in 100 mM Tris-HCl pH 7.5, 20 mM ATP, 20 mM $MgCl_2$, 80 mM phosphoenolpyruvate, 40 units/ml pyruvate kinase and 1.5 mM radiolabeled nucleoside substrate. The reaction mixture was incubated with enzyme for 10 minutes at 37°C and the PEI-adsorbable counts determined by LSC.

Nucleoside phosphotransferase- The assay procedure was the same as for the kinase except for that the buffer was 100 mM NaOAc pH 5.4 with 1.0 mM radiolabeled nucleoside and that p-nitrophenyl phosphate (10 mM) was used as the phosphate donor.

Other enzymes- Nucleoside phosphorylases were assayed in 50 mM Tris-HCl pH 7.5, 1.0 mM radiolabeled nucleoside and 10 mM KH_2PO_4 pH 7.5 . Deaminase activities were determined in 50 mM Tris-HCl pH 7.5 and 0.2 mM radiolabeled substrate. Reactions were run at 37°C for various times up to 60 minutes and terminated by $HClO_4$/KOH treatment.

The products of the reaction were analyzed by reverse phase HPLC. Thymidylate synthetase was assayed by the method of Santi and McHenry (133) using 5-flurodeoxy-[^{3}H]uridine monophosphate (18Ci/mmole). Dihydrofolate reductase reductase was assayed spectrophotometrically by the procedure of Hillcoat et al (134).

PREPARATION OF T. foetus EXTRACTS

Midlogarithmic phase cells were washed and resuspended in 1 volume of 25 mM Tris-HCl pH 7.2, 20 mM KCl, 6 mM $MgCl_2$ and 1 mM DTT. The cell suspension was homogenized with a Brinkman Polytron at 4°C. The cell homogenate was centrifuged at 10,000g for 30 minutes to remove cell debris and then at 100,000g for 1 hour to separate soluble and pelletable fractions. Protein concentrations were determined by method of Bradford (135) using BSA as standard.

RESULTS

De Novo Pyrimidine Nucleotide Synthesis

Radiolabeled bicarbonate, L-aspartate and orotic acid was not incorporated into the nucleotide pool after 60 a minute incubation with T. foetus cells at 37°C, as analyzed by HPLC.

Incorporation of radiolabeled precursors of de novo pyrimidine biosynthesis into nucleic acids was also examined by incubation of T. foetus with a radiolabeled precursor over a 2 hour period (Table 1.1). There was no detectable incorporation of radiolabeled bicarbonate, L-aspartate or orotic acid into RNA or DNA. L-Aspartate was incorporated only to a limited extent into T. foetus protein fraction. T. foetus extracts were found to be devoid of any orotate phosphoribosyltransferase (Table 1.2).

Salvage of Pyrimidines and Pyrimidine Nucleotides

The uptake and salvage of exogeneous pyrimidine bases and nucleosides are shown in Figure 1.4. Uracil is by far the most readily incorporated by T. foetus into the nucleotide pool. The uptake of uracil has an initial rate of 1.7 pmole/min-10^6 cells while that for uridine and cytidine were incorporated at 1/10 the rate of uracil. Cytosine and thymine are not incorporated at all while the uptake of thymidine is at a very low rate, about 1/100 that of the uracil rate. Results of competition experiments examining the incorporation of a radiolabeled substrate in the presence of a 10-fold higher concentration of unlabeled substrate is shown in Figure 1.5. The results

indicate; 1) uracil incorporation is inhibited by uracil and uridine, 2) uridine incorporation is inhibited by uracil and uridine, 3) cytidine incorporation is inhibited by uracil, uridine and cytidine and 4) thymidine is only inhibited by thymidine. The uptake of uracil, uridine, cytidine and thymidine is unaffected by a 10-fold excess of thymine or cytosine.

The incorporation of radiolabeled thymidine, uracil and uridine into T. foetus nucleic acids were also examined (Table 1.1). Both labeled uracil and uridine were found associated only in the RNA fraction while labeled thymidine was found only with the DNA fraction.

HPLC Analysis of the Nucleotide Pool

T. foetus cells were labeled with pyrimidines and pyrimidine nucleosides, washed free of label, and then chased by incubation with unlabeled substrate. The cells were lysed, nucleotides extracted and analyzed by HPLC (See Figures 1.6-1.9). The figures illustrate: 1) thymidine is converted to TMP, TDP and TTP; with chasing decreasing all three levels; 2) uracil and uridine are converted to UMP, UDP-hexose, UDP and UTP; with a substantial decrease in UMP upon chasing and 3) cytidine was found with CMP, UMP, UDP-hexose, UDP, CDP, UTP and CTP, then chasing reduces UMP, CMP, CDP, CTP to a large extent.

Enzyme Profiles

After a preliminary spin at 10,000g, the crude extract of T. foetus was centrifuged at 100,000g to separate pelletable (membrane associated) enzyme activities from the supernatant (cytosol associat-

ed) activities. The pyrimidine salvage enzyme profiles are shown in Table 1.2. There were no detectable dihydrofolate reductase or thymidylate synthetase activity. The only activity found for thymidine salvage was a 100,000g sedimentable phosphotransferase. The thymidine phosphotransferase utilized p-nitrophenyl phosphate, AMP, GMP, UMP, and CMP equally well as phosphate donors. Sugar phosphates such as fructose 1,6-diphosphate, were not recognized as substrate phosphate donors. Guanosine was shown to be a noncompetitive inhibitor of thymidine phosphotransferase while uridine and cytidine had no effect on enzyme activity.

Drug Testing

T. foetus was cultivated in TYM in the presence of several known inhibitors of thymidylate synthetase, (0.1 mM azomycin riboside, 0.1 mM 5-bromovinyldeoxyuridine) and of dihydrofolate reductase (0.5 mM methotrexate, 0.25 mM pyrimethamine, 0.5 mM trimethoprim). The drugs were without any effect on the growth of the trichomonad during a 24 hour period. 5-Flourouracil, a potent inhibitor of thymidylate synthetase, inhibited T. foetus growth. The incorporation of thymidine was not effected by 5-F-uracil but uracil, uridine and cytidine uptake were inhibited. The use of 5-F-[6-^{3}H]uracil (32.8 mCi/mmole) as a substrate by T. foetus cells revealed, after nucleotide extraction and HPLC analysis, the emergence of 3 radioactive peaks corresponding to the nucleoside mono-, di- and triphosphate of 5-F-uracil (See Chapter 3).

TABLE 1.1 Incorporation of radiolabeled substrates into T. foetus nucleic acids.

Substrate	Conc., mM	Label mCi/ mmol	Incorporation, pmol per 10^6 cells DNA fraction	RNA fraction
$H^{14}CO3^-$	2.0	58.0	<0.05 (3)	<0.05 (3)
[^{14}C]Aspartate	6.8	14.8	<0.05 (3)	<0.05 (3)
[5-^{14}C]Orotate	2.5	15.1	<0.05 (3)	<0.05 (3)
[methyl-^{3}H]-Thymidine	1.6	61.9	0.64 ± 0.11 (6)	<0.05 (3)
[6-^{3}H]Uracil	2.2	40.6	<0.05 (6)	5.77 ± 0.79 (4)
[6-^{3}H]Uridine	3.3	30.1	<0.05 (6)	5.30 ± 1.60 (3)

Incorporation was determined after 2 hr of incubation. Conc., concentration. Numbers in parentheses represent numbers of experiments. Results represent mean or mean ± SEM.

TABLE 1.2. Pyrimidine salvage enzyme activities in extracts of T. foetus.

Enzyme type	Substrate	Activity (nmol/min)/mg of protein	
		Supernatant	Pellet
Phosphoribosyl-transferase	Uracil	0.516 ± 0.004	<0.001
	Cytosine	<0.001	<0.001
	Thymine	<0.001	<0.001
	Orotate	<0.001	<0.001
Kinase	Uridine	<0.001	<0.001
	Cytidine	<0.001	<0.001
	Thymidine	<0.001	<0.001
Phosphotransferase	Uridine	<0.001	0.254 ± 0.050
	Cytidine	<0.001	0.039 ± 0.003
	Thymidine	<0.001	0.144 ± 0.022
Phosphorylase	Uridine	1.64 ± 0.02	<0.001
	Cytidine	<0.001	<0.001
Deaminase	Cytosine	<0.001	<0.001
	Cytidine	1.84 ± 0.02	<0.001
Dihydrofolate reductase	Dihydrofolate	<0.01	<0.01
Thymidylate synthetase		<0.0001*	<0.0001*

Each enzyme activity value is derived from three independent assays. Results represent mean or mean ± SEM.

*Binding value expressed as nmol of 5-fluorodeoxyuridine monophosphate bound per mg of protein.

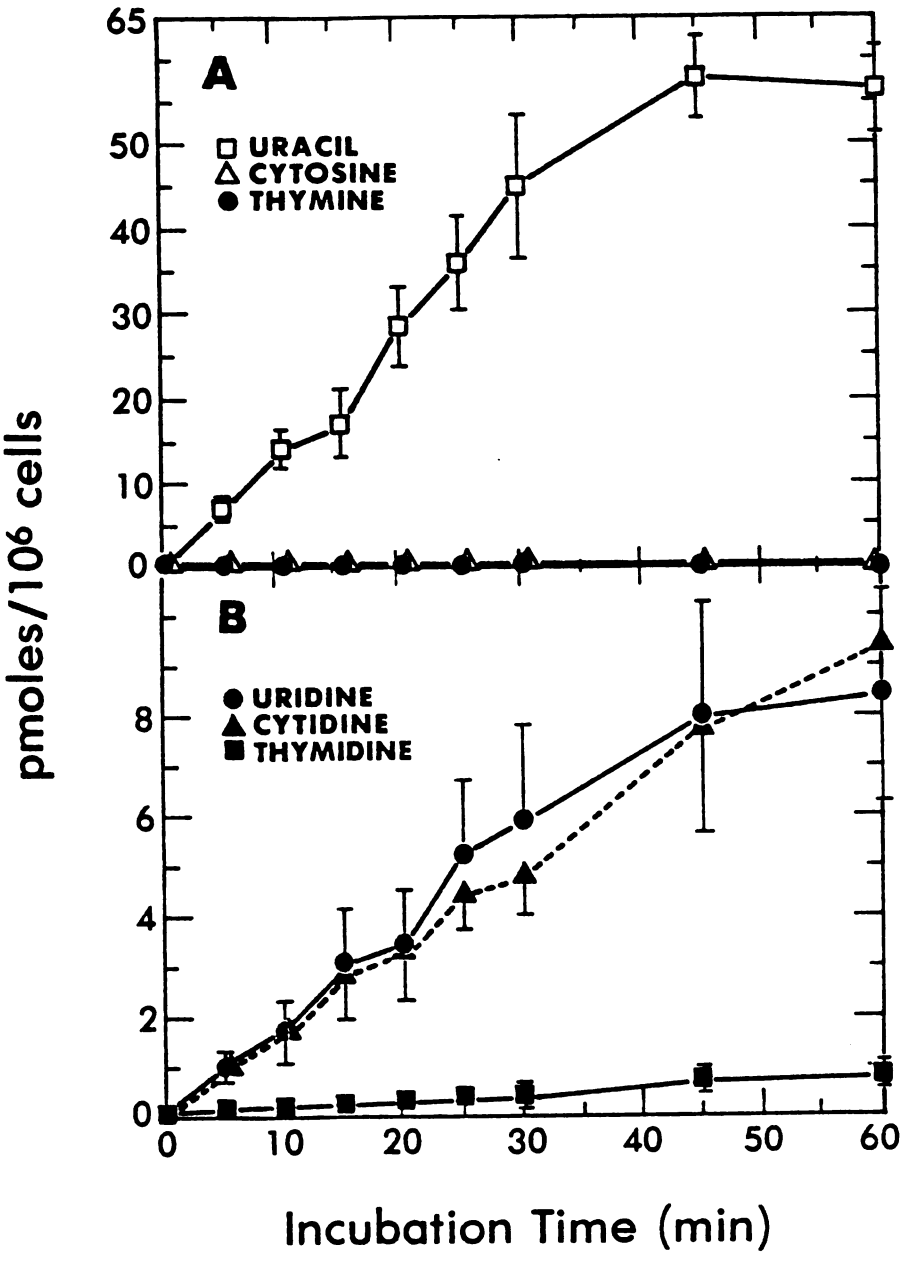

FIGURE 1.4. Substrate incorportion into T. foetus nucleotides. Substrates were used at 20 μM. (A)□, [2-^{14}C]uracil (58 mCi/mmol); △, [2-^{14}C]cytosine (61 mCi/mmol);●, [methyl-^{14}C]thymine (54 mCi/mmol). (B)●, [5,6-^{3}H]uridine (50 mCi/mole);▲, [5-^{3}H]cytidine (40 mCi/mmol);■ [methyl-^{3}H]thymidine (47 mCi/mmol).

FIGURE 1.5. Incorporation of radiolabeled uracil (A), uridine (B), cytidine (C), and thymidine (D) into T. foetus nucleotides in the presence of a 10-fold excess of unlabeled substrate. □, No unlabeled substrate; ○, unlabeled uracil; △, unlabeled uridine; ▽, unlabeled cytidine; ◇, unlabeled thymidine.

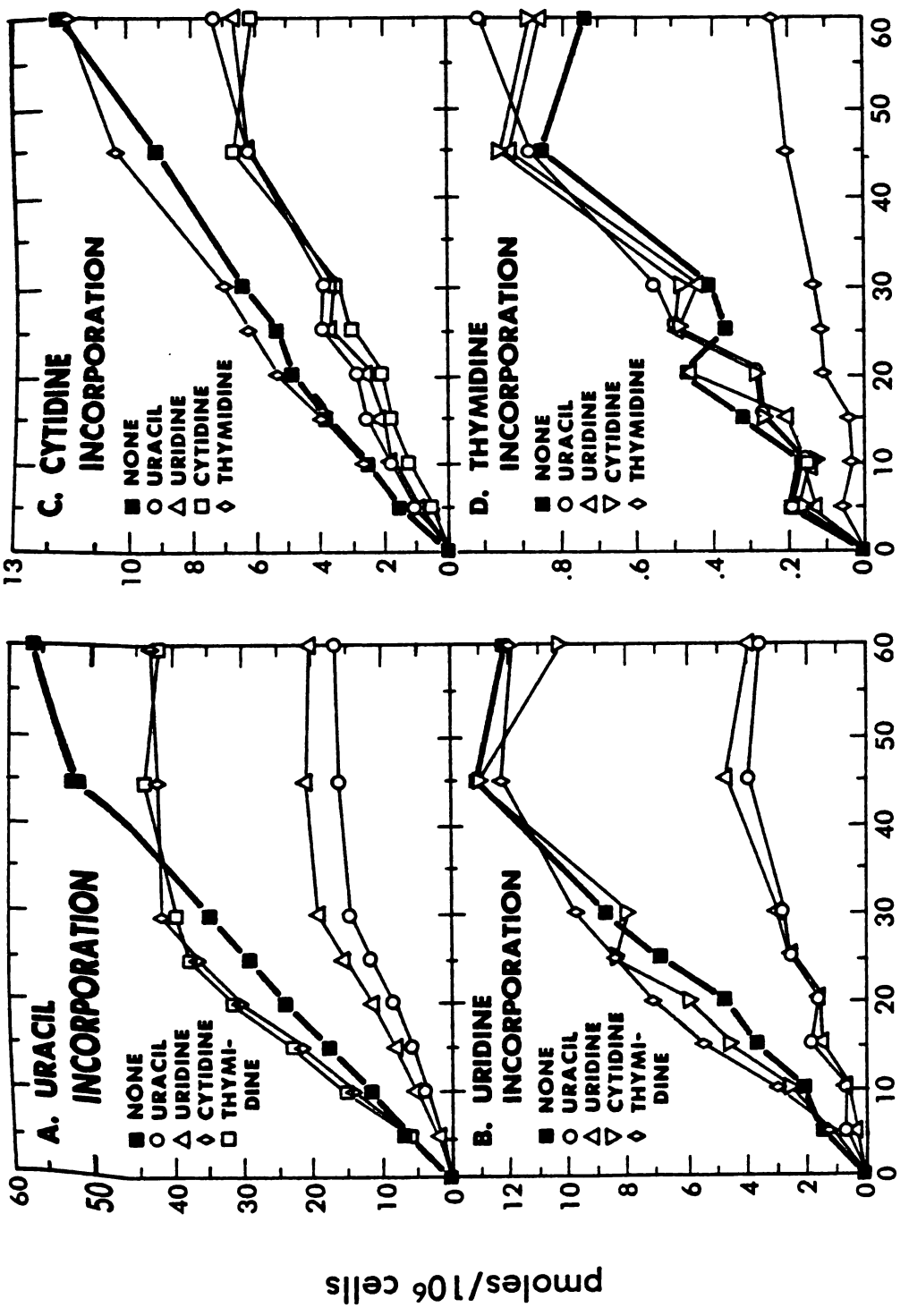
A. URACIL INCORPORATION
B. URIDINE INCORPORATION
C. CYTIDINE INCORPORATION
D. THYMIDINE INCORPORATION
NONE
URACIL
URIDINE
CYTIDINE
THYMI-DINE
THYMIDINE
pmoles/10⁶ cells
Incubation Time (min)

FIGURE 1.5.

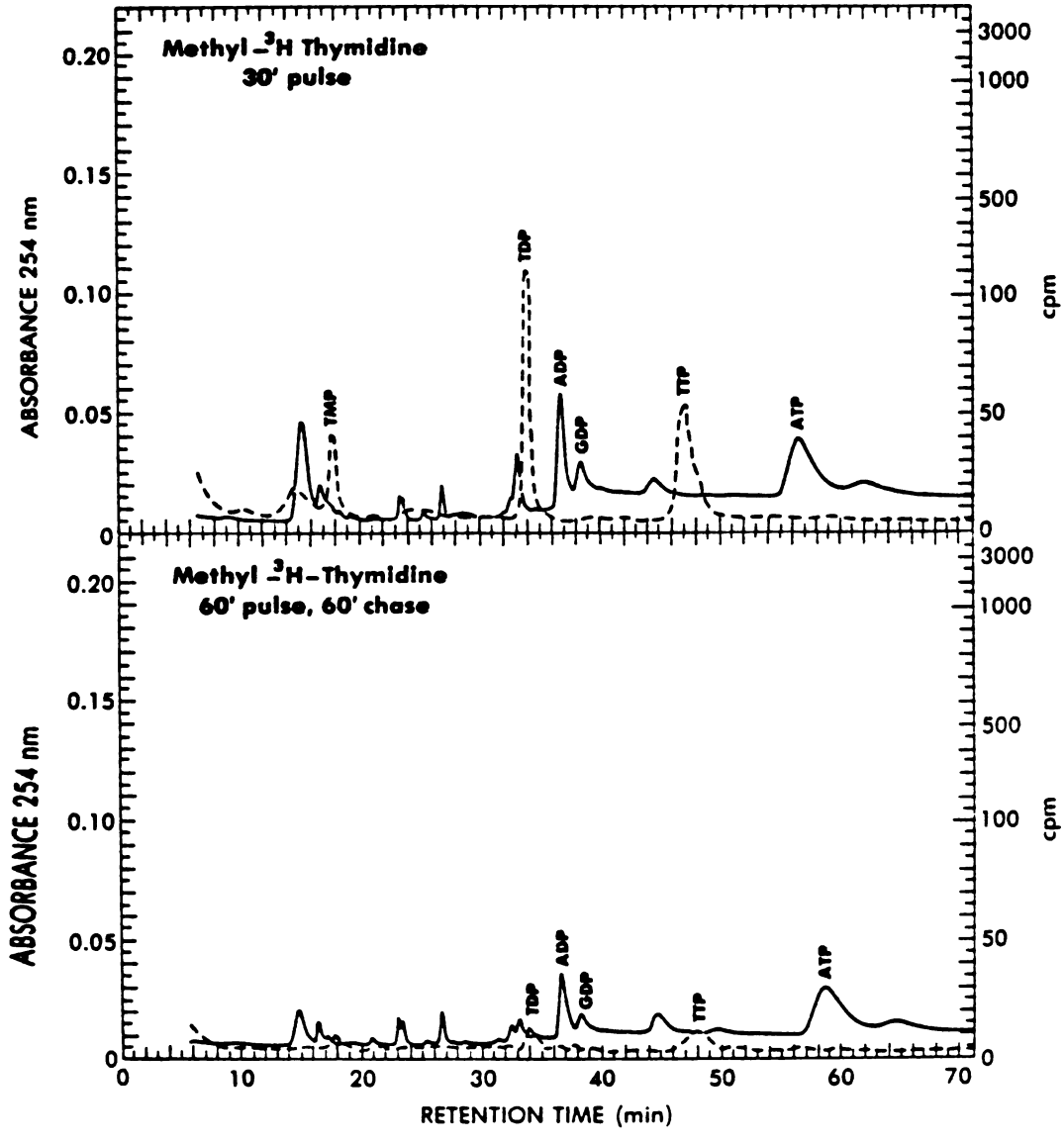

FIGURE 1.6. HPLC analysis of T. foetus nucleotides labeled for 30 minutes with 20 μM [methyl-^{3}H]thymidine (500mCi/mmol) (A) and labeled for 60 minutes and then chased for 60 minutes with 20 μM unlabeled thymidine (B). ——, A_{254}; - - - -, radioactivity.

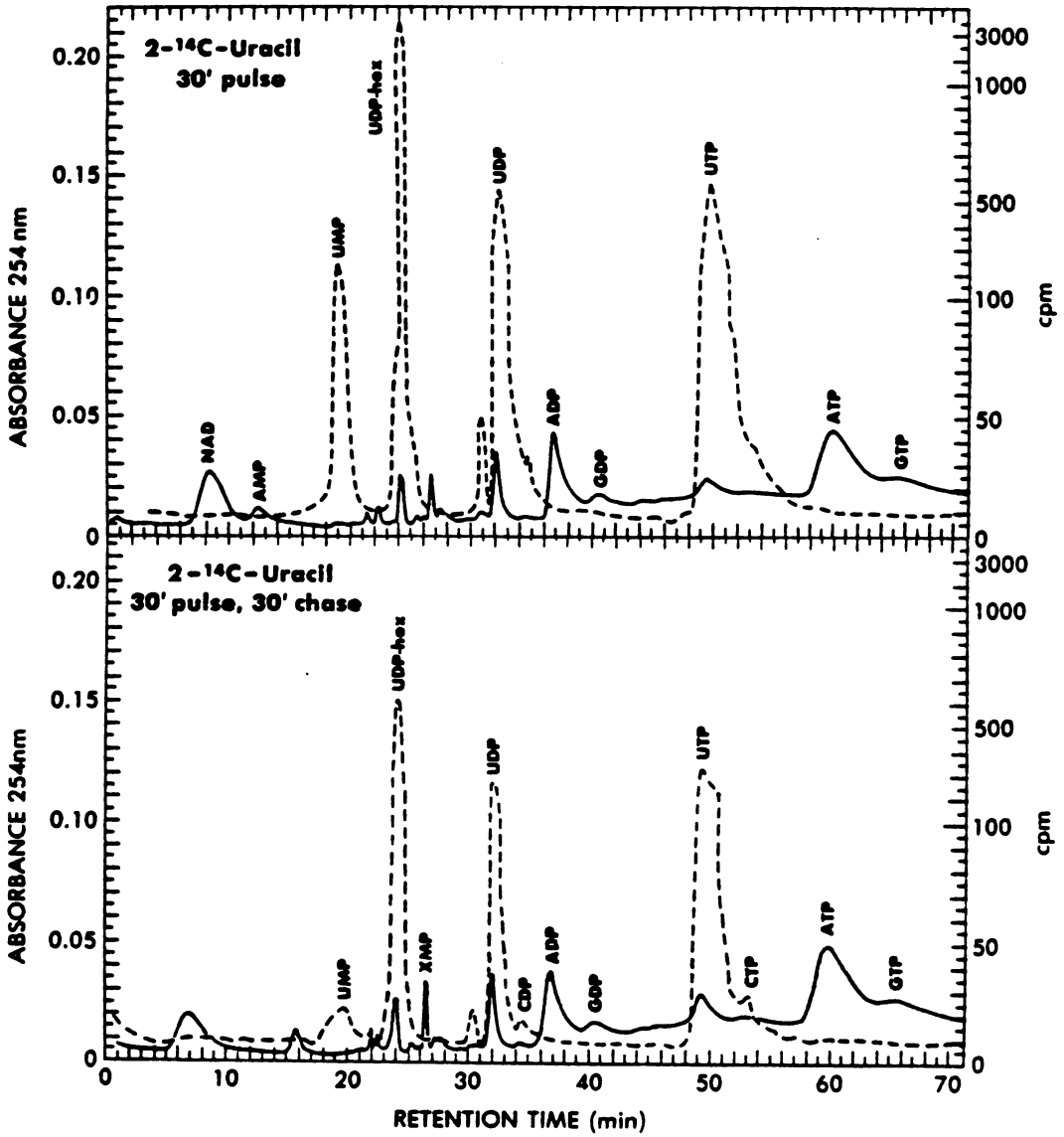

FIGURE 1.7. HPLC analysis of T. foetus nucleotides labeled for 30 minutes with 20 μM [2-^{14}C]uracil (58mCi/mmol) (A) and labeled for 30 minutes and then chased for 30 minutes with 20 μM unlabeled uracil (B). ——, A_{254}; ---- , radioactivity.

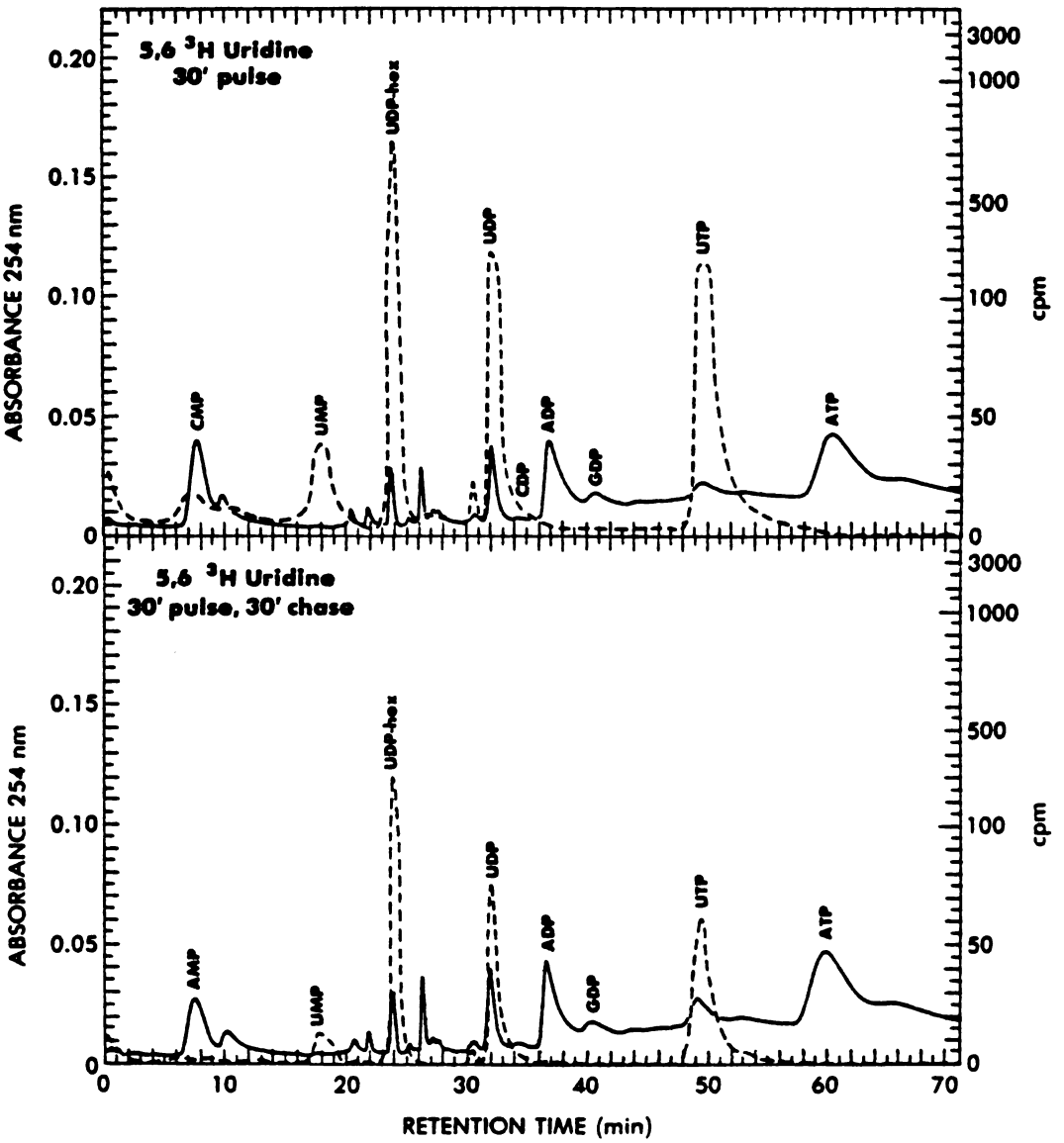

FIGURE 1.8. HPLC analysis of T. foetus nucleotides labeled for 30 minutes with 20 μM [5,6-^{3}H]uridine (49.4 mCi/mmol) (A) and labeled for 30 minutes and then chased for 30 minutes with 20 μM unlabeled uridine (B). ——, A_{254}; - - - -, radioactivity.

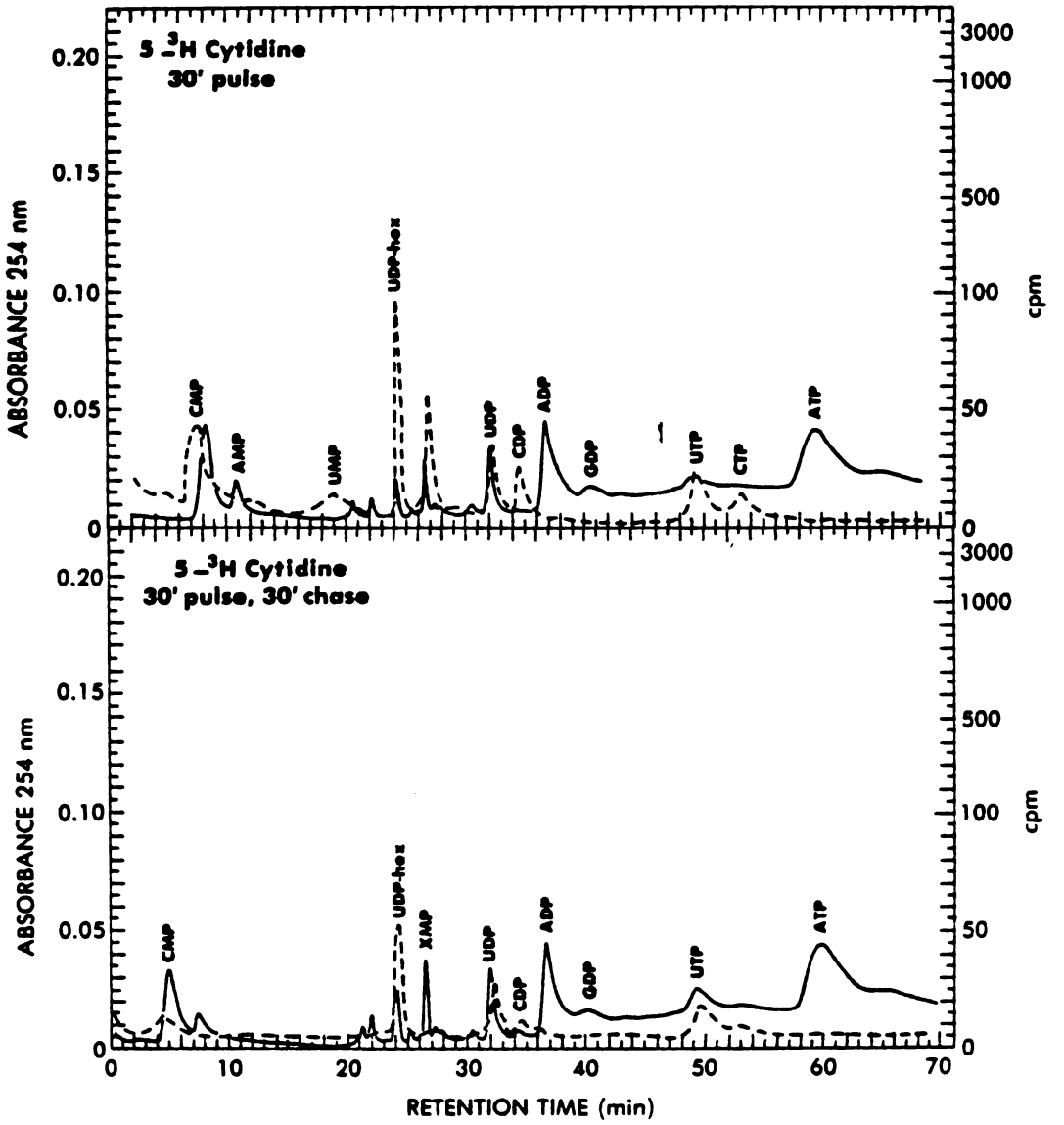

FIGURE 1.9. HPLC analysis of T. foetus nucleotides labeled for 30 minutes with 20 μM [5-^{3}H]cytidine (500mCi/mmol) (A) and labeled for 30 minutes and then chased for 30 minutes with 20 μM unlabeled cytidine (B). ——, A_{254}; -----, radioactivity.

DISCUSSION

Tritrichomonas foetus does not incorporate exogeneous bicarbonate, aspartate or ortate into its nucleotide pool or nucleic acids. This and the absence of orotidylate phosphoribosyltransferase (OPRTase) activity in crude extracts indicates that the parasite is incapable of de novo pyrimidine biosynthesis. This conclusion is also supported by the requirement of preformed pyrimidines in minimal defined media (118) and the absence of activities of de novo pyrimidine synthesis enzymes (139).

Examination of the trichomonads salvage pathway reveals that uracil and thymidine are used to fulfill the majority of the parasites pyrimidine requirements. The absence of thymidylate synthetase and dihydrofolate reductase activities in crude extracts, the inability of uracil to incorporate into DNA and of thymidine to incorporate into RNA, the lack of effect of potent thymidylate synthetase and dihydrofolate reductase inhibitors on T. foetus growth and the nucleotide pool evidence showing the absence of TMP formation from UMP indicates that T. foetus is incapable of forming TMP and is reliant upon thymidine salvage. This evidence also indicates that the uptake of uracil and thymidine occurs by two discrete and independent pathways. Thymidine phosphotransferase is responsible for the salvage of thymidine to form TMP while uracil phosphoribosyltransferase (UPRTase) converts uracil to UMP. Thymidine phosphotransferase is a unique and key enzyme providing for the parasites entire thymidine requirement.

Calculations indicate that the observed specific activity of thymidine phosphotransferase can more than account for the rate of thymidine incorporation into the nucleotide pool of T. foetus. The enzyme is sedimentable and utilizes several nucleoside 5'-monophosphates as well as p-nitrophenylphosphate as phosphate donor for thymidine. The same pelletable material containing thymidine phosphotransferase also contained guanosine phosphotransferase (See Chapter 2). It is not unlikely that GMP may be the natural phosphate donor for thymidine phosphotransferase and that the utilization of a purine nucleotide in a pyrimidine pathway may serve to balance the formation of pyrimidine and purine nucleotides.

The salvage of cytidine and uridine occurs most likely by prior conversion to uracil via cytidine deaminase and uridine phosphorylase, respectively, and then becomes incorporated in the trichomonads nucleotide pool with the aid of UPRTase. The importance of UPRTase is exemplified by the requirment of uracil to support the growth of T. foetus (118) and the inhibition of in vitro growth by 5-F-uracil (a moderate competive inhibitor of T. foetus UPRTase). It is yet unclear whether the inhibition of UPRTase by 5-F-uracil or its metabolites is/are responsible for the observed inhibition of growth. The UPRTase in T. foetus is different than that from mammalian sources in that it does not exhibit any OPRTase activity (141). The pyrimidine salvage network of Tritrichomonas foetus is summarized in Figure 1.10.

The absence of thymidylate synthetase and dihydrofolate reductase activities and the inability to perform de novo pyrimidine synthesis

may be not unique to T. foetus but perhaps may be a common deficiency in anaerobic parasites. Both Trichomonas vaginalis (138) and Giardia lamblia (140) are insensitive to millimolar concentrations of potent antifolates or thymidylate synthetase inhibitors such as methotrexate, pyrimethamine, trimethoprim and 6-azauridine. T. vaginalis, like T. foetus, exhibits a simple although different network of pyrimidine salvage. T. vaginalis incorporates uridine, cytidine and thymidine into its nucleotide pool via uridine, cytidine and thymidine phosphotransferase, respectively (138). Detailed knowledge on pyrimidine salvage in G. lamblia is not yet available, but preliminary findings suggest a similar network as in T. vaginalis.

Tritrichomonas foetus is a unique parasite in that it is unable to form pyrimidines de novo and lacks thymidylate synthetase and dihydrofolate reductase. The deficiencies of parasites in pyrimidine metabolism and reliance upon exogeneous pyrimidines has created two potential sites for chemotherapeutic attack. It is easy to envision that inhibition of either uracil phosphoribosyltransferase or thymidine phosphotransferase may lead to inhibition of T. foetus growth.

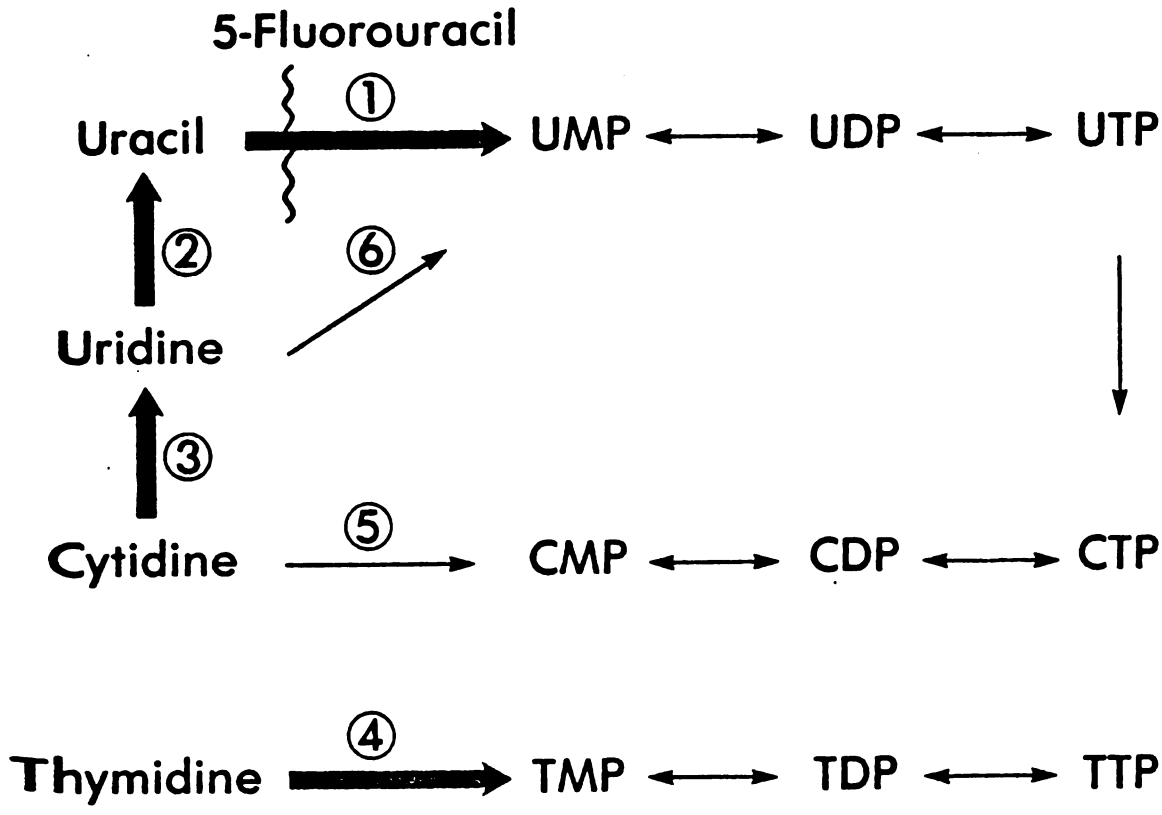

FIGURE 1.10. Pyrimidine salvage pathways in T. foetus. 1, Uracil phosphoribosyltransferase; 2, uridine phosphorylase; 3, cytidine deaminase; 4, thymidine phosphotransferase; 5, cytidine phosphotransferase; 6, uridine phosphotransferase.

CHAPTER 2

PURINE METABOLISM IN TRITRICHOMONAS FOETUS

INTRODUCTION

There are two general pathways available for the synthesis of purine nucleotides; 1) de novo synthesis assembles the purine ring on ribose-5-phosphate and 2) salvage pathways utilizing preformed purines or purine nucleosides for the formation of purine nucleotides. In mammals, the liver is the major site of de novo purine synthesis secreting synthesized purines and purine nucleosides to be salvaged by other tissues. The purine ring is assembled on ribose-5-phosphate from glycine, formate, CO_2, glutamine and aspartate (Figure 2.1). The salvage of purines in mammals is accomplished by kinases, phosphoribosyltransferases, deaminases and phosphorylases. A complete scheme for salvage and interconversion of purines is shown in figure 2.2.

All parasitic protozoa examined to date including, Trypanosoma cruzi (89), Leishmania donovani (96), Plasmodium lophurea (97), Eimeria tenella (98), Trichomonas vaginalis (99) and Giardia lamblia (144) are incapable of de novo purine nucleotide biosynthesis. The evidence for this conclusion has come mainly from studies on the chemical composition of minimal defined media and the failure of glycine or formate to incorporate into the parasite nucleic acids. Absence of the ability to synthesize purines de novo implies dependence on a salvage pathway. This dependence on the salvage of purines might be expected to render the parasite more susceptable to

the cytotoxic action of purine analogues. Allopurinol, a hypoxanthine analogue recognized by the parasitic salvage enzymes, exhibits anti-trypanosomal and antileishmanial activities (101,102). Likewise, the purine nucleoside analogues, allopurinol riboside (103), formycin B (104) and 4-thiopyrazolopyrimidine riboside (105) have anti-leishmanial activity because of their recognition as substrates by the nucleoside phosphotransferase in leishmania.

Recent evidence on the pyrimidine metabolism of T. foetus (142) indicated the absence of dihydrofolate reductase. Lack of this enzyme and the previous history of other protozoa examined, suggest that this parasite is also deficient in de novo purine nucleotide biosynthesis. In this chapter we propose to examine the purine nucleotide biosynthesis and purine salvage in Tritrichomonas foetus and identify potential targets for chemotherapeutic attack.

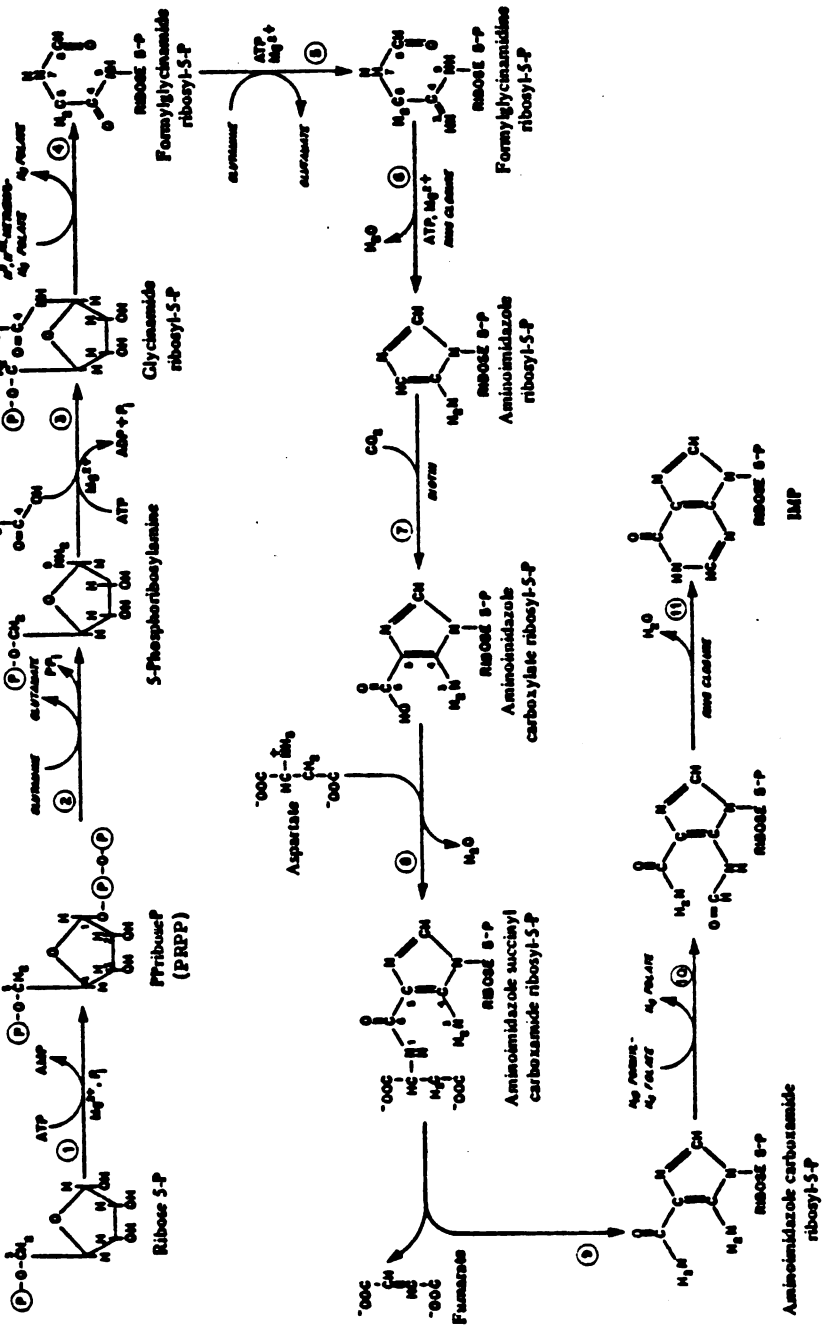

FIGURE 2.1. Purine de novo synthesis in mammalian cells.

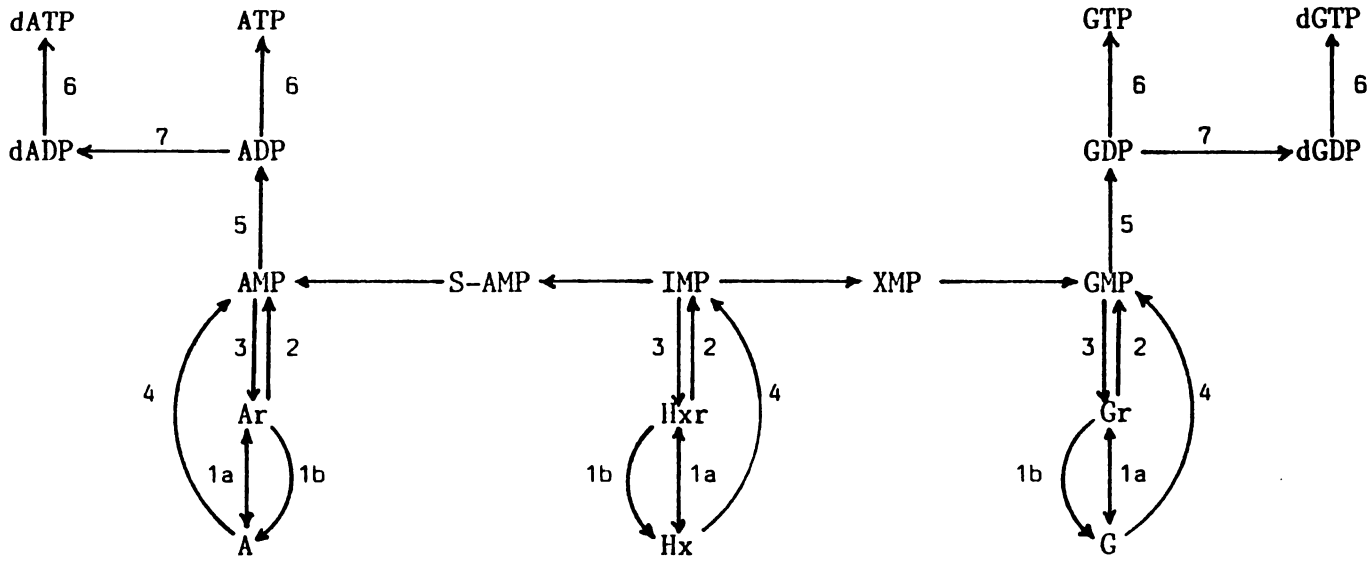

FIGURE 2.2. Salvage and interconversion of purines. Enzymes: 1a, nucleoside phosphorylase; 1b, nucleoside kinase; 2, nucleoside kinase; 3, nucleotide phosphatase; 4, phosphoribosyltransferase; 5, NMP kinase; 6, NDP kinase; 7, ribonucleotide reductase; 8, adenosine deaminase. IMP, inosine monophosphate; Hxr, inosine; Hx, hypoxanthine; Ar, adenosine; A, adenine; Gr, guanosine; G, guanine.

MATERIALS AND METHODS

CULTURES

T. foetus, strain KV_1, was cultivated in Diamonds TYM medium pH 7.2 supplemented with 10% heat inactivated horse serum and 1% antibiotic/antimycotic mixture at 37°C (114). See Chapter 1 for details.

CHEMICALS

[8-^{14}C]Hypoxanthine (51.1 mCi/mmol), [8-^{14}C]adenine (49.1 mCi/mmol), [8-^{14}C]xanthine (41.0 mCi/mmol), [8-^{14}C]guanine (56.7 mCi/mmol), [8-^{14}C]inosine (112.0 mCi/mmol), [2,8-^{3}H]adenosine (49.4 mCi/mmol), [8-^{3}H]guanosine (45.7 mCi/mmol), [^{14}C]formate (2.43 mCi/mmol), [^{14}C]bicarbonate (58.0 mCi/mmol) and [2-^{14}C]glycine were purchased from New England Nuclear, Amersham or ICN. All other chemicals were of the purest grade available.

PRECURSOR INCORPORATION INTO THE NUCLEOTIDE POOL

Midlogarithmic phase of growth cells were washed and resuspended in PSG. Radiolabeled substrate, 3 microcurie, was added to the cell suspension and incubated at 37°C. Nucleotides were extracted and the PEI-adsorbable radioactivity determined. See Chapter 1 for details.

HPLC

Nucleotides were identified by ion-exchange HPLC using an

Ultrasil-AX (10 micron) 4.6 x 250 mm column. Nucleosides and bases were identified by reverse phase chromatography with an ODS-Ultrasphere (5 micron) 4.6 x 250 mm column. See Chapter 1 for details.

ENZYME ASSAYS

Phosphoribosyltransferase activities were measured by a modified procedure of Schmidt et al (136). Nucleoside kinase activities were assayed by method of Nelson et al (103). Nucleoside phosphotransferase activities were measured simarily to the nucleoside kinase procedure. Nucleoside phosphorylase activities and deaminase activities were assayed as described in Chapter 1. See Chapter 1 for details.

PREPARATION OF T. foetus EXTRACT

Midlogarithmic phase cells were washed and homogenized at 4°C. The cell homogenate was centrifuged at 10,000g and then 100,000g. Protein concentrations were determined by method of Bradford (135) using BSA as standard.

RESULTS

DE NOVO PURINE NUCLEOTIDE SYNTHESIS

Mid log phase T. foetus cells (10^8 cells/ml) were incubated with 2.0 mM of [^{14}C]formate (2.43 mCi/mmol), [^{14}C]bicarbonate (58.0 mCi/mmol) or [2-^{14}C]glycine (37.69 mCi/mmol) in phosphate-buffered-saline-glucose (PBSG) at 37°C for up to two hours. The nucleotide pools were extracted and PEI-cellulose adsorbable radioactivity was determined. There was no detectable radioactivity incorporated into the parasite purine nucleotide pool.

SALVAGE OF PURINE AND PURINE NUCLEOSIDES

T. foetus cells were washed, resuspended in PBSG and incubated with radiolabeled purines and purine nucleosides. All purines and purine nucleosides examined were found to be incorporated into the nucleotide pool (Figure 2.3). Hypoxanthine, adenine and inosine were most readily incorporated with adenine reaching 60 pmol/10^6 cells after 1 hour. Guanine, xanthine and guanosine were incorporated to a much lower extent while adenosine was incorporated at an intermediate level.

Competition of the radiolabeled substrates with a 10-fold excess of unlabeled substrates revealed that adenine is the most potent inhibitor of uptake for all purine bases. Adenine and hypoxanthine were found to profoundly effect the incorporation of adenine, hypoxanthine, guanine and xanthine. Guanine and xanthine had little effect on adenine incorporation but did have moderate inhibiton on the incor-

poration of hypoxanthine, xanthine and guanine (Figure 2.4). Competition of radiolabeled nucleosides with their corresponding bases were also examined (Figure 2.5 and 2.6). The results indicated that 1) hypoxanthine and inosine compete equally well in inosine incorporation, 2) guanine is less effective an inhibitor as guanosine in guanosine incorporation and 3) adenine is less effective an inhibitor as adenosine in adenosine incorporation. The data suggest that inosine and hypoxanthine share a similar pathway of incorporation while guanosine and adenosine may have alternate routes of entering the nucleotide pool.

HPLC ANALYSIS OF THE NUCLEOTIDE POOL

HPLC analysis of the nucleotide pool of T. foetus incubated with radiolabeled hypoxanthine, adenine and inosine show very similar incorporation profiles. The labels were found predominately in IMP with some also in XMP, AMP, ADP, ATP, GMP, GDP and GTP. Upon chasing with cold substrate, the radioactivity in IMP decreased dramatically with a concommitant increase in ATP and GTP (Figures 2.7,2.8,2.12). Guanine and guanosine are mostly incorporated into IMP, XMP, GMP, GDP and GTP. Upon chasing, the labels decrease in IMP and XMP but appear in ADP and ATP. This evidence suggests a strong GMP reductase responsible for the rapid conversion of GMP to IMP (Figure 2.9). Xanthine is mainly converted to XMP with some label seen in IMP, GMP, GDP and GTP. After chasing, radioactivity decreases in XMP, IMP, GMP, GDP and GTP but also appears in ATP (Figure 2.10). Adenosine is primarily incorporated into NAD, AMP, IMP, XMP, ADP and ATP after a 30 minute

pulse. Upon chasing, the label in IMP dissappears and we see a decrease in radioactivity of NAD, AMP, XMP, ADP and ATP (Figure 2.11).

ENZYME PROFILES

The various salvage enzyme activities found in T. foetus crude extracts are summarized in Table 2.1. High hypoxanthine, guanine and xanthine phosphoribosyl transferase activity would account for the rapid uptake of these bases. The lack of adenine phosphoribosyl transferase and the presence of adenine deaminase could explain the incorporation of adenine by prior conversion to hypoxanthine. T. foetus lacks both inosine kinase and phosphotransferase and the conversion is dependent upon the presence of inorganic phosphate. Inosine uptake seems to occur only by way of an inosine phosphorylase. There is also high adenosine and guanosine phosphorylase present which converts the nucleosides to their respective bases in the presence of inorganic phosphate. The presence of guanine deaminase could explain why we see the early labeling of XMP by both guanine and guanosine. The salvage of adenosine occurs by an adenosine kinase forming AMP and guanosine by a phosphotransferase forming GMP directly. Guanosine phophotransferase was the only enzyme found to be sedimentable (100,000g). The enzyme utilizes p-nitrophenylphosphate as well as UMP, CMP, TMP and AMP as the phosphate donor.

TABLE 2.1. Purine salvage enzyme activities in Tritrichomonas foetus

Enzyme	Substrate	Activity* (nmol/min/mg protein)	
		Supernatant	Pellet
Phosphoribosyl-transferase	Hypoxanthine	0.915 ± 0.003	<0.001
	Guanine	1.137 ± 0.050	<0.001
	Adenine	<0.001	<0.001
	Xanthine	0.825 ± 0.005	<0.001
Kinase	Inosine	<0.001	<0.001
	Guanosine	<0.001	<0.001
	Adenosine	0.921 ± 0.100	<0.001
Phosphotransferse	Inosine	<0.001	<0.001
	Guanosine	0.233 ± 0.015	0.567 ± 0.030
	Adenosine	<0.001	<0.001
Phosphorylase	Inosine	44.0 ± 5.0	<0.001
	Guanosine	21.8 ± 2.0	<0.001
	Adenosine	16.0 ± 1.5	<0.001
Deaminase	Adenine	0.66 ± 0.07	<0.001
	Guanine	1.46 ± 0.06	<0.001
	Adenosine	29.0 ± 2.0	<0.001
	Guanosine	<0.001	<0.001

*Each activity value is derived from three independent assays.

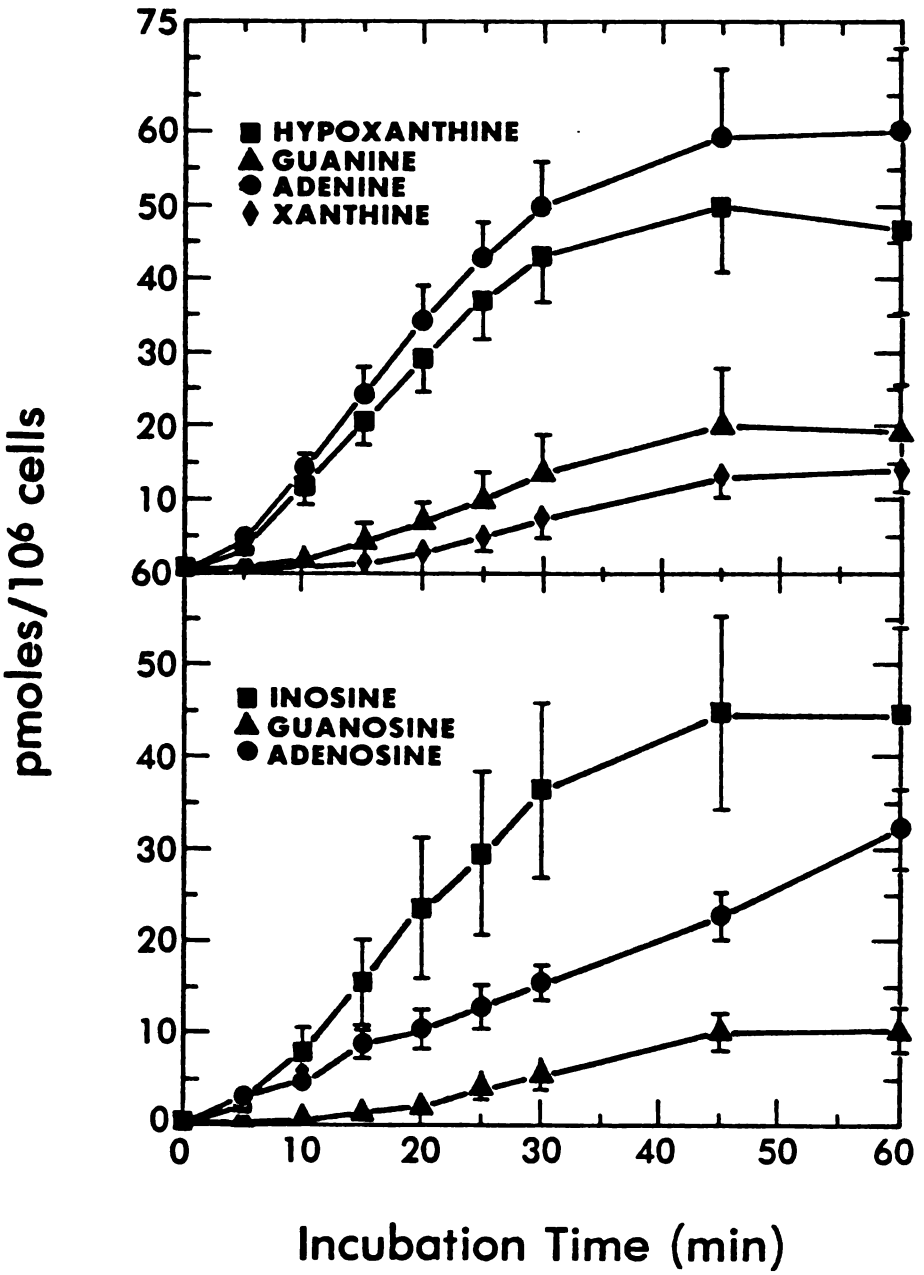

FIGURE 2.3. Incorporation of radiolabeled purines (A) and purine nucleosides (B) into T. foetus nucleotides. Each substrate was present at 20 μM in the incubation mixture; [8-^{14}C]hypoxanthine, (53.0 mCi/mmol); [8-^{14}C]guanine (56.7 mCi/mmol); [8-^{14}C]adenine (49.1 mCi/mmol); [8-^{14}C]xanthine (15.5 mCi/mmol); [8-^{14}C]inosine (22.5 mCi/mmol); [8-^{3}H]guanosine (45.7 mCi/mmol); [2,8-^{3}H]adenosine (49.4 mCi/mmol).

FIGURE 2.4. Incorporation of radiolabeled purines: (A) hypoxanthine; (B) guanine; (C) adenine; (D) xanthine into T. foetus nucleotides in the presence of another unlabeled base at ten fold higher concentration. Levels of radiolabeled purines are as described in Figure 2.3.

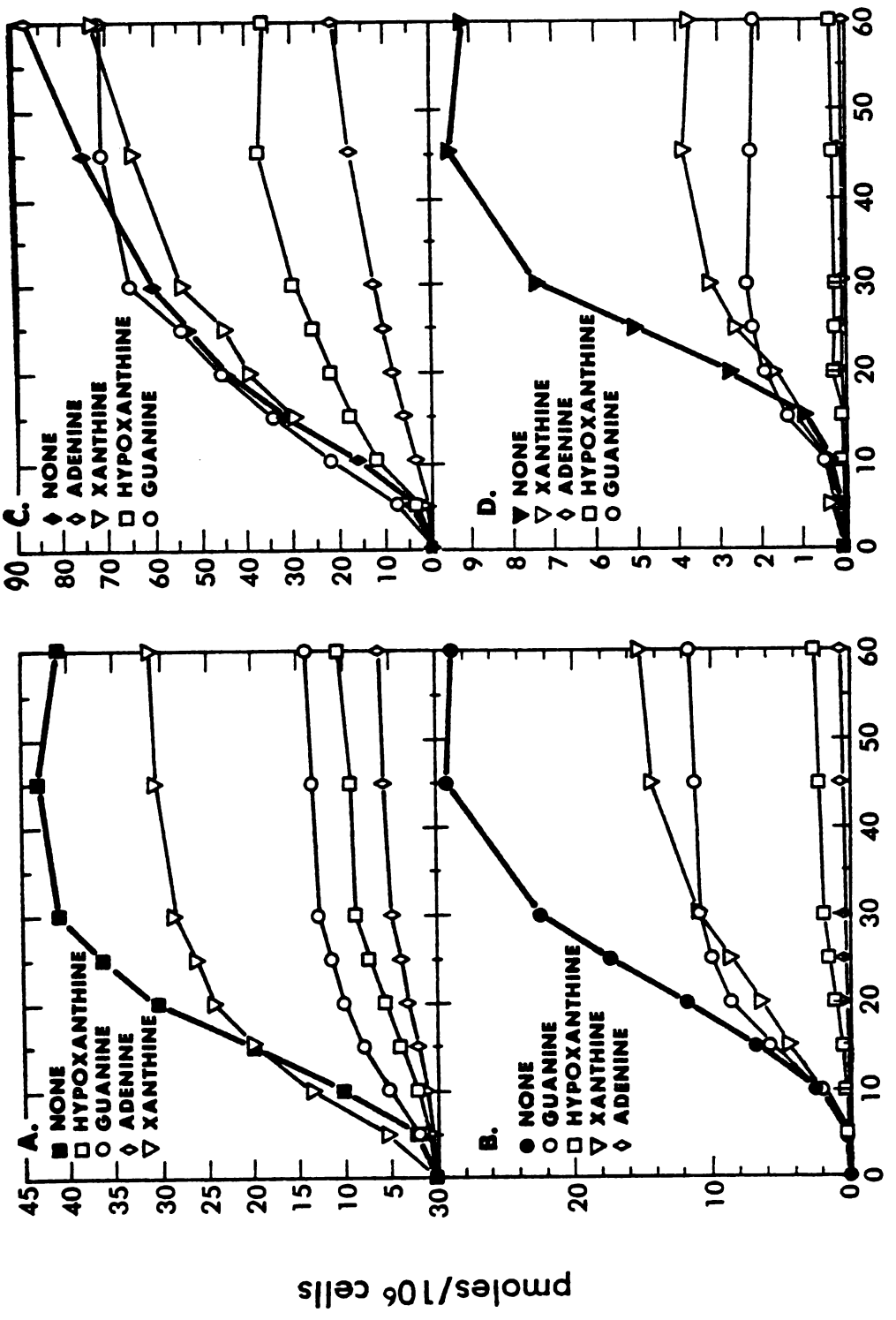
A.
NONE
HYPOXANTHINE
GUANINE
ADENINE
XANTHINE
B.
NONE
GUANINE
HYPOXANTHINE
XANTHINE
ADENINE
C.
NONE
ADENINE
XANTHINE
HYPOXANTHINE
GUANINE
D.
NONE
XANTHINE
ADENINE
HYPOXANTHINE
GUANINE
pmoles/10⁶ cells
Incubation Time (min)

FIGURE 2.4.

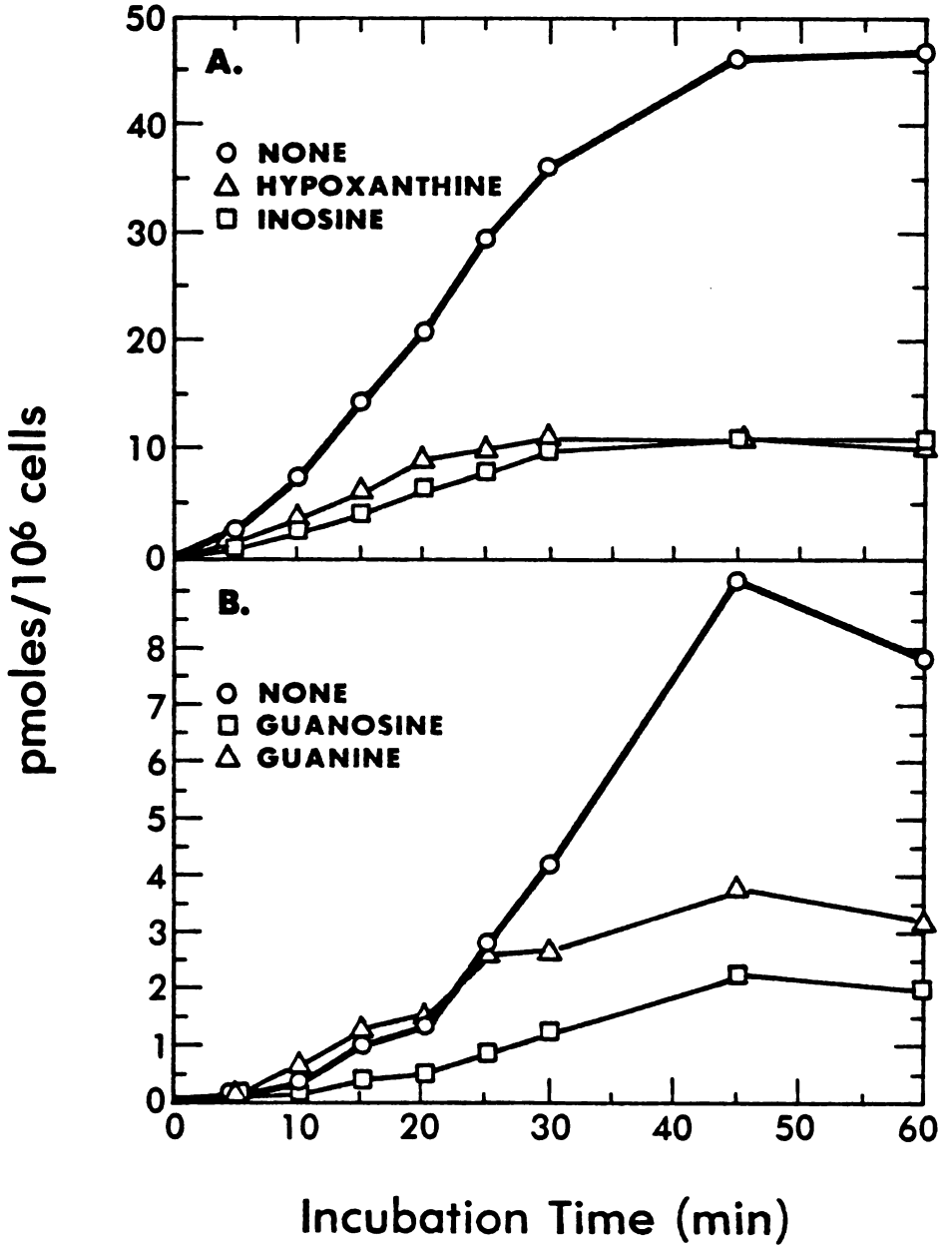

FIGURE 2.5. Incorporation of radiolabeled; (A) inosine and (B) guanosine into T. foetus nucleotides in the presence of another unlabeled substrate at ten fold higher concentration. Levels of radioactive substrates are as described in Figure 2.3.

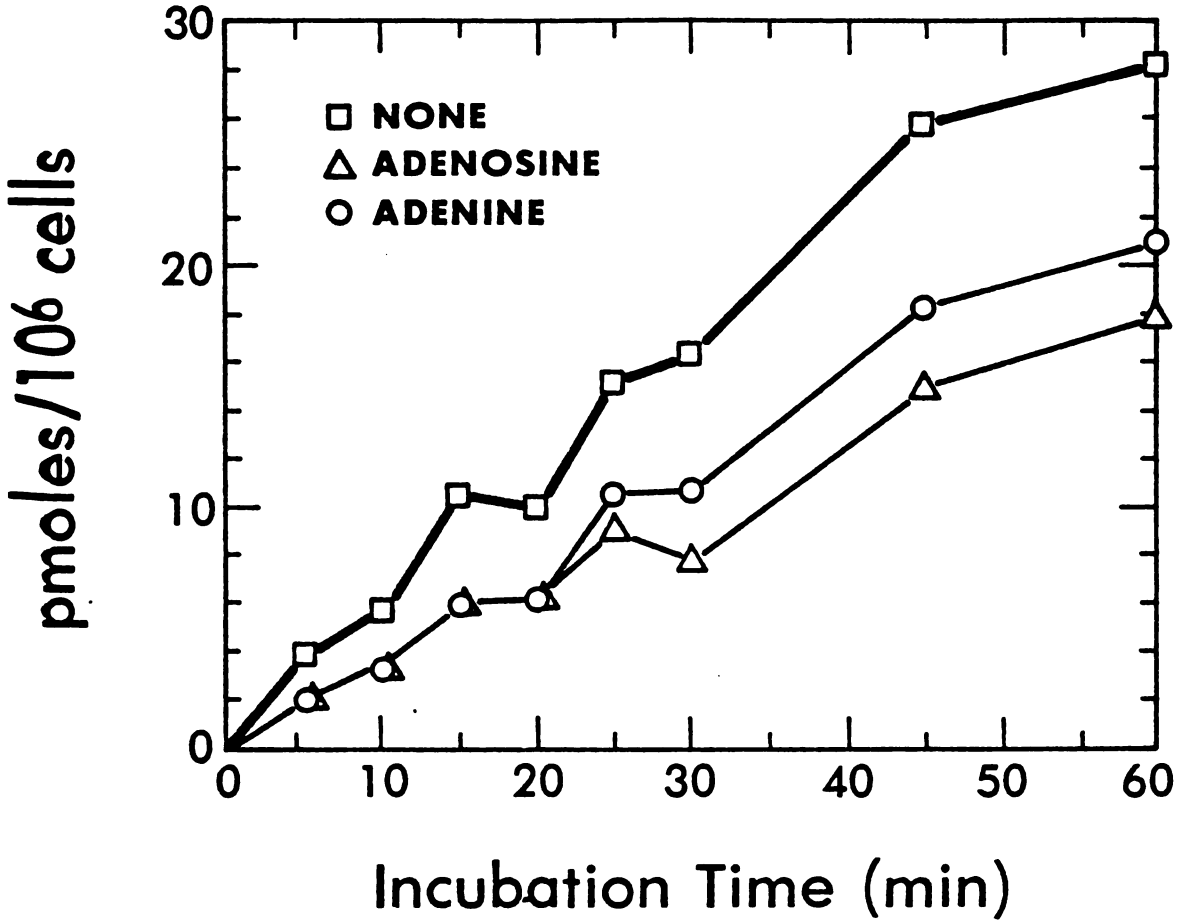

FIGURE 2.6. Incorporation of radiolabeled adenosine into T. foetus nucleotides in the presence of another unlabeled substrate at ten fold higher concentration. Levels of radioactive substrates are as described in Figure 2.3.

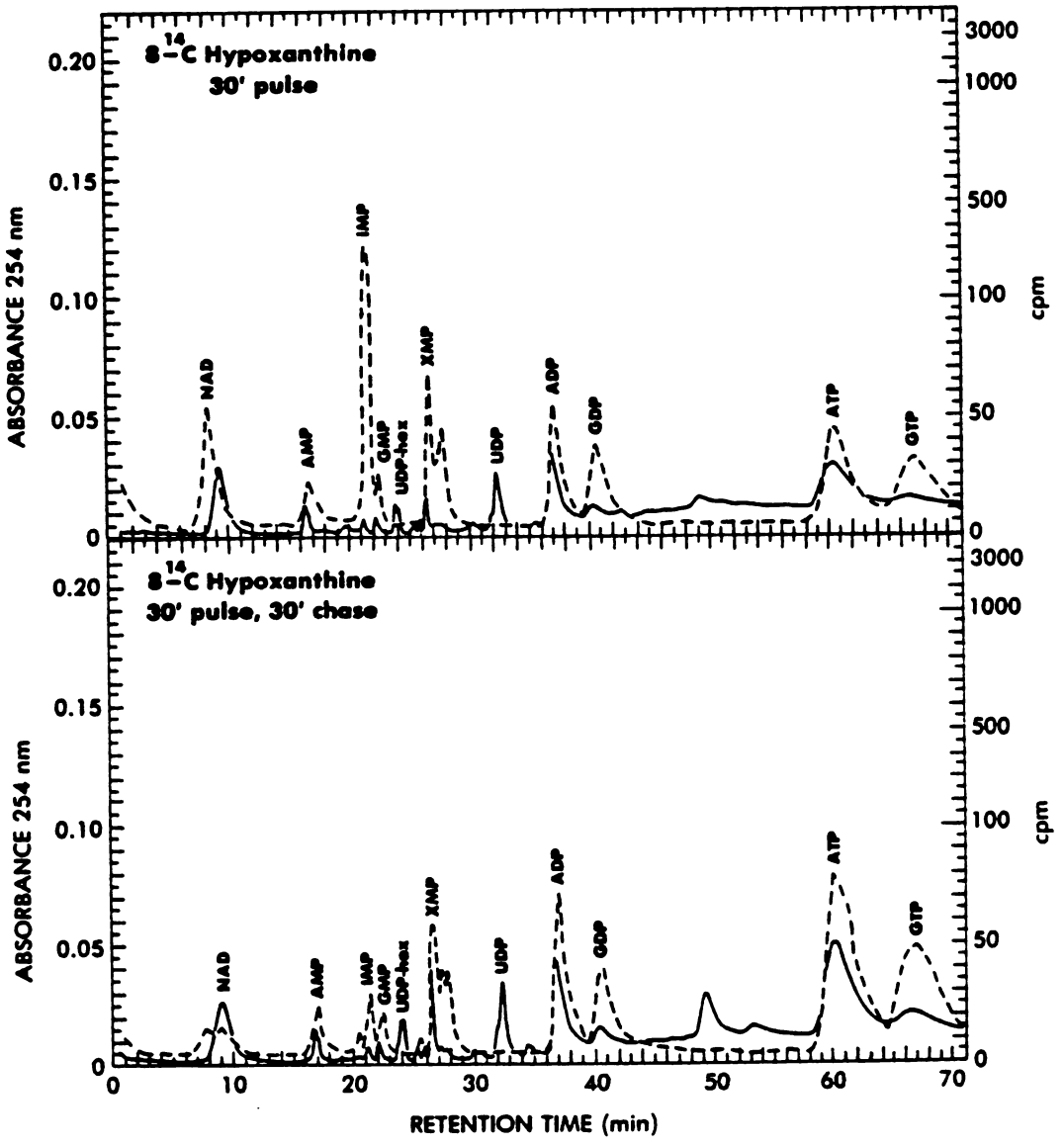

FIGURE 2.7. HPLC analysis of T. foetus nucleotides pulse-labeled by 20 μM [8-^{14}C]hypoxanthine (53.0 mCi/mmol) for 30 minutes, then chased by unlabeled hypoxanthine of the same concentration for 30 minutes. ——, A_{254}; ----, cpm.

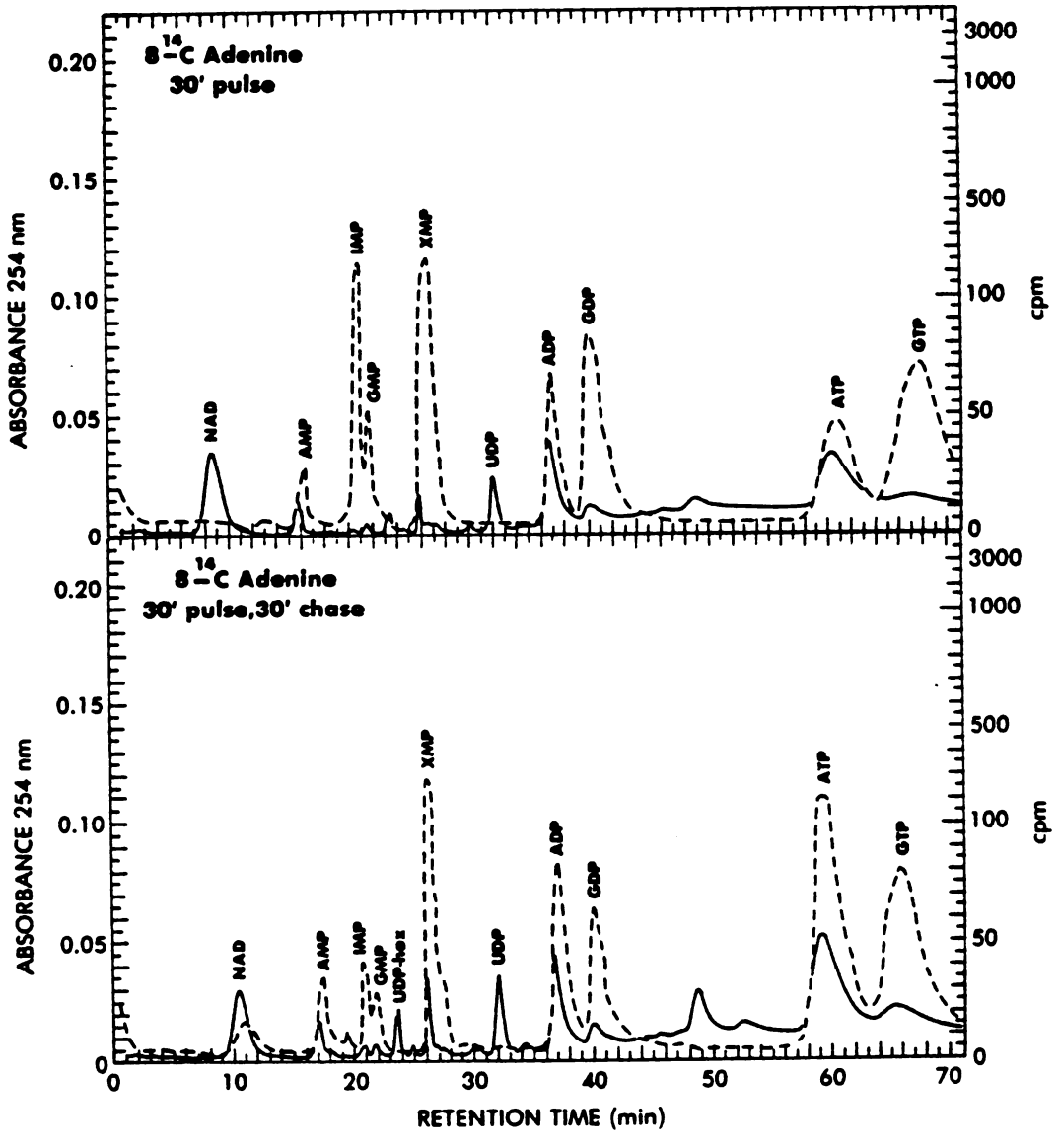

FIGURE 2.8. HPLC analysis of T. foetus nucleotides pulse-labeled by 20 μM [8-^{14}C]adenine (49.1 mCi/mmol) for 30 minutes, then chased by unlabeled adenine of the same concentration for 30 minutes.

——, A_{254};----, cpm.

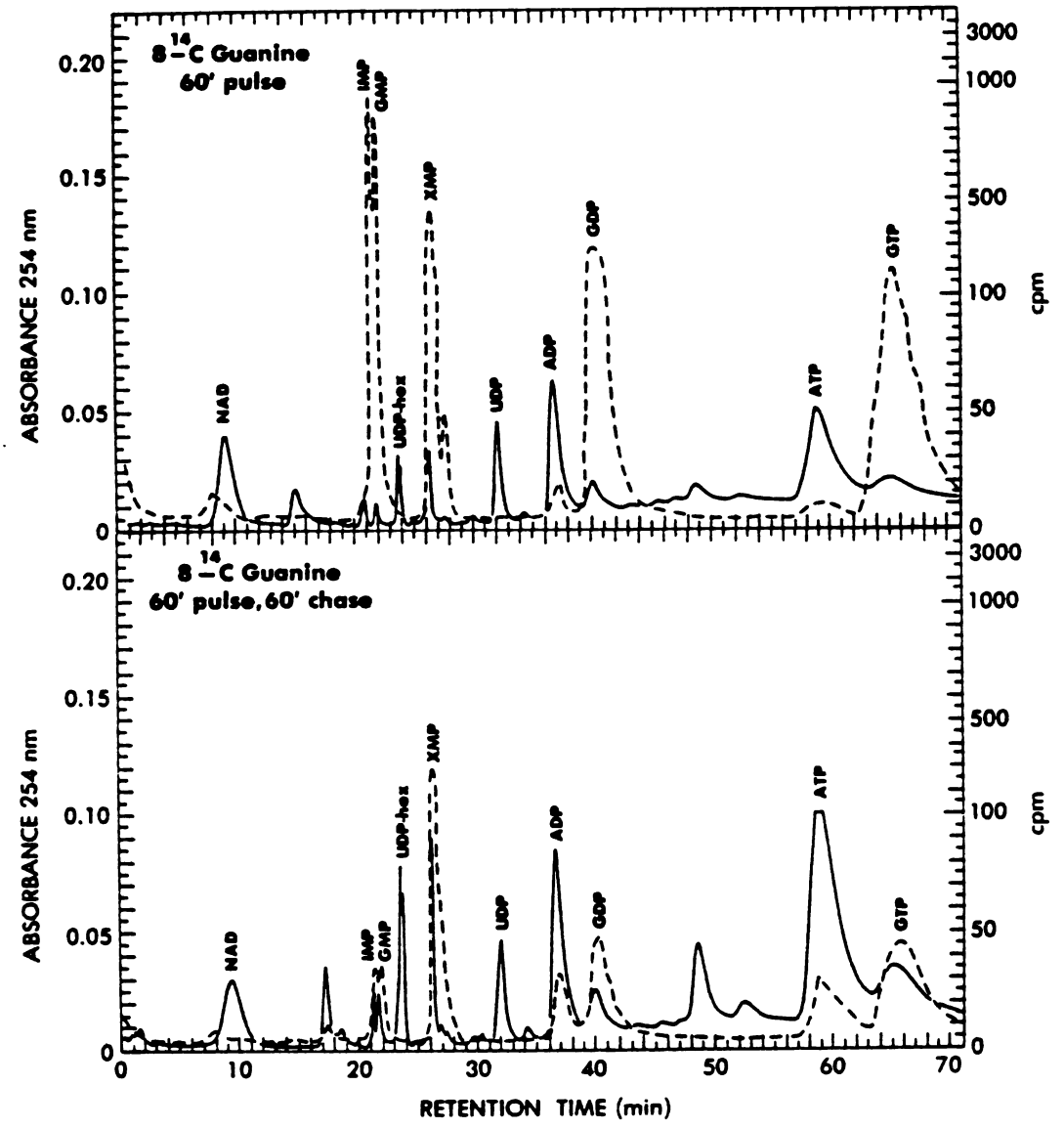

FIGURE 2.9. HPLC analysis of T. foetus nucleotides pulse-labeled by 20 μM [8-^{14}C]guanine (56.7 mCi/mmol) for 60 minutes, then chased by unlabeled guanine of the same concentration for 60 minutes.

——, A_{254}; ----, cpm.

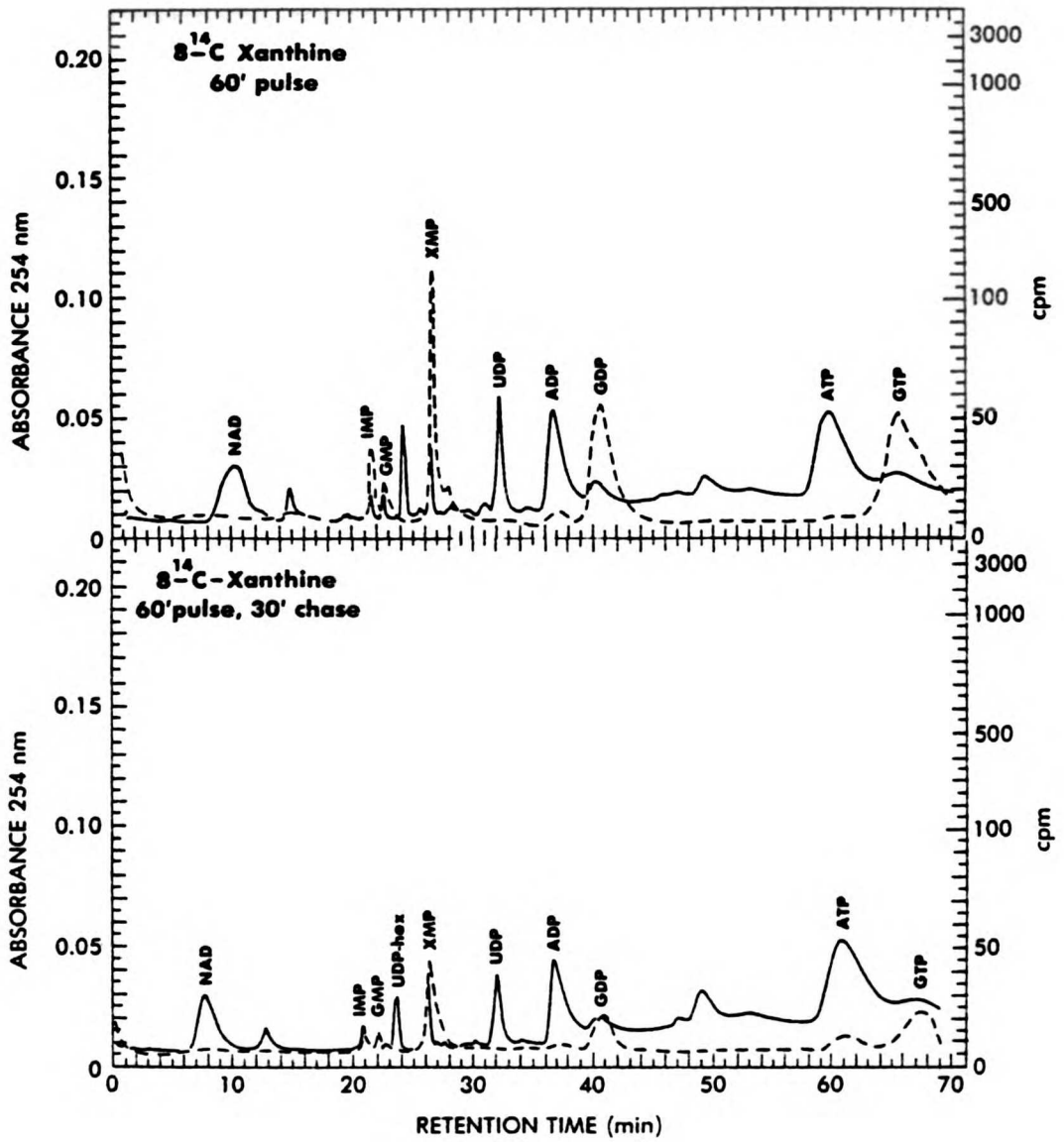

FIGURE 2.10. HPLC analysis of T. foetus nucleotides pulse-labeled by 20 μM [8-^{14}C]xanthine (15.5 mCi/mmol) for 60 minutes, then chased by unlabeled xanthine of the same concentration for 30 minutes.

——, A_{254}; ----, cpm.

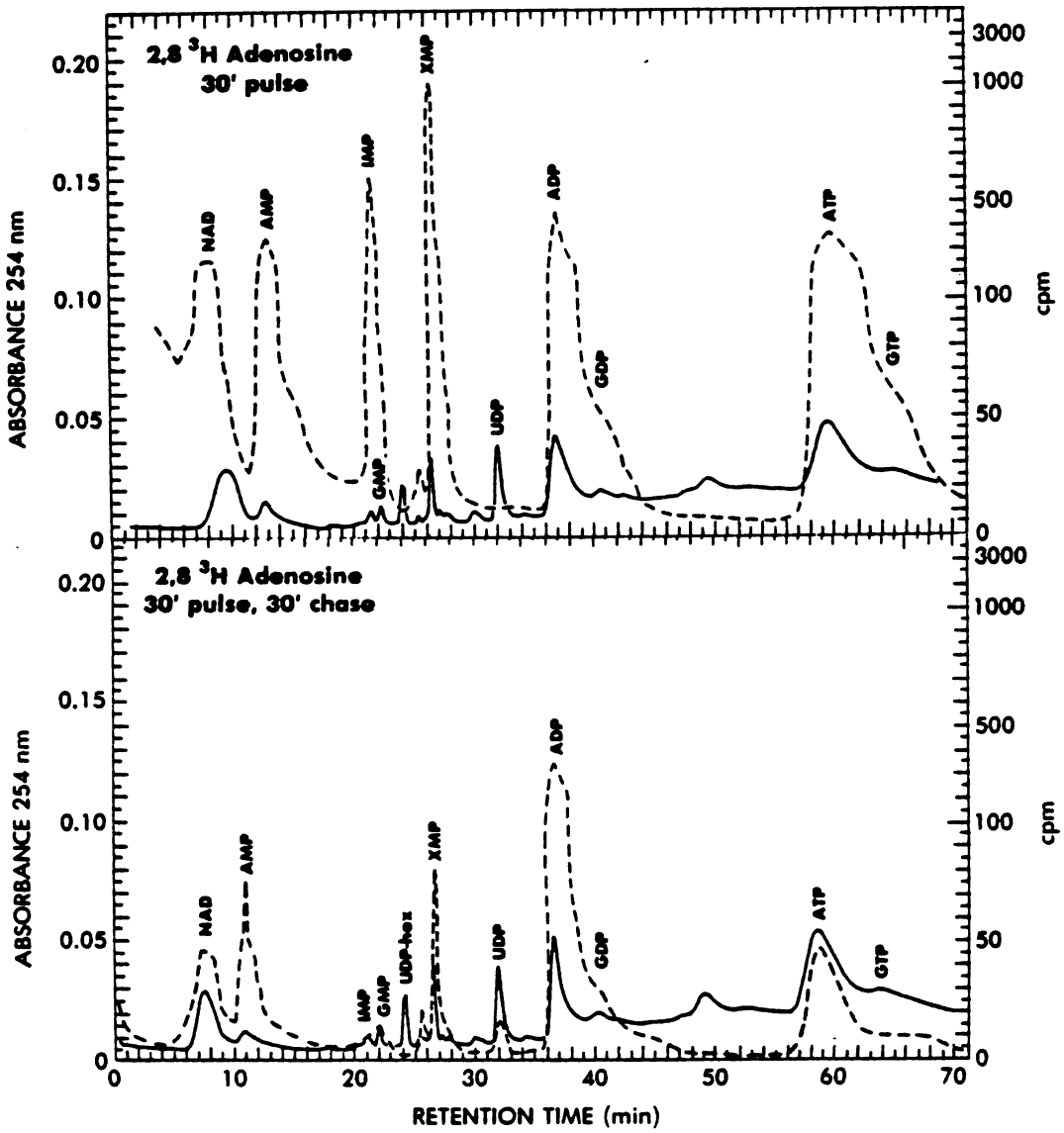

FIGURE 2.11. HPLC analysis of T. foetus nucleotides pulse-labeled by 20 μM [2,8-^{3}H]adenosine (88.3 mCi/mmol) for 30 minutes, then chased by unlabeled adenosine of the same concentration for 30 minutes.

——, A_{254};----, cpm.

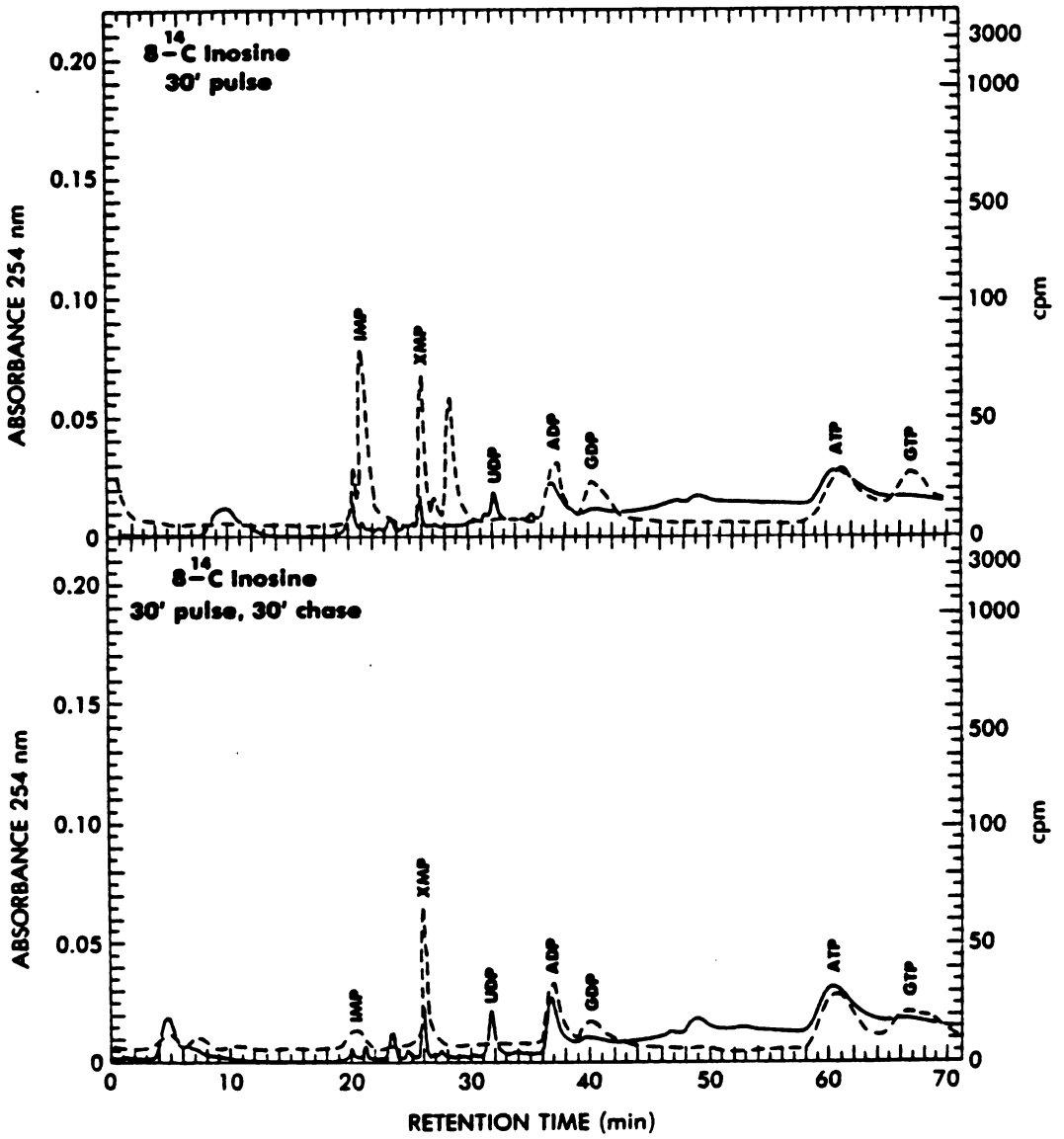

FIGURE 2.12. HPLC analysis of T. foetus nucleotides pulse-labeled by 20 μM [8-^{14}C]inosine (22.5 mCi/mmol) for 30 minutes, then chased by unlabeled inosine of the same concentration for 30 minutes.

——, A_{254}; ----, cpm.

DISCUSSION

All parasitic protozoa examined to date are unable to make their own purines, and T. foetus is no exception. The lack of dihydrofolate reductase (142) and the inability to incorporate precursors of purine nucleotide into the nucleotide pool indicates that T. foetus is incapable of purine de novo biosynthesis. The complete salvage pathway is summarized in Figure 2.13.

As is illustrated, the hypoxanthine-guanine-xanthine phosphoribosyl transferase activities play a key role in the salvage of purines. It is yet unknown whether this is indeed one, two or three separate enzymes. There are instances of all cases occuring among other protozoans (98,143). It was surprising to find no adenine phosphoribosyl transferase and difficult to explain the large uptake of adenine at first. The uptake of adenine apparently proceeded by way of hypoxanthine with the help of adenine deaminase. But adenine uptake was faster than hypoxanthine incorporation. This can be explained if we imagined that uptake is a two step process. Step 1 requires the transport of the substrate into the cell and step 2 is the actual conversion to nucleotide. If access across the membrane was the rate limiting step and adenine transport was quicker for adenine than hypoxanthine transport, we would expect to see a faster rate for adenine incorporation, even though it requires two catalytic steps to become incorporated. Adenosine uptake seems to have two pathways to become incorporated. One way is via adenosine kinase and the other way eventually involves hypoxanthine phosphoribosyl transferase.

Adenosine kinase is probably the main pathway, as the HPLC nucleotide pool chromatograms for adenosine uptake is so different from hypoxanthine uptake (Figures 2.7, 2.11).

Adenine, hypoxanthine and inosine are the most readily incorporated of the purines (Figure 2.3) and all proceed via the same phosphoribosyl transferase. The hypoxanthine-guanine-xanthine phosphoribosyl transferase plays a key role in supplying the parasites purine requirments. An inhibitor designed to exploit this enzyme could perhaps inhibit T. foetus growth as well.

Another interesting enzyme was the guanosine phosphotransferase. As was reported earlier, thymidine phosphotransferase was also found associated with this same pelletable material (142). The thymidine phosphotransferase represented the sole method for T. foetus to obtain a TMP supply. This enzyme was also shown to be inhibited by guanosine. This guanosine phosphotransferase / thymidine phosphotransferase could be another potential site for chemotherapeutic design.

Comparison of the purine metabolism of T. foetus to two other anaerobic protozoan parasites, Trichomonas vaginalis and Giardia lamblia, reveals quite a differance. Both T. vaginalis and G. lamblia are incapable of de novo purine biosynthsis but have simpler purine salvage networks than T. foetus. G. lamblia relies on adenosine and guanosine hydrolase to form adenine and guanine, repectively, which is then incorporated into the nucleotide pool by adenine and guanine phosphoribosyl transferases (144). T. vaginalis, on the other hand, lacks purine phosphoribosyl transferase activity (138). Instead, the

parasite relies on kinases and nucleoside phosphorylase activity for its purine needs. So, even though these anerobic parasites may share some similarities, they are quite different in their purine metabolism.

T. foetus is unable to synthesize its own purines de novo and must rely upon the salvage of exogeneous purines. Two enzymes, hypoxanthine-guanine-xanthine phosphoribosyl transferase and guanosine phosphotransferase have been identified as potential targets for chemotherapeutic drug design. Further work is required to examine these enzymes more closely.

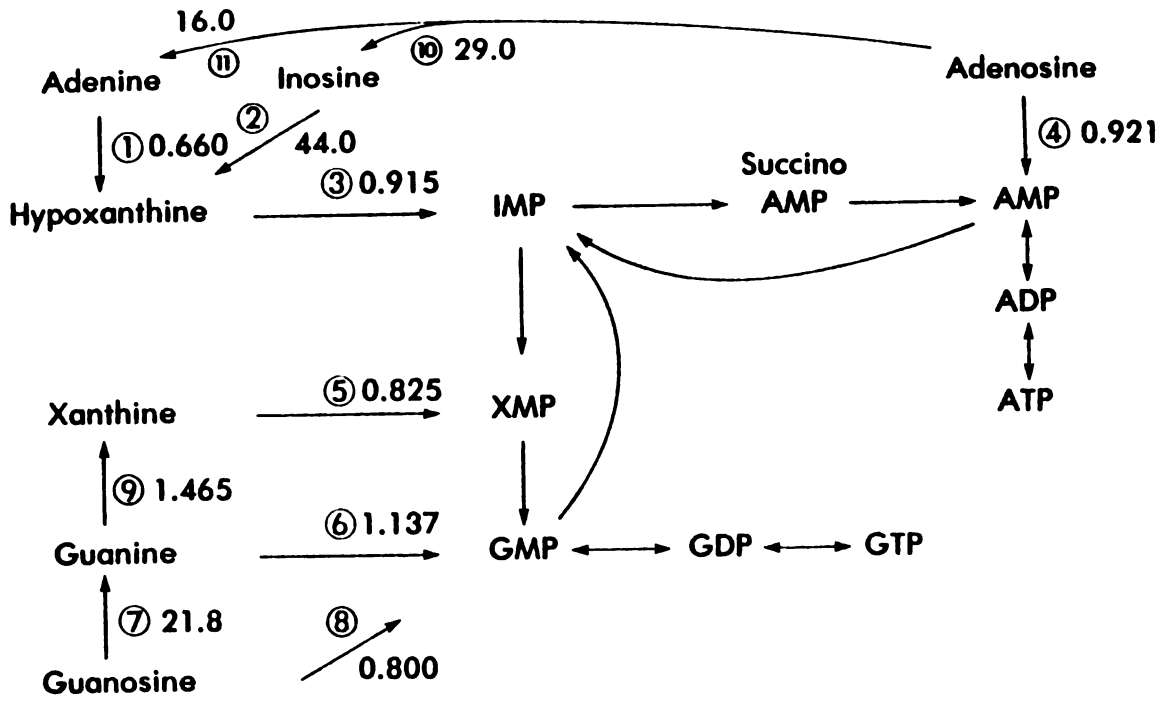

FIGURE 2.13. Purine salvage pathways in Tritrichomonas foetus. Enzymes; 1) adenase, 2) inosine phosphorylase, 3) hypoxanthine phosphoribosyltransferase, 4) adenosine kinase, 5) xanthine phosphoribosyltransferse, 6) guanine phosphoribosyltransferase, 7) guanosine phosphorylase, 8) guanosine phosphotransferase, 9) guanine deaminase, 10) adenosine deaminase and 11) adenosine phosphorylase. Numbers designate specific activities of the enzymes in nmol/min/mg protein.

CHAPTER 3

EFFECTS OF INHIBITORS ON THE PURINE AND PYRIMIDINE METABOLISM IN TRITRICHOMONAS FOETUS

INTRODUCTION

Our investigation has indicated that Tritrichomonas foetus is incapable of de novo purine (157) and pyrimidine biosynthesis (142). Survival of the parasite depends upon its ability to salvage exogeneous purines and pyrimidines. The main source of purines for T. foetus is provided by the salvage and conversion of hypoxanthine to IMP while the main channel for pyrimidine nucleotides involves the incorporation of uracil into UMP. The uptake of hypoxanthine and uracil is accomplished by hypoxanthine phosphoribosyltransferase and uracil phosphoribosyltransferase, respectively. Figure 3.1 summarizes the salvage scheme for hypoxanthine. T. foetus has also evolved a very specific and independent pathway for thymidine salvage because of its lack of dihydrofolate reductase and thymidylate synthetase. As a result of this evidence, a semi-defined minimal medium capable of supporting the growth of the parasite has been formulated and contains hypoxanthine, uracil and thymidine as the sole precursors of purine and pyrimidine nucleotides (118). This minimal media has also been used in our present investigation to analyze the relationship between drug effects on the growth of T. foetus and purine and pyrimidine supply in the media.

In this chapter we have examined the effects of two known inhibitors of adenylosuccinate synthetase; alanosine (146) and hadacidin (153), and specific inhibitors of IMP dehydrogenase; mycophenolic acid (MPA) (155) and virazole (158). Mycophenolic acid was tested and found to be partially effective against Leishmania tropica amasigotes by inhibiting guanosine nucleotide synthesis (159). Other purine analogues such as formycin B (FoB) and 8-azaguanine (8-AG) have also been tested on T. foetus. Formycin B has been shown to be an effective antileishmanial agent (104), being converted by Leishmania spp. (149, 151) and Trypanosoma cruzi (150) to formycin A- 5'-triphosphate (See Figure 3.13). A more in depth understanding of the purine and pyrimidine metabolism in Tritrichomonas foetus can be achieved by studying the effects of inhibitors on; 1) the in vitro growth of T. foetus, 2) substrate incorporation into the nucleotide pool of T. foetus and 3) changes in nucleotide concentrations within the nucleotide pool.

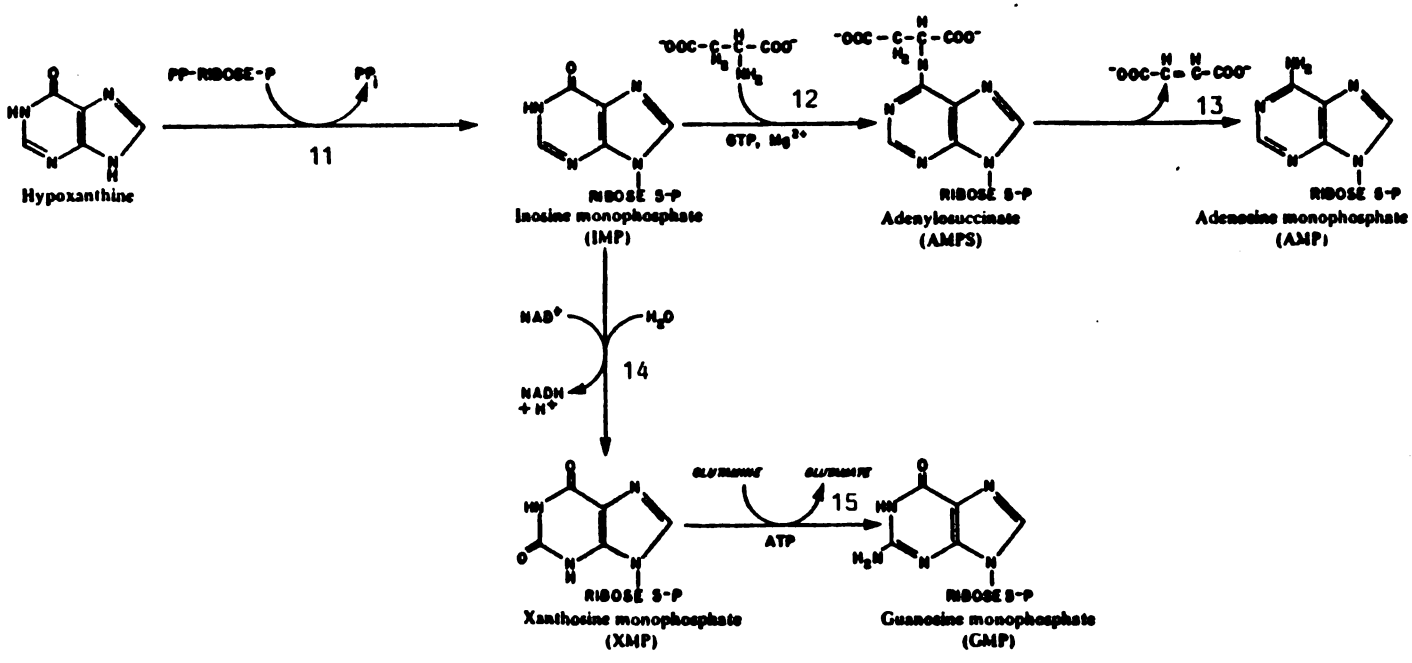

FIGURE 3.1. The salvage and conversion of hypoxanthine into both adenylate and guanylate nucleotides. Enzymes: 11, hypoxanthine phosphoribosyltransferase; 12, adenylosuccinate synthetase; 13, adenylosuccinase; 14, IMP dehydrogenase; and 15, GMP synthetase.

MATERIALS AND METHODS

CULTURES

T. foetus, KV_1 strain, was cultivated in Diamonds TYM medium pH 7.2, supplemented with 10% heat inactiviated horse serum (114). Cultures after 24 hours growth, 10^7 cells/ml, were transferred to fresh media in a 1:10 ratio. *In vitro* drug testing was done by adding the drug to the fresh media prior to innoculation with *T. foetus*. The cultures were then incubated at 37°C in a Forma anaerobic incubator Model 1024 under N_2 for 24 hours. Cell numbers were determined at the end of the incubation period using a Coulter counter Model ZF. In some instances, a more defined medium was chosen for in vitro drug testing. A semi-defined HUT medium containing; hypoxanthine, uracil and thymidine as the only source of exogeneous purines and pyrimidines was used (118). The procedures for innoculation, incubation and cell counting were preformed as previously described for TYM.

CHEMICALS

Radiolabeled purine bases, pyrimidine bases, purine nucleosides and pyrimidine nucleosides were purchased from Amersham (Arlington Heights, IL.) New England Nuclear (Boston, MA.) and ICN (Irvine, CA.). [^{3}H]-5-F-Uracil (32.8 mCi/mmol) and [^{3}H]-5-F-deoxyuridine (43.3 mCi/mmol) were provided to us by Dr. C. A. Hunt of the School of Pharmacy, UCSF. [^{3}H]-Formycin-B (400 mCi/mmol) was a gift from Dr. P. Rainey (151). Formycin B, 8-azaguanine, 5-F-uracil, 5-F-deoxyuridine, 2-aminothiadiazole, 6-mercaptopurine, thioallopurinol and metron-

idazole were obtained from the Sigma Chemical Co., (St. Louis, Mo.). Alanosine, hadacidin, and mycophenolic acid were a generous gift from Dr. W. Sadee of the School of Pharmacy, UCSF. All other chemicals used in the study were of the highest purity commericially available.

PRECURSOR INCORPORATION INTO THE NUCLEOTIDE POOL

Mid-log phase T. foetus were washed and resuspended in phosphate-buffered (pH 7.2)-saline glucose (PBSG) to a final cell density of 10^8 cells/ml. Parasites were incubated with radioactive substrates at 37°C and the intracellular nucleotide pool was extracted by the per chloric acid-KOH procedure (142). The extract was analyzed by ion exchange HPLC as previously described (142). Quantitative measure ments of the incorporation of radiolabeled substrates into the nucleo-tide pool were determined by passing the extract through a glass fiber, PEI-cellulose loaded filter and then counting the adsorbed radioactivity in a Beckman LS-3133T liquid scintillation spectrometer (142).

RESULTS

Uracil Phosphoribosyltransferase (UPRTase) Inhibitors

Two pyrimidine analogues, 5-flourouracil and 5-flourodeoxyuridine (Figure 3.2) were examined as possible inhibitors of the growth of Tritrichomonas foetus. 5-Flourouracil was found to have moderate inhibitory effect with a 50% inhibitory concentration (IC_{50}) of 25 µM while 5-flourodeoxyuridine was without effect on the in vitro growth of T. foetus in TYM over a 24 hour period. In the presence of 0.1 mM 5-F-uracil, the incorporation of 2.0 mM uracil, uridine and cytidine were inhibited 44%, 32% and 20% respectively. The drug, up to 0.5 mM, had no effect on thymidine incorporation into TMP, TDP or TTP. HPLC analysis of uracil, uridine and cytidine incorporation experiments showed that in the presence of 5-F-uracil, incorporated label in the nucleotide pool by each of the three substates was reduced. 5-F-Uracil was shown to be a competitive inhibitor of UPRTase with an IC_{50} of 70 µM against 20 µM uracil. When 5-F-[6-^{3}H]uracil (32.8 mCi/mmol) was used to label cells and the products analyzed by HPLC, radioactive peaks corresponding to 5-F-uridine mono-, di- and triphosphates were detected, suggesting that the compound may eventually be incorporated into T. foetus RNA (Figure 3.3). On the other hand, 5-F-[6-^{3}H]deoxyuridine (43.3 mCi/mmol) was not incorporated into the parasites nucleotide pool to a detectable extent.

Hypoxanthine phosphoribosyltransferasse (HPRTase) Inhibitors

Three potential inhibitors of T. foetus hypoxanthine phospho-

ribosyltransferase (HPRTase), 8-azaguanine (8-AG) (145), 6-mercaptopurine and thioallopurinol (Figure 3.4), were weak inhibitors of T. foetus growth in TYM. 8-Azaguanine, the most potent growth inhibitor of the three, limited the parasites in HUT medium with an estimated IC_{50} of 30 μM (Figure 3.12). 6-Mercaptopurine was the most effective inhibitor of purine uptake, decreasing the uptake of exogeneous guanine, hypoxanthine, and adenine by 74%, 60% and 40% respectively. 8-AG and thioallopurinol were not as effective inhibitors of purine uptake (Table 3.1). HPLC analysis of the nucleotide pool labeled with [8-^{14}C]hypoxanthine in the presence of 1 mM of inhibitor revealed a similar pattern for all three inhibitors. There was an overall decrease of labeled nucleotides, with the mono- and diphosphates depleted the most and the triphosphates accounting for the majority of the remaining label. The inhibitory effects of 8-AG on T. foetus growth in HUT and its effects on hypoxanthine incorporation into the parasite's nucleotide pool both support the hypothesis that 8-AG is a substrate of HPRTase (147). Additional evidence from incubation experiments of T. foetus with 1 mM 8-AG and HPLC analysis of the nucleotide pool revealed the emergence of three new peaks with retention times corresponding to the mono-, di- and triphosphates of 8-azaguanine (Figure 3.5) (147). Therefore, it is likely that the mode of anti-T. foetus action of 8-AG is that of incorporation into the parasites nucleic acids.

Adenylosuccinate Synthetase Inhibitors

Inhibitors of adenylosuccinate synthetase, L-alanosine, hadacidin and formycin B (FoB) (Figure 3.6) were tested on T. foetus. T. foetus growth in TYM was uneffected by 1 mM of L-alanosine or hadacidin while formycin B reduced the in vitro growth dramatically, after a 24 hour period (Figure 3.12). The uptake of labeled hypoxanthine, adenine and adenosine were inhibited about 40% by 1 mM FoB. Hadacidin (1 mM) was inhibitory to hypoxanthine and adenine uptake but stimulated adenosine uptake. The uptake of all three substrates, hypoxanthine, adenine and adenosine were stimulated by 100 μM alanosine (Table 3.2). In the presence of 1 mM hadacidin or formycin B, the nucleotide pool indicated a decrease in the adenine mono-, di- and triphosphates in HPLC analysis(Figure 3.7 C, D). The inhibitory strength of FoB appeared to be stronger than that of hadacidin. T. foetus was incubated with 3 μM [^{3}H]formycin B for 2 hours and the nucleotide pool extracted and analyzed. The results showed the appearance of only a single radiolabeled peak whose retention time corresponded to that of formycin B-5'-monophosphate (Figure 3.8) (151). If this monophosphate of formycin B is the active agent responsible for the growth inhibition observed in T. foetus, then it could possibly act by inhibition of adenylosuccinate synthetase as suggested by; the hypoxanthine incorporation experiments (Table 3.2), the HPLC analysis of incorporation experiments (Figure 3.7 C, D), and the postulation made by Carson and Chang (104). A test of this hypothesis involved the cultivation of T. foetus in HUT medium with added adenosine. The

added adenosine would be expected to reverse the inhibiton of FoB because adenosine can be converted directly to AMP by adenosine kinase. The data in Figure 3.10 however, indicated that adenosine had no rescueing effect for the parasite treated with 100 µM FoB, which could mean that either adenosine alone can not fulfill the requirements of T. foetus for purines or that FoB-5'-monophosphate may have other activities leading to inhibited growth of T. foetus.

IMP Dehydrogenase Inhibitors

Mycophenolic acid (MPA) and virazole (Figure 3.9) were examined as possible inhibitors of T. foetus growth. Virazole (1 mM) had no effect on T. foetus growth while mycophenolic acid was a moderate inhibitor of T. foetus growth with an estimated IC_{50} of 50 µM in TYM. The incorporation of [8-^{14}C]adenine was unaffected by 1 mM virazole and subsequent HPLC analysis of the nucleotide pool showed no change in the distribution of labeled nucleotides. Mycophenolic acid had a stimulatory effect on the uptake of adenine, hypoxanthine and guanine but inhibited xanthine uptake by 25%. HPLC analysis of the nucleotide pool labeled with [8-^{14}C]hypoxanthine in the presence of 100 µM MPA revealed the absence of labeled XMP, GMP, GDP and GTP (Figure 3.7 B). Which is consistent with the knowledge that MPA is a specific inhibitor of IMP dehydrogenase (155) in bacterial and mammalian cells. Additional evidence for the site of action of MPA could be provided by examining the effect of the drug in HUT medium, where the only purine source is hypoxanthine. With the addition of guanine or guanosine to

the medium, the parasite should be able to bypass the block and provide GMP by the actions of guanine phosphoribosyltransferase and guanine phophotransferase (157). Experimental evidence indicated that both guanine and guanosine are indeed capable of reversing the inhibitory effect of MPA on T. foetus growth (Figure 3.10), thus further proved that MPA is an inhibitor of T. foetus IMP dehydrogenase.

Other inhibitors of purine metabolism

2-Aminothiadiazole and metronidazole (Figure 3.11) were examined for their possible inhibition of purine metabolism in the bovine trichomonad. 2-Aminothiadiazole (1 mM) was without effect on the growth of T. foetus in TYM over a 24 hour period. Metronidazole on the other hand, one of the most effective agents against trichomoniasis, inhibited the growth of the trichomonad in TYM with an IC_{50} of 6 μM. 2-Aminothiadiazole had no effect on adenine uptake while the uptake of adenine, hypxanthine and adenosine were all 100% inhibited by 100 μM metronidazole. The rapidity in which the drug acts can also be visually seen. Upon the addition of metronidazole to a cell suspension, the cells immediately (within 1 minute) become orange in color. This orange color is also extractable in our nucleotide extraction procedure. Metronidazole seems to be a potent non-specific inhibitor of purine metabolism but its exact mode of action still remains to be elucidated.

TABLE 3.1. Effect of HPRTase inhibitors on purine uptake.

	% INHIBITION OF UPTAKE		
Substrate (20 μM)	6-Mercaptopurine (1 mM)	8-Azaguanine (1 mM)	Thioallopurinol (100 μM)
Hypoxanthine	60	31	19
Guanine	74	-15	--
Adenine	40	7	6
Adenosine	-2	-11	--

-- not done.

TABLE 3.2. Effect of inhibitors of adenylosuccinate synthetase on purine uptake.

	% INHIBITION OF UPTAKE		
Substrate (20 μM)	L-Alanosine (100 μM)	Hadacidin (1 mM)	Formycin B (1 mM)
Hypoxanthine	-18	24	40
Adenine	-152	40	38
Adenosine	-111	-21	38

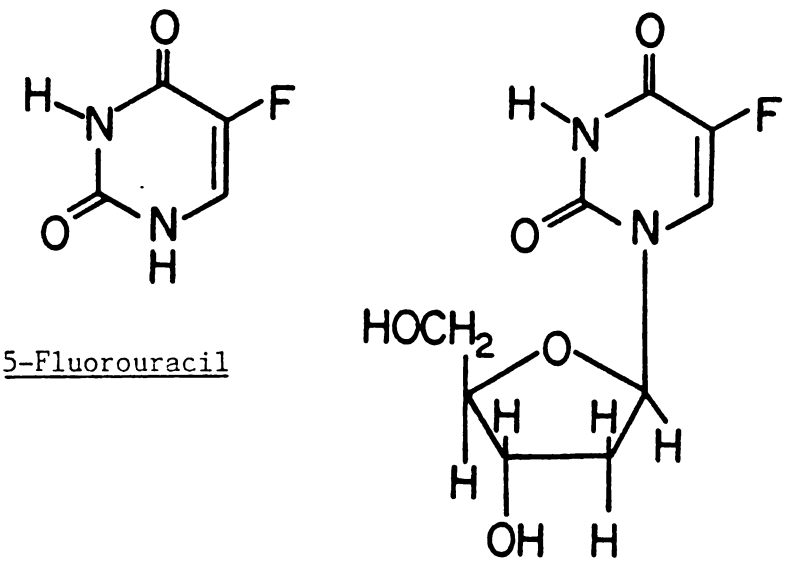

5-Fluorouracil

5-Fluorodeoxyuridine

Figure 3.2. Structures of 5-fluorouracil and 5-fluorodeoxyuridine.

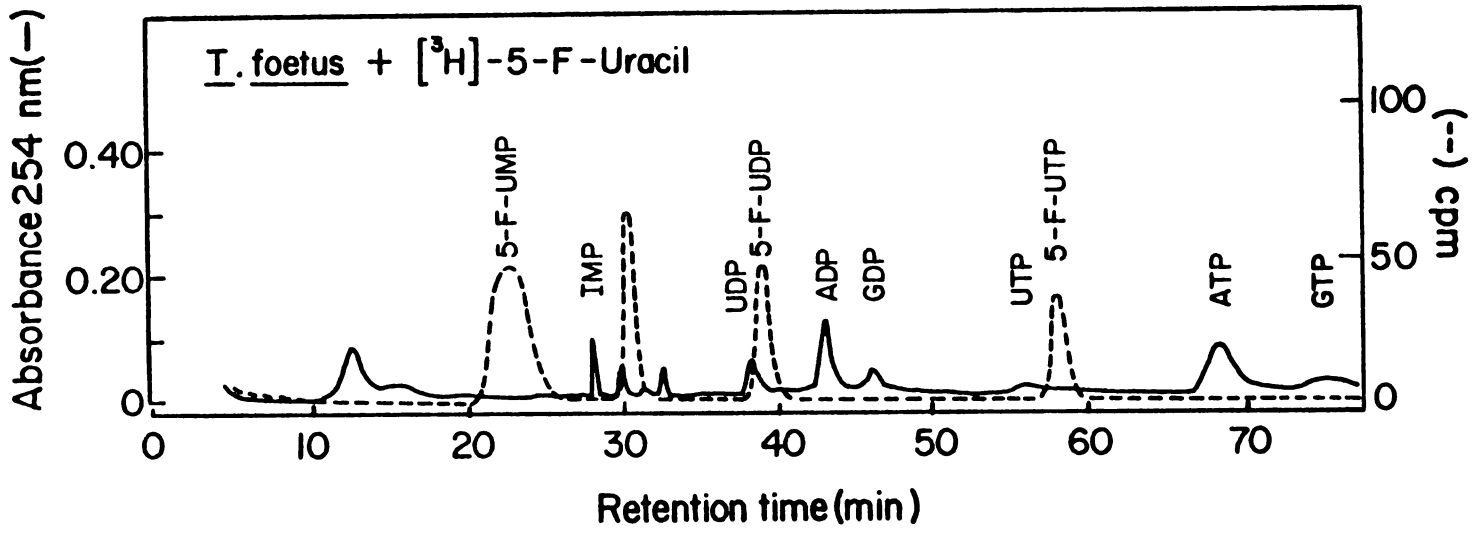

FIGURE 3.3. Incorporation of 5-F-[^{3}H]uracil (48.33 mCi/mmole) into the nucleotide pool of T. foetus.

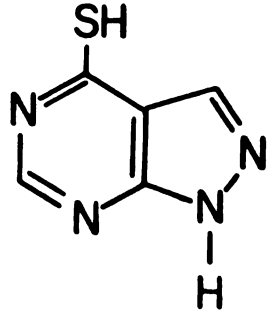

Thioallopurinol

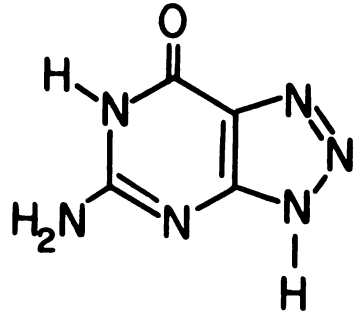

8-Azaguanine

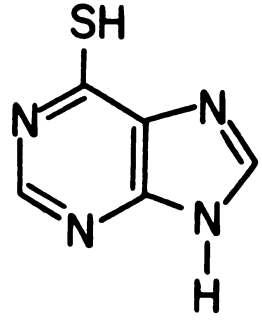

6-Mercaptopurine

Figure 3.4. Structures of 8-azaguanine, 6-mercaptopurine and thioallopurinol.

FIGURE 3.5. Incorporation of 8-azaguanine into the nucleotide pool of T. foetus. A) no drug control and B) with 1 mM 8-azaguanine for a 2 hour incubation at 37°C.

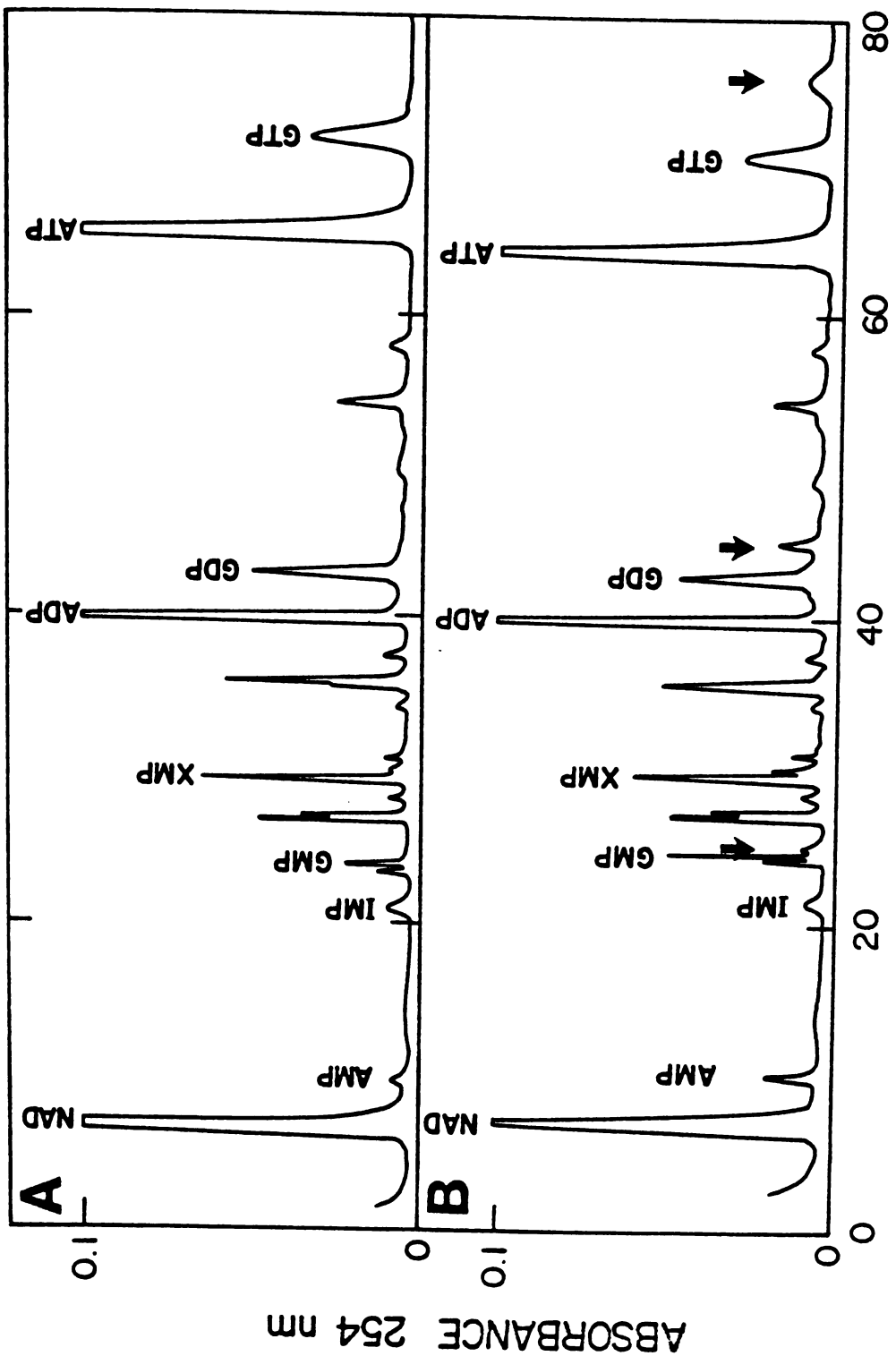
A
B
NAD
AMP
IMP
GMP
XMP
ADP
GDP
ATP
GTP
1.0
0
0
20
40
60
80
ABSORBANCE 254 nm
RETENTION TIME (min)

FIGURE 3.5.

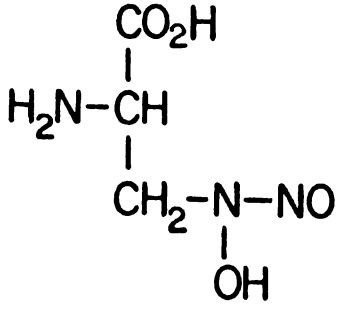

L-Alanosine

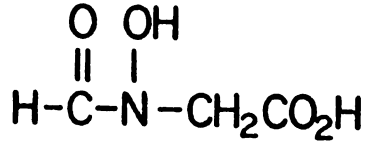

Hadacidin

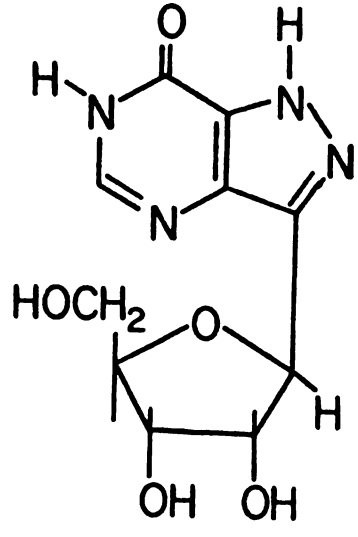

Formycin B

Figure 3.6. Structures of L-alanosine, hadacidin and formycin B.

FIGURE 3.7. HPLC profiles of nucleotides in T. foetus pulse-labeled with 20μM [8-^{14}C]hypoxanthine (51.1 mCi/mmole) for 45 minutes in the presence of A) no drug control, B) 100 μM mycophenolic acid, C) 1 mM hadacidin and D) 1 mM formycin B.

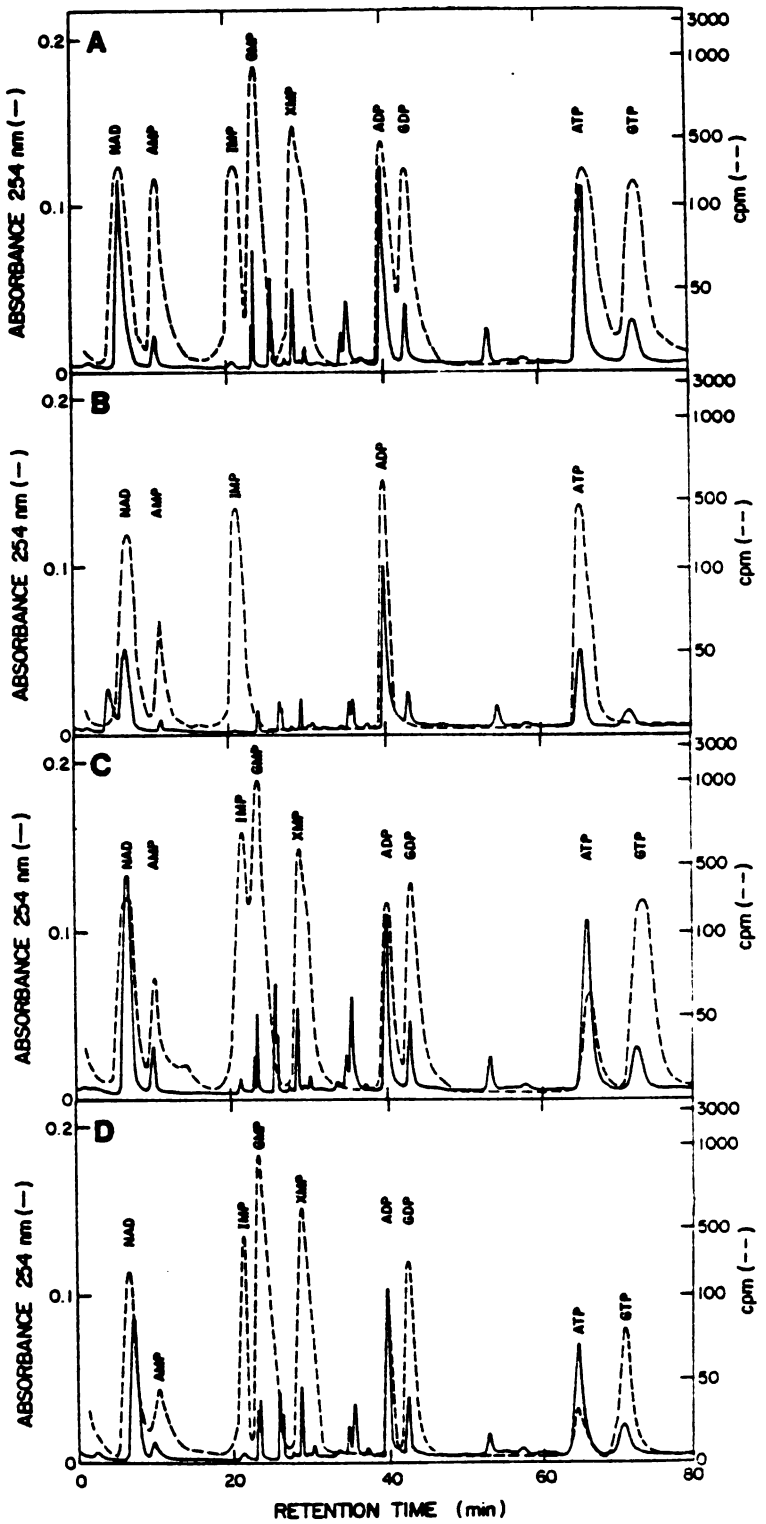
A
B
C
D
NAD
AMP
IMP
GMP
XMP
ADP
GDP
ATP
GTP
ABSORBANCE 254 nm (—)
cpm (- - -)
RETENTION TIME (min)
0
20
40
60
80
0.2
0.1
3000
1000
500
100
50

FIGURE 3.7.

FIGURE 3.8. Incorporation of formycin B into the nucleotide pool of *T. foetus*. *T. foetus* was incubated with 3 μM [^{3}H]forymcin B (450 mCi/mmole) for 2 hours.

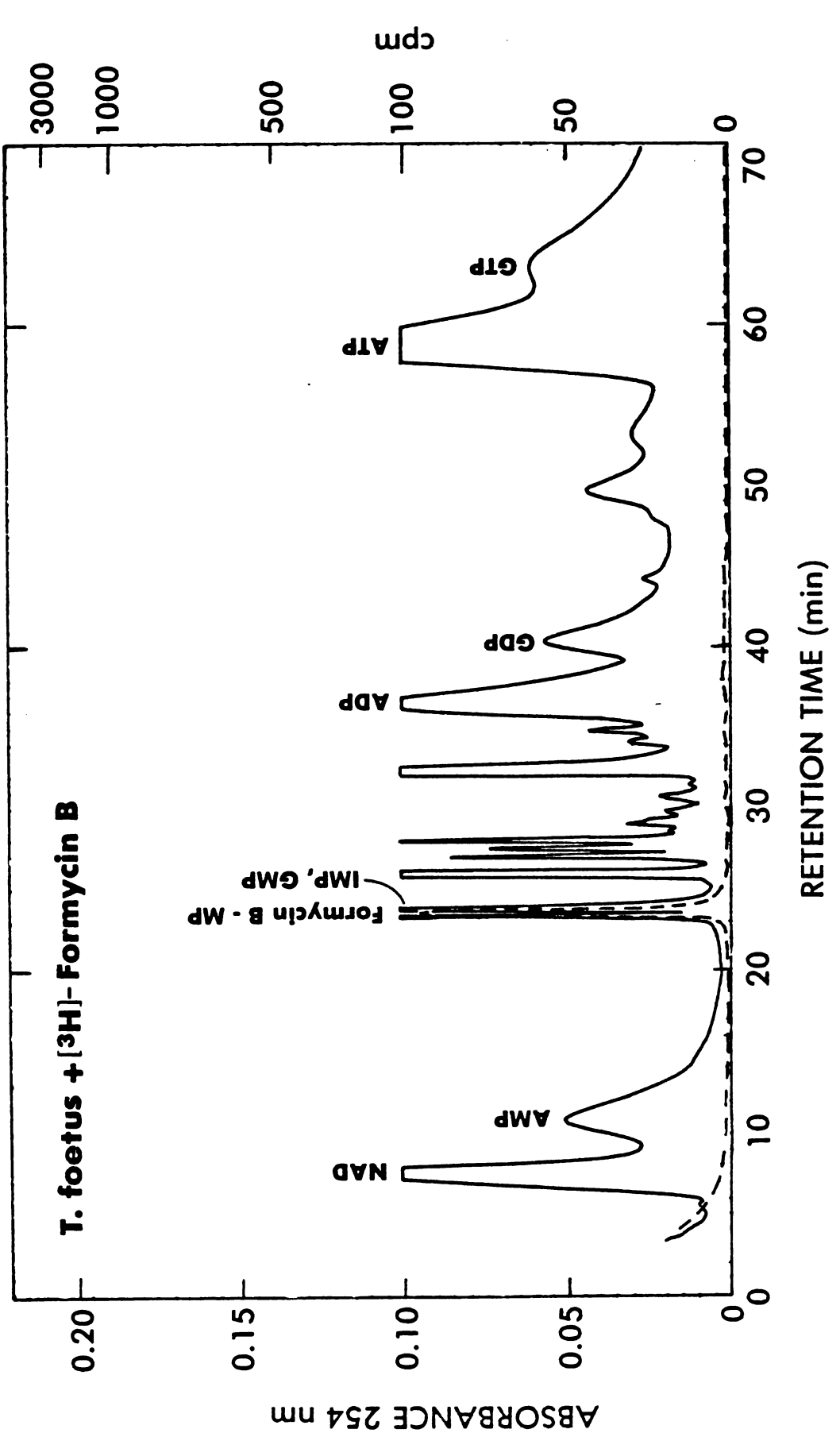
T. foetus + [3H]- Formycin B
NAD
AMP
Formycin B - MP
IMP, GMP
ADP
GDP
ATP
GTP
ABSORBANCE 254 nm
cpm
RETENTION TIME (min)
0.20
0.15
0.10
0.05
0
3000
1000
500
100
50
0
10
20
30
40
50
60
70

FIGURE 3.8.

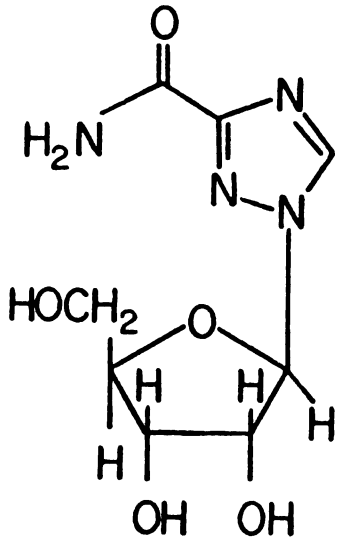

Virazole

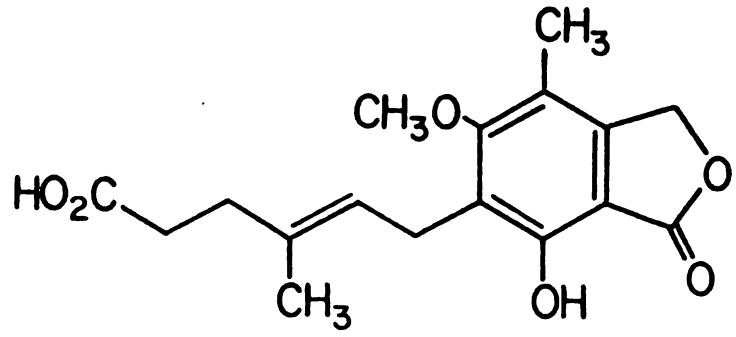

Mycophenolic acid

Figure 3.9. Structures of mycophenolic acid and virazole.

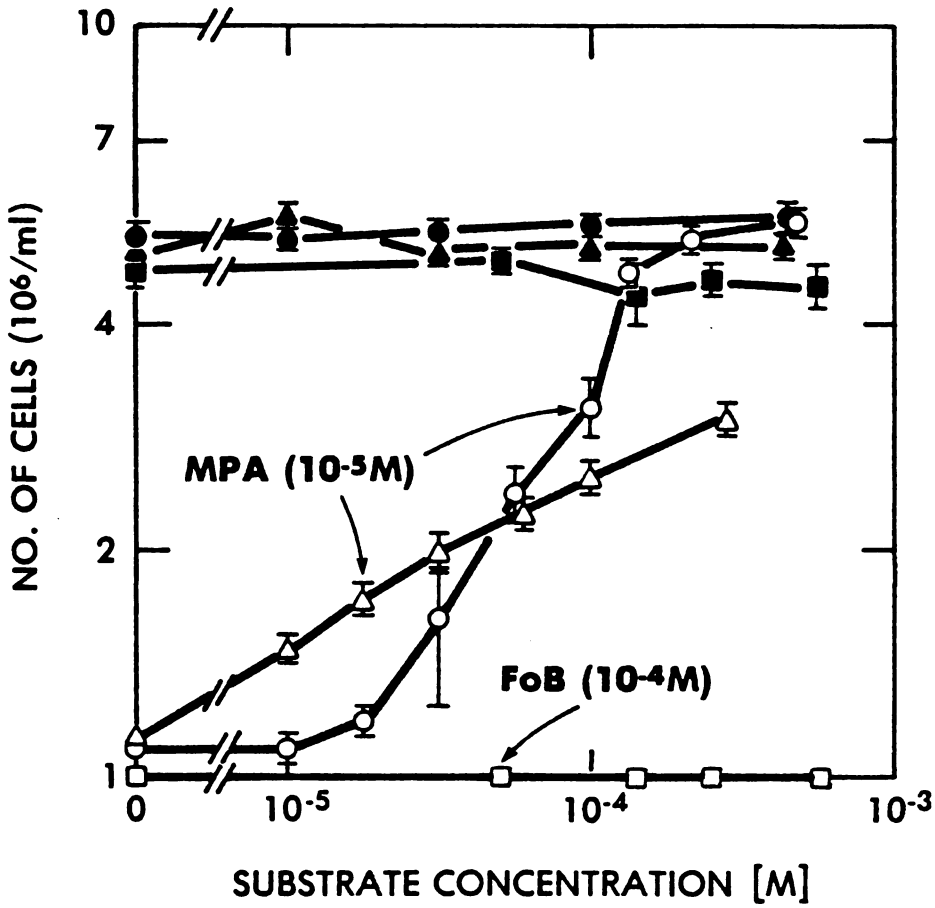

FIGURE 3.10. Reversal of growth inhibition exerted by mycophenolic acid (MPA) or forymcin B (FoB) on T. foetus cultivated in HUT medium. The added substrates were; guanine (○●), guanosine (△▲) and adenosine (□■), without inhibitor (●▲■), or with inhibitor (○△□).

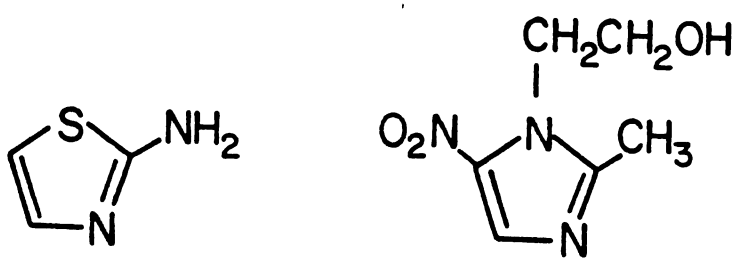

2-Aminothiadiazole

Metronidazole
"Flagyl"

Figure 3.11. Structures of 2-aminothiadiazole and metronidazole.

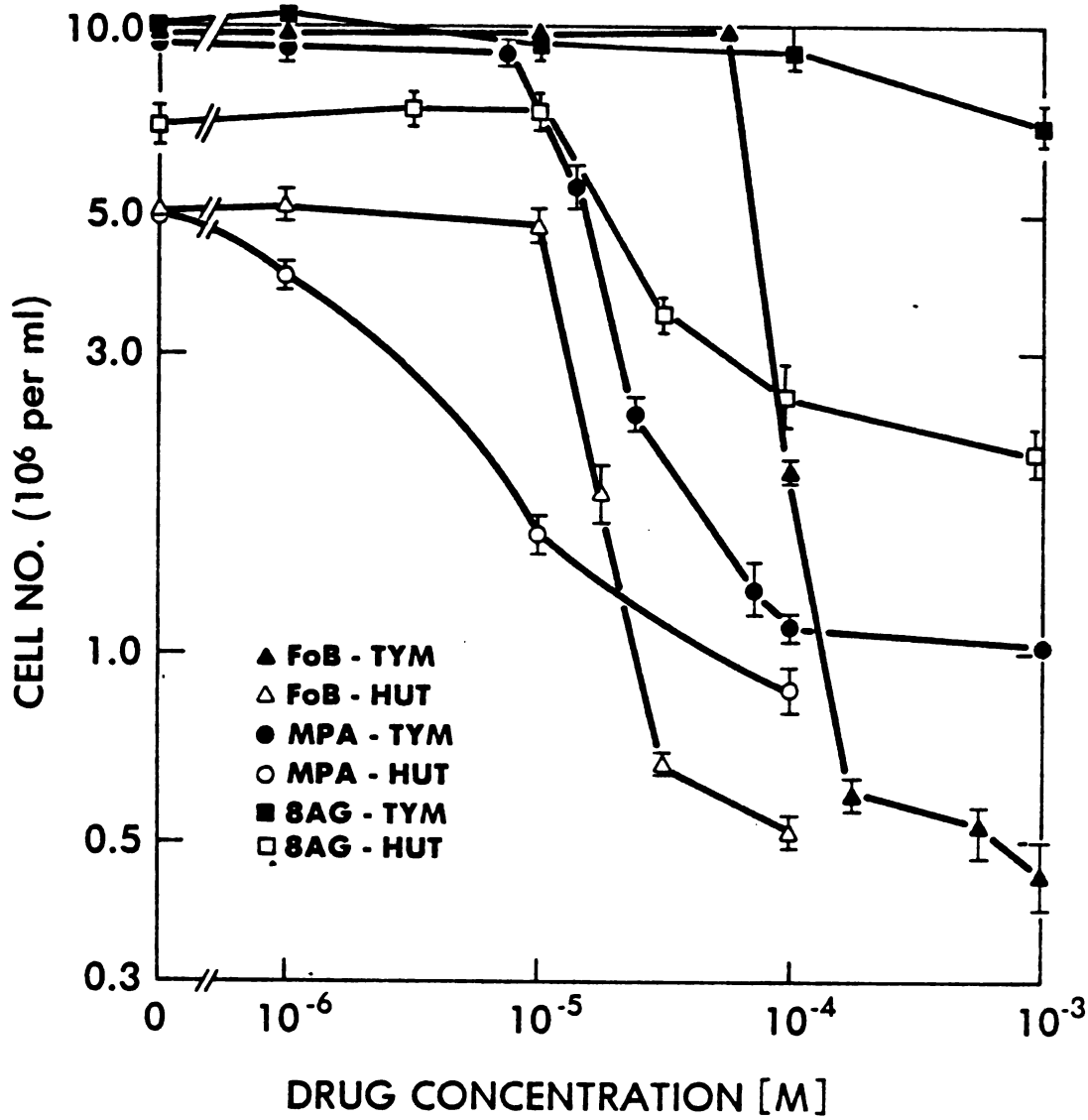

FIGURE 3.12. Effects of drugs on the growth of T. foetus in the TYM medium vs growth in the HUT medium.

DISCUSSION

Tritrichomonas foetus is reliant upon the salvage of exogeneous purines and pyrimidines for its survival (142,157). It is capable of being grown in a semi-defined minimal medium with uracil, thymidine and hypoxanthine as its only purine and pyrimidine source (118). The salvage of uracil was found to be competively inhibited by 5-F-uracil but this is probably not the drugs primary mode of action. Instead, the uptake and conversion of 5-F-uracil to the mono-, di and triphosphates (Figure 3.3) and its eventual incorporation into the parasites RNA is most likely its mechanism of action. On the other hand, T. foetus does not incorporate 5-F-deoxyuridine into the nucleotide pool which implies that the enzymes involved with nucleoside salvage and interconversion may be more substrate specific than UPRTase.

Since T. foetus can survive on hypoxanthine alone as the purine source (118), the hypoxanthine phosphoribosyltransferase, IMP dehydrogenase and adenylosuccinate synthetase in the parasite have important roles in purine salvage (See Figure 3.1). This is exemplified by the recognition of 8-AG as substrate by HPRTase, the uptake and conversion of 8-AG to the mono-, di- and triphosphate (Figure 3.5), its postulated incorporation into nucleic acids and the observed growth inhibition. This is also supported by a similar mode of action of 8-AG reported in bacterial and mammalian systems (147). The partial inhibition of HPRTase by 8-AG is probably not the primary mode of action because further increases in hypoxanthine levels in HUT medium

failed to reverse the inhibited growth (data not shown).

Several inhibitors of adenylosuccinate synthetase were tested including hadacidin (153), alanosine (146) and formycin B. Hadacidin, up to 1 mM concentration, shows no inhibition of T. foetus growth, and only weak activity in reducing the incorporation of hypoxanthine into AMP (Figure 3.7 D). This lack of activity in hadacidin is quite in contrast to its activity on Escherichia coli adenylosuccinate synthetase where it has a K_i value of 4.2 μM(153). The other inhibitor of adenylosuccinate synthetase, alanosine, was also without effect on T. foetus growth or on hypoxanthine incorporation into nucleotides. This lack of activity is probably because alanosine itself is a poor inhibitor of adenylosuccinate synthetase (K_i = 57.23 mM) and needs to be converted to L-alanosyl-5-amino-4-imidazole carboxylic acid ribonucleotide before becoming a potent inhibitor (K_i = 0.23 μM) (156) (See Figure 3.14). The enzyme catalyzing this conversion, 5-amino-4-imidazole-N-succinocarboxamide ribonucleotide synthetase, is part of the de novo purine synthetic pathway which is absent in T. foetus (157). Formycin B-5'-monophosphate is another inhibitor of adenylosuccinate synthetase although its mode of action is not clear. Formycin B exhibits an IC_{50} value of 20 μM for growth inhibition in HUT medium, with 147 μM hypoxanthine (Figure 3.12). This is in contrast to the IC_{50} of 1 mM of Formycin B needed for inhibiting 20 μM hypoxanthine incorporation (Figure 3.7 D and Table 3.2). The primary mode of action of formcyin B is thus not by blocking the purine salvage in T. foetus. The conversion of FoB to FoB-5'-monophosphate

(Figure 3.8) and the inhibition of hypoxanthine conversion to AMP, ADP and ATP (Figure 3.7D), are suggestive that one of the actions of FoB in T. foetus is inhibition of adenylosuccinate synthetase by its 5'-monophosphate. This was the postulated mechanism of action for FoB in Leishmania as suggested by Carson and Cheng (104). But this may not be the sole mechanism of inhibition in T. foetus because we were unable to reverse the inhibited growth in HUT by adenosine (Figure 3.10). An alternative mechanism of action of FoB was postulated by work done on Leishmania (104, 149) and Trypanosoma cruzi (150). In those cases, the conversion of FoB to formycin A-5'-triphosphate (FoATP) are observed and the eventual incorporation of FoATP into nucleic acids was postulated (See Figure 3.13). This could not, however occur in T. foetus because there was no FoATP formed from FoB (Figure 3.8).

The mode of action of mycophenolic acid was much simpler to determine. The inhibition of T. foetus growth by MPA in HUT medium was reversible by the addition of either guanine or guanosine (Figure 3.10). This and its inhibition of hypoxanthine incorporation into XMP, GMP, GDP and GTP (Figure 3.7 B) support the conclusion that MPA inhibits T. foetus growth by inhibiting its IMP dehydrogenase. The inhibition of IMP dehydrogenase by MPA has also been observed in mammalian cells (148,154) and other parasites (159). Virazole, a potent inhibitor of IMP dehydrogenase in mammalian cells, with an IC_{50} of 50 μM (154), was found to have no effect on the growth of T. foetus. The ribonucleotides of 6-mercaptopurine (160-162) and

8-azaguanine (163) found inhibiting IMP dehydrogenase in intact animal and bacterial cells, were also found to be not specific inhibitors of IMP dehyrogenase in T. foetus. The ineffectiveness of these agents against IMP dehydrogenase in the parasite may be because; 1) insufficient uptake of the drug, 2) lack of conversion to their corresponding ribonucleotides, or 3) lack of recognition as substrate by the enzyme.

The antitrichomonal agent, metronidazole, was found (as expected) to be a potent inhibitor of T. foetus growth with an IC_{50} of 6 μM. Metronidazole also completely inhibited the incorporation of hypoxanthine, adenine and adenosine. The non-specific nature of its inhibition is not so surprising since the mode of action of metronidazole has been suggested to proceed via a very reactive reactive reduced intermediate (See Dissertation Introduction). This intermediate could concievably react with any and all neighboring proteins. The inactivation of purine metabolism by metronidazole seems to be an additional cause for inhibition of T. foetus growth. The exact mode of action for metronidazole and its reactive intermediate is still unknown.

Several inhibitors and their modes of action have been examined on the purine and pyrimidine metabolism of T. foetus. The importance of uracil phosphoribosyltransferase, hypoxanthine phosphoribosyltransferase, adenylosuccinate synthetase and IMP dehydrogenase have been demonstrated with the use of authentic inhibitors and have corroborated the pathway elucidated from previous work (142,157). These four

enzymes are indeed potential sites for chemotherapeutic drug design. Inhibition of any one of these enzymes will inhibit the growth of T. foetus in HUT medium. Further work will be required to examine these potential sites more closely.

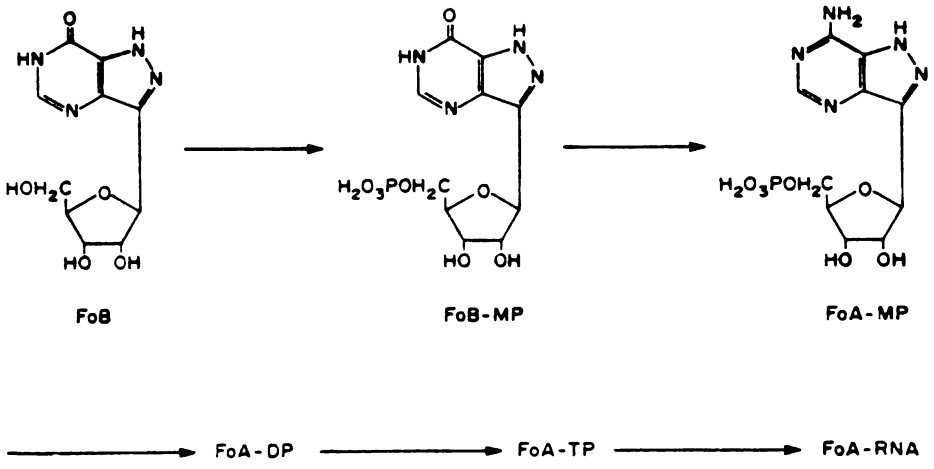

FIGURE 3.13. Proposed metabolism of formycin B in Trypanosoma cruzi epimastigotes (150).

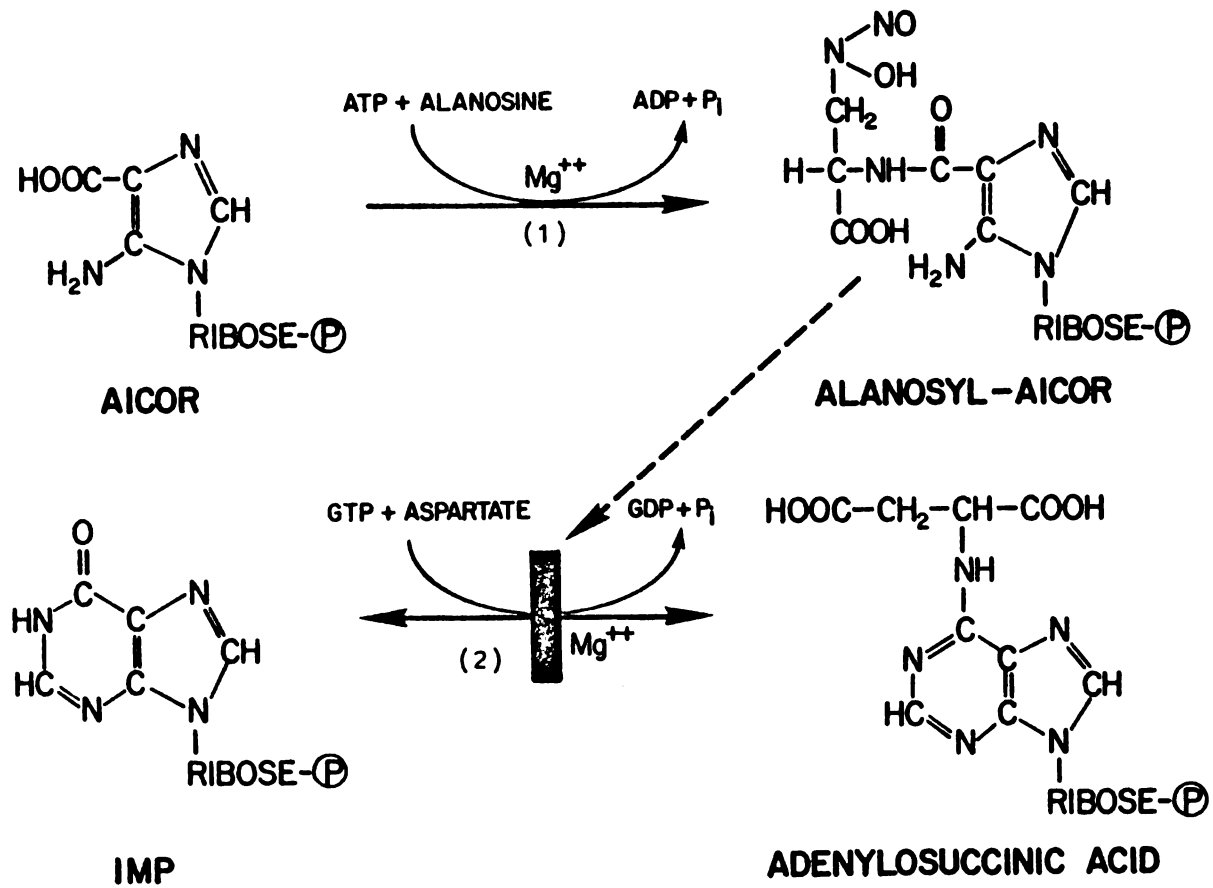

FIGURE 3.14. Proposed mode of action by the active anabolite of L-alanosine on adenylosuccinate synthetase (156). Enzymes: 1, SAICAR synthetase; 2, Adenylosuccinate synthetase.

CHAPTER 4

INOSINE 5'-MONOPHOSPHATE DEHYDROGENASE FROM TRITRICHOMONAS FOETUS

INTRODUCTION

Tritrichomonas foetus is a protozoan anaerobic parasite infecting the urogenital tract of cattle. The parasite has been reported to be incapable of de novo purine synthesis and dependent upon the salvage of hypoxanthine to fulfill its purine requirements (157). The parasite's reliance upon exogeneous sources for its purine needs would likely make it more susceptable to inhibitors of purine salvage. One such inhibitor of purine metabolism, mycophenolic acid, is an inhibitor of two enzymes which are essential for the synthesis of guanine nucleotides, inosinate dehydrogenase and guanylate synthetase, in mammalian cells (165). Recent work by Wang et al (165), have revealed that mycophenolic acid inhibits the growth of T. foetus in vitro and also inhibits the conversion of hypoxanthine and adenine to guanine nucleotides. This and additional work showing the reversal of growth inhibition by guanine or guanosine suggested that the IMP dehydrogenase of T. foetus was susceptable to mycophenolic acid inhibition and that the enzyme inhibition will lead to cessation of growth.

Inosine-5'-monophosphate occupies a key position in T. foetus purine metabolism, being the common precursor for the de novo biosynthesis of adenine and guanine nucleotides. IMP dehydrogenase

(IMP:NAD^+ oxidoreductase, E.C. 1.2.1.14) catalyzes the oxidation of IMP to xanthosine-5'-monophosphate (XMP) with the concommitant reduction of NAD^+ (167-169). It has been shown in extracts of bacteria (168, 170, 171), higher plants (172,173) and animals (161, 169, 173). The enzyme represents the first reaction unique to the biosynthesis of guanine nucleotides and is a potential site for metabolic control of guanine nucleotide and nucleic acid biosynthesis. The activity of IMP dehydrogenase is subject to repression in bacterial cells (174) and to negative feedback control by GMP (175).

Early kinetic studies and end product inhibition studies with the Aerobacter aerogenes IMP dehydrogenase enzyme had indicated that IMP is bound to the enzyme first followed by the coenzyme NAD^+, and that XMP was the last product to be released from the active site (162, 176,177). Subsequent investigations into steady state kinetics and isotope exchange at equilibrium in the presence of several different concentrations of K^+ ions have shown that the mechanism is random with respect to the addition of IMP and K^+ to the enzyme but that NAD^+ reacts only with the enzyme-K^+ and enzyme-K^+-IMP complexes (178). This binding sequence differs markedly with most other NAD^+-dependent dehydrogenases, such as lactate dehydrogenase (L-lactate:NAD^+ oxidoreductase, E.C. 1.1.1.27). The latter is a typical bisubstrate enzyme with compulsory order of addition of substrates; the coenzyme is the leading substrate to generate the enzyme-NAD^+ binary complex which then accepts the specific substrate, lactate, to form the ternary enzyme-NAD^+-lactate complex.

The purpose of this study is to purify and examine the IMP dehydrogenase found in T. foetus. A close examination of its physical and kinetic characteristics are performed so that a comparison of the enzyme between the mammalian and this protozoan source may be made. The potential of IMP dehydrogenase as a site for chemotherapeutic intervention may then be evaluated.

MATERIALS AND METHODS

CHEMICALS

[8-^{14}C]Hypoxanthine (50.0 mCi/mmol), [8-^{14}C]guanine (51.0 mCi/mmol) and [8-^{14}C]xanthine (41.0 mCi/mmol) were purchased from New England Nuclear. DEAE-Sepaharose was obtained from Pharmacia Fine Chemicals. Gel filtration standards, Bio-Gel A 0.5m, Ultrapure PAGE chemicals and PAGE standards were purchased from BIO-RAD. Mycophenolic acid was a generous gift from Prof. Wolfgang Sadee. All other chemicals used were of the highest purities commercially available.

CULTURES

T. foetus strain KV_1, was cultivated in Diamonds TYM (100) medium pH 7.2 supplemented with 10% heat inactivated horse serum and 1% antibiotic/antimycotic mix at 37°C. Stationary cultures having a cell density of about 2 x 10^7 cells/ml were used to inoculate fresh media at a 1:10 ratio (10%). Midlogarithmic phase of growth, with a cell density of 10^7/ml, was achieved by using a 4% inoculum and harvesting cells after 16 hours of incubation. Cell number was determined in a Coulter ZF counter.

ENZYME ASSAYS

Assay of IMP Dehydrogenase. IMP dehydrogenase was assayed by a modified procedure of Brox and Hampton (177). Enzyme activity was measured by following the increase in absorbance at 290 nm due to the

conversion of IMP to XMP (ε = 3,910 M^{-1} cm^{-1} at 290 nm). Each cuvette (1.0 cm light path) contained 50 mM Tris-HCl pH 8.1, 100 mM KCl, 1 mM DTT, 1.6 mM NAD and the enzyme. The mixture was warmed for 5 minutes at 37°C and the reaction initiated by addition of IMP (0.5 mM final). The resulting change in absorbance at 290 nm was recorded against a blank which lacked IMP, in a Beckman Model DU-7 spectrophotometer. The unit of enzyme activity was defined as that which effected an increase in absorbance of 1.0 in 1 minute. In kinetic experiments, inhibitors were added to the assay system before the addition of enzyme. Protein was determined by the method of Lowry (179) using bovine serum albumin as standard.

Assay of Adenylosuccinate Synthetase. Adenylosuccinate synthetase was measured by the procedure of Fischer, Muirhead and Bishop (180). The reaction mixture contained 50 mM HEPES pH 7.0, 0.2 mM IMP, 0.5 mM GTP, 4 mM $Mg(OAc)_2$ and enzyme. The mixture incubated at 37°C for 5 minutes and the reaction started by the addition of L-aspartate (4 mM final). The change in absorbance at 280 nm was recorded against a blank without the L-aspartate.

Assay of GMP Synthetase. GMP synthetase activity was measured by the method of Sakamoto (181). The reaction mixture consisted of 0.17 M Tris-HCl pH 8.5, 4 mM ATP, 16 mM $MgCl_2$, 24 mM XMP and 333 mM $(NH_4)_2SO_4$. After warming to 37°C, an enzyme sample was added to start the reaction. The change in absorbance at 290 nm was recorded against a blank which contained no XMP.

Assay of Phosphatase. Acid Phosphatase activity was assayed for

by following the appearance of p-nitrophenol at 405 nm. The reaction mixture contained 6 mM p-nitrophenyl phosphate, 50 mM NaOAc pH 4.8 and enzyme. The reaction was monitored by following the change in absorbance at 405 nm at 37°C for 30 minutes. When a nucleotide was used as substrate instead of p-nitrophenyl phosphate the reaction products were analyzed by HPLC.

Assay of Phosphoribosyltransferase. Phosphoribosyltransferase activity was assayed by the modified procedure of Schmidt et al (136). The assay mixture consisted of 100 mM Tris-HCl pH 7.8, 8 mM $MgCl_2$, 1 mM PRPP, 50 µg/ml BSA and 20 µM radiolabeled purine or pyrimidine base. The reaction was initiated by the addition of enzyme, incubated for 10 minutes at 37°C, and terminated by the addition of a 10-fold excess of cold 5 mM NH_4OAc pH 5.0. The mixture was filtered through a PEI-cellulose covered GF/B filter and the adsorbed counts determined using a Beckman Model 3133T liquid scintillation counter.

Assay of NADH oxidase. NADH oxidase activity was determined in 50 mM Tris-HCl pH 8.1, 100 mM KCl, 1 mM DTT and 0.4 mM NADH at 37°C. The reaction was initiated by adding enzyme and recording the decrease in absorbance at 340 nm.

HPLC ANALYSIS OF NUCLEOTIDES

Concentration and identification of nucleotides by HPLC, formed in the various assays, were performed as described previously (142). Briefly, nucleotides were separated by anion exchange on an Ultrasil AX (10 micron) 4.6 x 250 mm column using gradient elution from 7 mM KH_2PO_4 pH 3.8 to 250 mM KH_2PO_4 plus 500 mM KCl pH 4.5. The flow rate

was 1 ml/min and the effluent was monitored at 254 nm in a Beckman Model 160 UV detector.

POLYACRYLAMIDE GEL ELECTROPHORESIS

Native polyacrylamide electrophoresis was performed with a Hoeffer apparatus employing the method of Chramback et al (182). Step 5 protein was suspended with 10% glycerol and layered onto polyacrylamide tube gels (6% T, 5% C_{BIS}). The samples were then electrophoresed at 4°C for 16 hours at 5 mA/gel. The gels were removed and stained for protein (183). Duplicate gels were also stained for IMP dehydrogenase activity by a modified dehydrogenase procedure (184). The activity stain mixture contained 100 mM IMP, 4 mM NAD, 0.5 mM $MgCl_2$, 10 mM KCl, 0.375 mM nitro-blue tetrazolium, 0.1 mM phenazine methosulfate (PMS) and 200 mM Tris-HCl pH 7.2. Gels were first soaked in 200 mM Tris-HCl pH 7.2 for 15 minutes and then incubated with the activity stain for 6 hours at 37°C. Gels stained without IMP served as controls. Bands of enzyme activity were excised from the gel, homogenized and prepared for SDS-PAGE. SDS-PAGE was done according to the method of Laemmli (185) using 10% T, 5% C_{BIS} polyacrylamide slabs. Slabs were run at 15 mA/slab for 16 hours at 8° C. The gels were then stained for protein using Coomassie Blue R-250.

NATIVE MOLECULAR WEIGHT DETERMINATION

Gel filtration of the crude extract was performed using Bio-Gel A 0.5m (1.5 x 100 cm) and 25 mM KH_2PO_4 pH 7.2 and 1 mM DTT as buffer. The column was first calibrated with Bio-Rad standard protein

mixtures. Samples were allowed to sit at 4°C with or without 1 M NaCl before loading onto the column. Gel filtration was done in the absence and presence of 1 M NaCl for comparisons.

$s_{20,w}$ DETERMINATION

The sedimentation behavior of purified IMP dehydrogenase (20 µg of step 5 protein) was determined on a 12 ml 10-30% (w/w) isokinetic sucrose gradient containing 25 mM Tris pH 7.2, 20 mM KCl, 6 mM $MgCl_2$ and 1 mM DTT. The gradient was formed by the procedure of McCarty et al (189) and centrifuged at 4° C with a SW 41 rotor in a Backman L8-M centrifuge at 148,000 x g for 48 hours. After centrifugation, a hole was punched in the bottom of the centrifuge tube and fractions were collected and analyzed. Sedimentation coefficient ($s_{20,w}$) values were determined by comparison to standards. The standards used for these measurements were yeast alcohol dehydrogenase (7.6 S), bovine serum albumin (4.5 S) and cytochrome C (1.7 S). The position of cytochrome C was determined by following the absorbance at 410 nm, that of bovine serum by following the absorbance at 280 nm, and that of yeast alcohol dehydrogenase by enzymatic assay (190).

RESULTS

PURIFICATION OF IMP DEHYDROGENASE

Step 1. Homogenization- T. foetus, in midlogarithmic phase of growth, were collected by centrifugation. The cells were washed three times and resuspended in an equal volume of buffer A (50 mM Tris-HCl pH 7.2 and 1 mM DTT). This and all subsequent steps were performed at 4°C. Protease inhibitors; 1 mM 1,10 phenanthroline, 1 mM benzamidine and 0.05 mM PMSF, were added to the cell suspension and then sonicated with a HEAT systems sonicator Model W-375, at 20% output, using three 30 second bursts. The routine addition of these protease inhibitors had no observed effect on IMP dehydrogenase activity per se but protected the enzyme from protease degradation. The homogenate was centrifuged at 78,000g for 135 minutes in a Beckman Model L-8M Ultracentrifuge. Subcellular fractionation studies showed that >95% of the total IMP dehydrogenase activity in T. foetus crude homogenate was in the 100,000g supernatant fraction.

Step 2. Ammonium Sulfate Fractionation- To the supernatant in step 1, saturated $(NH_4)_2SO_4$ pH 7.2 was added to 45% saturation and stirred for 1 hour. After centrifugation at 10,000 x g for 20 minutes, more $(NH_4)_2SO_4$ was added to the supernatant to reach 75% saturation. After 1 hour the precipitate was collected by centrifugation like before and resuspended in a minimum volume of buffer A. Ammonium sulfate fractionation precipated 80-90% of the total activity

from the previous step.

Step 3. Gel Filtration- Step 2 protein was applied to a Bio-Gel A 0.5m column (2.6 x 48 cm) previously equilibrated with buffer B (25 mM KH_2PO_4 pH 7.2, 1 mM DTT). The column was eluted with the starting buffer and fractions containing IMP dehydrogenase activity were pooled. The enzyme eluted near the void volume on a Bio-Gel A 0.5m column (Figure 4.1). Calibration of the column with proteins of known molecular weights (Figure 4.2, 4.3) allowed an estimation of the native molecular weight of IMP dehydrogenase as 380,000.

Step 4. Ion Exchange- The pooled fractions from step 3 were loaded onto a DEAE-Sepharose column (1.8 x 67 cm) equlibrated with buffer B. The column was washed with 200 ml of buffer B + 50 mM KCl and the enzyme eluted by a 200 ml linear gradient of buffer B + 75 mM KCl to buffer B + 225 mM KCl. Fractions containing IMP dehydrogenase activity were pooled and dialysed/concentrated against buffer A using a Micro-ProDicon. The salt gradient was monitored using a YSI Model 32 Conductance meter with K = 1.0/cm for the cell. The IMP dehydrogenase was coeluted with a yellow colored protein exhibiting high NADH oxidase activity from the DEAE-Sepharose column (Figure 4.4).

Step 5. Cibacron Blue-Sepharose- Optimum conditions for enzyme binding to Cibacron blue (Step 5) was found to be within a pH range of 7.2-7.7 with a 50 mM Tris-HCl and 1 mM DTT buffer. The dialyzed enzyme from step 4 was loaded onto a Cibacron Blue column (1.0 x 4.0 cm) previously equilibrated with buffer A. The column was washed with

60 ml of buffer A + 150 mM KCl. The enzyme was eluted from the column with buffer A + 120 mM KCl + 30 mM IMP (Figure 4.5). Fractions with activity were pooled and concentrated/dialyzed against buffer A. The enzyme could also be eluted with 20 mM NAD in the same buffer but the specific activity was much lower. Washing the Cibacron blue column with 150 mM KCl removed the NADH oxidase activity from the preparation. The results of the purification procedure are summarized in Table 4.1. The overall yield, with the outlined purification procedure was about 42% with a 500 fold purification. Step 5 protein is free of contaminating enzyme activities such as; AMP synthetase, GMP synthetase, NADH oxidase, Hypoxanthine-Guanine-Xanthine phosphoribosyltransferases, Adenylosuccinate synthetase and acid phosphatase. The enzyme preparation obtained after Step 5 was stable for up to 6 weeks at -80°C in the indicated buffer.

PHYSICAL PROPERTIES AND SUBUNIT MOLECULAR WEIGHT

When the purified enzyme (Step 5) was denatured with sodium dodecyl sulfate, dithiothreotol and β-mercaptoethanol (SDS-PAGE) and electrophoresed on 10% polyacrlyamide gels, one major and several minor Coomassie blue stained bands were observed (Figure 4.7 lane 4). Step 5 protein was also electrophoresed on native tube gels of 7.5% polyacrylamide, and stained for IMP dehydrogenase activity (Figure 4.6). The single activity band which corresponds to the major protein band was excised, minced and loaded onto SDS-PAGE. After Coomassie blue staining, this excised protein showed up as closely associated

double bands (Figure 4.7 lane 2). By comparison of the migration of these bands to proteins of known subunit molecular weight, the subunit molecular weight of IMP dehyrogenase appears to be about 58,000.

Gel filtration of the Step 2 preparation with Bio-Gel A 0.5m yielded one or two peaks of activity depending upon the procedure employed. When the pelleted enzyme obtained after ammonium sulfate fractionation were resuspended in buffer and immediately applied to the gel filtration column, two activity peaks with estimated molecular weights of 380,000 and 270,000 would be eluted. While, if the resuspended pellet was allowed to incubate at 4°C for a short duration only one peak of activity, of molecular weight 380,000, would be eluted. Further examination of this phenomenon entailed eluting the gel filtration column with and without 1 M NaCl added to the buffer. Bio-Gel A 0.5m (191) and Ve/Vo ratios of standard proteins used in calibrating the column (Vitamin B_{12}, Myoglobin, Ovalbumin, IgG and Thyroglobulin) were unaffected by the added salt. When IMP dehydrogenase is run on Bio-Gel A 0.5m using 25 mM KH_2PO_4 pH 7.2 and 1 mM DTT, only one peak of activity is eluted with a native molecular weight of 380,000. In the presence of 1M NaCl, a single peak of IMP dehydrogenase activity is eluted with a corresponding molecular weight of 270,000 (Figure 4.8). IMP dehydrogenase appears as two peaks of activity (Figure 4.12) following isokinetic sucrose centrifugation with sedimentation coefficients of 8.8 and 11.4 S. The smaller form is similar to the IMP dehydrogenase found in Aerobacter aerogenes, 9.1 S (177).

PROPERTIES OF THE ENZYMIC REACTION

The effect of pH on the enzyme activity within the range of 4.0-9.0 was tested. Citrate/phosphate/borate (100 mM) were used for the pH range 3-9, 50 mM NaOAc pH 4-5.7, 50 mM NaH_2PO_4 pH 5.7-8.0 and 50 mM Tris-HCl pH 7.2-9.0. IMP dehydrogenase was found active in both Tris and phosphate buffers and exhibited a pH optimum of 8.0 (Figure 4.9). The effect of various inorganic salts was examined using 50 mM Tris-HCl pH 8.1, 1 mM DTT, 2 mM NAD and 0.5 mM IMP. The results show IMP dehydrogenase inhibited by Mg^{++}, Na^+, and NH_4^+, and slightly activated by K^+ (Figure 4.10). High concentrations of NAD^+ (>3 mM) is also inhibitory to IMP dehydrogenase activity (Figure 4.11). Incubation of the enzyme at pH 8.1 with 2.3 mM XMP and 0.2 mM NADH did not result in a decrease in the absorbance at 340 nm. Such a decrease would be due to the net conversion of NADH and XMP to NAD^+ and IMP, respectively. The reaction is apparently irreversible.

INITIAL VELOCITY KINETICS

The activity of IMP dehydrogenase was measured by the change in absorbance at 290 nm; under the conditions used the reaction velocity was constant for about 20 minutes and was a linear function of the amount of enzyme used in the assay. The initial velocity of the enzymatically catalyzed reaction was determined at several concentrations of NAD^+ and IMP in 50 mM Tris-HCl pH 8.1, 1 mM DTT and 100 mM KCl. The reciprocal of the initial velocity was graphed as a function

of the reciprocal of the concentration of IMP or NAD^+ at several fixed concentrations of one of the other reaction components (Figure 4.20, 4.21) The lines in Figures 4.20 and 4.21 intersect in the upper left hand quadrants. The extrapolated V_{max} were essentially the same, 14.3 and 18.1 μM/min. The K_m values for IMP and NAD^+ were 18 μM and 445 μM, respectively.

PRODUCT INHIBITION PATTERNS

Inhibition of IMP dehydrogenase by XMP was competitive with respect to IMP (K_i = 27 μM) (Figure 4.22) and noncompetitive with respect to NAD^+ (K_i = 640 μM) (Figure 4.23). GMP, not a product of this reaction but the product of the reaction catalyzed by GMP synthetase, is a dead end inhibitor of IMP dehydrogenase and we examined its effect on IMP dehydrogenase of T. foetus. It was a competitive inhibitor with IMP (K_i = 95 μM) (Figure 4.24) but had no effect on NAD^+; 5 mM GMP did not affect the reaction with respect to NAD^+ at a fixed IMP concentration of 2 mM. When the effects of GMP were examined at subsaturating IMP or NAD^+ levels, we found a similar competitive inhibition pattern for GMP with respect to IMP (Figure 4.25) but GMP was a noncompetitive inhibitor with respect to NAD^+ (Figure 4.26).

The other product of the reaction, NADH, also inhibited IMP dehydrogenase activity. Kinetically the inhibition by NADH was noncompetitive with respect to IMP and NAD^+ with K_i's of 320 μM and 210 μM respectively (Figure 4.27, 4.28).

INHIBITION OF IMP DEHYDROGENASE

Mycophenolic acid was a potent uncompetitve inhibitor of IMP dehydrogenase with respect to both NAD^+ and IMP with K_i's of 6 μM and 9 μM, respectively (Figure 4.29, 4.30). The inhibition was not reversible by the addition of either more IMP or NAD^+ to the inhibited enzyme. IMP dehydrogenase was unaffected by up to 1 mM of virazole.

Table 4.1. Purification of IMP Dehydrogenase

	Volume (ml)	Total Activity (Units)	Total Protein (mg)	%Recovery	Specific Activity (U/mg)	Purification
1. 10^5 crude supernatant	289	54.0	2834	100	0.019	1
2. 45-75% $(NH_4)_2SO_4$	27	44.7	2210	83	0.020	1
3. Bio-Gel A 0.5m	154	46.8	782	87	0.059	3
4. DEAE-Sepharose	11.8	28.2	34.5	52	0.818	43
5. Cibacron Blue	3.2	22.6	2.3	42	9.699	506

FIGURE 4.1. Gel filtration of IMP dehydrogenase on Bio-Gel A-0.5m. The column (2.6 x 65 cm) was equilibrated with 25 mM KH_2PO_4, 1 mM DTT pH 7.2 and loaded with 10 ml of step 2 protein. The column was then eluted with starting buffer at a flow rate of 10 ml/hr.

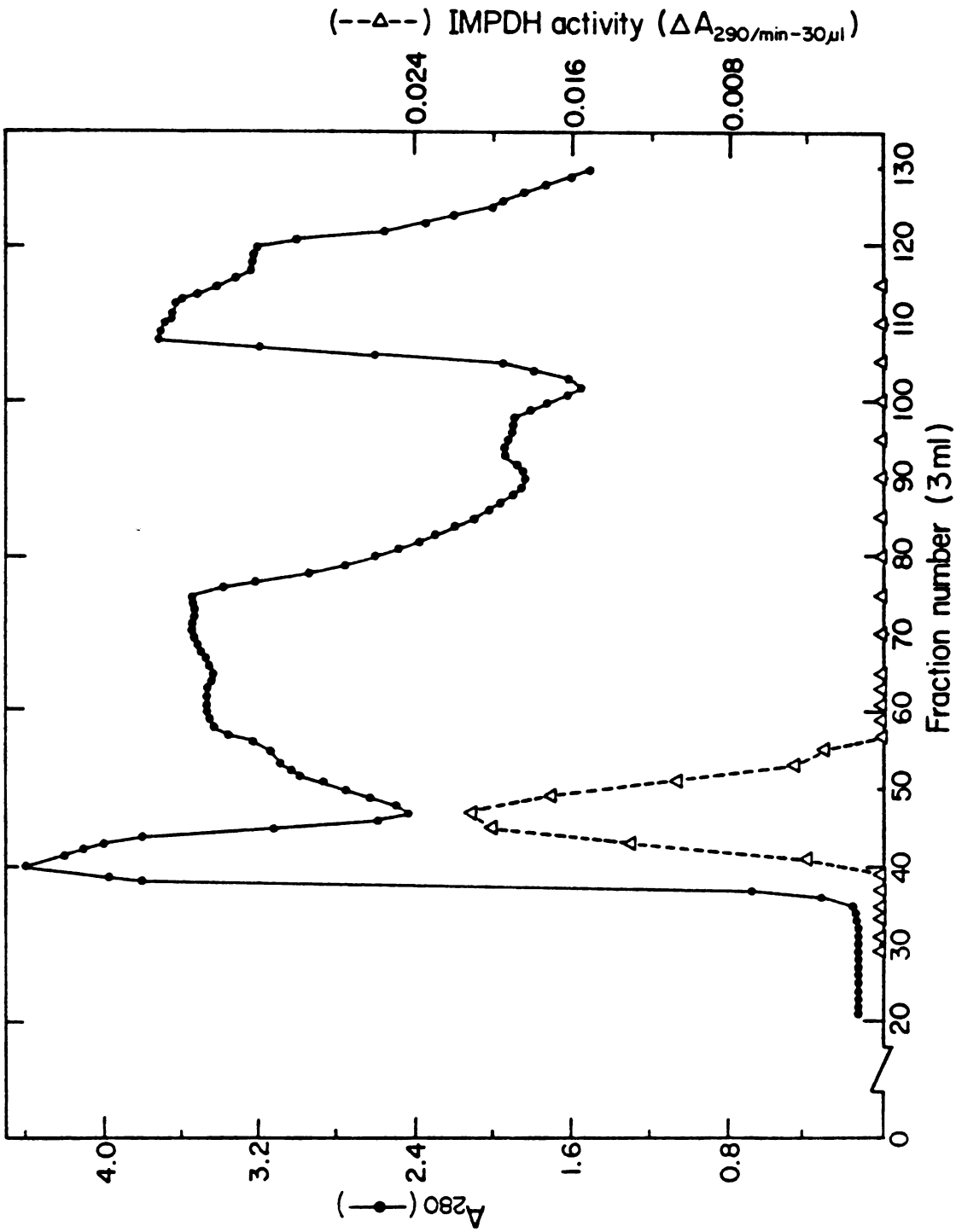
(--Δ--) IMPDH activity (ΔA290/min-30μl)
0.024
0.016
0.008
Fraction number (3ml)
A280 (—●—)
4.0
3.2
2.4
1.6
0.8
0
20
30
40
50
60
70
80
90
100
110
120
130

FIGURE 4.1.

FIGURE 4.2. Calibration of Bio-Gel A 0.5m column (2.6 x 65 cm). The column was equilibrated with 25 mM KH_2PO_4, 1 mM DTT pH 7.2 and loaded with 1 ml of Bio-Rad standards. The proteins were eluted in starting buffer at a flow rate of 10 ml/hr.

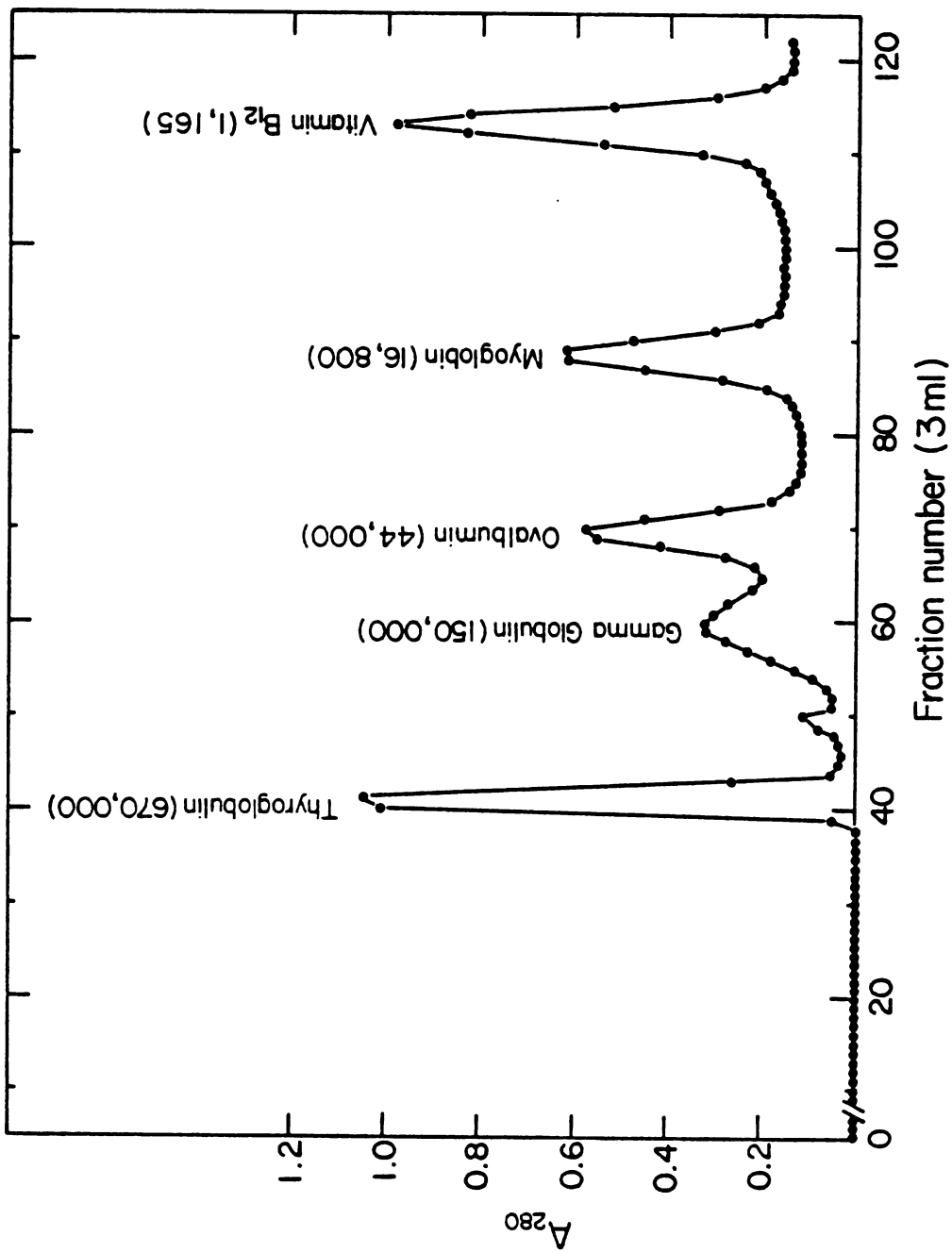
Thyroglobulin (670,000)
Gamma Globulin (150,000)
Ovalbumin (44,000)
Myoglobin (16,800)
Vitamin B12 (1,165)
A280
0.2
0.4
0.6
0.8
1.0
1.2
0
20
40
60
80
100
120
Fraction number (3ml)

FIGURE 4.2.

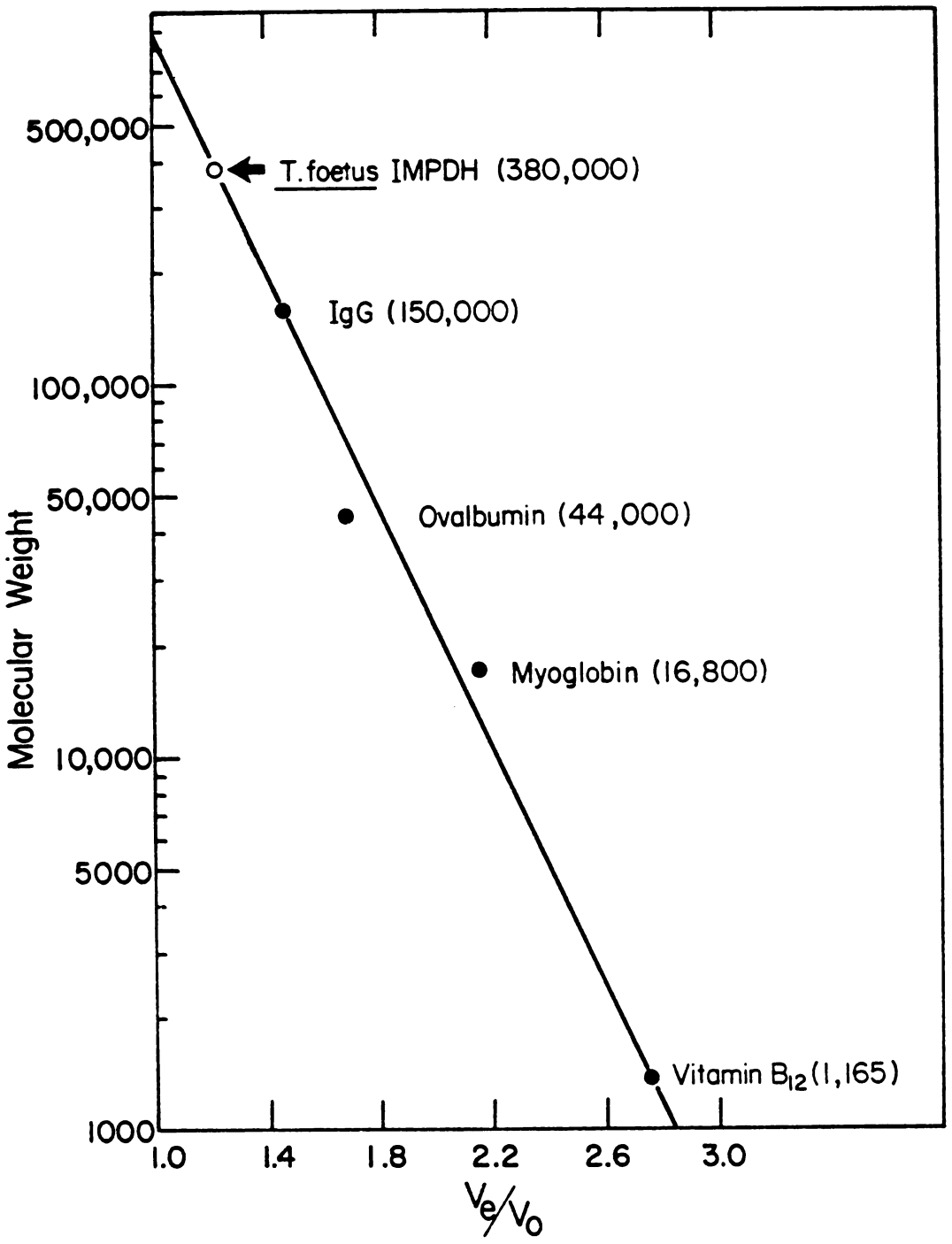

FIGURE 4.3. Standard curve for the determination of molecular weights on a Bio-Gel A 0.5m column (2.6 x 65 cm). The native molecular weight of IMPDH is 380,000 daltons.

FIGURE 4.4. Elution of IMP dehydrogenase from DEAE-Sepharose. Step 3 protein, 218 mg was loaded on the column (1.6 x 18 cm) and eluted with a linear KCl gradient at a flow rate of 20 ml/hr.

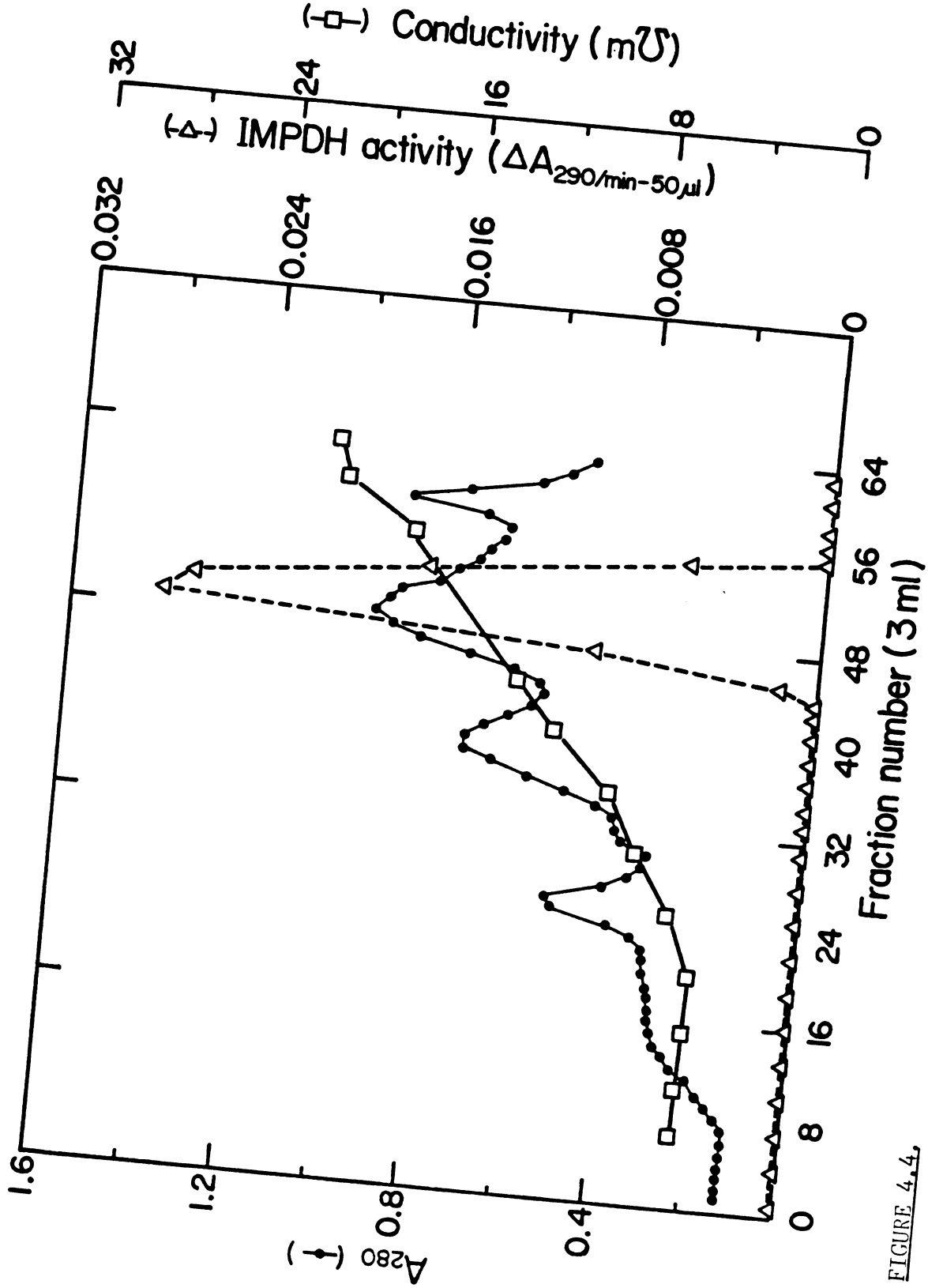
(-□-) Conductivity (m℧)
32
24
16
8
0
(-△-) IMPDH activity (ΔA290/min-50μl)
0.032
0.024
0.016
0.008
0
A280 (-•-)
1.6
1.2
0.8
0.4
0
0
8
16
24
32
40
48
56
64
Fraction number (3 ml)

FIGURE 4.4.

FIGURE 4.5. Step 4 protein, 23 mg, is loaded onto a (2.1 x 10.0 cm) Cibacron blue column. The column is washed with starting buffer, 50 mM Tris-Cl, 1 mM DTT pH 7.2, and then with 150 mM KCl. IMP dehydrogenase activity is eluted by the addition of 30 mM IMP at a flow rate of 11 ml/hr.

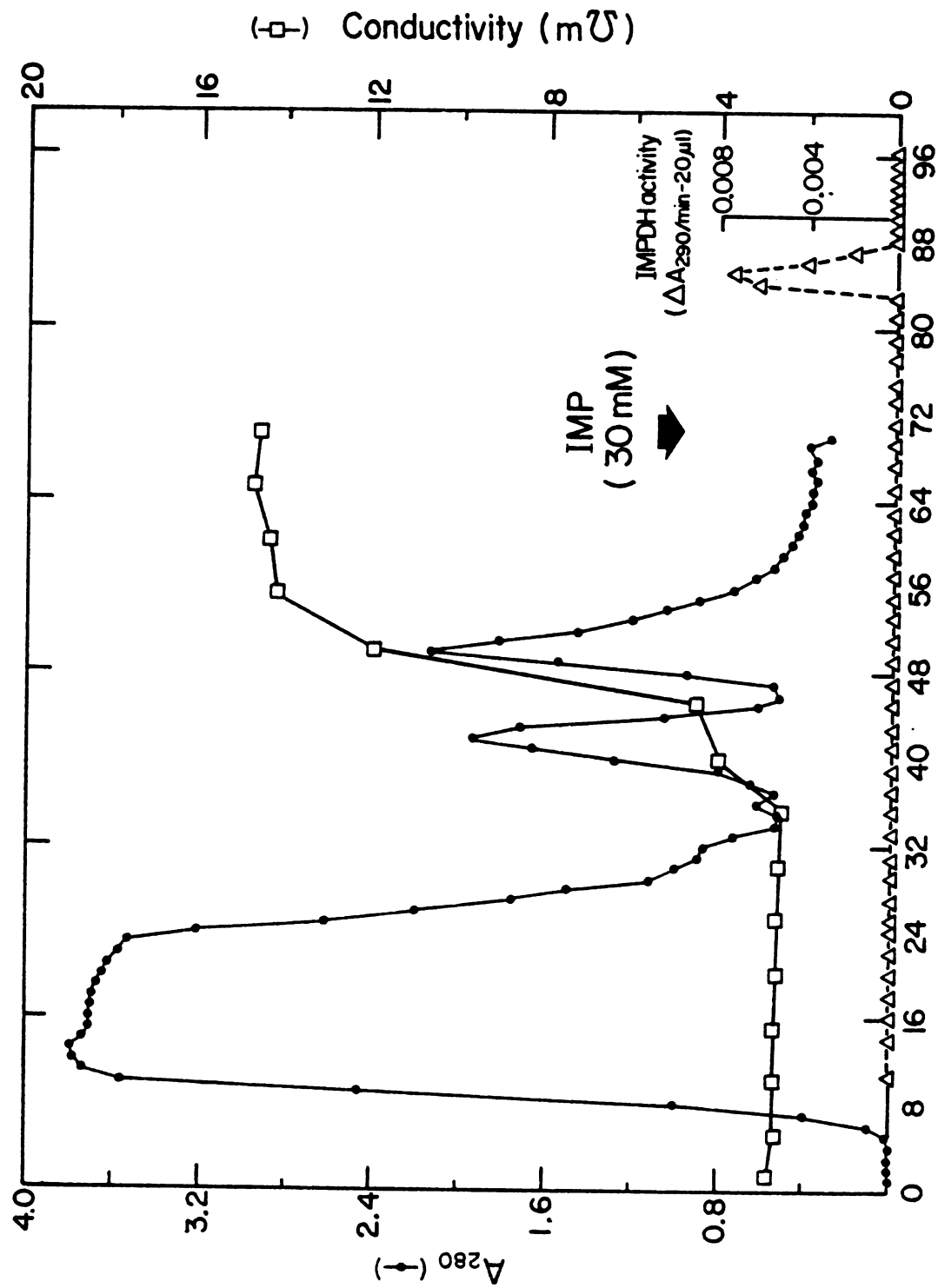
(-□-) Conductivity (m℧)
20
16
12
8
4
0
IMPDH activity
(ΔA290/min-20μl)
0.008
0.004
IMP
(30 mM)
4.0
3.2
2.4
1.6
0.8
A280 (-●-)
0
8
16
24
32
40
48
56
64
72
80
88
96
Fraction number (3 ml)

FIGURE 4.5.

FIGURE 4.6. Native PAGE, 7.5%T and 5%C, of step 5 protein. Loaded 0.1 mg of protein per gel. Gel 1) Coomassie blue stain, Gel 2) activity stain for IMP dehydrogenase and Gel 3) activity stain control - no IMP.

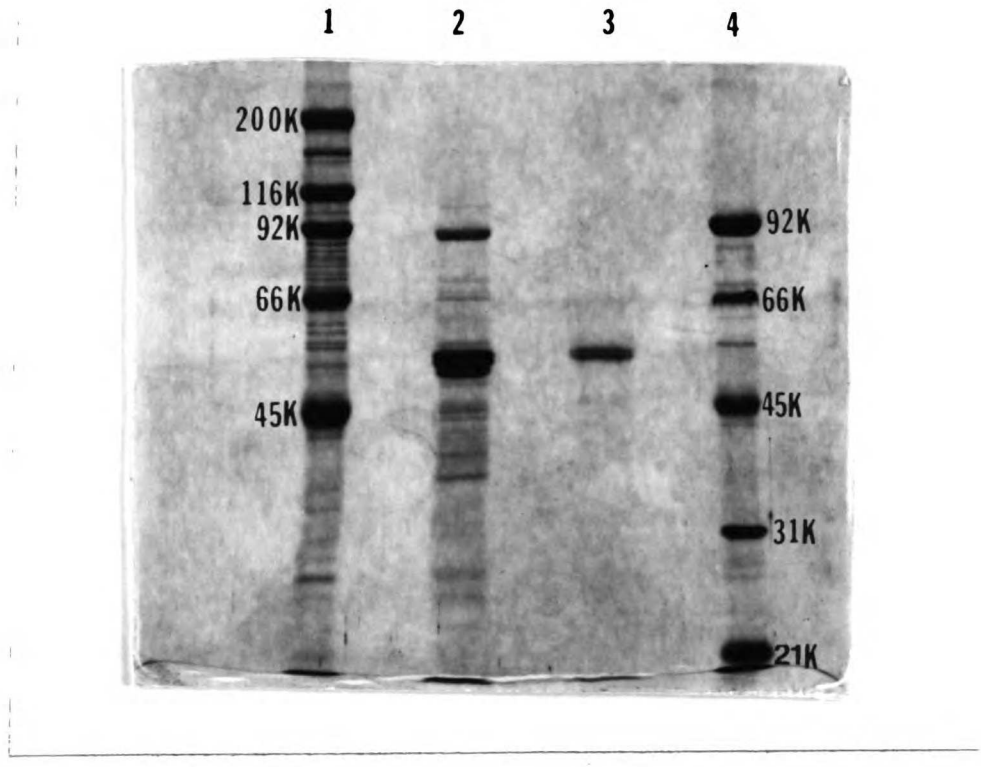

FIGURE 4.7. SDS-PAGE, 10%T and 2.7%C, stained by Coomassie Blue. Lane 1) High M.W. standards, Lane 2) 0.05mg of step 5 protein, Lane 3) Excised protein from native gel which showed IMPDH activity and Lane 4) High M.W. standards.

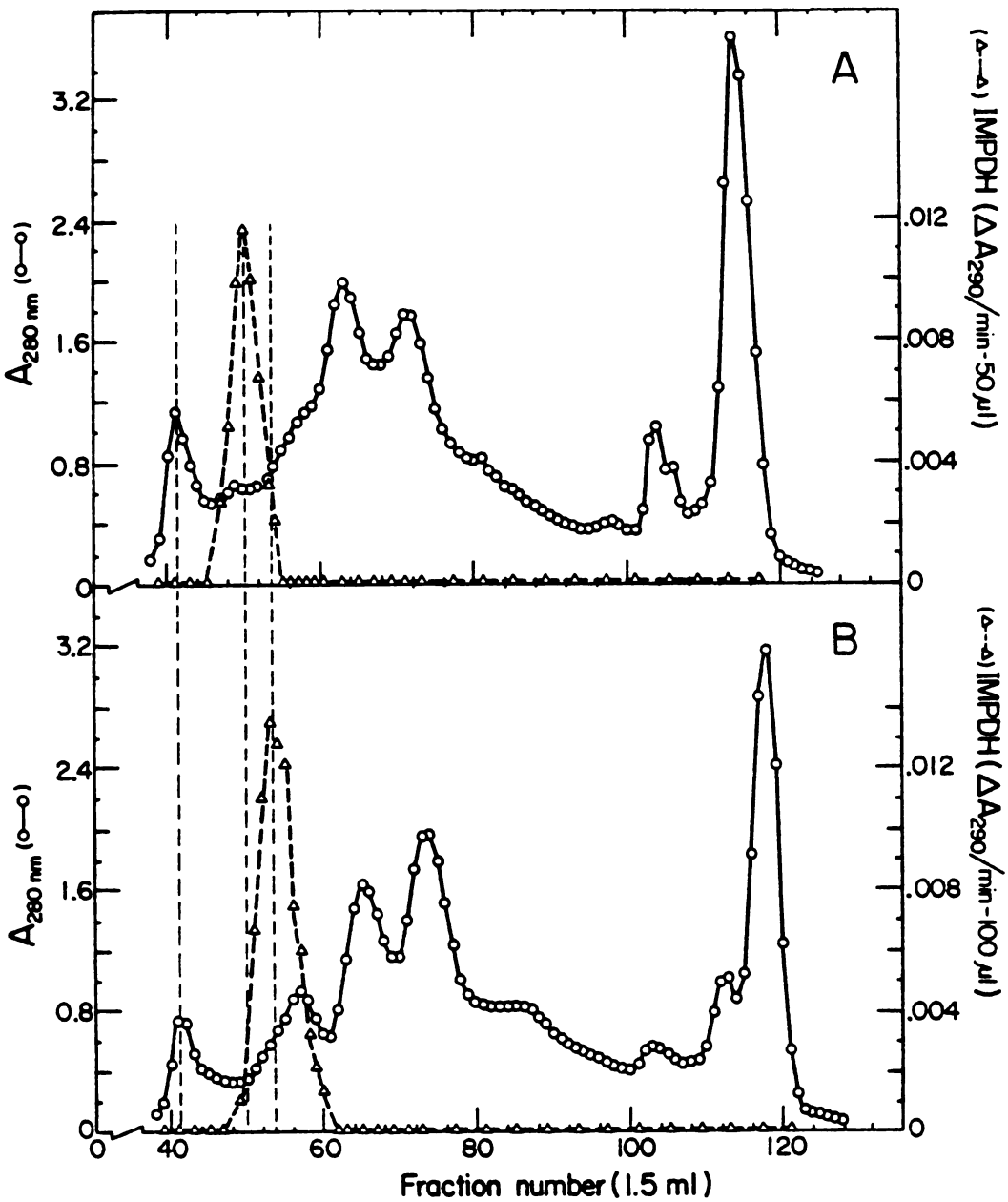

FIGURE 4.8. Gel filtration of IMP dehydrogense on Bio-Gel A 0.5m. The column (1.5 x 100 cm) was equilibrated with 25 mM KH_2PO_4 pH 7.2, 1 mM DTT (A) and with 1 M NaCl (B). One ml of step 2 protein was loaded and the column eluted with starting buffer at a flow rate of 3.5 ml/hr.

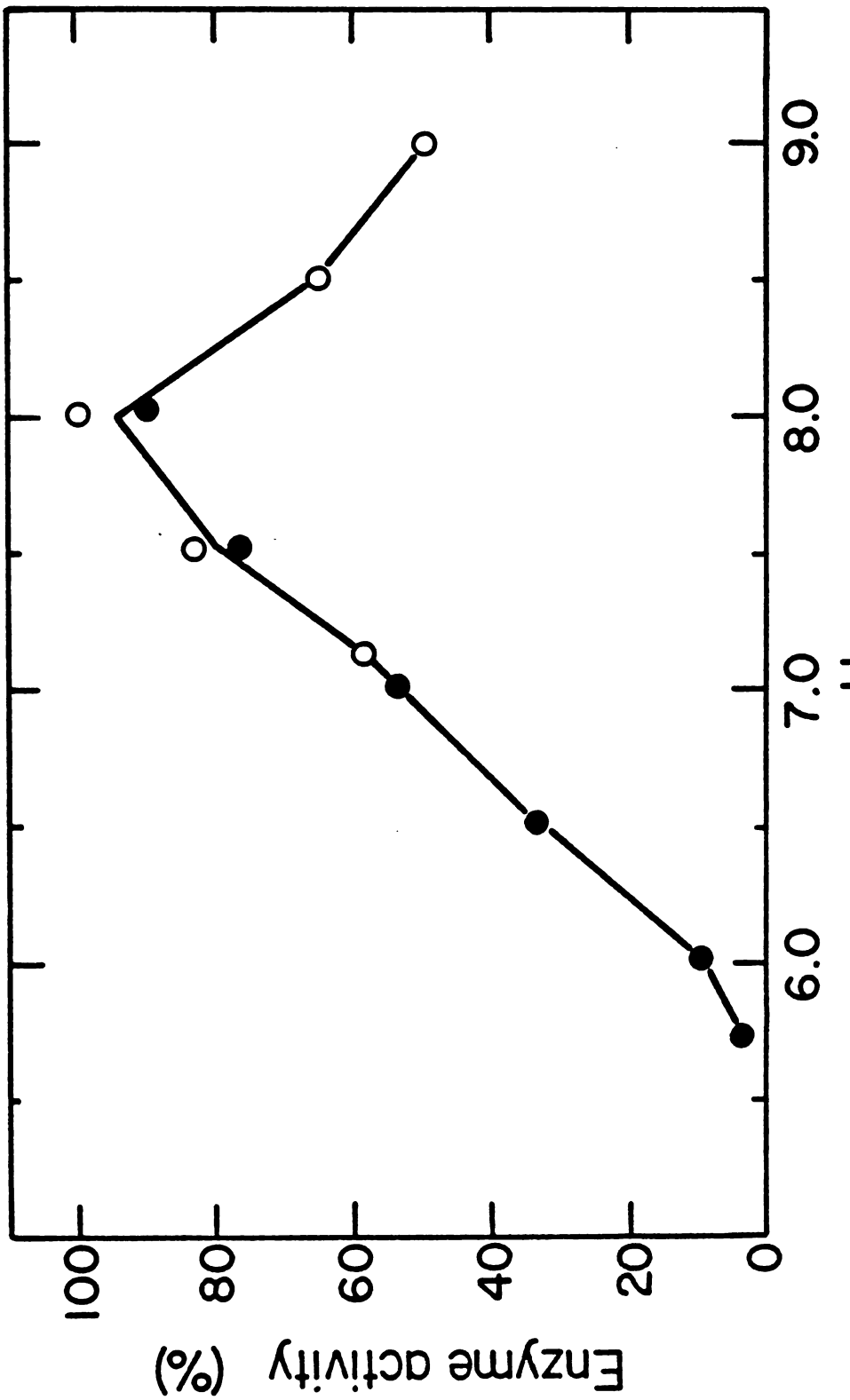

Figure 4.9. Effect of pH on IMP dehydrogenase activity. The buffers used were 50 mM NaH_2PO_4 pH 5.7-8.0 and 50 mM Tris-Cl pH 7.2-9.0. The enzyme was not active below pH 5.7.

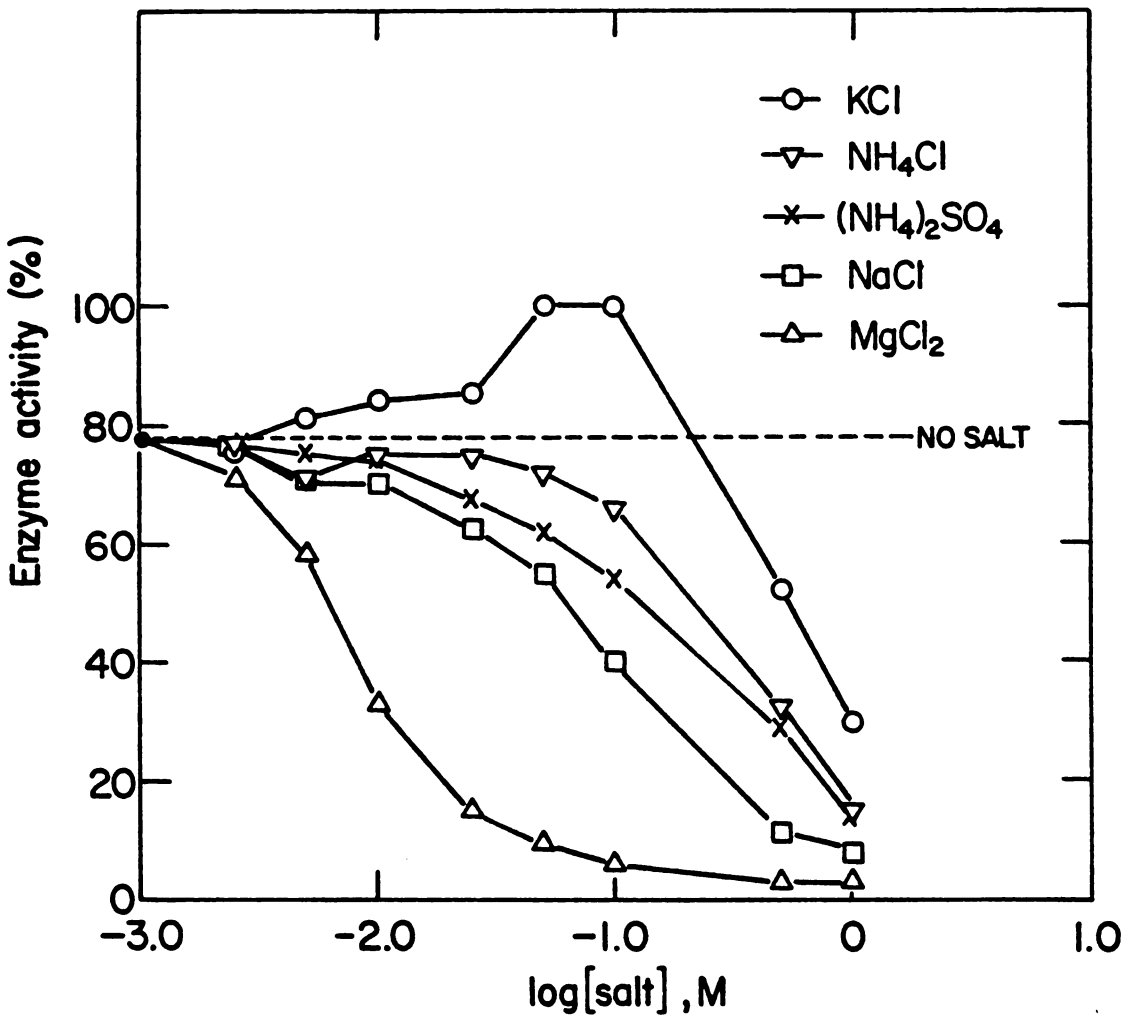

FIGURE 4.10. Effect of inorganic salts on the activity of IMP dehydrogenase. The reactions were conducted with 50 mM Tris-Cl pH 8.1, 2 mM NAD^+ and 0.5 mM IMP.

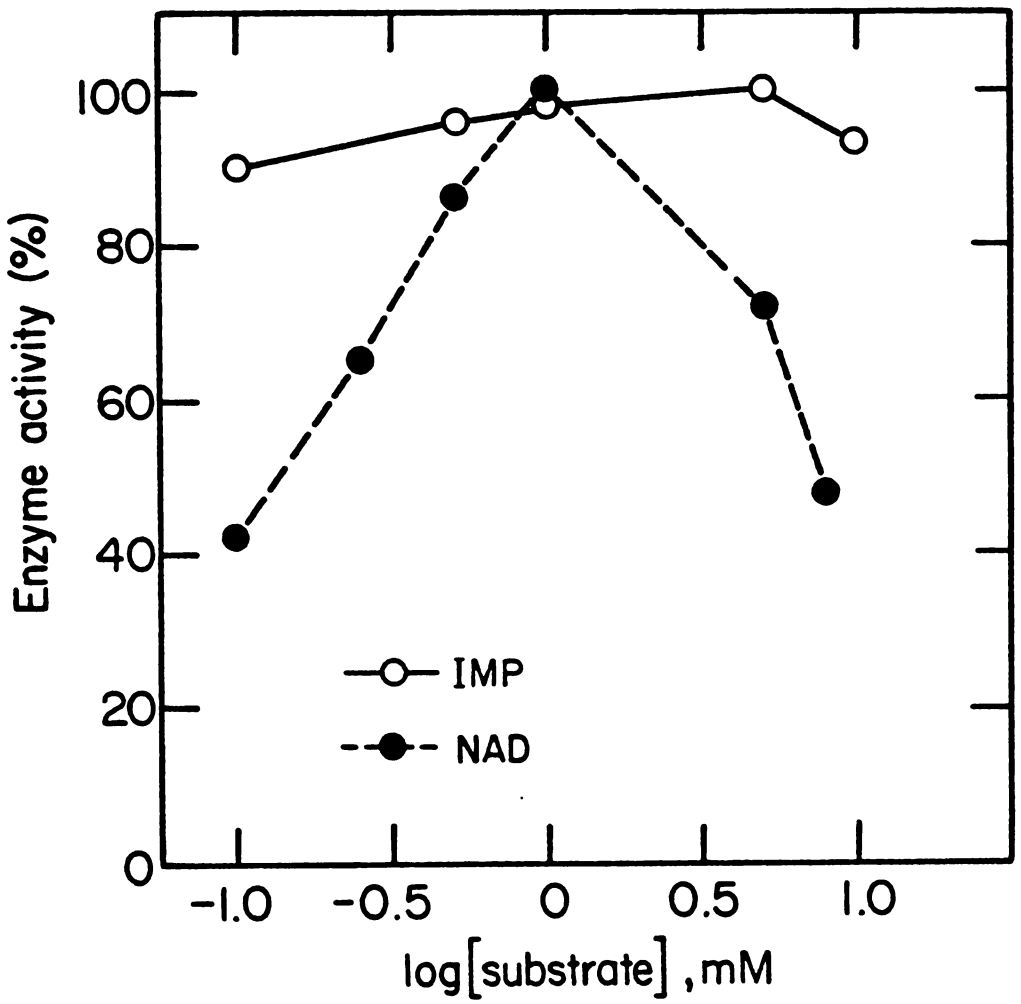

FIGURE 4.11. Effect of the concentration of IMP and NAD^+ on the activity of IMP dehydrogenase. The assays were done in 50 mM Tris-Cl pH 8.1 with varying concentrations of NAD^+ (IMP = 1mM) or IMP (NAD^+ = 2mM).

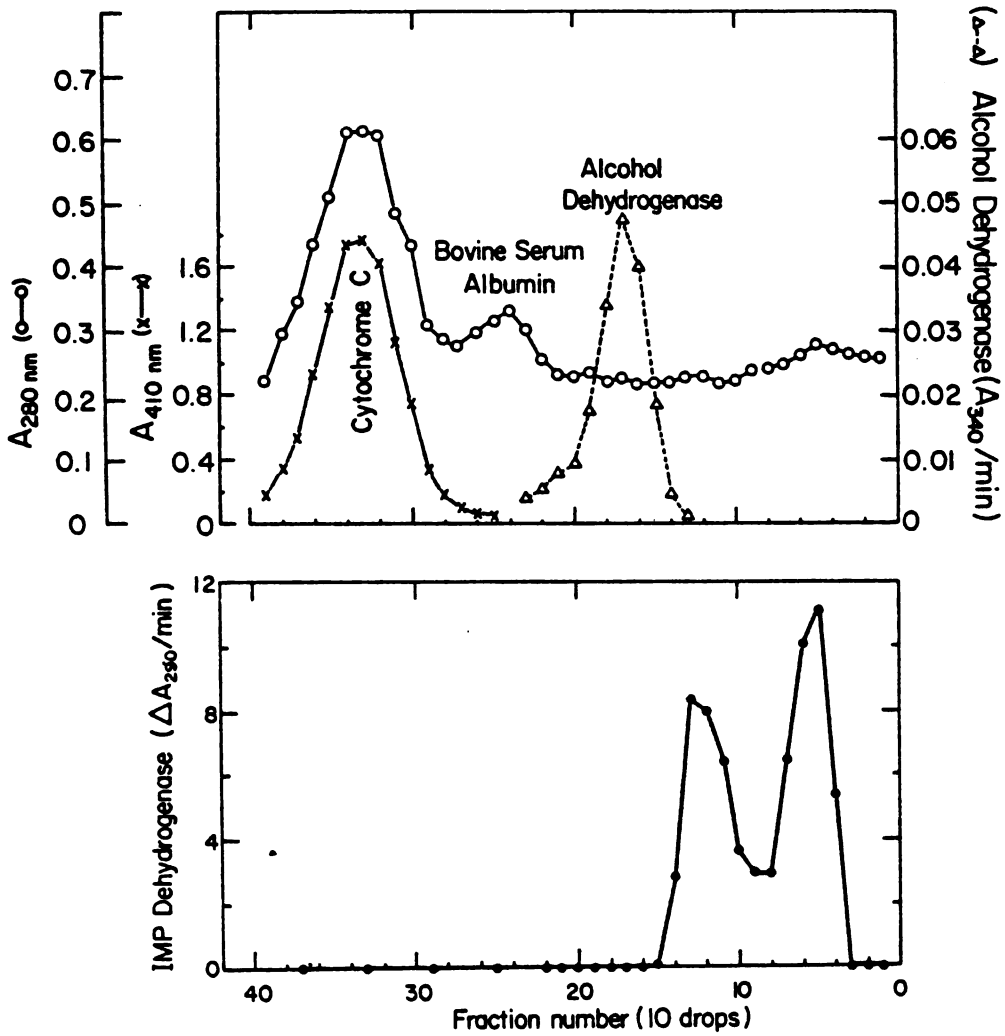

Figure 4.12. Sedimentation behavior of purified IMP dehydrogenase along with the indicated standards, on an isokinetic sucrose gradient as described under "Materials and Methods".

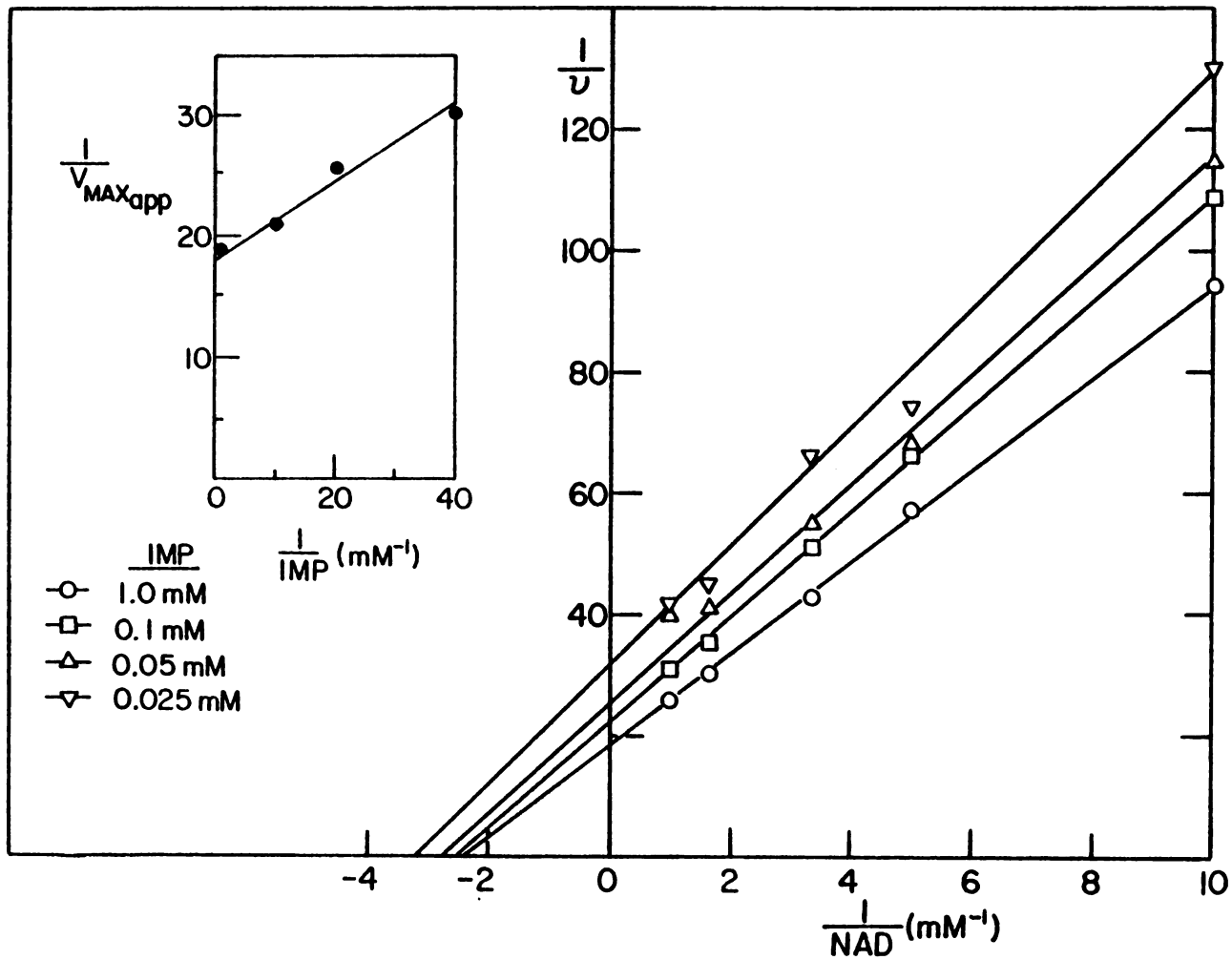

FIGURE 4.20. Lineweaver-Burke plots of initial velocity vs NAD^+ concentration at several constant levels of IMP. Velocities were measured at 290 nm. K_m IMP = 18 μM

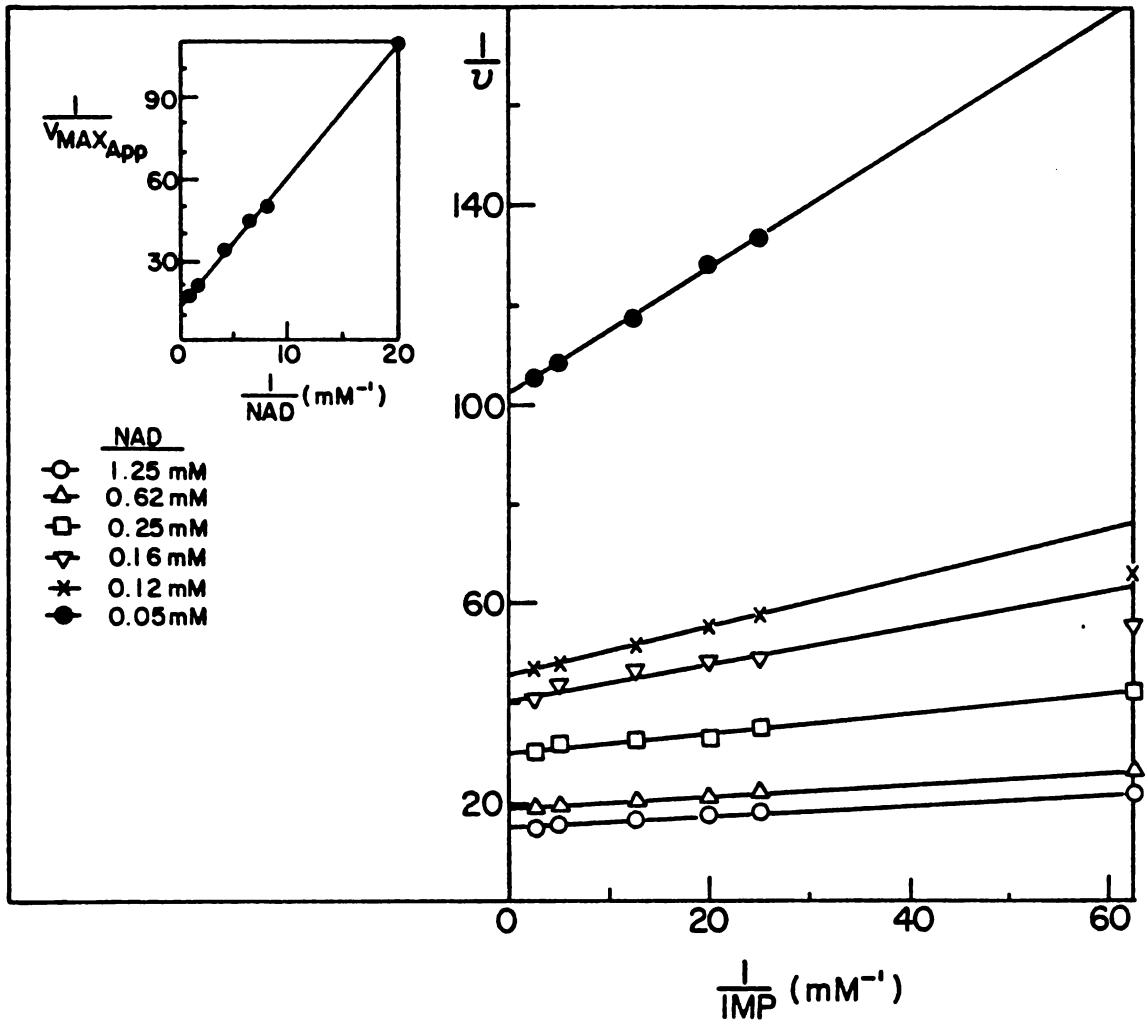

FIGURE 4.21. Lineweaver-Burke plots of initial velocity vs IMP concentration at several constant levels of NAD^+. Velocities were measured at 290 nm. K_m NAD^+ = 445 μM

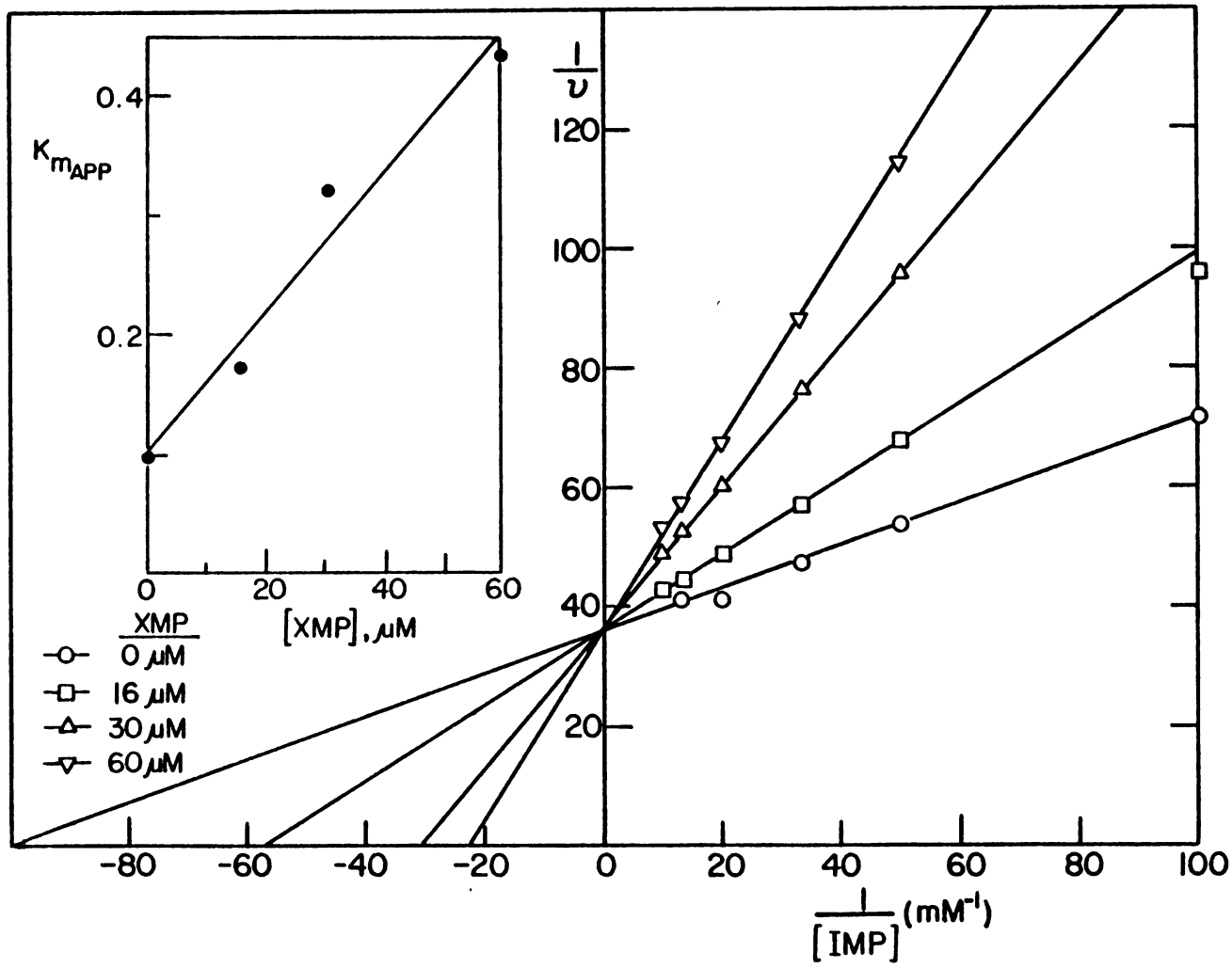

FIGURE 4.22. Lineweaver-Burke plots of initial velocity vs IMP concentration at several constant levels of XMP. Velocities were measured at 290 nm. $[NAD^+]$ = 0.6 mM, Ki XMP = 27 μM

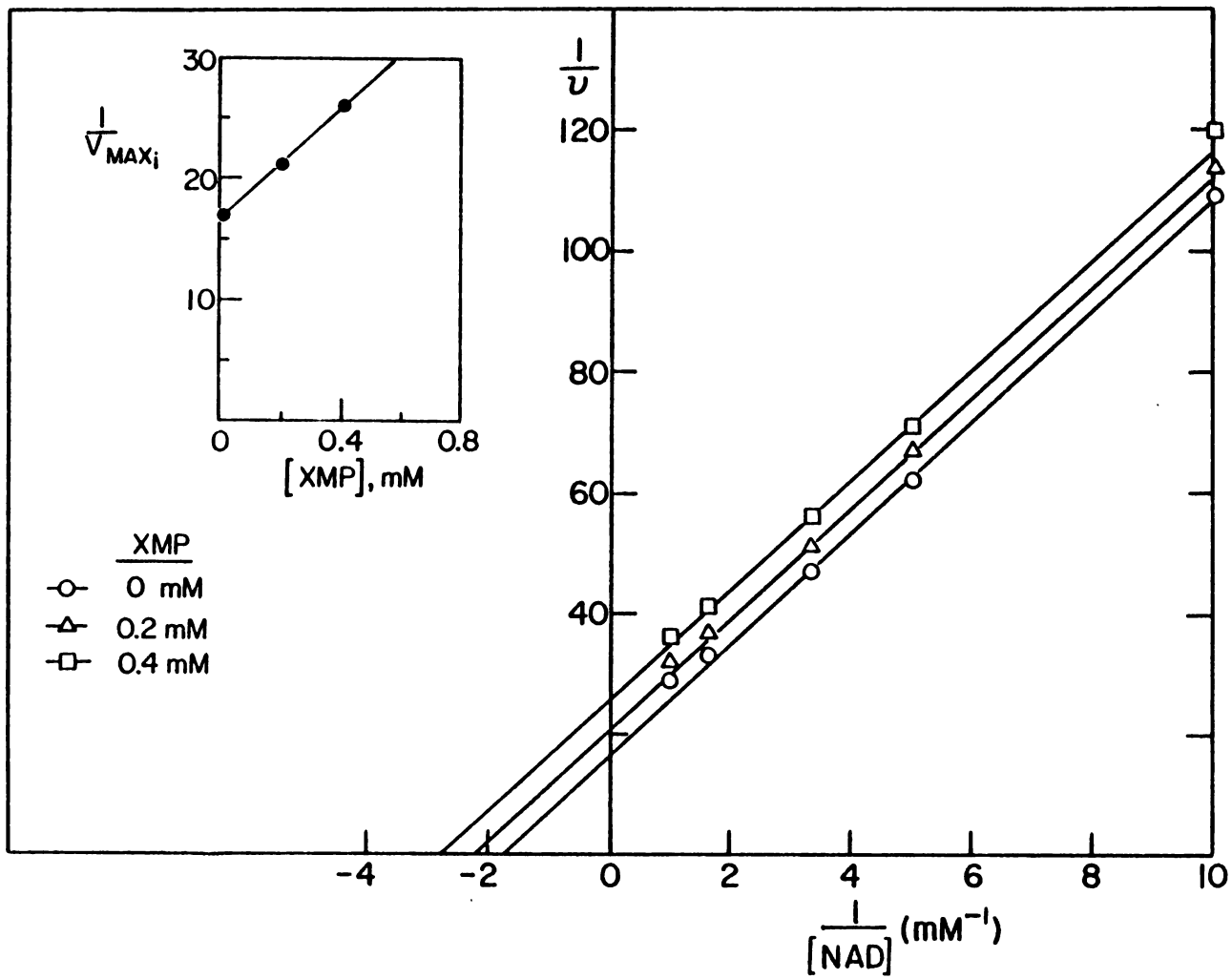

FIGURE 4.23. Lineweaver-Burke plots of initial velocity vs NAD^+ concentration at several constant levels of XMP. Velocities were measured at 290 nm. [IMP] = 0.75 mM, Ki XMP = 640 μM.

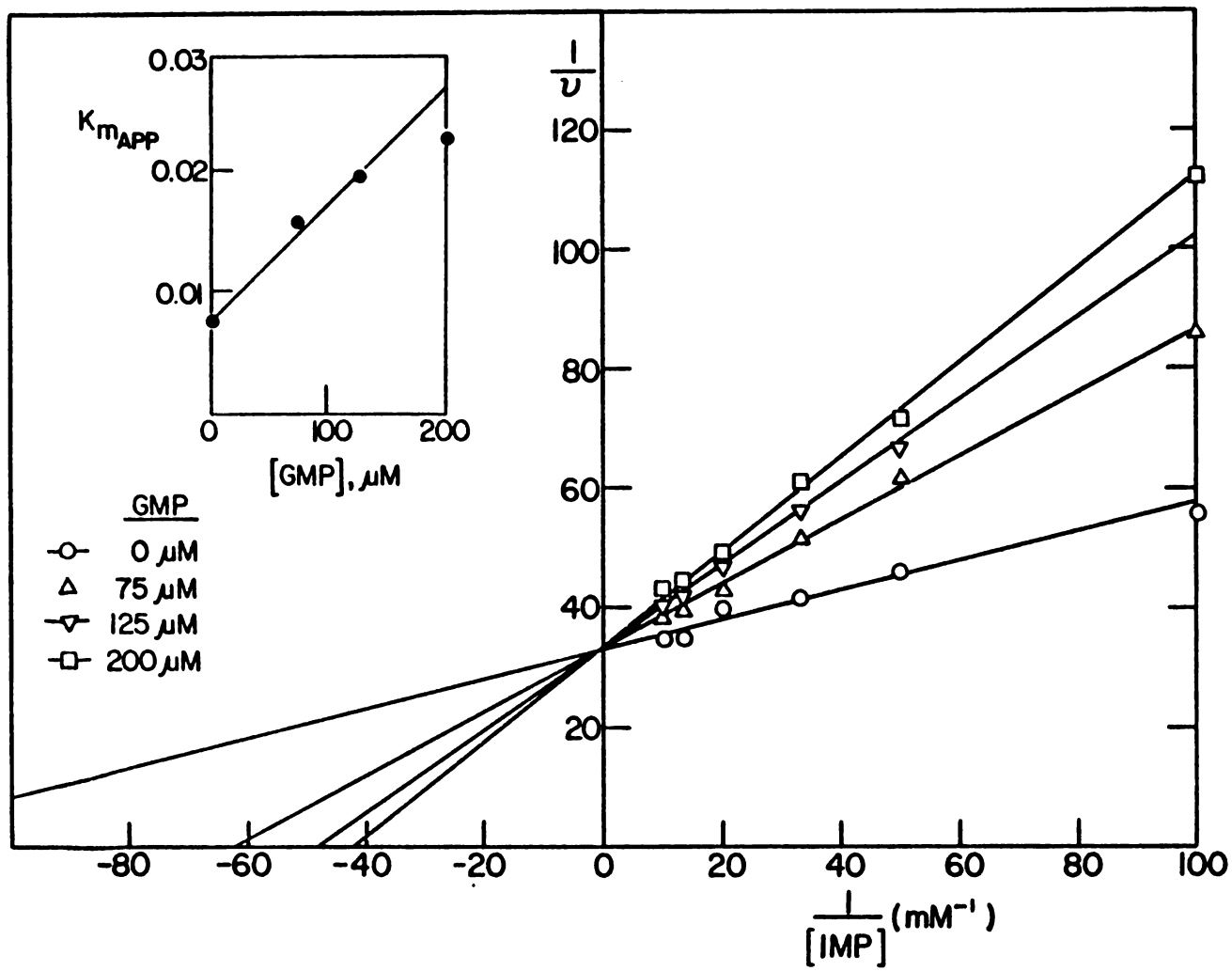

FIGURE 4.24. Lineweaver-Burke plots of initial velocity vs IMP concentration at several constant levels of GMP. Velocities were measured at 290 nm. $[NAD^+]$ = 1 mM, Ki GMP = 95 μM.

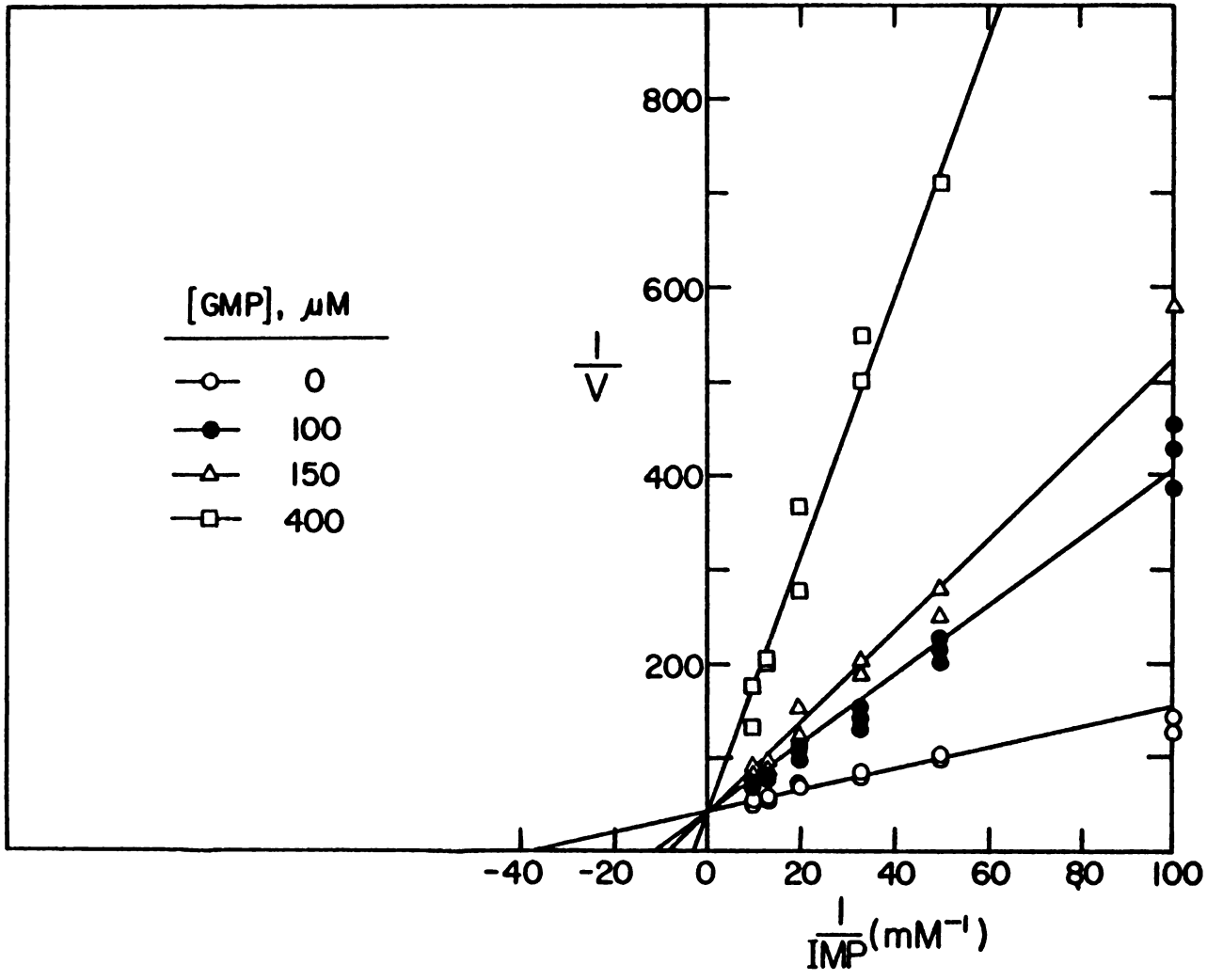

FIGURE 4.25. Lineweaver-Burke plots of initial velocity vs IMP concentration at several constant levels of GMP and with subsaturating levels of NAD^+ (0.5 mM). Velocities were measured at 290 nm.

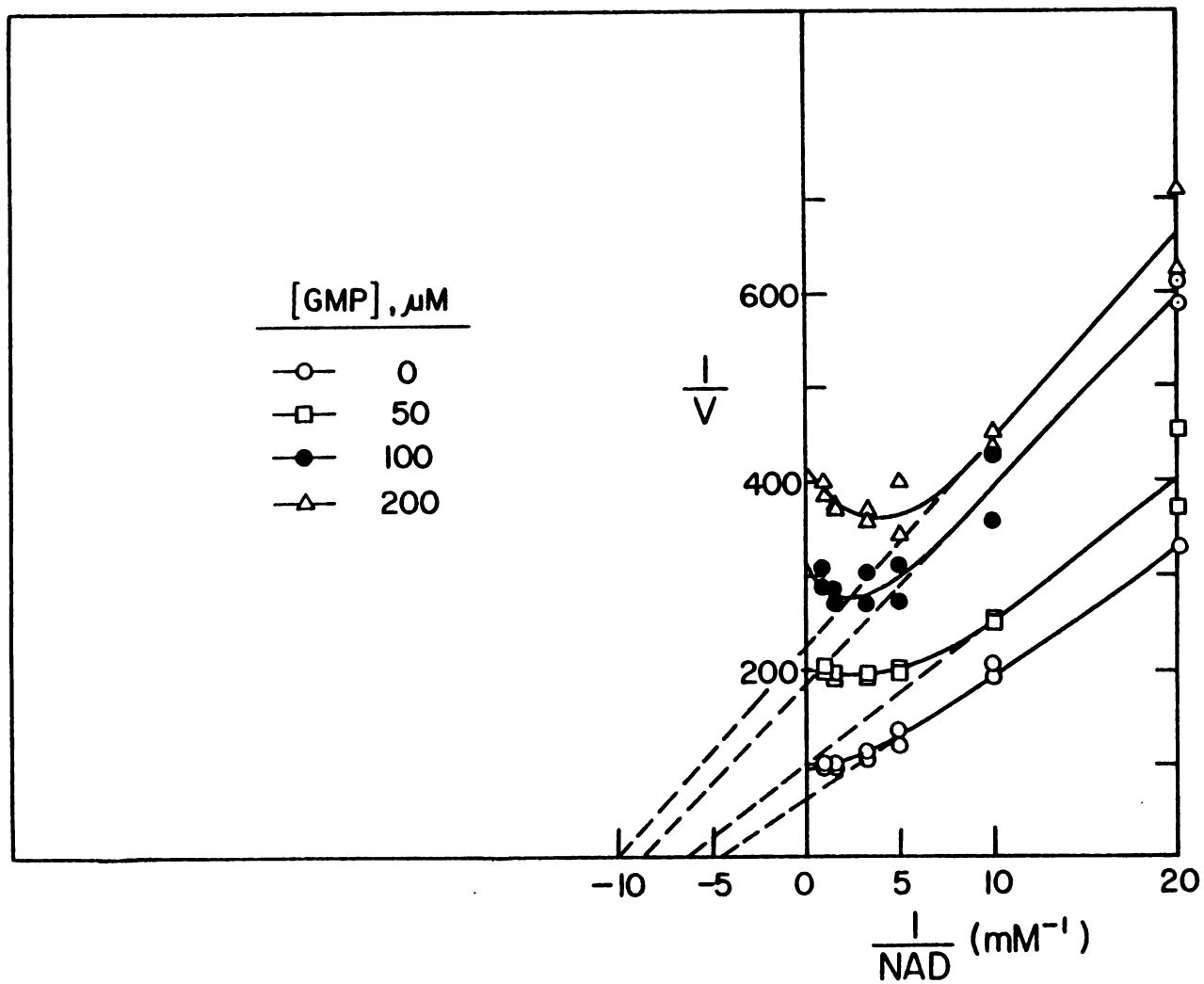

FIGURE 4.26. Lineweaver-Burke plots of initial velocity vs NAD^+ concentration at several constant levels of GMP and with subsaturating levels of IMP (20 μM). Velocities were measured at 290 nm.

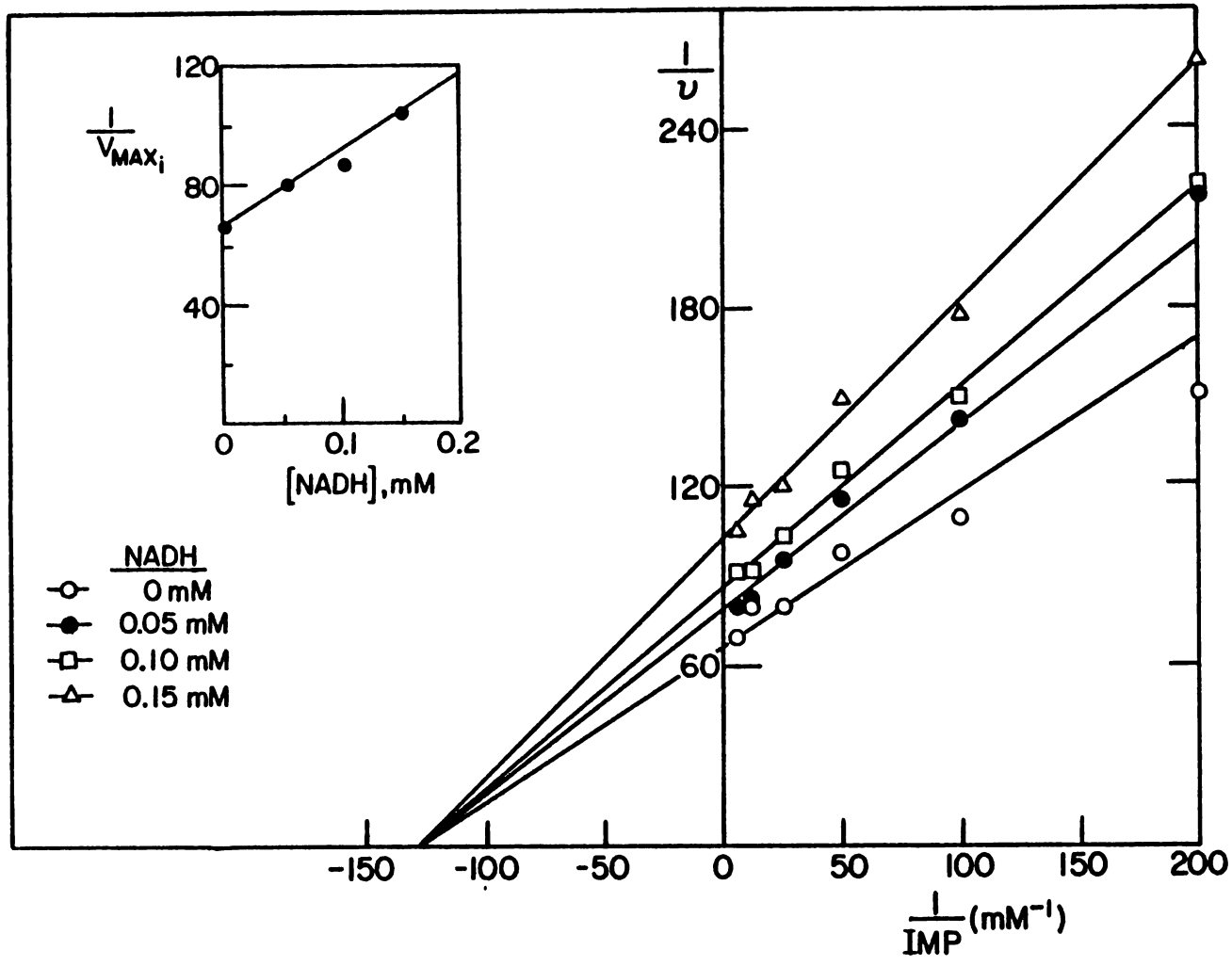

FIGURE 4.27. Lineweaver-Burke plots of initial velocity vs IMP concentration at several constant levels of NADH. Velocities were measured at 290 nm. $[NAD^+]$ = 1 mM, Ki NADH = 322 μM.

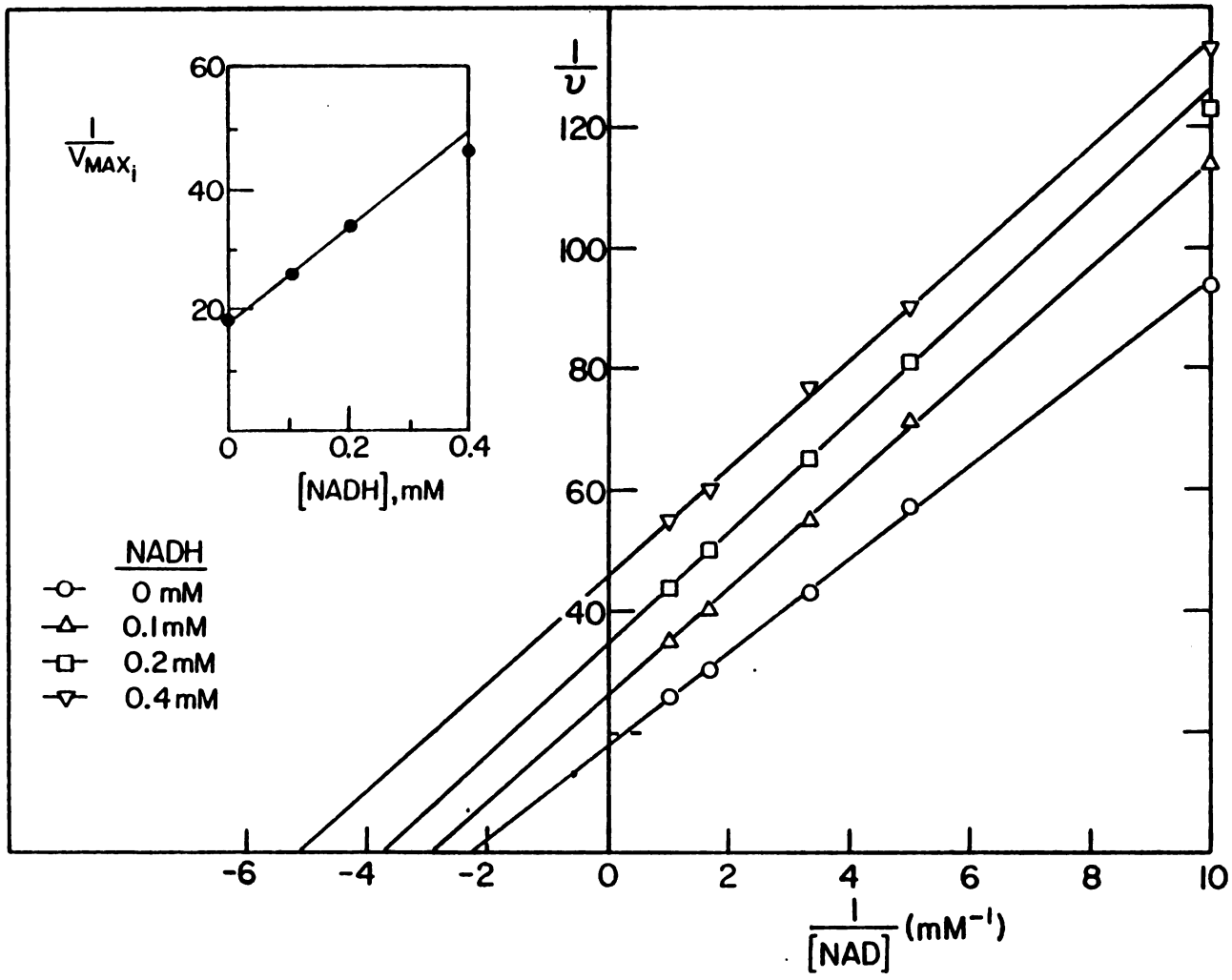

FIGURE 4.28. Lineweaver-Burke plots of initial velocity vs NAD^+ concentration at several constant levels of NADH. Velocities were measured at 290 nm. [IMP] = 1 mM, Ki NADH = 320 μM.

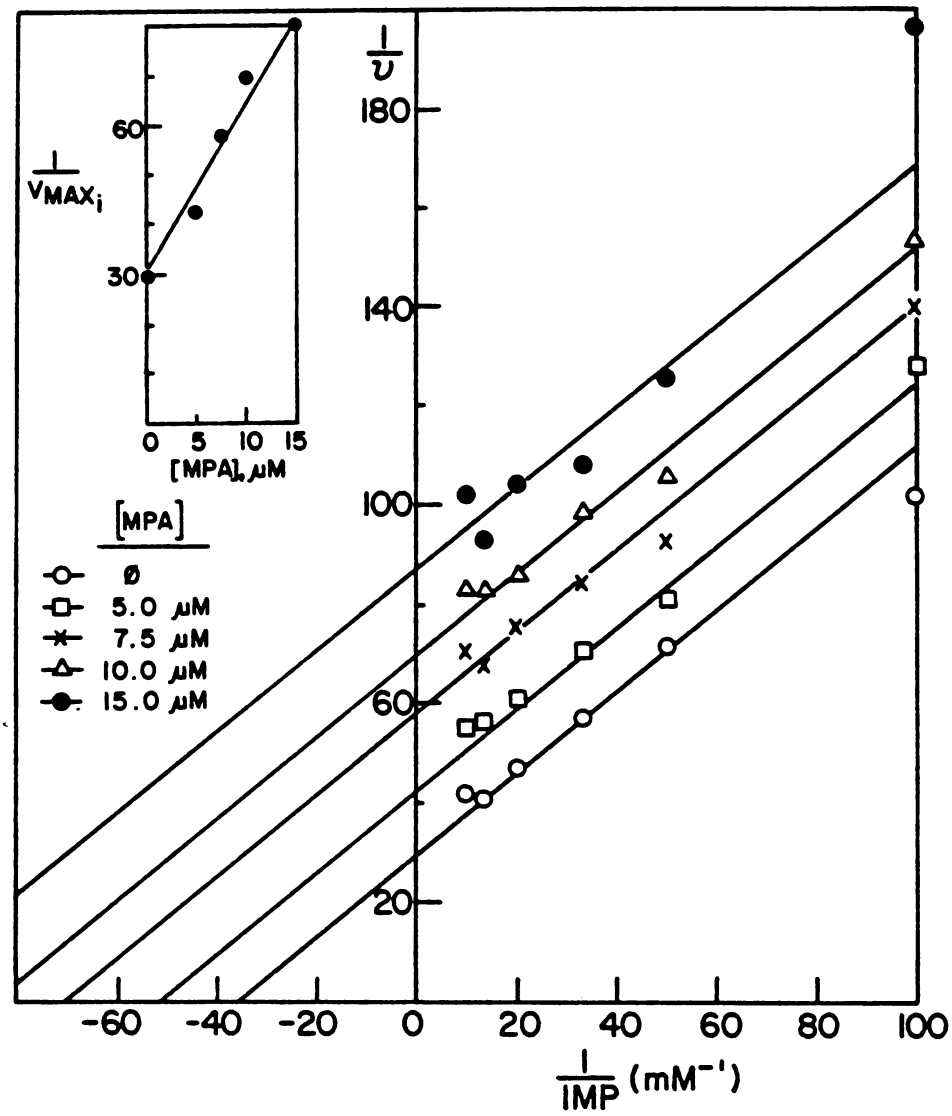

FIGURE 4.29. Lineweaver-Burke plots of initial velocity vs IMP concentration at several constant levels of mycophenolic acid. Velocities were measured at 290 nm. $[NAD^+]$ = 2.0 mM, Ki = 9 μM.

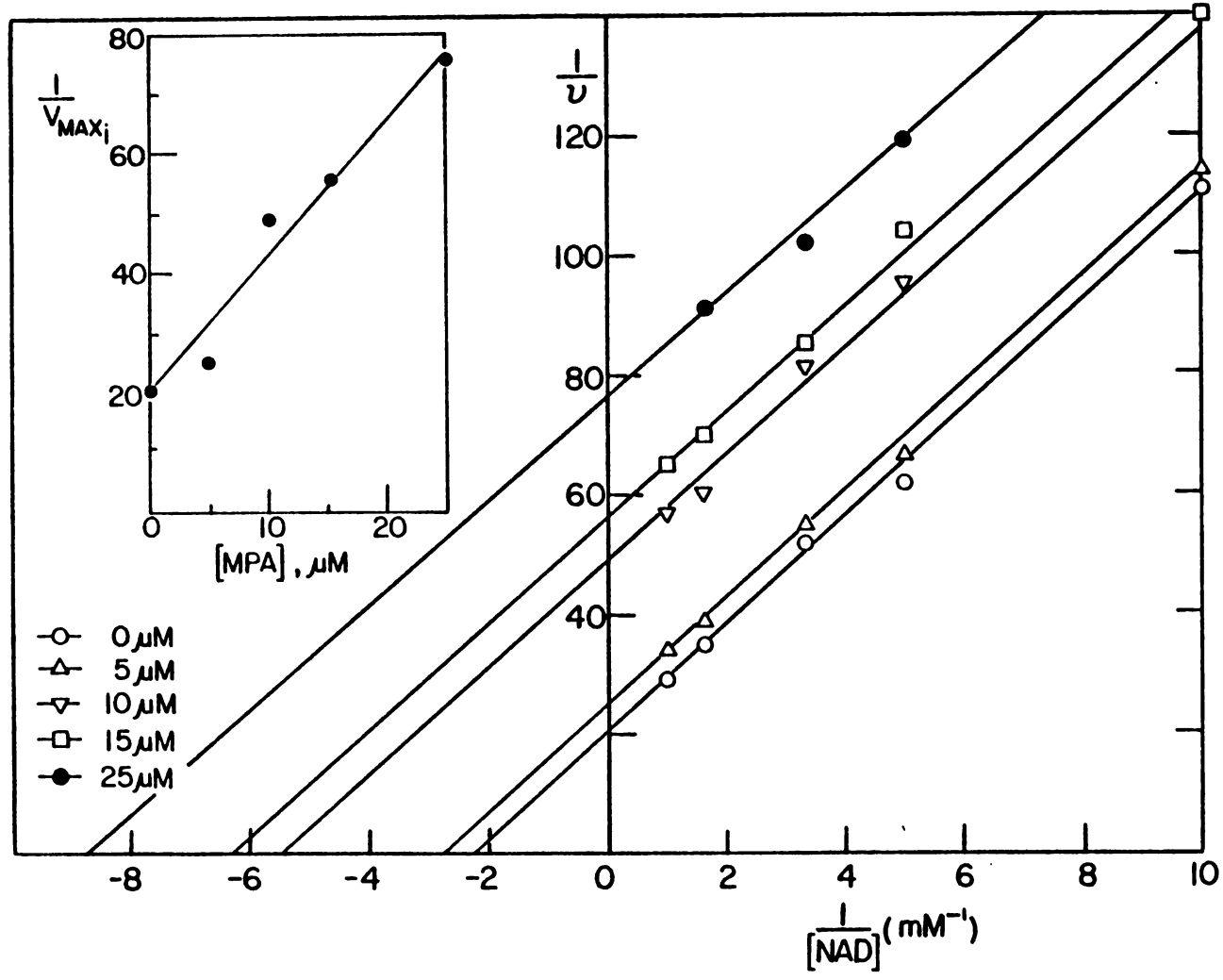

FIGURE 4.30. Lineweaver-Burke plots of initial velocity vs NAD^+ concentration at several constant levels of mycophenolic acid. Velocities were measured at 290 nm. [IMP] = 0.4 mM, Ki = 6 μM.

DISCUSSION

The IMP dehydrogenase of T. foetus is similar to the IMP dehydrogenases obtained from other sources with respect to pH optimum, apparent irreversibilty of the reaction and kinetic parameters. The K_m value for IMP is similar (18 μM) for the IMP dehydrogenases of Aerobacter aerogenes (162,168), pea seedlings (172), Sarcoma 180 cells (186) and Ehrlich ascites tumor cells (161). The K_m value for NAD^+ is similar to that found for the IMP dehydrogenase of Sarcoma 180 cells and Aerobacter aerogenes. The parasite enzyme is also similar to other IMP dehydrogenases in terms of reaction sequence. The findings that the double reciprocal plots of the initial velocities of IMP dehydrogenase activity intersect (Figure 4.21, 4.22) indicate that the enzymatic reaction mechanism involves either ordered addition or rapid equilibrium random addition of the substrates to the enzyme to form active enzyme-substrate complexes. The results of the product inhibition experiments are, however, inconsistant with a rapid equilibrium random addition mechanism. In a random addition mechanism, each product would be expected to compete with each substrate for binding to the free enzyme (187). But the data in Figure 4.27 and 4.28 show noncompetitive inhibition by NADH. On the other hand, an ordered addition reaction mechanism, with IMP binding first and XMP leaving last, is consistant with the data. An ordered mechanism is also observed in Aerobacter aerogenes (162) and Sarcoma 180 cells (186). It seems that IMP dehydrogenase from T. foetus is similar to other IMP dehydrogenases in that they differ from other dehydrogenases in

general which usually bind the pyridine nucleotide first (188).

The enzyme obtained from T. foetus is also very different from other IMP dehydrogenases in several aspects. A native molecular weight of 380,000 is almost twice as large as that observed in Aerobacter aerogenes (177). The subunit weight of 58,000 suggests that the native enzyme is composed of 6 subunits.

Gel filtration studies on Bio-Gel A 0.5m, in the presence of 1 M NaCl, suggested a decrease in Stokes radii which extrapolated to a loss of 110,000 daltons in the proteins molecular weight (Figure 4.8). This implies a loss of two subunits in high salt but that the remaining 4 subunits are still catalytically active. These varied mobilities of IMP dehydrogenase in gel filtration may not be due to an artifact of the experimental procedure because; 1) the filtering property of Bio-Gel A 0.5m is unaffected by changes in salt concentration (191), 2) calibration profiles of the column with and without the added salt are identical and 3) both types of IMP dehydrogenase, 380K and 270K daltons, were observed during the same run. In addition, two peaks of activity were found for IMP dehydrogenase during isokinetic sucrose centrifugation (Figure 4.12). Further work is required to elucidate the nature of the differances in sedimentation behavior for the two forms.

Another difference in IMP dehydrogenase obtained from T. foetus, to other IMP dehydrogenases is the absence for an inorganic salt requirment (Figure 4.10). Both Aerobacter aerogenes (168) and Sarcoma 180 cells (186) are markedly stimulated by the presence of potassium

salts. For the T. foetus enzyme, only about 10-20% maximal increase was observed at a K^+ concentration of 100 mM (186).

Mycophenolic acid (MPA) is an inhibitor of T. foetus growth (IC_{50} of 50 μM) and blocker of guanine nucleotide synthesis (166). Mycophenolic acid is also a potent uncompetitive inhibitor of IMP dehydrogenase with respect to both IMP (K_i = 9 μM) and NAD^+ (K_i = 6 μM) (Figure 4.29, 4.30). The addition of either NAD^+ or IMP was not able to reverse the inhibition by mycophenolic acid. The exact nature of the inhibition is not known.

IMP dehydrogenase from T. foetus has been purified 500 fold and physically and kinetically characterized. The enzyme exhibits a native molecular weight of 380,000 and a subunit molecular weight of 58,000. The enzymatic mechanism is ordered with IMP binding first and XMP leaving last and shows no requirment for inorganic salt. Both the lack of an inorganic salt requirement and its unusually large molecular weight make T. foetus IMP dehydrogenase unique from the others. We have already shown that inhibition of this enzyme can lead to growth inhibition of T. foetus (166). The differences discovered between this enzyme and that from mammalian sources, supports the idea that IMP dehydrogenase in Tritrichomonas foetus is a potential site for chemotherapeutic drug design.

CHAPTER 5

HYPOXANTHINE-GUANINE-XANTHINE PHOSPHORIBOSYLTRANSFERASE FROM TRITRICHOMONAS FOETUS

INTRODUCTION

Purine phosphoribosyltransferases catalyze the condensation of the 5-phosphoribosyl moiety derived from PP-ribose-P (PRPP) with purine bases to form purine 5'-ribonucleotides. These enzymes represent the major metabolic pathway for the salvage of preformed purines and are found widely distributed in nature.

A deficiency of hypoxanthine-guanine phosphoribosyltransferase (HGPRTase) in man may have several clinical consequences. A complete absence of enzyme activity is found in patients with the Lesch-Nyhan syndrome (192). This disease is characterized chemically by hyperuricemia due to an overproduction of uric acid and clinically by self-mutilation, choreoathetosis, spasticity, growth and mental retardation. A partial deficiency of HGPRTase activity has been described in some patients suffering from a severe form of gout (193). These patients though, differed from the former group in that they did not have the devastating neurological and behavioral abnormalities characteristic of the Lesch-Nyhan syndrome. The precise genetic mechanisms leading to a deficiency of HGPRTase in man are not well understood (209-213). The normal human enzyme has been purified to homogeneity from erythrocytes and its physical properties have been

well described (194-196). Fundamental differences between some bacterial, protozoal and mammalian purine phosphoribosyltransferases have been observed (143, 197, 198).

All parasitic protozoa examined to date lack the ability to synthesize purines de novo and are dependent upon the salvage of exogeneous preformed purines (89, 96-99, 144). The abilities to catalyze phophoribosyl transfer to adenine (9-11), hypoxanthine and guanine (143, 199-201) have been found at high levels in the cell-free extracts of several protozoa. Promastigotes of Leishmania donovani when exposed to allopurinol, a hypoxanthine analogue, accumulate large quantities of allopurinol ribonucleoside 5'-monophosphate (202, 203) and the parasites growth is inhibited (204). In contrast, mammalian cells accumulate only minute amounts of this ribonucleotide (205).

Tritrichomonas foetus is an anaerobic protozoan parasite and the causative agent of bovine trichomoniasis. The parasite has been found to be incapable of de novo purine biosynthesis and dependent primarily upon the salvage of hypoxanthine and guanine to fulfill its purine requirements (166). Adenine uptake is facilitated by prior conversion to hypoxanthine and then incorporated into the parasites nucleotide pool by a hypoxanthine phosphoribosyltransferase. An analogue of guanine, 8-azaguanine, has been shown to be recognized as substrate by Tritrichomonas foetus and incorporated into the parasites nucleotide pool as 8-azaguanine mono-, di-, and triphosphates (See Figure 3.5). In addition, 8-azaguanine exhibits an IC_{50} of 30 M on the growth of T. foetus in HUT medium (See Figure 3.11).

Differances in the substrate specificities of the purine phosphoribosyltransferases in mammalian and protozoal sources may be

exploited in our effort for chemotherapeutic inhibitor design. This chapter describes the hypoxanthine-guanine-xanthine phosphoribosyl-transferase present in Tritrichomonas foetus. The enzyme has been partially purified and characterized. A comparison of the HGXPRTase from T. foetus to the HGPRTase in mammmals wil be used to evaluate if the protozoan enzyme is a potential site for chemotherapeutic inhibitor design.

MATERIALS AND METHODS

CHEMICALS

[8-^{14}C]Hypoxanthine (48.7 mCi/mmol), [8-^{14}C]guanine (51.0 mCi/mmol), [8-^{14}C]xanthine (55.0 mCi/mmol) and [2-^{14}C]uracil (53.0 mCi/mmol) were purchased from ICN (Irvine, CA.). Sephadex G-75 and DEAE-Sepaharose were obtained from Pharmacia Fine Chemicals. Gel filtration standards were purchased from BIO-RAD. Yeast alcohol dehydrogenase, cytochrome c, GMP agarose, 6-mercaptopurine, allopurinol, adenine, 8-thioguanine, 2-amino-6-thiopurine and 8-aza-guanine were bought from Sigma Chemical Co. 4-Thiopyrazolo-[3,4-d-]-pyrimidine was a generous gift from Dr. Richard Miller of the Burroughs Wellcome Research Laboratories. All other chemicals used were of the highest purities commercially available.

CULTURES

T. foetus strain KV_1, was cultivated in Diamonds TYM (100) medium pH 7.2 supplemented with 10% heat inactivated horse serum and 1% antibiotic/antimycotic mix at 37°C. Stationary cultures having a cell density of about 2 x 10^7 cells/ml were used to inoculate fresh media at a 1:10 ratio (10%). Mid-logarithmic phase of growth, with a cell density of 10^7/ml, was achieved by using a 4% inoculum and harvesting cells after 16 hours of incubation. Cell number was determined in a Coulter ZF counter.

ENZYME ASSAYS

Assay of Phosphoribosyltransferase. Phosphoribosyltransferase activity was assayed by the modified procedure of Schmidt et al (136).

The assay mixture consisted of 100 mM Tris-HCl pH 7.8, 8 mM $MgCl_2$, 1 mM PRPP, 50 µg/ml BSA and 20 µM radiolabeled purine or pyrimidine base. The reaction was initiated by the addition of enzyme, incubated for 10 minutes at 37°C, and terminated by the addition of a 10-fold excess of cold 5 mM NH_4OAc pH 5.0. The mixture was filtered through a PEI-cellulose covered GF/B filter and the adsorbed counts determined using a Beckman Model 3133T liquid scintillation counter. The reaction mixture without PRPP served as controls. The products of the reaction were also analyzed by ion exchange HPLC (See appendix for details). An alternative phosphoribosyltransferase assay is a modified procedure of Tuttle and Krenitsky (143). The assay mixture contains 100 mM Tris-HCl pH 7.8, 8 mM $MgCl_2$, 1 mM PRPP, 50 µg/ml BSA and 0.1 mM hypoxanthine or xanthine or 0.04 mM guanine. The formation of nucleotides was followed at 243, 250 and 255 nm for hypoxanthine ($\Delta\varepsilon$ = 2.2 mM^{-1} cm^{-1}), xanthine ($\Delta\varepsilon$ = 3.9 mM^{-1} cm-1) and guanine ($\Delta\varepsilon$ = 4.2 mM^{-1} cm^{-1}), respectively. The reaction was initiated by the addition of enzyme. Protein concentrations were determined by the method of Lowry (179) using bovine serum albumin as standard.

Assays for Interfering Enzyme Activities-

Deaminase activities were assayed by a modified procedure of Tuttle and Krenitsky (143). The assay mixture contained 100 mM Tris-HCl pH 7.8, 8 mM $MgCl_2$, 1 mM DTT and 0.1 mM adenine or 0.04 mM guanine. Enzyme samples were passed down a Sephadex G-25 column (0.5 x 10 cm) which had been equilibrated at 4°C with 50 mM Tris-HCl pH 7.2, 10mM $MgCl_2$ and 1 mM DTT to remove PRPP. Activities were determined by following the change in absorbance at 265 nm and 246 nm for adenase ($\Delta\varepsilon$ = -5,700 M^{-1} cm^{-1}) and guanase ($\Delta\varepsilon$ = -4,230 M^{-1} cm^{-1}).

The products of the reaction were also analyzed by reverse phase HPLC (See appendix for details). Xanthine oxidase assay mixture contained 100 mM Tris-HCl pH 7.8, 8 mM $MgCl_2$, 0.1 mM hypoxanthine or xanthine. The reaction was followed at 292 nm ($\Delta\varepsilon$ = 11,500 M^{-1} cm^{-1}) which corresponded to uric acid formation. The reaction was initiated by the addition of enzyme. IMP dehydrogenase assay mixture contained 50 mM Tris-HCl pH 8.1, 100 mM KCl, 1 mM DTT, 1.6 mM NAD^+ and the enzyme. The rate increase in absorbance at 290 nm (ε = 3,910 M^{-1} cm^{-1}) resulting from the formation of IMP was measured. The reaction was initiated by the addition of IMP (0.5 mM final concentration).

$s_{20,w}$ DETERMINATION

The sedimentation behavior of purified HGXPRTase (Step 3 protein containing 1 mM PRPP) was determined on a 12 ml 10-30% (w/w) isokinetic sucrose gradient containing 25 mM Tris pH 7.2, 20 mM KCl, 6 mM $MgCl_2$ and 1 mM DTT. The gradient was formed by the procedure of McCarty et al (189) and centrifuged at 4° C with a SW 41 rotor in a Backman L8-80M centrifuge at 148,000 x g for 48 hours. After centrifugation, a hole was punched at the bottom of the centrifuge tube and fractions were collected and analyzed. Sedimentation coefficient ($s_{20,w}$) values were determined by comparison with standards. The standards used for these measurements were yeast alcohol dehydrogenase (7.6 S), bovine serum albumin (4.5 S) and cytochrome c (1.7 S). The position of cytochrome c was determined by following the absorbance at 410 nm, that of bovine serum by following the absorbance at 280 nm, and that of yeast alcohol dehydrogenase by enzymatic assay (190).

POLYACRYLAMIDE GEL ELECTROPHORESIS

SDS-PAGE was done according to the method of Laemmli (185) using 10%T, 5%C_{BIS} polyacrylamide slabs. Samples of step 5 protein were precipatated by 10% TCA and resuspended in .05 ml of buffer A. Slabs were run at 15 mA/slab for 8 hours at 8° C. The gels were then stained for protein using a silver staining procedure (215).

RESULTS

ENZYME PURIFICATION

Step 1. Homogenization- T. foetus in mid-logarithmic phase of growth, were collected by centrifugation. The cells were washed three times and resuspended in an equal volume of buffer A (50 mM Tris-HCl pH 7.2, 10 mM $MgCl_2$ and 1 mM DTT). This and all subsequent steps were performed at 4°C. Protease inhibitors; 1 mM 1,10-phenanthroline, 1 mM benzamidine, 50 µM PMSF, 20 µg/ml leupeptin, 50 µg/ml crude trypsin ovomucoid inhibitor, 50 µg/ml crude soybean trypsin inhibitor and 50 µg/ml aprotinin, were added to the cell suspension and then sonicated with a HEAT systems sonicator Model W-375, at 20% output, using three 30 second bursts. The homogenate was centrifuged at 78,000 x g for 135 minutes in a Beckman Model L8-80M Ultracentrifuge. Both the stability and activity of the phosphoribosyltransferases (PRTases) in T. foetus were significantly enhanced by the addition of the protease inhibitors. Hypoxanthine, guanine and xanthine phosphoribosyltransferase activities were increased 7.7, 13.3 and 15.3 fold respectively in the presence of these protease inhibitors. HPLC analysis of the reaction mixtures indicated a comparable increase in IMP and GMP levels for the HPRTase assay, GMP and XMP levels for GPRTase assay and XMP level for XPRTase assay. Uracil phosphoribosyltransferase was unaffected by the addition of protease inhibitors. The PRTases are stable for up to two weeks at -80°C with greater than 90% activity remaining.

Step 2. Ammonium Sulfate Fractionation- To the supernatant in step 1, saturated $(NH_4)_2SO_4$ pH 7.2 was added to 45% saturation and

stirred for 1 hour. After centrifugation at 10,000 x g for 20 minutes, more $(NH_4)_2SO_4$ was added to the supernatant to reach 75% saturation. After 1 hour the precipatate was collected by centrifugation like before and resuspended in a minimum volume of buffer A. More than 90% of the total activity was precipatated between 45-75% saturation.

Step 3. Gel Filtration- Step 2 protein (10 ml) was applied to a Sephadex G-75 column (2.5 x 98 cm) previously equilibrated with buffer A. The column was eluted with starting buffer and fractions containing hypoxanthine, guanine, and xanthine PRTase activities were pooled. The HPRTase, GPRTase and XPRTase activities coeluted (Figure 5.1) while UPRTase activity appeared in another fraction closer to the void volume (data not shown). Calibration of the column with proteins of known molecular weights (Figures 5.2 and 5.3) allowed the determination of the native molecular weight of T. foetus HGXPRTase as 25,000 daltons. The native molecular weight of UPRTase was estimated to be 90,000 daltons (data not shown).

Step 4. GMP Agarose- The pooled enzyme from step 3 was added to 15 ml of a GMP agarose suspension (10 ml packed bed volume) and processed batch wise. Weak affinity of the enzyme for the GMP agarose at pH 7.2 required incubation of the enzyme with the gel for 15 minutes at 4°C. About 70% of the activity was adsorbed to the GMP agarose which was then sequentially washed with 100 ml of buffer A, 100 ml buffer A + 25 mM KCl and then with 50 ml of buffer A. The enzyme was then eluted by 50 ml of buffer A + 5 mM PRPP. HPRTase, GPRTase and XPRTase activities were eluted as a single peak. The

substantial decrease in total recovery in this step (Table 5.1) is due to the loss of activity not adsorbed to the gel.

Step 5. DEAE Sepharose- The eluted enzyme from step 4 was applied to a DEAE Sepharose column (1.4 x 5.0 cm) previously equilibrated with buffer A at a flow rate of 40 ml/hr. The column was washed with 50 ml of buffer A and then the enzyme was eluted by 200 ml of a linear KCl gradient consisting of buffer A to buffer A + 200 mM KCl. HPRTase, GPRTase and XPRTase activities were eluted as a single peak of activities at a KCl concentration equivalent to 80 mM. Fractions containing activity were pooled and PRPP added to a final concentration of 1 mM. A summary of the above purification procedure is shown in Tables 5.1 and 5.2. The coelution of all three enzyme activities durine purification is indicative of a single protein with three activities. The enzyme obtained from this procedure was stored at -80°C without loss of activity for at least 4 weeks. The final specific activity for HPRTase, GPRTase and XPRTase are 137.7, 71.1 and 3.9 nmol/min/mg protein. The preparation is free of adenase, guanase, xanthine oxidase or IMP dehydrogenase activities as determined spectrophometrically. However, HPLC analysis of the radiolabeled assay mixture after a 20 minute incubation with 15 µg of step 5 protein revealed an interesting phenomenon. When hypoxanthine was used as substrate, the products IMP and XMP were formed; guanine produced GMP and XMP and xanthine produced only XMP. SDS-PAGE of step 5 protein revealed a single band of approximate molecular weight of 24,000 daltons.

ENZYME STABILITY

The relative stabilities at 37°C of the PRTase activities in the absence of PRPP is shown in Figure 5.5. UPRTase was the most stable while H-, G-, and XPRTase behaved simarily and were the least stable.

Magnesium and PRPP are known stabilizers of PRTase activity and their stabilizing effect was examined on T. foetus PRTases. All three activities, hypoxanthine, guanine and xanthine PRTase were simarily stabilized by PRPP but unaffected by magnesium (Table 5.3).

SEDIMENTATION COEFFICIENT

Hypoxanthine, guanine and xanthine phosphoribosyltransferase activities in T. foetus appear as a single peak of activities (Figure 5.4) following isokinetic sucrose centrifugation with a sedimentation coefficient of 3.7 S. An approximate molecular weight can be determined by comparison to the standards and corresponds to an approximate molecular weight ranging from 38,000-58,000 daltons.

PROPERTIES OF THE ENZYMIC REACTION

The effect of pH and buffers on the activity of hypoxanthine phosphoribosyltransferase is shown in Figure 5.6. The pH profiles for guanine and xanthine phosphoribosyltransferase activity were identical as that for hypoxanthine. Maximal enzyme activity was observed in a pH range of 7.5 to 9.0 using a Tris-HCl buffer. The phosphoribosyltransferase was active in all buffers used but was inactive below pH 4.5.

The effect of various inorganic salts were examined using 100 mM Tris-HCl pH 7.8, 1 mM PRPP, 50 µg/ml BSA, 1 mM DTT and 20 µM radiolabled hypoxanthine. The results (Figure 5.7) were identical for

hypoxanthine, guanine and xanthine PRTases and showed an increase in activity with Mg^{++} at 5-10 mM. Higher concentrations of magnesium or other salts were inhibitory to the activity of the PRTases.

INHIBITION OF HYPOXANTHINE-GUANINE-XANTHINE PHOSPHORIBOSYLTRANSFERASE

Adenine and several purine analogs were examined for inhibition on HGXPRTase of T. foetus (Table 5.3). The inhibitors 6-mercaptopurine, 2-amino-6-thiopurine and 8-thioguanine at 0.5 mM were the most effective in inhibiting HGXPRTase activity when hypoxanthine concentration was 100 µM. At 1 mM, the growth of T. foetus in TYM was inhibited significantly by 6-mercaptopurine, 8-azaguanine, 4-thiopyrazolo-[3,4d]pyrimidine and 8-thioguanine.

Table 5.1. Purification of HGXPRTase from T. foetus.

	Volume (ml)	Total Activity* (Units)	Total Protein (mg)	%Recovery	Specific Activity (U/mg)	Purification
1. 10^5 crude supernatant	40	492	1532	100	0.3	1
2. 45-75% $(NH_4)_2SO_4$	10	285	695	58	0.4	1
3. Sephadex G-75	39	827	63.0	168	13.3	41
4. GHP Agarose	18	223	7.4	45	30.2	100
5. DEAE Sepharose	25	1032	7.5	210	137.7[1]	459

*Activity was measured using 20 μM [8-^{14}C]hypoxanthine (48.7 mCi/mmol).

[1]The specific activities for guanine and xanthine are 71.1 and 3.9 nmol/min/mg protein.

TABLE 5.2. Purification summary of Hypoxanthine, Guanine and Xanthine Phosphoribosyltransferase specific activities from T. foetus.

	Specific Activities (nmol/min/mg protein)			Ratio of activities
	HPRTase	GPRTase	XPRTase	H:G:X
1. 10^5 crude	0.32	0.34	0.16	2:2:1
2. 45-75% $(NH_4)_2SO_4$	0.41	0.26	0.09	4:3:1
3. Sephadex G-75	13.31	8.37	0.59	22:14:1
4. GMP-agarose	30.16	22.76	2.76	11:8:1
5. DEAE-Sepharose	147.50	71.10	3.90	38:8:1

TABLE 5.3. Stabilizers of the purine phosphoribosyltransferase activities in Tritrichomonas foetus.

	% activity remaining after 10 minutes at 37° C*		
Additions	Hypoxanthine	Guanine	Xanthine
None	42	45	52
10 mM $MgCl_2$	33	34	46
1 mM PRPP	98	112	114
10 mM $MgCl_2$, 1 mM PRPP	95	105	117

*Incubation mixtures containing 100 mM Tris-HCl pH 7.8, 1 mM DTT 20 µM radiolabeled base and 16 µg of step 3 protein were incubated at 37° C for 10 minutes.

TABLE 5.4. Effect of inhibitors on T. foetus growth and HGXPRTase activity.

	% Inhibition of PRTase activity*	% Inhibition of T. foetus growth[2]
1. Adenine	23	0
2. Allopurinol	7	0
3. 6-Mercaptopurine	44	27
4. 8-Azaguanine	6	24
5. 4-Thiopyrazolo-[3,4d-]pyrimidine	13	23
6. 2-Amino-6-thiopurine	64	6
7. 8-Thioguanine	51	89

*Assay mixtures contained 100 mM Tris-HCl pH 7.8, 1 mM DTT, 100 µM [8^{14}C]hypoxanthine (48.7 mCi/mmol), 3 µg of step 5 protein and 0.5 mM inhibitor.

[2]T. foetus grown in TYM in the presence of 1 mM purine or purine analogue. Cells were counted after 24 hours of growth.

FIGURE 5.1. Gel filtration of Hypoxanthine-Guanine-Xanthine Phosphoribosyltransferase on Sephadex G-75. The column (2.5 x 98 cm) was equilibrated with 50 mM Tris-HCl pH 7.2, 10 mM $MgCl_2$, 1 mM DTT and loaded with 10 ml of step 2 protein. The column was then eluted with starting buffer at 20 ml/hr. Activities were determined as described under "Materials and Methods".

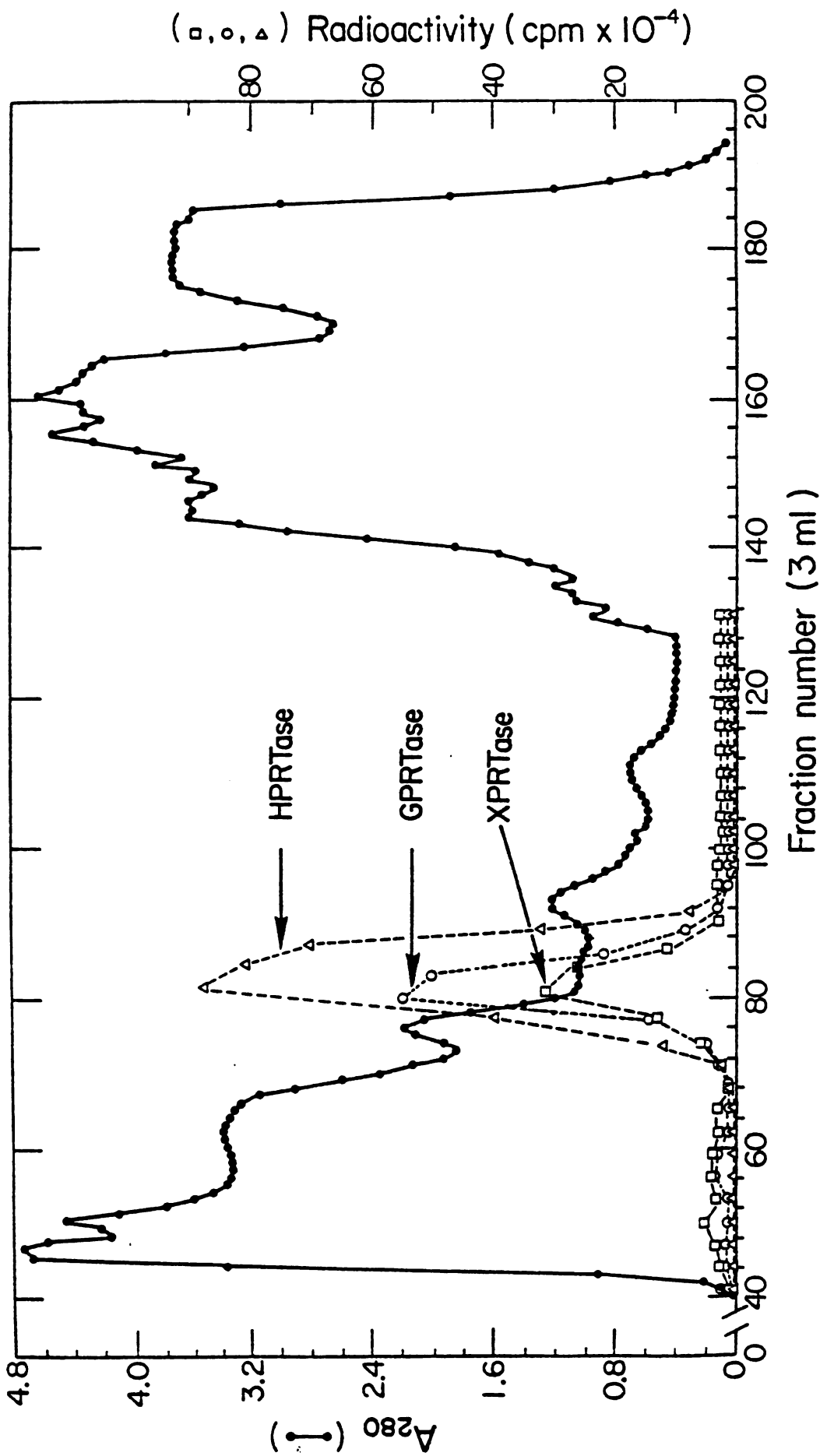
(□, ○, △) Radioactivity (cpm x 10^{-4})
80
60
40
20
200
180
160
140
120
100
80
60
40
0
Fraction number (3 ml)
HPRTase
GPRTase
XPRTase
4.8
4.0
3.2
2.4
1.6
0.8
0
A_{280} (—●—)

FIGURE 5.1.

FIGURE 5.2. Calibration of Sephadex G-75 column (2.5 x 98 cm). The column was equilibrated with 50 mM Tris-HCl pH 7.2, 10 mM $MgCl_2$, 1 mM DTT and loaded with 1 ml of Bio-Rad gel filtration standards with 10 mg Chymotrypsinogen A and 10 mg bovine serum albumin. The column was eluted with starting buffer at a flow rate of 20 ml/hr.

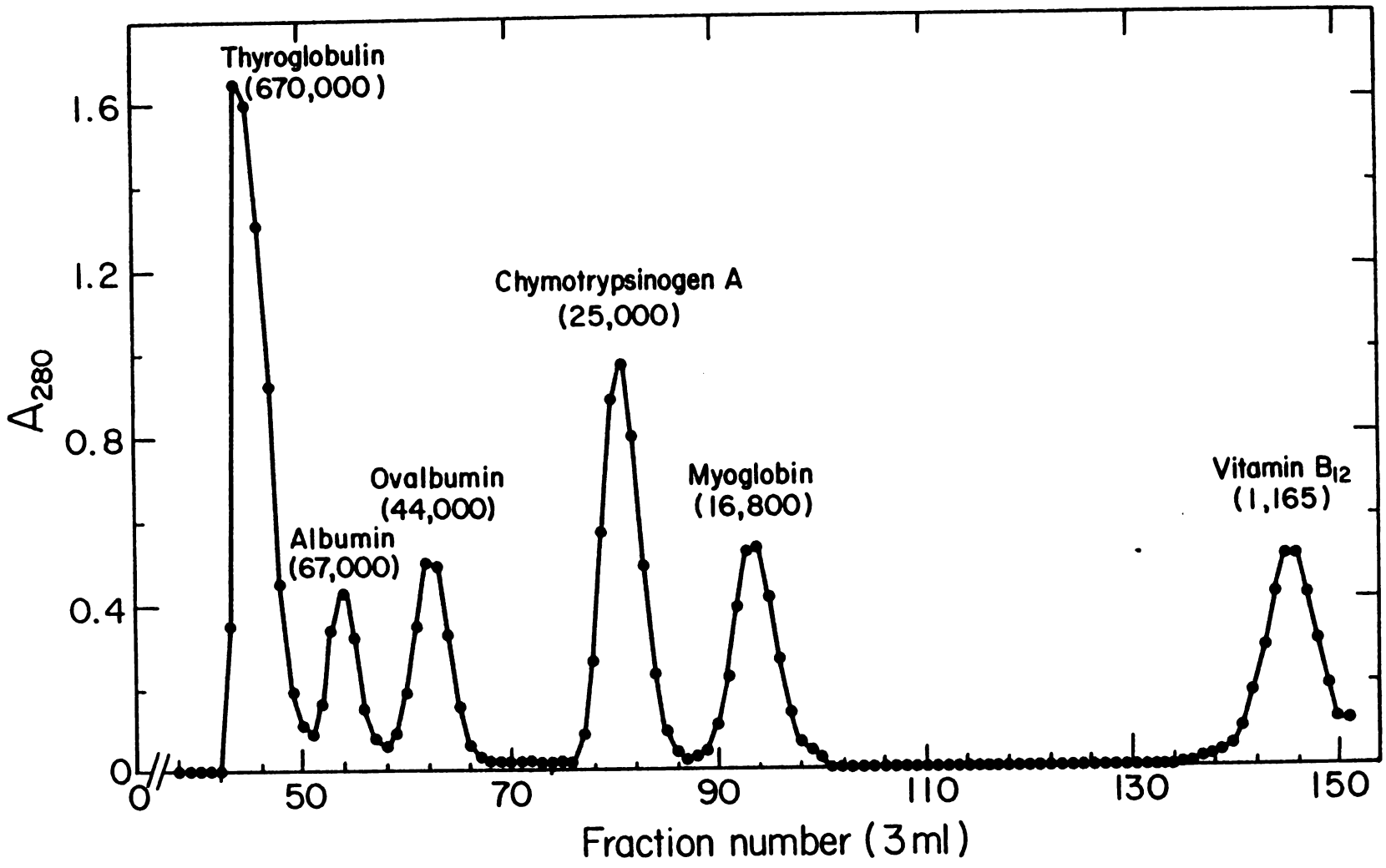
Thyroglobulin
(670,000)
Chymotrypsinogen A
(25,000)
Ovalbumin
(44,000)
Albumin
(67,000)
Myoglobin
(16,800)
Vitamin B_{12}
(1,165)
A_{280}
1.6
1.2
0.8
0.4
0
0
50
70
90
110
130
150
Fraction number (3ml)

FIGURE 5.2.

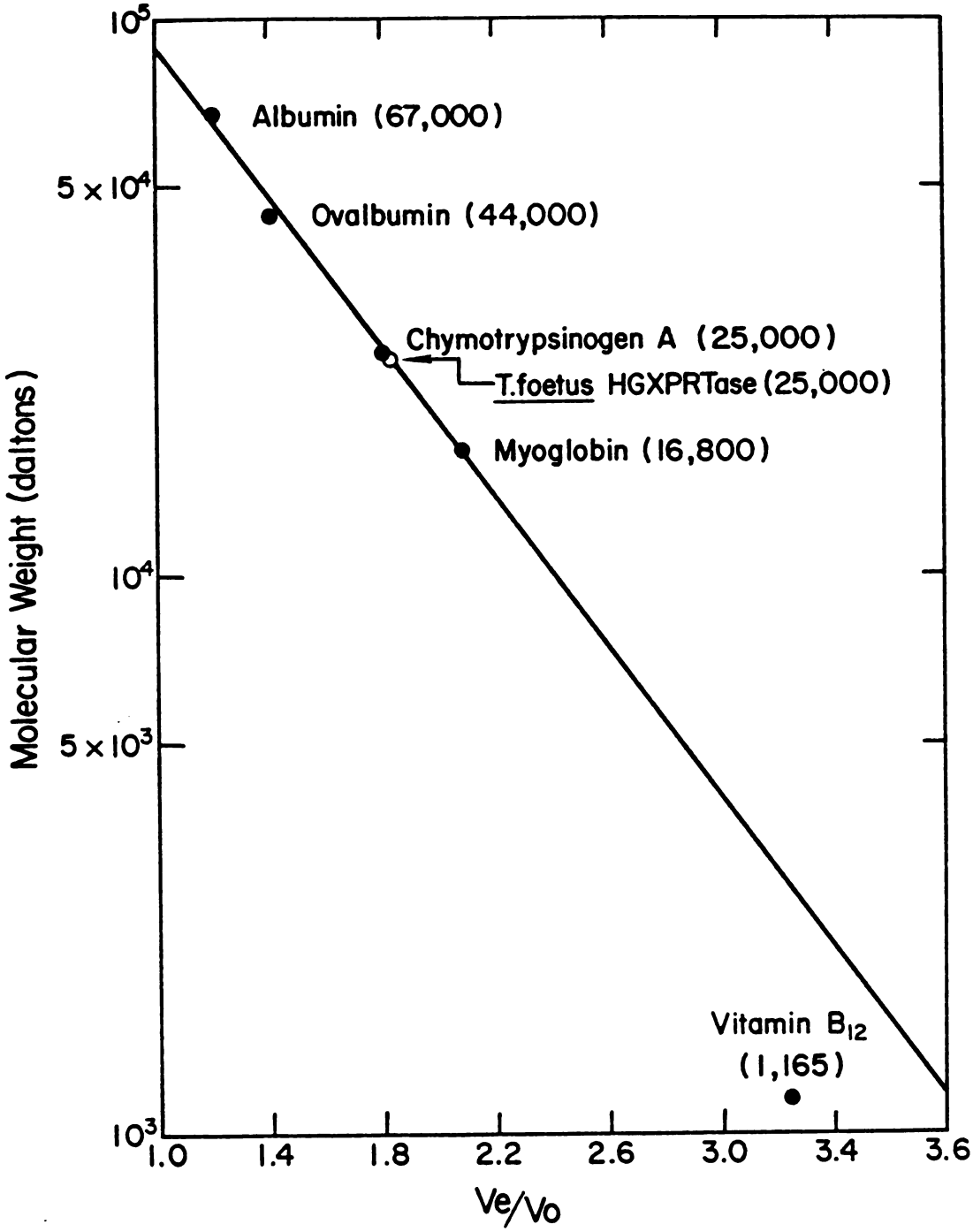

FIGURE 5.3. Standard curve for the determination of molecular weights on a Sephadex G-75 column (2.5 x 98 cm). The native molecular weight of HGXPRTase from T. foetus is 25,000 daltons.

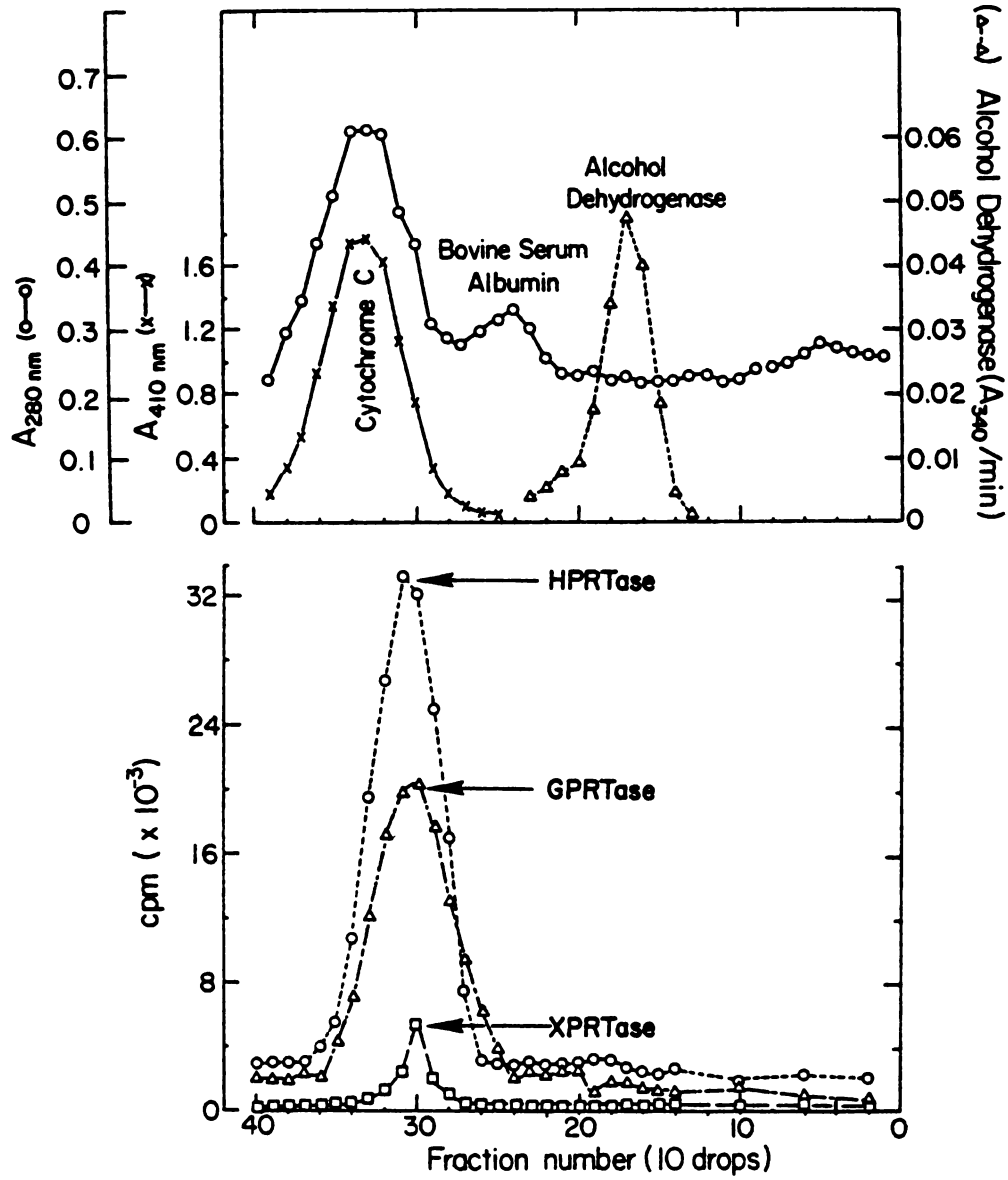

FIGURE 5.4. The partially purified enzyme (Step 3) was sedimented in an isokinetic sucrose gradient along with the indicated standards. The sedimentation coefficient of HGXPRTase from T. foetus is 3.7 S. Activity was determined using 50 μM of [8-^{14}C]hypoxanthine (48.7 mCi/mmol), [8-^{14}C]guanine (51 mCi/mmol) and [8-^{14}C]xanthine (55 mCi/mmol).

FIGURE 5.5. Rate of inactivation of phosphoribosyltransferase activities from T. foetus at 37°C. Incubation mixtures contained 50 mM Tris-HCl pH 7.2, 10 mM $MgCl_2$ and 1 mM DTT. Step 3 protein was used for HGXPRTase activity and an equivalently purified (after G-75) UPRTase from T. foetus was also examined.

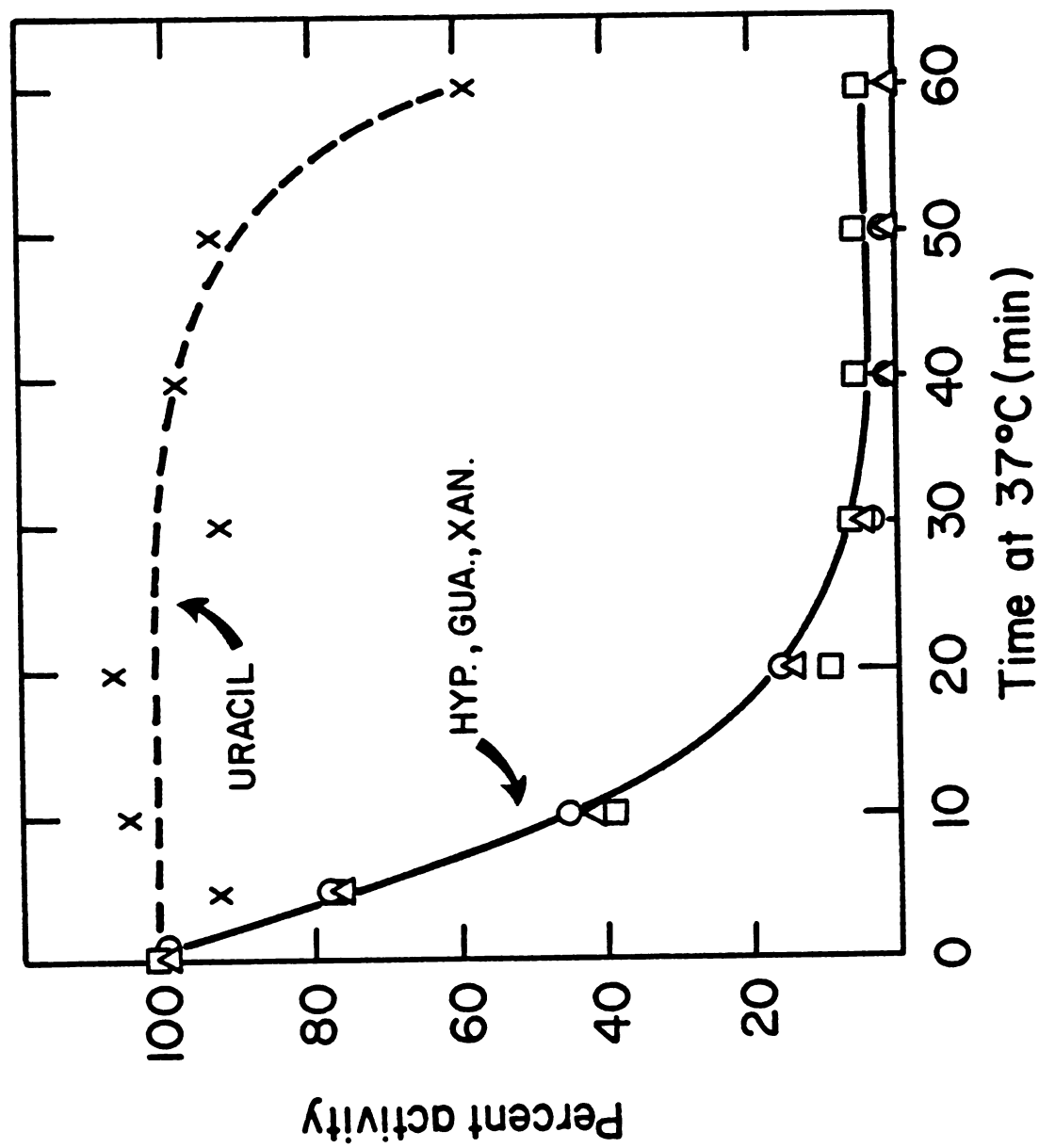
Percent activity
100
80
60
40
20
0
10
20
30
40
50
60
Time at 37°C (min)
URACIL
HYP., GUA., XAN.

FIGURE 5.5.

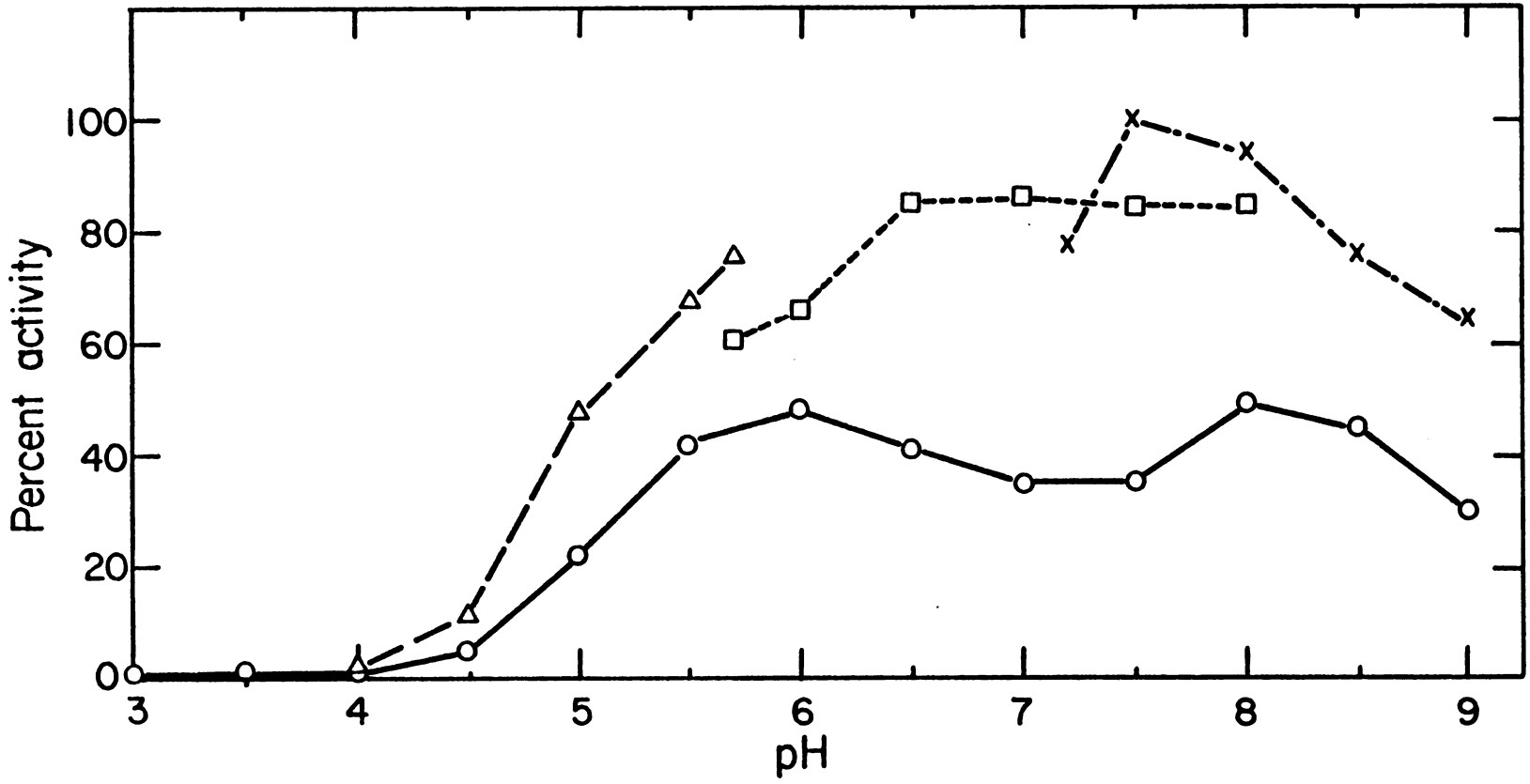

FIGURE 5.6. The effect of buffer and pH on hypoxanthine phosphoribosyltransferase activity. The buffers used are; 100 mM citrate/phosphate/borate pH 3-9 (○), 50 mM NaOAc pH 4-5.7 (△), 50 mM $NaHPO_4$ pH 5.7-8.0 (□) and 50 mM Tris-HCl pH 7.2-9.0 (×). Activity was determined using [8-^{14}C]hypoxanthine (48.7 mCi/mmol).

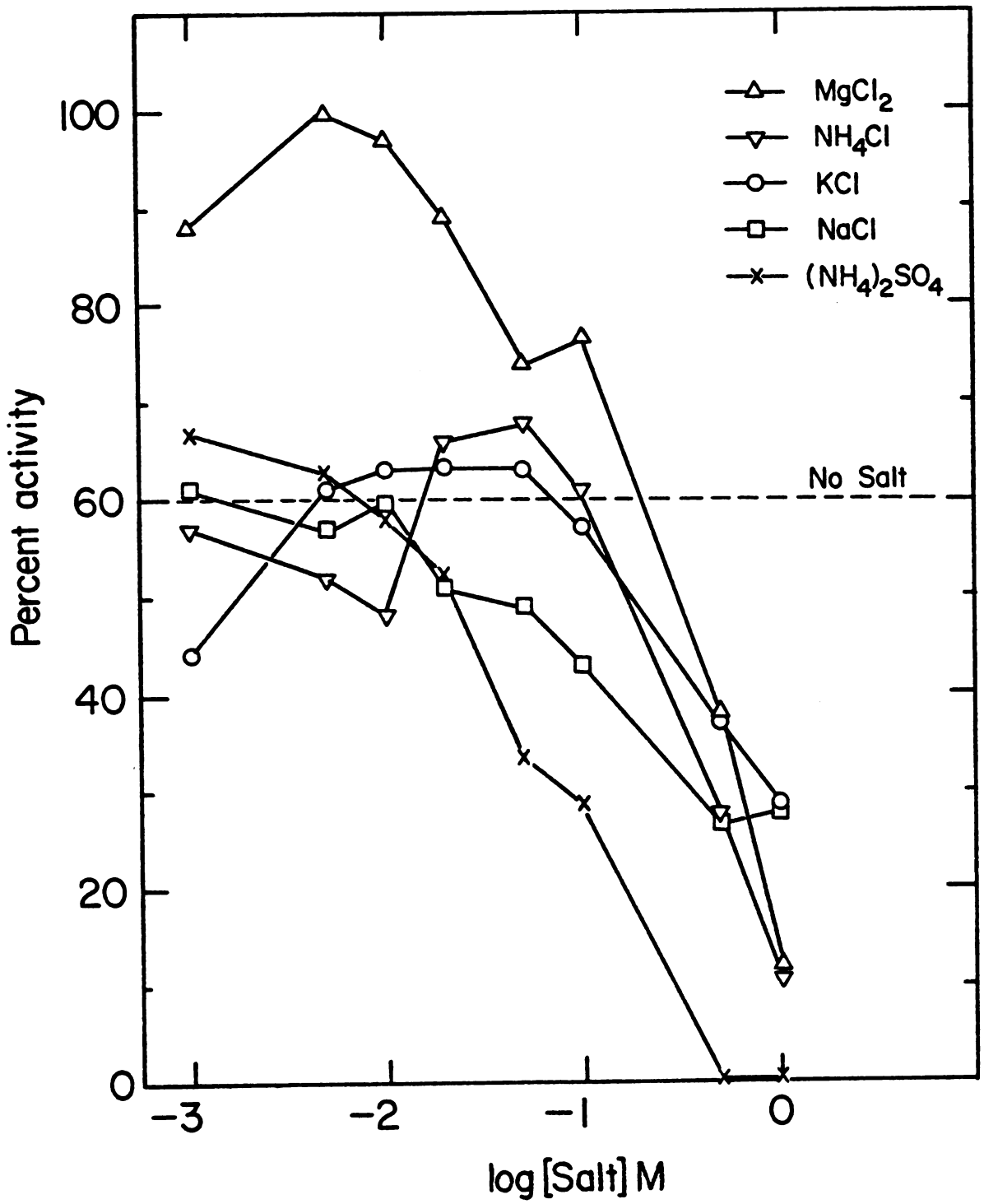

FIGURE 5.7. Effect of inorganic salts on the activity of HGXPRTase of T. foetus. The reactions were conducted with 100 mM Tris-HCl pH 7.8, 1 mM PRPP, 50 µg/ml BSA, 1 mM DTT and 20 µM [8-^{14}C]hypoxanthine (48.7 mCi/mmol).

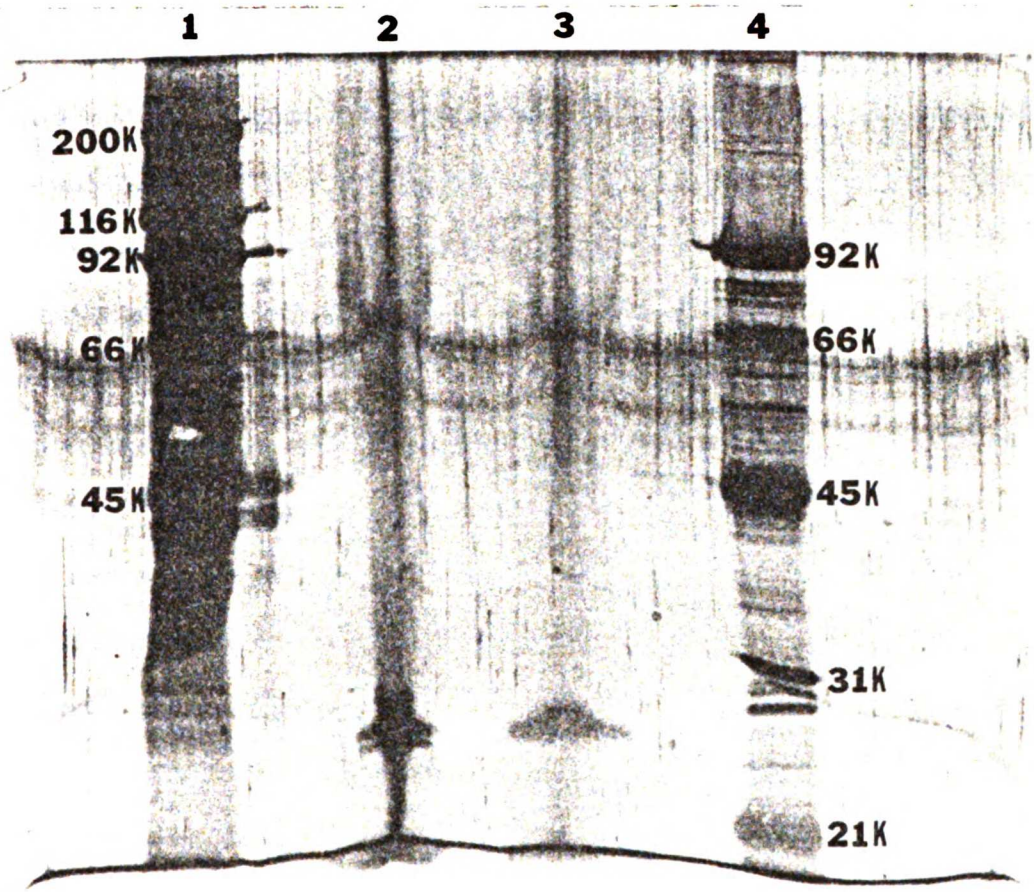

FIGURE 5.8. SDS-PAGE, 10%T and 2.7%C, stained by Silver stain (215). Lane 1) High M.W. standards, Lane 2 and 3) 100µℓ and 20µℓ, repectively, T. foetus HGXPRTase Step 5 protein and Lane 4) Low M.W. standards.

DISCUSSION

The phosphoribosyltransferases in T. foetus seem to be quite susceptable to protease activity as demonstrated by a dramatic increase of activity in crude extracts in the presence of protease inhibitors. T. foetus has been shown to have a single protease of 20,000 molecular weight and found associated with the "large cytoplasmic particle" population (206-208). This protease is inhibited by compounds effective against thiol proteinases such as; p-chloromercuribenzoate, iodoacetate, N-α -tosyl-L-lysine chloromethylketone, L-tosylamide-2-phenylethyl chloromethylketone, leupeptin, antipain and chymostatin (207). Leupeptin, present in our protease inhibitor mixture may account for a decrease in protease activity and the resultant increase in phosphoribosyltransferase activity.

Hypoxanthine, guanine and xanthine phosphoribosyltransferase activities seem to be associated with a single protein as evidenced by; 1) coelution of all three activities from Sephadex G-75 filtration, GMP agarose and DEAE-Sepharose chromatographies (Figure 5.1), 2) identical heat inactivation profiles (Figure 5.5), 3) similar pH optimum (Figure 5.6), 4) similar requirements for magnesium ion (Figure 5.7) and stabilization by PRPP (Table 5.3), 5) similar sedimentation rate in isokinetic sucrose centrifugation (Figure 5.4) and 6) single protein band in SDS-PAGE (Figure 5.8.).

The native molecular weight of T. foetus HGXPRTase, as determined by gel filtration is 25,000 daltons (Figure 5.3). Gel filtration also created a dramatic change in activity of HGXPRTase perhaps because of the removal of guanase and xanthine oxidase by this purification step.

Work by Tuttle and Krenitsky (143) have shown that gel filtration of adenine phosphoribosyltransferase activity from L. donovani is eluted at a volume corresponding to a particle weight of 25,000 in the absence of PRPP and 54,000 in the presence of PRPP. The molecular weight of T. foetus HGXPRTase is unique in being so small as compared to the phosphoribosyltransferases found in other protozoans such as Leishmania donovani HGPRTase, molecular weight of 56,000 (143) or in mammmalian erythrocyte HGPRTase, molecular weight of 96,000 (214). A sedimentation coefficient of 3.7 S for T. foetus HGXPRTase is also smaller than the 5.9 S (214) observed for human erythrocyte HGPRTase. This supports the gel filtration finding that this protozoan HGXPRTase is indeed smaller than phosphoribosyltransferases in general.

Substrate specificty of the protozoan HGXPRTase is hypoxanthine > guanine >> xanthine while product formation is not as specific. A unique catalytic feature of HGXPRTase was discovered when the products of the phosphoribosyltransferase assay was analyzed by HPLC. We observed the formation of IMP and XMP from hypoxanthine and GMP and XMP from guanine. This phenomenon is difficult to explain because the enzyme preparation is free of contaminating activities such as guanase, xanthine oxidase and IMP dehydrogenase.

The enzyme is similar to other phosphoribosyltransferses with respect to its broad pH optimum (on the alkaline side), requirement for magnesium ion and stabilization by PRPP.

Preliminary inhibition studies indicate a correlation between HGXPRTase inhibition and inhibition of T. foetus growth in TYM (Table 5.2). As illustrated in Table 5.2, 8-thioguanine is a good inhibitor of both HGXPRTase activity and in vitro growth.

This investigation supports the hypothesis that HGXPRTase plays a key role in purine salvage in Tritrichomonas foetus. This enzyme is capable of recognizing hypoxanthine, guanine and xanthine as substrates and producing IMP, GMP and XMP. The trichomonads HGXPRTase is unusually small in native molecular weight and is inhibitable by several purine analogs. The enzyme is thus an attractive target for chemotherapeutic inhibition. Further work will be required to uncover the enzyme's mechanism of XMP formation from both hypoxanthine and guanine.

CHAPTER 6

SUMMARY

Tritrichomonas foetus is an anaerobic protozoan parasite, worldwide in distribution and infects the urogenitial tract of cattle. Characteristic features of this trichomonad include three anterior flagella, an undulating membrane, absence of mitochondria and the presence of the small organelles, hydrogenosomes. The present drug of choice, metronidazole, is carcinogenic in rats and mice and mutagenic in bacteria. This and the emergence of metronidazole resistant strains of *T. vaginalis* has provided impetus for the development of safe and effective agents against trichomoniasis.

Tritrichomonas foetus has been chosen to be a model system in our "rational" approach to antiparasitic drug design. Our effort entails a comparative biochemical study of the parasite and the host and then exploiting any differences that we may find.

All parasitic protozoa examined to date are incapable of *de novo* synthesis of purine nucleotides and thus dependent upon salvage of exogeneous preformed purines to fulfill their purine requirements. This deficiency has led to discoveries of some purine and purine nucleoside analogs as antileishmanial and antitrypanosomal agents.

De novo pyrimidine biosynthesis, on the other hand, takes place in most of the parasitic protozoa examined. Recent evidence however indicates that the anerobic flagellates, *Trichomonas vaginalis* and *Giardia lamblia* may not be able to synthesize pyrimidines *de novo*. This suggests that anerobic flagellates may be incapable of both *de*

novo purine and pyrimdine biosynthesis and these defects in the parasite metabolism may provide us with several potential sites for antiparasitic chemotherapeutic attack. The purine and pyrimidine metabolism of Tritrichomonas foetus, another anerobic flagellate, has been studied and potential sites for chemotherapeutic intervention identified.

Tritrichomonas foetus is incapable of incorporating radiolabeled bicarbonate, asparatate or orotate into its pyrimidine nucleotide pool, or its nucleic acids. No orotate phosphoribosyltransferase can be detected in the extracts of the trichomonad. The parasite thus likely lacks the capability of de novo pyrimidine synthesis. In similar experiments, however, active incorporation of uracil into UMP, UDP and UTP is observed due to a high level of uracil phosphoribosyltransferase (UPRTase) and, presumably high nucleotide kinases, in the cellular cytoplasm of T. foetus. Uridine and cytidine are also incorporated into the nucleotide pool; but mainly through prior conversion to uracil by uridine phosphorylse and cytidine deaminase found in T. foetus. 5-Fluorouracil is an inhibitor of the UPRTase as well as an inhibitor of T. foetus growth with similar IC_{50} values of 60 μM and 25 μM respectively. In addition, 5-fluorouracil is incorporated and converted to 5-fluorouridine mono-, di-, and triphosphates. Uracil, uridine and deoxyuridine cannnot be incorporated into the parasites DNA. The parasite contains no detectable dihydrofolate reductase or thymidylate synthetase and is resistant to millimolar concentrations of methotrexate, pyrimethamine, trimethoprim or 3-bromovinyldeoxyuridine. The only apparent means of obtaining TMP for the parasite is by an enzyme, thymidine phosphotransferase found in the pelletable

cellular fraction of T. foetus. Guanosine phosphotransferase is also found in the same pelletable fraction and guanosine serves as a competitive inhibitor of thymidine phosphotransferase. This independent pathway of exclusive thymidine salvage could be another valuable target for controlling bovine trichomoniasis.

Tritrichomonas foetus is also incapble of de novo purine synthesis by its failure to incorporate radiolabeled glycine or formate into the nucleotide pool. It has high activities of incorporating adenine, hypoxanthine or inosine. HPLC analysis of the nucleotides extracted from T. foetus following radiolabel pulse-chase experiments indicate that adenine, hypoxanthine and inosine all enter the nucleotide pool through prior conversion to IMP. This observation is supported by the high hypoxanthine phosphoribosytransferase, adenine deaminase and inosine phosphorylase, but no adenine phosphoribosyltransferase, inosine kinase or inosine phosphotransferase activities in T. foetus crude extracts. Adenine and inosine are thus converted to hypoxanthine before incorporation.

Adenosine is also rapidly convered to hypoxanthine, but the adenosine kinase in the parasite also converts some adenosine directly to AMP. There are direct incorporations of guanine and xanthine into GMP and XMP, due to guanine and xanthine phosphoribosyltransferase. There are also activities which convert guanosine to guanine and guanine to xanthine. A guanosine phosphotransferase is found in the sedimentable fraction of T. foetus, and is capable of converting some guanosine to GMP. This overall network of T. foetus purine salvage suggests the importance of hypoxanthine-guanine-xanthine phosphoribosyltransferase activities. It is postulated that specific

inhibition of this enzyme(s) could lead to effective chemotherapeutic control of T. foetus.

The parasites reliance upon the salvage of exogeneous purines and their conversion to nucleotides may provide us with opportunities for inhibitor design. As a consequence of this study, several purine inhibitors were tested on Tritrichomonas foetus. Mycophenolic acid, hadacidin, 8-azaguanine and forymycin B inhibited the growth of the parasite. Mycophenolic acid inhibited IMP dehydrogenase (IMP to XMP conversion), hadacidin blocked adenylosuccinate synthetase (IMP to AMP conversion) whereas 8-azaguanine was incorporated into the nucleotide pool of T. foetus as 8-azaguanosine mono-, di-, and triphosphates. Formycin B is converted to formycin B 5'-monophosphate and inhibits IMP to AMP conversion. Alanosine, a potent inhibitor of mammalian adenylosuccinate synthetase and virazole, an inhibitor of mammmalian IMP dehydrogenase in the intact cells, had no effect on the growth of T. foetus or hypoxanthine incorporation in T. foetus.

Tritrichomonas foetus is dependent primarily on the salvage of exogenous hypoxanthine to fulfill its needs for purine nucleotides. Two enzymes involved in this conversion, hypoxanthine-guanine-xanthine phosphoribosyltransferase and IMP dehydrogenase have been more closely examined. The IMP dehydrogenase activity in T. foetus must be essential for survival of the parasite in a natural enviroment where the main source of purine comes from degradation of adenine nucleotides to hypoxanthine. When T. foetus is cultured in vitro supplemented with hypoxanthine as the only source of purines, the cell growth is effectively inhibited by mycophenolic acid (MPA), a known inhibitor of IMP dehydrogenase, with an IC_{50} value of 30 μM. HPLC

analysis of the nucleotide pool in MPA-treated T. foetus suggested inhibition of hypoxanthine incorporation into guanine nucleotide as the cause of growth inhibition which could be reversed by adding guanine or guanosine to the culture medium.

IMP dehydrogenase has been purified some 500 fold by 45-75% ammonium sulfate fractionation, Bio-Gel A 0.5m filtration, DEAE-Sepharose and Cibacron blue column chromatographies with an overall yield of 42%. The purified enzyme preparation does not have activites of GMP synthetase, adenylosuccinate synthetase, hypoxanthine-guanine-xanthine phosphoribosyltransferase or NADH oxidase. IMP dehydrogenase activity stained by tetrazolium salts in polyacrylamide electrophoretic gels indicated the presence of a single activity band which by Coomassie Blue stain constitute about half of the proteins in the purified preparation. Gel filtration and SDS polyacrylamide gel electrophoresis (PAGE) showed an unusually high molecular weight of 380,000 for the native enzyme with an estimated subunit molecular weight of 58,000. The enzyme has a pH optimum of 8.0 and K_m values of 18 μM and 445 μM for IMP and NAD^+ respectively. XMP and GMP are both inhibitors of the enzyme by competing with IMP at the K_i values of 27 μM and 95 μM respectively. The enzymatic reaction mechanism is ordered with IMP binding first and XMP the last product to leave and shows no requirement for inorganic salt. Both the lack of an inorganic salt requirement and its unusually large molecular weight make T. foetus IMP dehydrogenase unique from the others. Mycophenolic acid is an uncompetitive inhibitor with IMP and NAD^+ at the K_i values of 9 μM and 6 μM; which is similar to its inhibitory potency on mammalian IMP dehydrogenase.

Hypoxanthine-Guanine-Xanthine phosphoribosyltransferase, another key enzyme in the conversion of hypoxanthine to purine nucleotides, has been purified 460 fold by 45-75% $(NH_4)_2SO_4$ fractionation, Sephadex G-75 filtration, GMP agarose and DEAE-Sepharose column chromatographies with an overall yield of 200% due to removal of endogenous inhibitors. The enzyme has a native molecular wight of 25,000 daltons and final specific activities of 137.7, 71.1 and 3.9 nmol/min/mg of protein for hypoxanthine, guanine and xanthine respectively. The HGXPRTase from T. foetus requires magnesium ion, is stabilized by PRPP and has a broad pH optimum of about 7.5-9. The purified enzyme is free of adenase, guanase, IMP dehydrogenase and xanthine oxidase activities as determined by spectrophometric assays. Several purine analogs were also found inhibitory to T. foetus HGXPRTase including 6-mercaptopurine, 2-amino-6-thiopurine and 8-thioguanine. In vitro growth studies indicate that 8-thioguanine is a good inhibitor of T. foetus growth in TYM while 6-mercaptopurine and 2-amino-6-thiopurine were weak inhibitors of growth. The data indicate that the HGXPRTase in T. foetus is quite unique and significantly different from mammalian HGPRTase. The enzyme's potential as a chemotherpeutic target is supported because of its differance from mammalian HGPRTase.

In conclusion, examination of the purine and pyrimidine metabolism in Tritrichomonas foetus has provided us with several potential sites as chemotherapeutic targets. Further examination of two of these enzyme sites, IMP dehydrogenase and HGXPRTase has uncovered major differances between the protozoan enzymes and its mammalian counter parts. Preliminary inhibitor screening has provided lead compounds in our "rational" approach to chemotherapeutic

inhibitor design. Further work will be required to follow up on these lead compounds and also to examine other "potential sites" for inhibitor design in T. foetus. This work is the initial phase in our "rational" approach to inhibitor design and we hope it will eventually lead to an effective and safe agent in the treatment of bovine trichomoniasis.

APPENDIX A

TRITRICHOMONAS FOETUS CULTIVATION

Since 1933, with the advent of and use of antibiotics, a medium capable of supporting growth of T. foetus in the absence of bacteria was devised (111). Axenic cultures of T. foetus can be readily cultivated in a variety of media. The media, none of them chemically defined, commonly used include Plastridges's medium as modified by Fritzgerald et al (112), TYM (114), CPLM (115), CTLM (116), NIH thioglycollate broth (34) and Brewer thioglycollate (34). All media were supplemented with normal sera in differant concentrations from various mammals. T. foetus has also been cultivated on agar plates (117).

In our experiments, T. foetus strain KV_1, was axenically cultivated in Diamonds TYM medium pH 7.2, supplemented with 10% heat inactivated horse serum and 1% antibiotic/antimycotic mixture at 37°C (114). TYM media consists of the following;

	g/liter H_2O
Tryptose	20.0
Yeast extract	10.0
Maltose	5.0
Cysteine HCL	1.0
Ascorbic Acid	0.2
K_2HPO_4	0.8
KH_2PO_4	0.8

The media was adjusted to pH 7.2 with KOH, dispensed into 500 ml bottles and autoclaved for 20 minutes at 121°C. The media can be stored for several weeks at 4°C. Prior to use, 10% heat inactivated horse serum and 1% antibiotic/antimycotic mix is added. Horse serum is heat inactivated by incubating the serum at 57°C for 30 minutes. The antibiotic/antimycotic mix contains (100X solution)- 10,000 U/ml Penicillin, 25 mcg/ml Fungizone and 10,000 mcg/ml streptomycin.

Stationary cultures having a cell density of about 14 x 10^6 cells/ml are transfered to fresh media in a 1:10 ratio. After 24 hours growth the cultures are again transferred to fresh media. Midlogarithmic phase of growth, with a cell density of 8.0 x 10^6 cells/ml can be achieved by using a 4% innoculum of a 24 hour old culture and harvesting cells 16 hours later. The growth of T. foetus is independent of vessal size as long as the amount of air in the container is kept to a minimum. Figure A.1 illustrates the growth of T. foetus in TYM. Cells were rountinely counted using a Coulter Counter Model Z_f, with Amplification 4, Threshold 18 and Aperture current at $\frac{1}{2}$.

Tritrichomonas foetus may also be cultivated in a semi-defined media (118). The composition of semi-defined media (HUT) is shown in Table A.1.

The pH of the HUT solution is adjusted to 7.5 and 10% heat inactivated Dialyzed Horse serum and 1% antibiotic/antimycotic mix is added. The media is then sterilized by passage through a 0.22 micron filter.

Cryopreservaton of T. foetus, with high recovery, is achivable from stabilates frozen in liquid nitrogen with dimethylsulfoxide serving as the cryoprotectant (119, 120, 121).

TABLE A.1 The composition of HUT medium.

	mg/Liter H_2O		mg/Liter H_2O
NaCl	2000	Nicotinamide	5
KCl	2000	Riboflavin	1
KH_2PO_4	1000	Choline	1
K_2HPO_4	500	Thiamine	1
Ferric Ammonium citrate	20	Pyridoxamine	5
$MgSO_4$	361	Pantothenic acid	10
$CaCl_2$	235		
Trace elements (10K X)	100 µl	Hypoxanthine	2
		Uracil	2
Maltose	5000	Thymidine	0.2

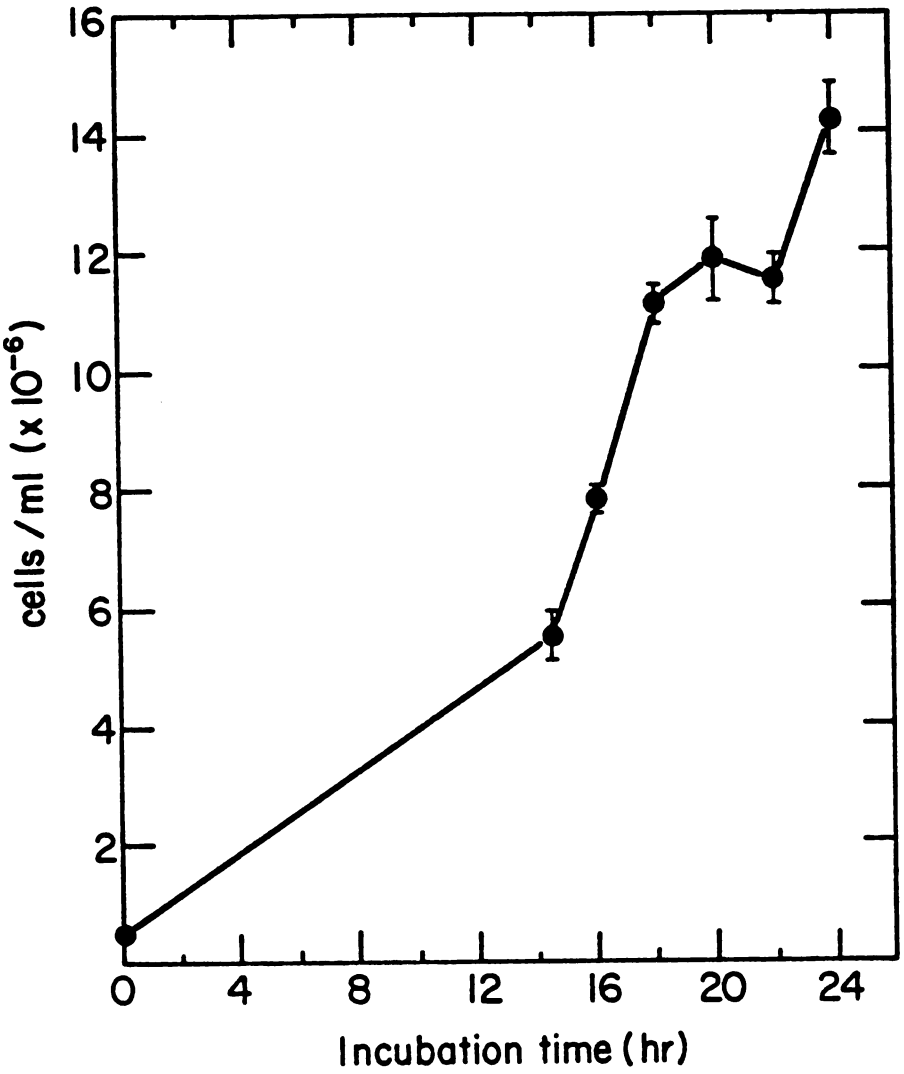

FIGURE A.1. Growth curve for Tritrichomonas foetus in TYM.

APPENDIX B

FLOW BETA-RADIOACTIVE DETECTION

The use of a radioactivity flow detector circumvented methods of collecting effluent fractions for subsequent measurement by static liquid scintillation spectroscopy (LSC). The optimal use of radioactivity flow detectors requires to balance a large number of interrelated instrumental parameters. Several workers have attemped a quantitative description of flow beta-counting, but none have presented general algorithms relating parameters of flow detector performance in usuable equations (122-124). Recently however, Klein and Hunt have developed realistic and general equations which define how eight chromatographic and instrumental parameters affect sensitivity in flow radioactivity detectors (125). Use of these equations allow the chromatographer to optimize sensitivity or calculate the experimental parameters required to achieve any desired sensitivity before experimentation is done. General equations interrelating column chromatography condition with factors of flow-beta-radiation detectors are shown below:

$$C = \frac{(cpm)seV}{100(fs + k)} \qquad (1)$$

The total counts registered by the detector after an entire HPLC peak has passed through the cell, C, can be calculated from; i) cpm,

the total cpm in the HPLC peak from LSC, ii) f, the HPLC flow rate (ml/min), iii) s, the splitting fraction (0-1.0), iv) e, the % counting efficiency, v) V, the volume of the flow cell (ml), and vi) k, the cocktail flow rate (ml/min). Equation 1 illustrates that we can maximize sensitivity by maximizing s, minimizing k, minimizing f and using the largest V consistant with out requirements of resolution.

Assuming that the radioactivity chart recorder peak is roughly triangular in shape, we can calculate w_r, the width of the radioactive chart peak at its base from w_c, the width of the UV detector chart peak at its base and other known parameters using equation 2.

$$w_r = w_c + \frac{V}{(fs + k)} \qquad (2)$$

Equation 1 and 2 can then be combined to calculate the sensitivity of flow detection with a given set of intrumental parameters. For example, for a signal/noise $\geq$ 2, the minimum detectable peak h_{min} is,

$$h_{min} = 2(BKgd) = 2C/w_r$$

$$= \frac{2(cpm)_{min}\ seV}{100(fs + k)w_r}$$

then rearranging,

$$(cpm)_{min} = \frac{100(Bkgd)(fs + k)w_r}{seV} \qquad (3)$$

Solving equation 3 with the following instrumental parameters; f = 1 ml/min, s = 3, e = 12% (^{3}H), 19% (^{14}C), V = 1.75 ml, k = 3 ml/min, w_c = 1 min and Bkgd = 40 cpm, we find that the minimum detectable ^{3}H peak is 1095 cpm and ^{14}C peak is 692 cpm above background. The HPLC parameters will be discussed further in another section.

In a flow radioactive detector, gelling of the scintillation cocktail must be avoided. Most commercially available scintillation cocktails contain gelling agents in order to avoid a two phase system with the addition of water. Modification of commercial cocktails was accomplished by mixing 1 part Aquasol 1 (NEN) with 1 part "scintillized" toluene. Scintillized tolune contains 40 ml Triton X-100, 1.2g Bis-MSB (p-bis-(o-methylstryrl)benzene) and 40g PPO (2,5-diphenyloxazole) per 4 liters of toluene. This new mixture still retains the same counting efficiency as Aquasol 1, but will not gel when mixed with water.

APPENDIX C

HPLC

High Performance Liquid Chromatography (HPLC) was done using Beckman Model 110A pumps and Model 420 controller. Column effluent was monitored with a Beckman 160 UV absorbance detector and a Radiomatic Flo-one radioactive flow detector hooked up in series. The output of the detectors was recorded synchronously on a Kipp and Zonen BD 41 dual pen chart recorder and analyzed with a Hewlett-Packard 3390A intergrator.

HPLC is used extensively in our work of purine and pyrimidine metabolism. Ion exchange chromatography was used to analyze nucleotides while reverse phase chromatography was used to separate bases and nucleosides. In addition, the HPLC was used to monitor the interconversion of labeled nucleotides and to analyze for products of enzymatic reactions. The separation of these various compounds not only required two different types of columns, but also entirely different separation schemes and instrumental parameters.

Analysis of the purine and pyrimidine nucleotide pool of T. foetus required that nucleotides be extracted from the parasites prior to HPLC. There are several methods to accomplish this and we settled on a modification of a procedure by van Haverbeke and Brown (126-128). T. foetus cells are lysed by the addition of 4.2M perchloric acid (final concentration of 0.2M). After 30 minutes in an ice bath the sample is spun to remove any precipatate and then neutralized by the

addition of an equal volume of Freon (1,1,2-trichloro-1,2,2-trifluoroethane)/trioctylamine (50:50 mix). This procedure ensures that the aqueous phase is in a pH range of 5-7. This extraction procedure has been shown to be very effective in the extraction and recovery of nucleotides from biological sources (128).

Most nucleotide analysis employing high pressure liquid chromatography depend on the use of microparticulate chemically bonded resins, usually strong anion exchangers or reverse phase adsorbents. Reverse phase HPLC of nucleotides involves the use of a phosphate buffer and low concentrations of an ion pairing reagent like tetrabutylammonium phosphate. The nucleotides are then eluted by an organic buffer either isocratically or with a gradient (131,132). We encountered several problems using reverse phase chromatography for nucleotide separation. The salts used, such as sodium and potassium phosphates, to make up the buffers contained large amounts of UV absorbing material which would stick to the column and then be eluted by the acetonitrile. This caused an upward baseline drift on the chromatograph as the organic eluting buffer concentration increased. This problem was corrected by passing the buffer over an appropriate resin to remove the UV absorbing organics or by usage of ammonium instead of potassium, or sodium phosphate. Another problem encountered with this procedure was poor peak resolution. Maximizing peak separation was important if this separation scheme was to be used in conjuction with flow beta detection.

Anion exchange chromatography of nucleotides (126,129,130) proved

to be more succesful and provided well separated peaks using a slow flow rate of 1 ml/min. A compromize was chosen between length of chromatographic runs, a consequence of a slow flow rate, and maximizing sensitivity of flow radioactive detection. The separation of nucleotides involved equilibration of a 4.6 x 250mm Partisil 10-SAX or Ultrasil AX column with 7 mM KH_2PO_4 pH 3.8. Samples are loaded and then eluted with a gradient starting from 7 mM KH_2PO_4 pH 3.8 to 250 mM KH_2PO_4, 500 mM KCl pH 4.5 at a flow rate of 1 ml/min. Figure C.1 shows a typical separation of nucleotides.

Reverse phase chromatography was used primarily for the analysis of nucleosides and bases. Samples are injected onto a 4.6 x 250mm Ultrasphere ODS column equilibrated with 7 mM KH_2PO_4 pH 6.0 and then eluted by a gradient of acetonitrile at a flow rate of 0.75 ml/min. Figure C.2 shows a typical separation of nucleosides and bases.

As has been mentioned earlier, all methods encountered in the literature for the separation of nucleotides, nucleosides or bases dealt with a "rapid" separation scheme, which inevitable meant a fast flow rate. The fast flow rate was not conducive to flow radioactive counting and HPLC procedures needed to be optimized at a much slower flow rate. These slow flow rates tended to increase analysis time. The nucleotide separation required 90 minutes and the nucleoside and base separation took 70 minutes. All buffers used for HPLC purposes were degassed and passed through a 0.45 micron filter before use.

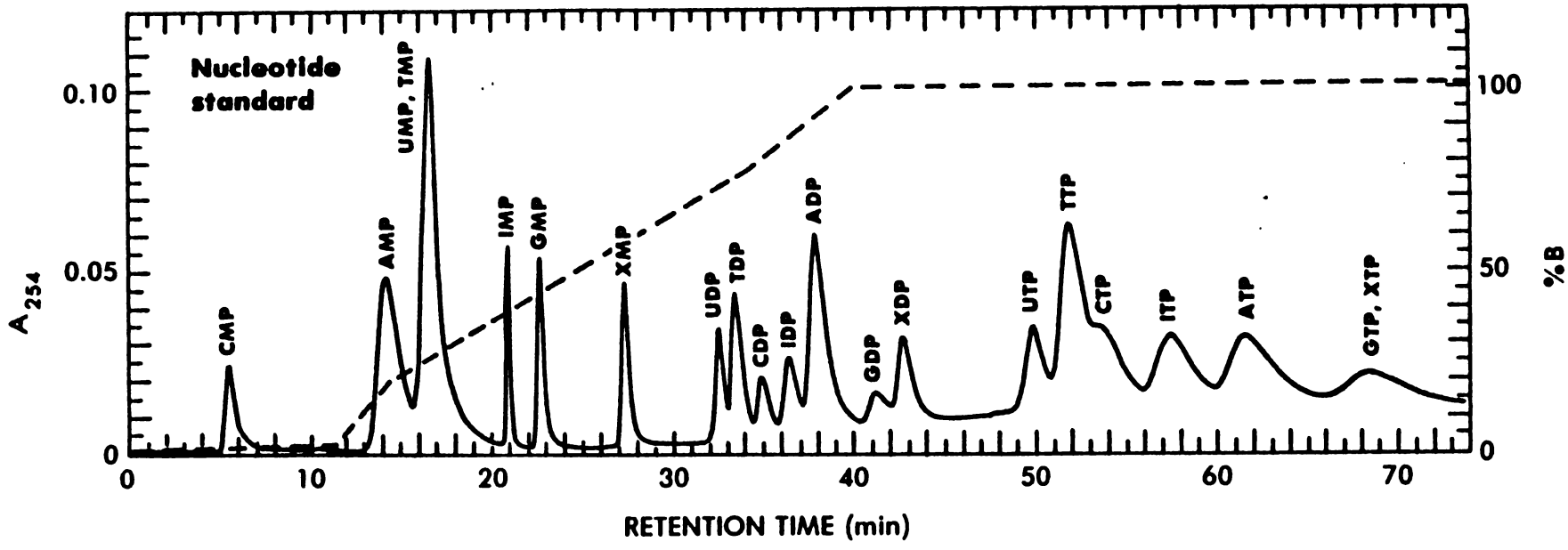

FIGURE C.1. Standard nucleotide elution profile using a Partisil 10 SAX column and gradient elution from 7 mM KH_2PO_4 pH 3.8 to 250 mM KH_2PO_4, 500 mM KCl pH 4.5.

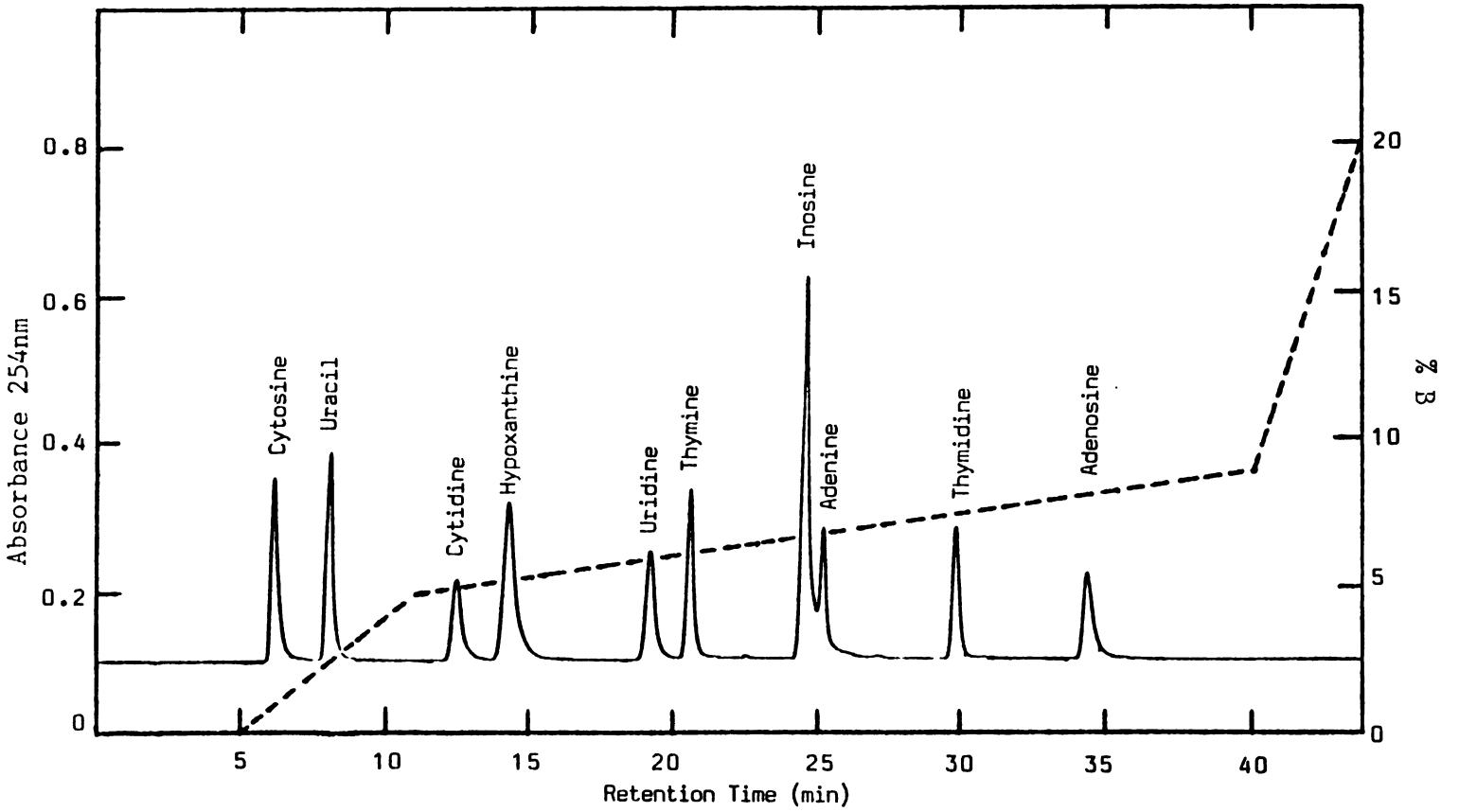

FIGURE C.2. Standard elution profile of bases and nucleosides using an Ultrasphere ODS column equilibrated with 7 mM KH_2PO_4 pH 6.0 and then eluted by a gradient of acetonitrile.

REFERANCES

1. Openshaw, H. (1953). In "The Alkaloids." (R. Manske and H. Holmes, eds.) pp. 101-118 Academic Press, New York-London.

2. Morgan, B. B., (1946). "Bovine Trichomoniasis," rev. ed. Burgess, Minneapolis, Minnesota.

3. Wenrich, D. H., and Emmerson, M. A. (1933). Studies on the morphology of Tritrichomonas foetus (Riedmuller) (Protozoa, Flagellata) from American cows. J. Morphol. 55, 193-206.

4. Morgan, B. B., and Hawkins, P. A. (1948). "Veterinary Protozoology." Burgess, Minneapolis, Minnesota.

5. Kirby, H. (1951). Observations on the trichomonad flagellate of the reproductive organs of cattle. J. Parasitol. 37, 445-459.

6. Honigberg, B. M. (1963). Evolutionary and systematic relationships in the flagellate order Trichomonadida Kirby. J. Protozool. 10, 20-63.

7. Levine, N. D. (1973). "Protozoan Parasites of Domestic Animals and of Man," 2nd ed. Burgess, Minneapolis, Minnesota.

8. Abraham, R., and Honigberg, B. M. (1964). Structure of Trichomonas gallinae (Rivolta). J. Parasitol. 50, 608-619.

9. Muller, M. (1973). Biochemical cytology of trichomonad flagellates. I. Subcellular localization of hydrolases, dehydrogenases, and catalase in Tritrichomonas foetus. J. Cell Biol. 57, 453-474.

10. Honigberg, B. M. (1970). Trichomonads. In "Immunity to Parasitic Animals" (J. G. Jackson, and I. Singer, eds.), Vol 2, pp. 469-550. Appleton, New York.

11. Hammond, D. M., and Bartlett, D. E. (1945). An instance of phagocytosis of Trichomonas foetus in bovine vaginal secretions. J. Parasitol. 31, 82.

12. Kulda, J., and Honigberg, B. M. (1969). Behavior and pathogenicity of Tritrichomonas foetus in chick liver cell cultures. J. Protozool. 16, 479-495.

13. Ito, Y., Furaya, M., Doi, M., Hayashi, H., Yayu, M., Oka, Y., and Osaki, H. (1975). Protective role of immune lymphoid cells and phagocytes in experimental trichomoniasis in mice. Jap. J. Parasitol. 24, 333-339.

14. Robertson, M. (1963). Antibody response in cattle to infection with Trichomonas foetus. In "Immunity to Protozoa" (P. C. C. Garnham, A. E. Pierce, and I. Roitt, eds.), pp. 336-345. Blackwell, Oxford.

15. Pierce, A. E. (1949). The agglutination reaction of bovine serum in the diagnosis of trichomoniasis. Br. Vet. J. 105, 286-294.

16. Robertson. M. (1960). The antigens of Trichomonas foetus isolated from cows and pigs. J. Hyg. 58, 207-213.

17. Kerr, W. R., and Robertson, M. (1945). A note on the appearance of serological varieties among T. foetus strains isolated from infected cattle. Vet. Rec. 57, 221-222.

18. Kerr, W. R. (1944). The intradermal test in bovine trichomoniasis. Vet. Rec. 56, 303-307.

19. Kerr, W. R., McGirr, J. L., and Robertson, M. (1949). Specific and nonspecific desensitization of the skin in Trichomonas-sensitive bovines. J. Comp. Pathol. Ther. 59, 133-154.

20. Kerr, W. R., Robertson, M., and McGirr, J. L. (1951). A study of the reaction of the white blood corpuscles in bovines at parturition with a consideration of the evidence of the action of the adrenal cortical hormone (cortisone). J. Hyg. 49, 67-80.

21. Feinberg, J. G., and Morgan, W. T. J. (1953). The isolation of a specific substance and a glycogen-like polysaccharide from Trichomonas foetus (var. Manley). Br. J. Exp. Pathol. 34, 104-118.

22. Endress, R. (1939). Verwertbarkeit der Komplementbindungsreaktion, der Agglomeration und der Trichomolyse fur die Erkennung der Trichomonaden-infecktion des Rindes. Arch. Wiss. Prakt. Tierheilkd. 75, 65-82.

23. Kerr, W. R., and Robertson, R. (1943). A study of the antibody response of cattle to Trichomonas foetus. J. Comp. Pathol. Ther. 53, 280-297.

24. Riedmuller, L. (1932). Zur Frage der atiologischen Bedeutung der bei Pyometra und sporadischen Abortus des Rindes gefundenen Trichomonaden. Schweiz. Arch. Tierheilkd. 74, 343-351.

25. Shorb, M. S. (1964). The physiology of trichomonads. In "Biochemistry and Physiology of Protozoa" (S. H. Hutner, ed.), Vol. 3, pp. 383-457. Academic Press, New York.

26. Danforth, W. F. (1967). Respiratory metabolism. In "Research in Protozoology" (T. T. Chen, ed.), Vol. 1, pp. 201-306. Pergamon, Oxford.

27. von Brand, T. (1973). "Biochemistry of Parasites," 2nd ed. Academic Press, New York.

28. Suzuoki, Z., and Suzuoki, T. (1951). Hydrogen evolution by Trichomonas foetus. Nature (London) 168, 610.

29. Suzuoki, Z., and Suzuoki, T. (1951). Carbohydrate metabolism of Trichomonas foetus. J. Biochem. (Tokyo) 38, 237-254.

30. Ryley, J. F. (1955). Studies on the metabolism of the parasite flagellate Trichomonas foetus. Biochem. J. 59, 361-369.

31. Manners, D. J., and Ryley, J. F. (1955). Studies on the metabolism of the protozoa. 6. The glycogens of the parasitic flagellates Trichomonas foetus and Trichomonas gallinae. Biochem. J. 59, 369-372.

32. Doran, D. J. (1957). Studies on trichomonads. I. The metabolism of Tritrichomonas foetus and trichomonads from the nasal cavity and cecum of swine. J. Protozool. 4, 182-190.

33. Doran, D. J. (1959). Studies on trichomonads. III. Inhibitors, acid production and substrate utilization by 4 strains of Tritrichomonas foetus. J. Protozool. 6, 177-182.

34. Lindblom, G. (1961). Carbohydrate metabolism of trichomonads: Growth, respiration and enzyme activity in four species. J. Protozool. 8, 139-150.

35. Cerkasovova, A. (1966). The respiration of the parasitic protozoa Trichomonas foetus; the influence of glucose and metabolic inhibitors. Acta Univ. Carol., Biol. pp. 171-177.

36. Cerkasovova, A. (1969). Energetic metabolism of Tritrichomonas foetus. II. Accumulation of pyruvic acid and thiamine deficient cultures. Folia Parasitol. (Prague) 16, 297-301.

37. Cerkasovova, A. (1970). Energy-producing metabolism of Tritrichomonas foetus. I. Evidence for control of intensity and contribution of aerobiosis to total energy production. Exp. Parasitol. 27, 165-178.

38. Cerkasovova, A., and Cerkasov, J. (1974). Location of NADH-oxidase activity in fractions of Tritrichomonas foetus homogenate. Folia Parasitol. (Prague) 21, 193-203.

39. Cerkasovova, A., and Cerkasov, J. (1974). Incorporation of ^{32}P into the microsomal fraction of Tritrichomonas foetus. Folia Parasitol. (Prague) 21, 204.

40. Cerkasovova, A., and Cerkasov, J. (1976). Some properties of the membrane of hydrogenosomes of Tritrichomonas foetus. In "Biochemistry of Parasites and Host-Parasite Relationships," (H. Van den Bossche, ed.), pp. 23-30. Elsevier/North Holland Biomedical Press, Amsterdam.

41. Muller, M. (1976). Carbohydrate and energy metabolism of Tritrichomonas foetus. In "Biochemistry of Parasites and Host-Parasite Relationships," (H. Van den Bossche, ed.), pp. 3-14. Elsevier/North Holland Biochemical Press, Amsterdam.

42. Lindmark, D. G., and Muller, M. (1973). Hydrogenosome, a cytoplasmic organelle of the anaerobic flagellate Tritrichomonas foetus, and its role in pyruvate metabolism. J. Biol. Chem. 248, 7724-7728.

43. Lindmark, D. G. and Muller, M. (1973). Subcellular distribution of flavins in two trichomonad species. J. Protozool. 20, 500.

44. Lindmark, D. G., and Muller, M. (1974). Superoxide dismutase in the anarobic flagellates, Tritrichomonas foetus and Monocercomonas sp. J. Biol. Chem. 249, 4634-4637.

45. Linkmark, D. G., and Muller, M. (1975). Acetate formation from pyruvate by hydrogenosomes of Tritrichomonas foetus. J. Protozool. 22, 13A.

46. Bauchop, T. (1971). Mechanism of hydrogen formation in Trichomonas foetus. J. Gen. Microbiol. 68, 27-33.

47. Muller, M. (1977). Regulation of carbohydrate metabolism in the anaerobic flagellate, Tritrichomonas foetus. Abstr. Pap. 5th Int. Cong. Protozool., New York, June-July, 1977. p. 226.

48. Muller, M., and Lindmark, D. G. (1974). Enzymes involved in succinate formation in Tritrichomonas foetus. Program Abstr. 49th Annu. Meet. Am. Soc. Parasitol. p. 43.

49. Lindmark, D. G. (1976). Acetate production by Tritrichomonas foetus. In "Biochemistry of Parasites and Host-Parasites Relationships," (H. Van den Bossche, ed.) pp. 15-21. Elsevier/North-Holland Biomedical Press, Amsterdam.

50. Honigberg, B. M., Mattern, C. F. T., and Daniel, W. A. (1971). Fine structure of the mastigont system in Tritrichomonas foetus (Riedmuller). J. Protozool. 18, 183-198.

51. Daniel, W. A., Mattern, C. F. T., and Honigberg, B. M. (1971). Fine structure of the mastigont system in Tritrichomonas muris (Grassi). J. Protozool. 18, 575-586.

52. Mattern, C. F. T., Honigberg, B. M., and Daniel, W. A. (1967). Mastigont system of Trichomonas gallinae (Rivolta) as revealed by electron microscopy. J. Protozool. 14, 320-339.

53. Baernstein, H. B. (1963). A review of electron transport mechanisms in parasitic protozoa. J. Parasitol. 49, 12-21.

54. Cerkasovova, A., Cerkasov, J., Kulda, J., and Reischig, J. (1976). Circular DNA and cardiolipin in hydrogenosomes, microbody-like organelles of trichomonads. Folia Parasitol. (Prague) 23, 33-37.

55. Cerkasovova, A., Cerkasov, J., and Kulda, J. (1974). Biochemical comparison of microbody-like granules (hydrogenosomes) of trichomonads with mitochondria of other cells. Proc. Inter. Congr. Parasitol., 3rd, 1974 Vol 1, pp. 68-69.

56. Harrap, G. J., and Warkins, W. M. (1970). Enzymes of Trichomonas foetus. Separation and properties of two beta-galactosidases. Biochem. J. 117, 667-675.

57. Stealey, J. R., and Watkins, W. M. (1972). Separation of alpha-L-fucosidases in extracts of Trichomonas foetus. Biochem. J. 126, 16P-17P.

58. Watkins, W. M. (1959). Enzymes of Trichomonas foetus. The action of cell-free extracts on blood-group substances and low-molecular-weight glycosides. Biochem. J. 71, 261-274.

59. Watkins, W. M., and Morgan, W. T. J. (1954). Inactivation of the H receptors on human erythrocytes by an enzyme obtained from Trichomonas foetus. Br. J. Exp. Pathol. 35, 181-190.

60. Romanowska, E., and Watkins, W. M. (1963). Fractionation of neuraminidases in extracts of Trichomonas foetus. Biochem. J. 87, 37P-38P.

61. Timofeev, B.A. (1962). Facteur de diffusion et l'hyaluronidase dans les Trichomonas porcins et Trichomonas foetus (Riedmuller, 1928). Tr. Vses. Inst. Eksp. Vet. 28, 300-306.

62. Fitzgerald, P. R., Johnson, A. E., Hammond, D. M., Thorne, J. L., and Hibler, C. P. (1958). Experimental infection fo young pigs following intranasal innoculation with nasal, gastric, or cecal trichomonads from swine or with Trichomonas foetus. J. Parasitol. 44, 597-602.

63. Hammond, D. M., and Bartlett, D. E. (1943). The distribution of Trichomonas foetus in the preputial cavity of infected bulls. Am. J. Vet. Res. 4, 143-149.

64. Florent, A. (1947). Pouvoir agglutinant du mucus vaginal vis-a-vis de Trichomonas foetus dans la trichomonose du betail. C. R. Seances Biol. Ses Fil. 141, 957-958.

65. Hogue, M. J. (1938). The effect of Trichomonas foetus on tissue culture cells. Am. J. Hyg. 28, 288-298.

66. Kulda, J. (1967). Effect of different species of trichomonads on monkey kidney cell cultures. Folia Parasitol. (Prague) 14, 295-310.

67. Michaels, R. M., and Strube, R. E. (1961). Antitrichomonal agents 5-nitrothiazoles, 5-nitropyridines and 5-nitropyrimidines. J. Pharm. Pharmacol. 13, 601-610.

68. Steck, E. A. (1968). Chemotherapy of urogenital trichomoniasis. In "The Chemotherapy of Protozoan Diseases" Vol. 2, Chap. 17. Walter Reed Army Inst. Res., Washington, D.C.

69. Keighley, E. E. (1971). Trichomoniasis in a closed community: Efficacy of metronidazole. Br. Med.J. 1, 207-209.

70. McLaughlin, D. K. (1965). Dimetridazole, a systemic treatment for bovine venereal trichomoniasis. I. Oral administration. J. Parasitol. 51, 835-836.

71. McLaughlin, D. K. (1968). Dimetridazole, systemic treatment for bovine venereal trichomoniasis. II. Intravenous administration. J. Parasitol. 54, 1038-1039.

72. McLaughlin, D. K. (1970). Dimetridazole, a systemic treatment for bovine venereal trichomoniasis. III. Trials with cows. J. Parasitol. 56, 39-40.

73. Bartlett, D. E. (1948). Further observations on experimental treatments of Trichomonas foetus infection in bulls. Am. J. Vet. Res. 9, 351-359.

74. Fitzgerald, P. R., Johnson, A. E., and Hammond, D. M. (1963). Treatment of genital trichomoniasis in bulls. J. Am. Vet. Med. Assoc. 143, 259-262.

75. Ings. R. M., McFadzean, J. A., and Ormerod, W. E. (1974). The mode of action of metronidazole in T. vaginalis and other microorganisms. Biochemical Pharmacology 23, 1421-1429.

76. Muller, M., Lindmark, D. G. and McLaughlin, J. (1976) In "Biochemistry of Parasites and Host-Parasite Relationships" (H. Van den Bossche ed.) pp. 537-544. Elsevier/North Holland. Biomedical Press, Amsterdam.

77. Muller, M., and Lindmark, D. (1976). Uptake of metronidazole and its effect on viability in trichomonads and Entamoebe invadens under anarobic and aerobic conditions. Antimicrob. Agents and Chemother. 9, 696-700.

78. Milne, S., Stokes, E., and Waterworth, P. (1978). Incomplete anaerobiosis as a cause of metronidazole "resistance". J. Clin. Pathol. 31, 933-938.

79. Lindmark, D. G., and Muller, M. (1976). Antitrichomonal action, mutagenicity and reduction of metronidazole and other nitroimidazoles. Antimicrob. Agents and Chemother. 10, 476-482.

80. Goldstein, B., Vidal-Plana, R., Cavalleri, B., Zerelli, L., Carniti, G., and Silvestri, L. (1977). The mechanism of action of nitro-heterocyclic antimicrobial drugs. Metabolic activation by microorganisms. J. Gen. Microbiol. 100, 283-289.

81. Searle, A., and Willson, R. (1976). Metronidazole (Flagyl): degradation by the intestinal flora. Xenobiotica 6, 457-463.

82. Stambaugh, J., Feo, L., and Manthei, R. W. (1968). The isolation and identification of the urinary oxidative metabolites of metronidazole in man. J. Pharmacol. Exp. Ther. 161, 373-381.

83. Manthei, R., Feo, L., and Stambaugh, J. (1969). Identification of the metabolites of metronidazole in the human vagina. Wiad. Parazytol. 15, 403-405.

84. Manthei, R., and Feo, J. (1964). Studies on the metabolism of metronidazole. Wiad. Parazytol. 10, 177-179.

85. Templeton, R. (1977). Metabolism and parmacokinetics of metronidazole. In "A Review in: Metronidazole." (S. M. Finegold ed.) pp.28-40. Excerpta Medica, Amsterdam.

86. Coombs, G. (1976). Studies on the activity of metronidazole. In "Biochemistry of Parasites and Host-Parasite Relationship," (H. Van den Bossche, ed.), pp. 545-552. Elsevier/North Holland Biomedical Press, Amsterdam.

87. Moreno, S., Mason, R., Muniz, R., Cruz, F., and Docampo, R. (1983). Generation of free radicals from metronidazole and other nitroimidazoles by Tritrichomonas foetus. J. Biol. Chem. 258, 4051-4054.

88. Docampo, R., Moreno, S., and Mason, R. (1984). Reduction of nitrofurans and metronidazole to free radical metabolites by Tritrichomonas foetus hydrogenosomes. Abstract 1984 ASBC meeting St. Louis.

89. Gutteridge, W. E., and Gaborak, M. (1979). A re-examination of purine and pyrimidine synthesis in the three main forms of Trypanosoma cruzi. Int. J. Biochem. 10, 415-422.

90. Chrystal, E., Koch, R., and Goldman, P. (1980). Metabolites from the reduction of metronidazole by xanthine oxidase. Molecular Pharmacology 18, 105-111.

91. Meingassner, J. G., and Thurner, J. (1979). Strain of Trichomonas vaginalis resistant to metronidazole and other 5-nitroimidazoles. Antimicro. Agents Chemother. 15, 254-257.

92. Ames, B., Durston, W., Yamasaki, E., and Lee, F. (1973). Carcinogens are mutagens: A simple test combining liver homogenates for activation and bacteria detection. Proc. Natl. Acad. Sci. USA. 70, 2281-2285.

93. Miller, E., and Miller, J. (1971). The mutagenicity of chemical carcinogens: Correlations, problems and interpretation. In "Chemical Mutagens", (A. Hollaender, ed.) Vol. 1 pp. 83-119. Plenum, New York.

94. Rustia, M., and Shubik, P. (1972). Induction of lung tumors and malignant lymphomas in mice by metronidazole. J. Natl. Cancer. Inst. 48, 721-729.

95. Ryley, J. F., and Stacey, G. J. (1963). Experimental approaches to the chemotherapy of trichomoniasis. Parasitology 53, 303-320.

96. Marr, J. J., Berens, R. L., and Nelson, D. J. (1978). Purine metabolism in Leishmania donovani and Leishmania braziliensis. Biochim. Biophys. Acta. 44, 360-371.

97. Walsh, C. J., and Sherman, I. N. (1968). Purine and pyrimidine synthesis by the avian malaria parasite, Plasmodium lophurae. J. Protozool. 15, 763-770.

98. Wang, C. C., and Simashkevich, P. M. (1931). Purine metabolism in the protozoan parasite Eimeria tenella. Proc. Natl. Acad. Sci. USA 78, 6618-6622.

99. Heyworth, P. G., Gutteridge, W. E., and Ginger, C. D. (1982). Purine metabolism in Trichomonas vaginalis. FEBS Lett. 141, 106-110.

100. Ceron, C., Caldas, R., Felix, C., Mundim, M., and Roitman, I. (1979). Purine metabolism in trypanosamatids. J. Protozool. 26, 479-481.

101. Marr, J. J., Berens, R. L., and Nelson, D. J. (1978). Antitrypansomal effect of allopurinol conversion in vivo to aminopyrazolopyrimidine nucleotides by Trypanosoma cruzi. Science 201, 1018-1020.

102. Pfaller, M. A., and Marr, J. J. (1974). Antileishmanial effect of allopurinol. Antimicrob. Agents. Chemother. 5, 469-472.

103. Nelson, D. J., LaFon, S. W., Tuttle, J. V., Miller, W. H., Miller, R. L., Krenitsky, T. A., Elion, G. B., Berens, R. L., and Marr, J. J. (1979). Allopurinol ribonucleoside as an antileishmanial agent. J. Biol. Chem. 254, 11544-11549.

104. Carlson, D. A., and Chang, K. -P. (1981). Phosphorylation and antileishmanial activity of formycin B. Biochem. Biophys. Res. Commun. 100, 1377-1388.

105. Marr, J. J., Berens, R. L., Nelson, D. J., Krenitsky, T. A., Spector, T., LaFon, S. W., and Elion, G. B. (1982). Antileishmanial action of 4-thiopyrazol-(3,4-d)pyrimidine and its ribonucleoside. Biochem. Pharmacol. 31, 143-148.

106. Hill, B., Kilsby, J. Rogerson, G. W., McIntosh, R. T., and Ginger, C. D. (1981). The enzymes of pyrimidine biosynthesis in a range of parasitic protozoa and helminths. Mol. Biochem. Parasitol. 2, 123-134.

107. Lindmark, D. G., and Jarroll, E. L. (1982). Pyrimidine metabolism in Giardia lamblia trophozoites. Mol. Biochem. Parasitol. 5, 291-296.

108. Gutteridge, W. E., and Coombs, G. H. (1977). Nucleic acid metabolism. In "Biochemistry of Parasitic Protozoa". University Park Press. Baltimore, Maryland. pp. 69-88.

109. Perrotto, J., Keister D., and Gelderman, A. (1971). Incorporation of precursors into Toxoplasma DNA. J. Protozool. 18, 470-473.

110. Booden, T., Shaffer, J. G., and Alback, R. A. (1973). Purine and pyrimidine nucleotide metabolism by Entameba histolytica. In "Progress in Protozoology". IV International Congress of Protozoology. Clermont, France. p. 52.

111. Witte, J. (1933). Bakterienfrele Zuchtung von Trichomonaden and dem Uterus des Rindes in einfachen Nahrboden. Zentrabl. Bakteriol., Parasitenkd., Infektionskr. Hyg., Abt. 1: Orig. 128, 188-195.

112. Plastridge, W. N. (1943). Cultivation of a bacteria-free strain of Trichomonas fetus. J. Bacteriol. 45, 196-197.

113. Fitzgerald, P. R., Hammond, D. M., and Shupe, J. L. (1954). The role of cultures in immediate and delayed examinations of preputial samples for Trichomonas foetus. Vet. Med. (Kansas City, Mo.) 49, 409-413.

114. Diamond, L.S. (1957). The establishment of various trichomonads of animals and man in axenic cultures. J. Parasitol. 43, 488-490.

115. Johnson, G., and Trussell, R. E. (1943). Experimental basis for the chemotherapy of Trichomonas vaginalis infestations. I. Proc. Soc Exp. Biol. Med. 54, 245-249.

116. McEntegart, M. G. (1952). The application of haemagglutination technique to the study of Trichomonas vaginalis infections. J. Clin. Pathol. 5, 275-280.

117. Samuels, R. (1962). Agar techniques for colonizing and cloning trichomonads. J. Protozool. 9, 103-107.

118. Wang C. C., Wang A. L., and Rice A. (1984). Tritrichomonas foetus: Partly defined cultivation medium for study of the purine and pyrimidine metabolism. Experimental Parasitology 57, 63-75.

119. Diamond, L.S. (1964). Freeze-preservation of protozoa. Cryobiology 1, 95-102.

120. Honigberg, B. M., Farris, V. K., and Livingston, M. C. (1965). Preservation of Trichomonas vaginalis and Trichomonas gallinae in liquid nitrogen. Prog. Protozool., Int. Conf. Protozool., 2nd, 1965 Excerpta Med. Found. Int. Congr. Ser. No. 91, p. 199.

121. Bosch, I., and Frank, W. (1972). Beitrag zur Gefrierkonservierung pathogener Amoeben und Trichomonaden. Z. Parasitenkd. 38, 303-312.

122. McGuinness, E. T., and Cullen M. C. (1970). Continuous flow measurement of beta radiation using suspended scintillators. J. Chem. Ed. 47, A9-24.

123. Sieswerda. G. B., Poppe, H., and Huber, J. F., (1975). Flow versus batch detection of radioactivity in column liquid chromatogaraphy. Anal. Chim. Acta 78, 343-358.

124. Reeve, D. R., and Crozier A. (1977). Radioactivity monitor for High-Performance Liquid Chromatography. J. Chromatogr. 137, 271-282.

125. Klein, F. K., and Hunt C. A. (1981). Optimizing parameters for flow counting of radioactivity in column chromatographic effluents. International Journal of Applied Radiation and Isotopes 32, 669-671.

126. Payne, S. M., and Ames. B. N. (1982). A procedure for rapid extraction and HPLC separation of the nucleotides and other small molecules from bacterial cells. Anal. Biochem. 123, 151-161.

127. Chen, S. C., Brown, P. R., and Rosie, D. M. (1977). Extraction procedures for use prior to HPLC nucleotide analysis using microparticle chemically bonded packings. J. of Chromatographic Science 15, 218-221.

128. Van Haverbeke, D. A., and Brown, P. R. (1978). Optimization of a procedure for extraction of nucleotides from plasma and erythrocytes prior to HPLC analysis. J. of Liquid Chromatography 1, 507-525.

129. Pogolotti, A. L., and Santi, D. V. (1982). HPLC-UV analysis of intracellular nucleotides. Anal. Biochem. 126, 335-345.

130. Van Dyke, K., Truch, M. A., Wilson, M. E., and Stealey, P. K. (1977). Isolation and analysis of nucleotides from erythrocyte-free malarial parasites (Plasmodium berghei) and potential relevance to malaria chemotherapy. Bull. W.H.O. 55, 253-264.

131. Darwish, A. A., and Prichard, R. K. (1981). Analysis of ribonucleotides by reverse-phase HPLC using ion pairing on radially compressed or stainless steel columns. J. of Liq. Chrom. 4, 1511-1524.

132. Shaw, N. M., Brown, E. G., and Newton, R. P. (1979). Analysis by HPLC of free nucleotide pools of rat tissues. Biochemical Society Trans. 7, 1250-1251.

133. Santi, D. V., and McHenry, C. S. (1972). 5-Fluoro-2'deoxyuridylate covalent complex with thymidylate synthetase. Proc. Natl. Acad. Sci., U.S.A., 69, 1855-1857.

134. Hillcoat, B.L., Nixon, P. F., and Blakley, R. L. (1967). Effect of substrate decomposition on the spectrophotometric assay of dihydrofolate reductase. Anal. Biochem., 21, 178-189.

135. Bradford, M. M. (1976). A rapid and sensitive method for the quantition of microgram quantities of protein utilizing the principle of protein dye binding. Anal. Biochem., 72, 248-254.

136. Schmidt, R., Foret, M., and Reichert, U. (1976). Improved microscale assay for purine phosphoribosyl transferase activities. Clin. Chem., 227, 67-69.

137. Morse, S. A., Stein, S., and Hines, J. (1974). Glucose metabolism in Neisseria gonorrhoeae. J. Bacteriol., 120, 702-714.

138. Wang, C. C., and Cheng, H, -W. (1984). Salvage of pyrimidine nucleosides by Trichomonas vaginalis. Molc. Biochem. Parasitology 10, 171-184.

139. Jarroll, E. L., Lindmark, D. G., and Paolella, P. (1983). Pyrimidine metabolism in Tritrichomonas foetus. J. Parasitol., 69, 846-849.

140. Wang, C. C. (1984). Purine and pyridine metabolism in Trichomonadidae and Giardia: Potential targets for chemotherapy. Mechanism of Drug Action, 133-145.

141. McLard, R. W., Black, M. J., Livingston, L. R., and Jones, M. E. (1980). Isolation and initial characterization of the single polypeptide that synthesizes uridine 5'-monophosphate from orotate in Ehrlich Ascites carcinoma. Purification by tandem affinity chromatography of uridine-5'-monophosphate synthase. Biochemistry 19, 4699-4706.

142. Wang, C. C., Verham, R., Tzeng, S., Aldritt. S., and Cheng W. -H., (1983). Pyrimidine metabolism in Tritrichomonas foetus. Proc. Natl. Acad. Sci. U.S.A. 80, 2564-2568.

143. Tuttle, J. V., and Krenitsky, T. A. (1980). Purine phosphoribosyltransferases from Leishmania donovania. J. Biol. Chem. 255, 909-916.

144. Wang, C. C., and Aldritt, S. (1983). Purine salvage networks in Giardia lamblia. J. Exp. Med. 158, 1703-1712.

145. Elion, G. (1969). Actions of purine analogs: Enzyme specificity studies as a basis for interpretation and design. Cancer Res. 29, 2448-2453.

146. Gale, G. R., and Schmidt, G. B. (1968). Mode of action of alanosine. Biochem. Pharmac. 17, 363-368.

147. Grunberger, D., and Grunberger, G. (1979). in Antibiotics (Ed. F. H. Hahn), Vol. V, Part 2, pp 110-123. Springerk, Berlin

148. Lowe, J. K., Brox, L. and Henderson, J. F. (1977). Consequences of inhibtion of guanine nucleotide synthesis by mycophenolic acid and virazole. Cancer Research 37, 736-743.

149. Nelson, D. J., LaFon, S. W., Jones, T. E., Spector, T. Berens, R. L., and Marr, J. J. (1982). The metabolism of formycin B in Leishmania donovani. Biochem. Biophys. Res. Commun. 108, 349-354.

150. Rainey, P., Garrett, C. E., and Santi, D. V. (1983). The metabolism and cytotoxic effects of formycin B in Trypanosoma cruzi. Pharmac. 32, 749-

151. Rainey, P., and Santi, C. V. (1983). Metabolism and mechanism of action of formycin B in Leishmania. Proc. Natl. Acad. Sci. U.S.A. 80, 288-292.

152. Santi, D. V. (1980) Perspectives on the design and biochemical pharmacology of inhibitors of thymidylate synthetase. J. Med Chem. 23, 103-111.

153. Shigeura, H. T., and Gordon, C. N. (1962). The mechanism of action of hadacidin. J. Biol. Chem. 237, 1937-1940.

154. Smith, C. M., Fonteneile, L. J., Muzik, H., Paterson, A. R., Unger, H., Brox, L. N., and Henderson, J. F. (1974). Inhibitors of inosinate dehydrogenase activity in Ehrlich Ascite tumor cells in vitro. Biochemical Pharmacology 23, 2727-2735.

155. Synder, F. F., Henderson, J. F., and Cook, D. Z. (1972). Inhibition of purine metabolism- computer-assisted analysis of drug effets. Biochem. Pharmacol. 21, 2351-2357.

156. Tyagi, A. K., and Cooney, D. A. (1980). Identification of the antimetabolite of L-alanosine, L-alanosyl-5-amino-4-imidazolecarboxylic acid ribonucleotide, in tumors and assessment of its inhibition of adenylosuccinate synthetase. Cancer Res. 40, 4390-4397.

157. Wang, C. C., Verham, R., Rice, A., and Tzeng, S. (1983). Purine salvage by Tritrichomonas foetus. Molc. Biochem.Parasit. 8, 325-337.

158. Streeter, D. G., Witkawaski, J. T., Knare, G. P., Sidwell, R. W., Baver, R. J., Robins, R. K., and Simon. L. N. (1973). Mechanism of action of 1-beta-D-ribofuranosyl-1,2,4-triazole-3-carboxamide (Virazole), a new broad spectrum agent. Proc. Natl. Acad. Sci. U.S.A. 70, 1174-1178.

159. Berman, J. D., and Webster, H. K. (1982). In vitro effects of mycophenolic acid and allopurinol against Leishmania tropica in human macrophages. Antimicrobial Agents and Chemotherapy 21, 887-891.

160. Hampton, A. (1963). Reactions of ribonucleotide derivatives of purine analogues at the site of inosine 5 -phosphate dehydrogenase. J. Biol. Chem. 238, 3068-3074.

161. Atkinson, M. R., Morton, R. K., and Murray, A. W. (1963). Inhibition of inosine 5′-phosphate dehydrogenase from Ehrlich Ascites Tumour cells by 6-thioinosine 5′-phosphate. Biochem. J. 89, 167-172.

162. Hampton, A., and Nomura, A. (1967). Inosine 5′-phosphate dehydrogenase. Site of inhibition by guanosine 5′-phosphate and of inactivation by 6-chloro and 6-mercaptopurine ribonucleoside 5′-phosphates. Biochem. 6, 679-689.

163. Anderson, J. H., and Sartorelli, A. C. (1969). Inhibition of inosinic acid dehydrogenase of Sarcoma 180 cells by nucleotides and their analogs. Biochem. Pharmac. 18, 2747-2757.

164. Muller, M. (1980). The hydrogenosome. Symposium of the Society of General Microbiology 30, 127-142.

165. Cohen, M. B., Maybaum, J., and Sadee, W. (1981). Guanine nucleotide depletion and toxicity in mouse T-Lymphoma (S-49) cells. J. Biol. Chem. 256, 8713-8717.

166. Wang, C. C., Verham, R., Cheng, H, -W., Rice, A., and Wang, A. L. (1984). Differential effects of inhibitors of purine metabolism on two trichomonad species. Biochem. Pharm. 33, 1323-1329.

167. Abrams, R., and Bentley, M. (1955). Biosynthesis of nucleic acid purines. II. Role of hypoxanthine and xanthine compounds. Archs. Biochem. Biophys. 58, 109-118.

168. Magasanik, B., Moyed, H. S., and Gerring, L. B. (1957). Inosine 5'-phosphate dehydrogenase. J. Biol. Chem. 226, 339-350.

169. Lagerkuist, U. (1958). Biosynthesis of Guanosine 5'-phosphate. I. Xanthosine 5'-phosphate as an intermediate. J. Biol. Chem. 233, 138-142.

170. McFull, E. and Magasanik, B. (1960). The control of purine biosynthesis in cultured mammmalian cells. J. Biol. Chem. 235, 2103-2108.

171. Powell, G. F., Rajagopalan, K. V., and Handler, P. (1966). Abstracts of the American Chemical Society Meeting. Sept. C 117.

172. Turner, J. F. and King, J. E. (1961). Inosine 5'-phosphate dehydrogenase of Pea seeds. Biochem. J. 79, 147-151.

173. Ackerman, C. J., Al-Mudhaffer, S., and Mah, V. (1966). The inhibition of GMP synthesis by thyroid hormones. Fed. Proc. 25, 618.

174 Moyed, H. S. (1961). Interferance with feedback control of enzyme activity. Cold Spring Harbor Symp. Quant. Biol. 26, 323-329.

175. Krishnaiah, K. V. (1975). Inosinic acid 5'-monophosphate dehydrogenase of Escherichia coli: purification by affinity chromatography and some properties. Archs. Biochem. Biophys. 170, 567-575.

176. Hampton, A., Brox, L. W., and Bayer, M. (1969). Analogs of inosine 5'-phosphate with phosphorus-nitrogen and phosphorus-sulfur bonds. Binding and kinetic studies with inosine 5'-phosphate dehydrogenase. Biochem. 8, 2303-2311.

177. Brox, L., and Hampton, A. (1968). Inosine 5'-phosphate dehydrogenase. Kinetic mechanism and evidence for selective reaction of the 6-chloro analog of inosine 5'-phosphate with a cysteine residue at the inosine 5'-phosphate site. Biochem. 7, 2589-2596.

178. Heyde, E., Nagabushanam, A., Vonarx, M., and Morrison, J. F. (1976). Studies on inosine monophosphate dehydrogenase. Steady state kinetics. Biochim. Biophys. Acta. 429, 645-660.

179. Lowry, O. H., Rosebrough, N. J., Farr, A. L., and Randall, R. J. (1951). Protein measurement with the folin-phenol reagent. J. Biol. Chem. 193, 265-275.

180. Fischer, H. E., Muirhead, K. M., and Bishop, S. H. (1978). Purine and Primidine nucleotide metabolism. In "Methods in Enzymology" (Hoffee, P.A., and Jones, M. E. eds.) Vol. 51, pp. 207-213. Academic Press, New York.

181. Sakamoto, N. (1978). Purine and Pyrimidine nucleotide metabolism. In "Methods in Enzymology" (Hoffee, P. A., and Jones, M. E. eds.) Vol. 51, pp. 213-218. Academic Press, New York.

182. Chrambach, A., Jovin, T. M., Svendsen P. J, and Rodbard, D. (1976). Analytical and preparative polyacrylamide gel electrophoresis. An objectively defined fractionation route, apparatus and prodedures. In "Methods of Protein Separation". Vol. 2. (Catsimpoolas, N. ed.), Plenum Publishing Corp., New York, pp. 27-144.

183. Blakesley, R. W., and Boezi, J. A. (1977). A new staining technique for proteins in polyacrylamide gels using Coomassie Brilliant Blue G 250. Anal. Bioch. 82, 580-582.

184. Gabriel, O. (1971). Enzyme purification and related techniques. In "Methods in Enzymology" (Jakoby, W. B. ed.) Vol. 22, pp. 578-603. Academic Press, New York.

185. Laemmli, U. K. (1970). Cleavage of structural proteins durine the assembly of the head of bacteriophage T_4. Nature (London) 227, 680-685.

186. Anderson, J. H., and Sartorelli, A. C. (1968). Inosinic acid dehydrogenase of Sarcoma 180 cells. J. Biol. Chem. 243, 4762-4768.

187. Cleland, W. W. (1963). The kinetics of enzyme-catalyzed reactions with two or more substrates or products. I. Nomenclature and rate equations. Biochim. Biophys. Acta. 67, 104-137.

188. Strittmatter, P. (1966). Dehydrogenases and flavoproteins. Annu. Rev. Biochem. 35, 125-156.

189. McCarty, K. S., Stafford, D., and Brown, O (1968). Resolution and fractionation of macromolecules by isokinetic sucrose density gradient sedimentation. Anal. Biochem. 24, 314-329.

190. Kersters, K., and DeLey, J. (1966). Carbohydrate metabolism. In "Methods in Enzymology". Vol. 9, (Wood, W. A. ed.) Academic Press, New York. pp. 346-350.

191. Bio-Rad Price List J. (1984). Gel Chromatography. pp 31-38.

192. Rosenbloom, F. M., Hendrson, J. F., Caldwell, I. C., Kelley, W. N., and Seegmiller, J. E. (1968). Biochemical bases of accelerated purine biosynthesis de novo in human fibroblasts lacking Hypoxanthine-Guanine phosphoribosyltransferase. J. Biol. Chem. 243, 116-1173.

193. Kelley, W. N., and Wyngaarden, J. B. (1974). Enzymology of gout in "Advances in Enzymology" (Meister, A. ed.) 41, pp. 1-33. John Wiley and Sons, New York.

194. Wood, T. (1968). The detection and identification of intermediates of the pentose phosphate cycle and related compounds. J. Chromatog. 35, 352-361.

195. Krenitsky, T. A., and Papainnou, R. (1969). Human hypoxanthine phophoribosyltransferase. II. Kinetics and chemical modification. J. Biol. Chem. 244, 1271-1277.

196. Kornberg, A., Lieberman, I., and Simms, E. S. (1955). Enzymatic synthesis of purine nucleotides. J. Biol. Chem. 215, 417-427.

197. Krenitsky, T. A., Neil, S. M., and Miller, R. L. (1970). Guanine and Xanthine phosphoribosyltransferase activities of Lactobacillus casei and Escherichia coli. J. Biol. Chem. 245, 2605-2611.

198. Gots, J. S., and Benson, C. E. (1974). Adv. Exp. Med. Biol. 41A, 33-39.

199. Hill, D. L. (1972). In "The Biochemistry and Physiology of Tetrahymena", pp. 125-162. Academic Press, New York.

200. Walter, R. D., and Konigk, E. (1974). Hypoxanthine-Guanine Phosphoribosyltransferase and Adenine Phosphoribosyltransferase from Plasmodium chabaudi, purification and properties. Tropenmed. Parasitol. 25, 227-235.

201. Kahn, V., and Blum, J. J. (1965). Effect of 8-azaguanine on phophorylation of purines in Astasia and Euglena. J. Biol. Chem. 240, 4435-4443.

202. Konigk, E. (1978). Purine nucleotide metabolism in promastigotes of Leishmania tropica: inhibitory effect of allopurinol and analogues of purine nucleosides. Tropenmed. Parasitol. 29, 435-438.

203. Nelson, D. J., Bugge, C. J., Elion, G. B., Berens, R. L., and Marr, J. J. (1979). Metabolism of pyrazolo[3,4d]pyrimidines in Leishmania braziliensis and Leishmania donovani. J. Biol. Chem. 254, 3959-3964.

204. Marr, J. J., and Berens, R. L. (1977). Antileishmanial effect of allopurinol. II. Relationship of adenine metabolism in Leishmania species to the action of allopurinol. J. Infect. Dis. 136, 724-732.

205. Nelson, D. J., Bugge, C. J., Krasny, H. C., and Elion, G. B. (1973). Formation of nucleotides of [6-^{14}C]allopurinol and [6-^{14}C]oxipurinol in rat tissues and effects on uridine nucleotide pools. Biochem. Pharmacol. 22, 2003-2022.

206. North, M. J. (1982). Comparative biochemistry of the proteinases of eucaryote microorganisms. Microbiological Reviews.

207. McLaughlin, J., and Muller, M. (1979). Purification and characterization of a low molecular weight thiol proteinase from the flagellate protozoan Tritrichomonas foetus. J. Biol. Chem. 254, 1526-1533.

208. Coombs, G. H., and North, M. J. (1983). An analysis of the proteinases of Trichomanas vaginalis by polyacrylamide gel electrophoresis. Parasitology 86, 1-6.

209. Kelley, W. N., and Arnold, W. J. (1972). Human hypoxanthine-guanine phosphoribosyltransferase studies on the normal and mutant forms of the enzyme. Fed. Proc. 32, 1656-1659.

210. Merril, C.A., Goldman, D., and Ebert, M. (1981). Protein variations associated with Lesch-Nyhan syndrome. Proc. Natl. Acad. Sci. USA 78, 6471-6475.

211. Johnson, G., Ramage, A., Littlefield, J. and Kazazian, H. H. (1982). Hypoxanthine-Guanine phosphoribosyltransferase in human erythroid cells: Posttranslational modification. Biochem. 21, 960-966.

212. Steyn, L. M., and Harley, E. (1984). Substrate inhibition in a human variant of hypoxanthine-guanine phosphoribosyltransferase. J. Biol. Chem. 259, 338-342.

213. Wilson, J. and Kelley, W. (1984). Human hypoxanthine-guanine phosphoribosyltransferase. J. Biol. Chem. 259, 27-30.

214. Holden, J., and Kelley, W. (1978). Human hypoxanthine-guanine phosphoribosyltransferase. J. Biol. Chem. 253, 4459-4463.

215. Wray, W., Boulikas, T., Wray, V. P., and Hancock, R. (1981). Silver staining of proteins in polyacrylamide gels. Anal. Biochem. 118, 197-203.

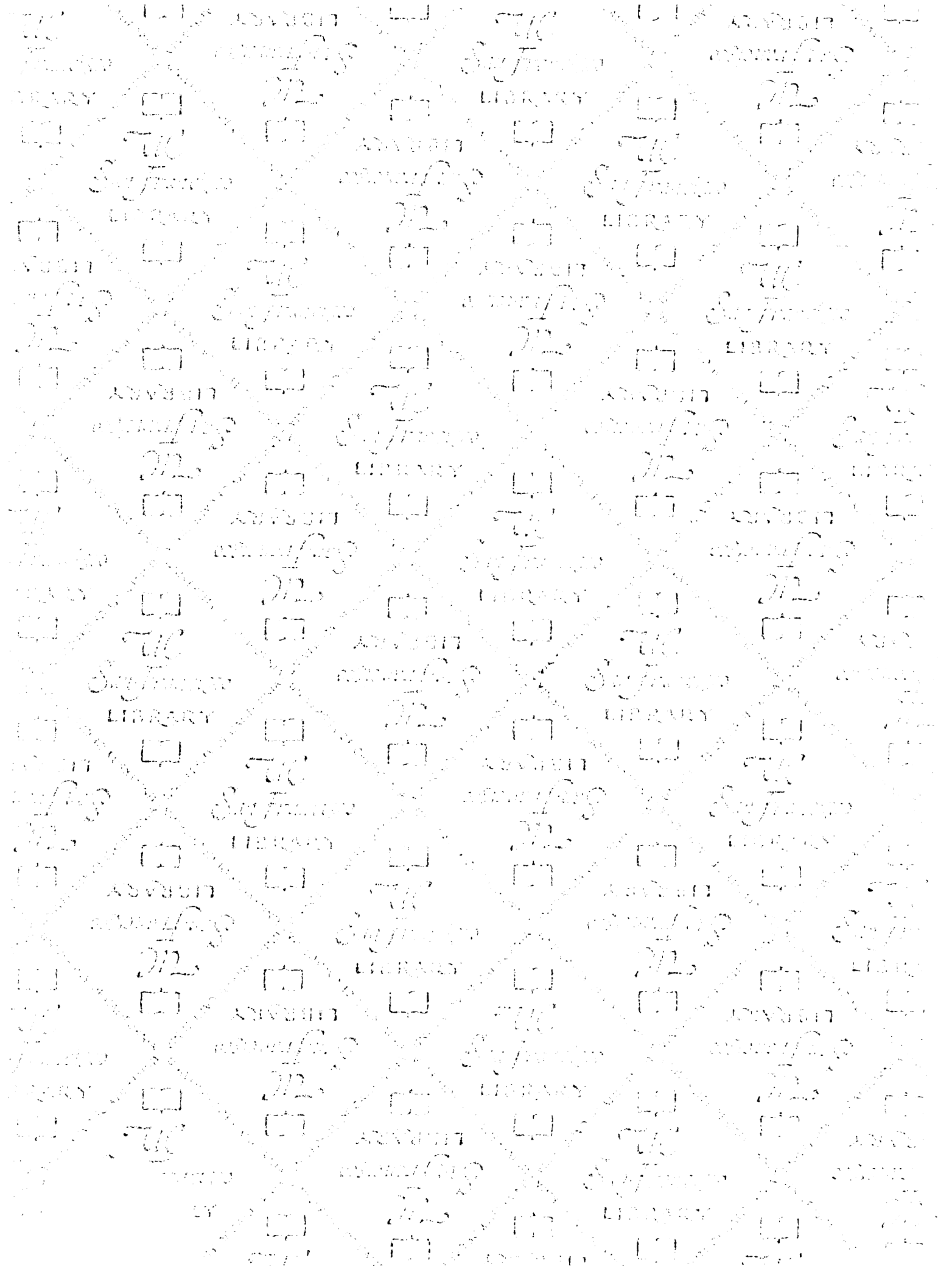

FOR REFERENCE

NOT TO BE TAKEN FROM THE ROOM

BRODART CAT. NO. 22 012 PRINTED IN U.S.A.